POLITECNICO DI MILANO

School of Civil, Environmental and Land Management Engineering

Master of science in Civil Engineering for Risk Mitigation

FLOOD HAZARD MODELLING FOR THE CITY OF LODI

Supervisor: Dr. Alessio Radice

Co-supervisor: Dr. Anna Rita Scorzini

Thesis of:
Andrea Agosti Matr.863427
Julien Crippa Matr.864568

Academic Year 2016/2017

ACKNOWLEDGEMENT

We would first like to thank our thesis advisor Dr. Alessio Radice of the school of Civil, Environmental and Land Management Engineering at Politecnico di Milano. The door to Prof. Radice's office was always open whenever we ran into a trouble spot or had a question about our research or writing. He consistently allowed this thesis to be our own work but steered us in the right direction whenever he thought we needed it.

We would also like to acknowledge Dr. Anna Rita Scorzini of the school of Civil, Environmental and Land Management Engineering at Politecnico di Milano as the co-advisor of this thesis, and we are gratefully indebted to her for her very valuable comments and help on this thesis.

Finally, we want to express our very profound gratitude to our friends, parents and to our girlfriends for providing us with unfailing support and continuous encouragement throughout our years of study and through the process of researching and writing this thesis. This accomplishment would not have been possible without them.

Thank you.

Andrea e Julien

April 2018

ENGLISH ABSTRACT

Every year riverine flooding affects a significant number of people, due to the exposure of population living in floodplains and the lack of adequate flood protection measures. Preparedness and monitoring are two effective ways to reduce the flood risk. The first one is related to the production of detailed hazard maps and it is the main objective of this study.

This thesis describes the procedures applied to develop the hazard scenario, which will be used for the hydrological risk assessment in the city of Lodi, considering a past event occurred on November 2002. In this study, two alternative ways of producing the hazard scenario are proposed.

The first procedure is based on a traditional hydraulic modelling procedure, which consists in the creation of a steady and an unsteady model. Sensitivity analysis and calibration are performed to achieve the results. The outputs of the model are hazard maps representing the flooded area, with water depth and velocity fields. Then, they are compared to the results of available reports and observed measurements. This procedure is time-consuming and requires a great computational effort.

The second is a fast and low computational demanding procedure, which consists in the calculation of water depth distribution from the flooded area. For the current work, the latter one is a hazard map (*Mappa della pericolosità e del rischio di alluvioni*) produced by the Po river basin authority (AdbPo), but it may be also provided by programmes as the European Flood Awareness System (EFAS)[1]. The approximations and limits of this method are described, in order to understand if it can be used for emergency planning purposes and after-event first damage estimation.

Overall this thesis provides precise results for both the traditional hydraulic modelling procedure and the fast as well as low computational demanding one.

This work has been performed within the Flood-IMPAT+[2] project, a procedure under development by Politecnico di Milano for the evaluation and mapping of the hydrogeological risk at different spatial scales.

[1] www.efas.eu

[2] www.floodimpatproject.polimi.it

ITALIAN ABSTRACT

Ogni anno, a causa dell'esposizione della popolazione che vive nelle aree golenali e della mancanza di adeguate misure di protezione, le alluvioni colpiscono un numero significativo di persone. Per ridurre il rischio d'alluvione, esistono due metodi efficaci: la prevenzione e il monitoraggi. Il primo, obiettivo principale di questo studio, è correlato alla produzione di dettagliate mappe di pericolosità.

Nella presente tesi, sono descritte le procedure utilizzate per sviluppare lo scenario di pericolosità, che sarà utilizzato per la valutazione del rischio idrologico della città di Lodi, considerando l'evento accaduto nel novembre 2002. Nell'elaborato, sono proposti due metodi alternativi per produrre lo scenario di pericolosità.

Il primo consiste in una procedura tradizionale di modellazione idraulica, che si basa sulla creazione di due modelli: uno di moto permanente e uno vario. Per ottenere i risultati vengono eseguite le procedure dell'analisi di sensitività e di calibrazione del modello. Gli output prodotti sono mappe di pericolosità che rappresentano l'area allagata con la profondità e la mappa della velocità dell'acqua. Infine, questi vengono confrontati con risultati di report e misure reali. Questa procedura è lunga e richiede un grande sforzo computazionale.

Il secondo metodo è una procedura veloce e con basse esigenze computazionali; questa consiste nel calcolo della profondità dell'acqua a partire dall'area allagata. Per questo studio, questa è rappresentata dalla mappa di pericolosità (*mappa della pericolosità e del rischio di alluvioni*) prodotta dall'Autorità del bacino del fiume Po (AdbPo), ma può anche essere fornita da programmi come il European Flood Awareness System (EFAS)[3]. Per ultimo sono descritte le approssimazioni e i limiti del metodo, per capire se questo può essere utilizzato per scopi di pianificazione di emergenza e per una prima stima del danno post-evento.

Complessivamente, per entrambi i metodi sopra descritti, la tesi in esame fornisce risultati dettagliati.

Questo lavoro è stato realizzato nell'ambito del progetto Flood-IMPAT+[4], una procedura in fase di sviluppo del Politecnico di Milano per la valutazione e la mappatura del rischio idrogeologico dal punto di vista della microscala.

[3] www.efas.eu

[4] www.floodimpatproject.polimi.it

INDEX

LIST OF FIGURES

LIST OF TABLES

APPENDIX INDEX

‘‘*…essentially, all models are wrong, but some are useful.*’’
(George E. P. Box)

1 INTRODUCTION

1.1 SCOPE OF THE THESIS

Worldwide, many important economic and social impacts are due to hydrogeological disasters. In particular during the last century urban flood events have been increasing in frequency and severity as a consequence of growing of the population and due to the climate change. These factors will contribute to increase urban risk in the future, and as a result improved modelling of urban flooding has been identified as a research priority (Poljanšek K. et al., 2017). To improve the hydrogeological risk management, a coordinated effort is needed, which strengthen all the component of the risk management cycle, including prevention, preparedness, response and recovery.

The key for a short and long-term emergency planning, which is needed to increase society's resilience to this risk, is the development of a suitable risk map. The methodology used to produce flood hazard maps is based on the determination of the probability of an area being flooded. Usually, this computation is performed with respect to a determined flood level (e.g. the 0.01 Annual Exceedance Probability threshold).

To compute the flood risk, the flood hazard is taken and combined with information on the potential damage, which are vulnerability and exposure of population and goods in the floodplains. The approaches available to determine the risk are different according to:

- temporal scale at which the hazard and risk assessment are applied;
- spatial scale at which the hazard and risk assessment are applied;
- modelling tools available;
- data available;
- type of flood hazard (e.g. fluvial, surface water or coastal flood).

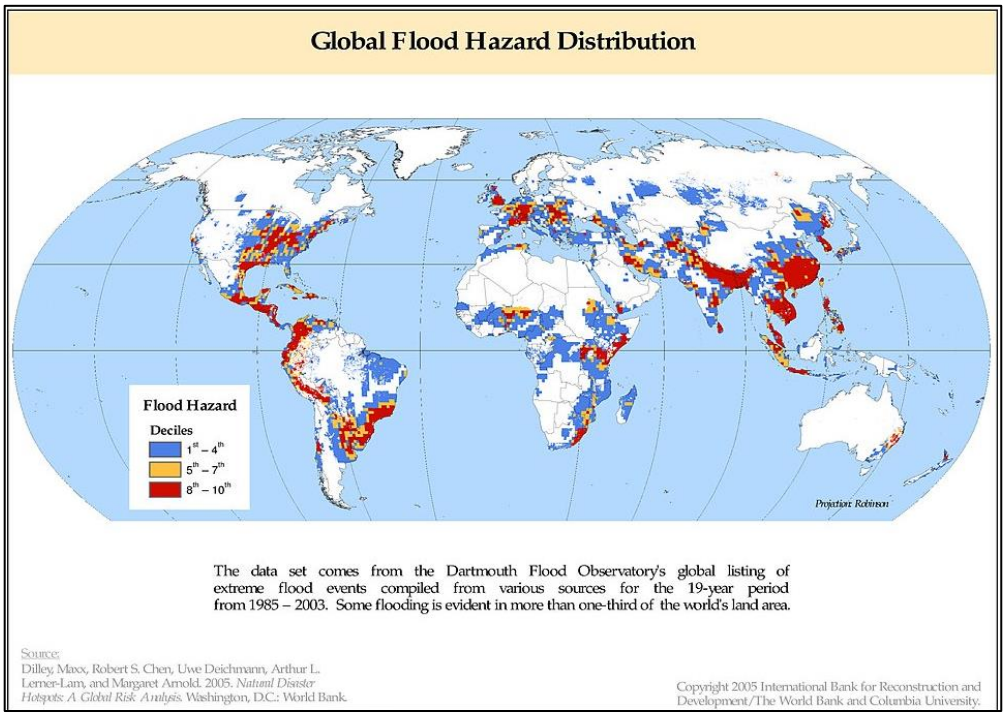

Figure 1 Global Flood Hazard Distribution

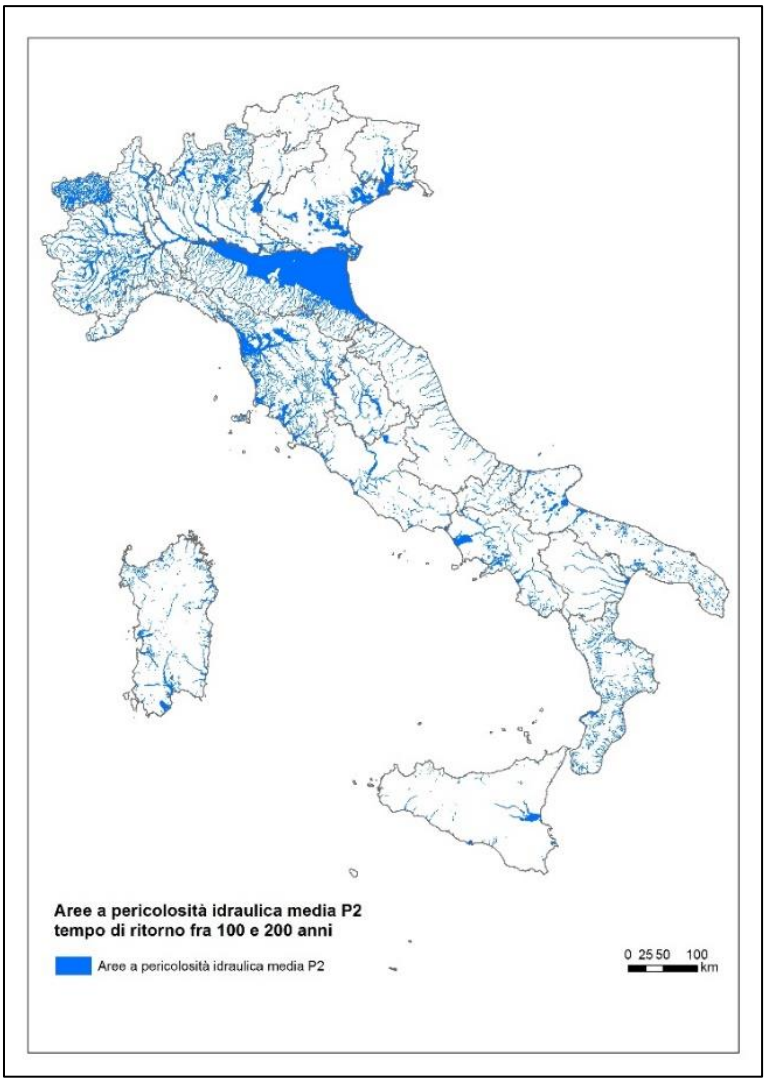

Figure 2 Italian Hazard Distribution with return period between 100 and 200 years

To create complete hydrogeological risk map it is needed a great amount of data, with a long-time series of events and a chain of models and assessments, that reflect the way of understanding of the physical process controlling hydrological events.

All the factors which were just expressed have some uncertainties, therefore the risk maps have uncertainties. Consequently, it is important that risk maps are harmonised with user requirements and needs, so that decision makers can understand and act upon the information deduced.

The main scope of this study is to develop the hazard scenario which will be used for the hydrogeological risk assessment in the city of Lodi, considering the event happened in November 2002.

Figure 3 Photo taken from the 2002 event, area of the city completely flooded

This work has been performed within the project Flood-IMPAT+[5], further development of a previous project called Flood-IMPAT. The latter is a procedure developed by Politecnico di Milano for the evaluation and mapping of the hydrogeological risk. The working scale of the project Flood-IMPAT is the mesoscale, therefore it is not useful for the development of emergency plans. In order to perform the plans, a microscale view is necessary.

Flood-IMPAT+ has the objective to extend the procedure to the microscale, in order to define quantitative methods for flood risk assessment that can be used also for the development of emergency plans.

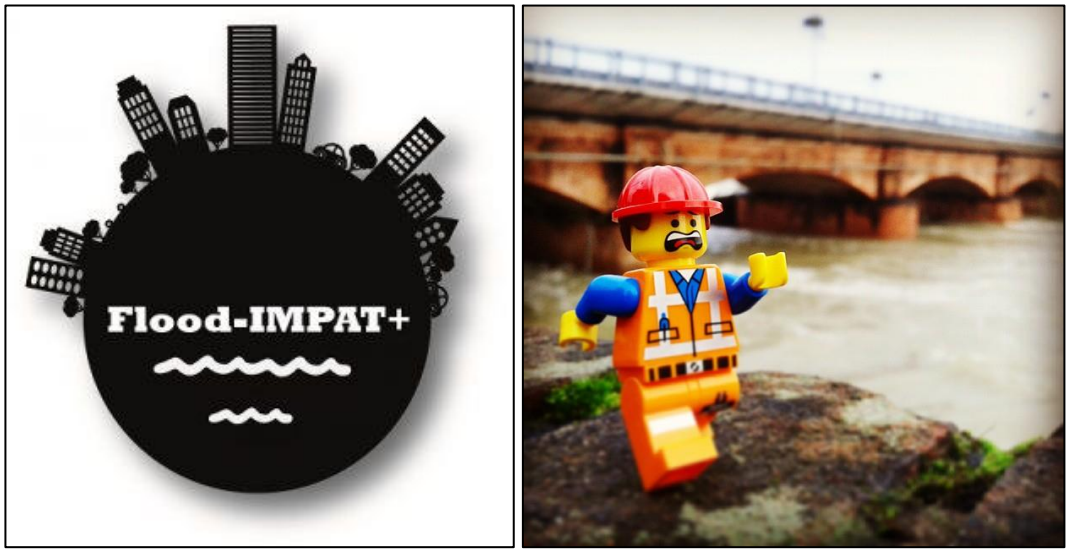

Figure 4 On the left Flood Impat+ logo, on the right the bridge Napoleone Bonaparte

[5] www.floodimpatproject.polimi.it

Starting from the definition, flood risk is defined as the expected losses for exposed elements having a specific vulnerability and affected by a given hazard (Menoni & Margottini, 2011) . This thesis focuses the attention on the last part of the risk definition: the hazard, probability of occurrence, and magnitude of a phenomenon.

At the microscale, it is necessary to calculate the hazard at the level of single exposed items (i.e. buildings), therefore the 2002 flood in Lodi is chosen as a test case. This event, as explained in the chapter 1.3, is documented in another study (Rossetti & Cella, 2010), commissioned by the municipality to design a flood protection system for the city. The availability of a large quantity of data as well as previous analyses, useful for comparison, made this event an optimal case study.

The thesis is subdivided in 2 parts:

- computation of the hazard with the traditional hydraulic modelling procedure;
- computation of the hazard with a fast procedure based on the flooded perimeter.

Considering the event occurred on November 2002, firstly the steady model of the event is created. Then, using all the information gained, the unsteady analysis is performed, and the hazard map is created. Later, it is proposed a new procedure that, starting from the flooded perimeter, is capable of producing the flood hazard map. Finally, the resultant hazard maps are compared to understand if a fast procedure is sufficient for an after-event damage estimation.

1.2 GEOGRAPHICAL CONTEXT

The city of Lodi is a municipality of 45.106 inhabitants[6] located in the south-centre of the Lombardy region (Northern Italy), in the area called as low land, *bassa pianura*. It is the capital of the Lodi province and the area of the municipality is around 41 km^2.

[6] www.comune.lodi.it/flex/cm/pages/ServeBLOB.php/L/IT/IDPagina/417

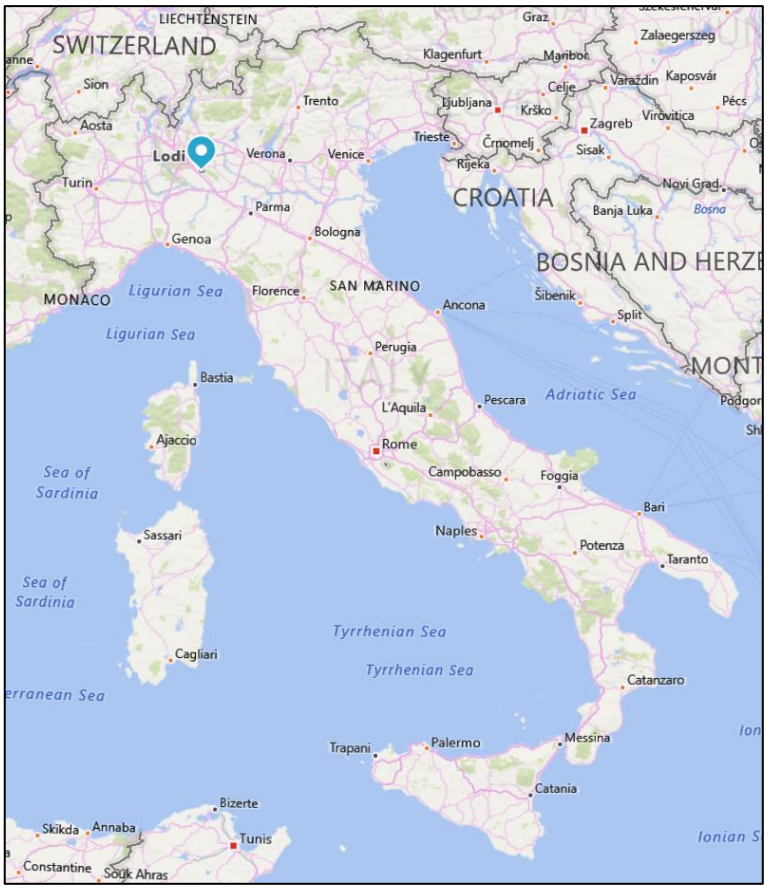

Figure 5 Map of Italy, geolocalization of Lodi

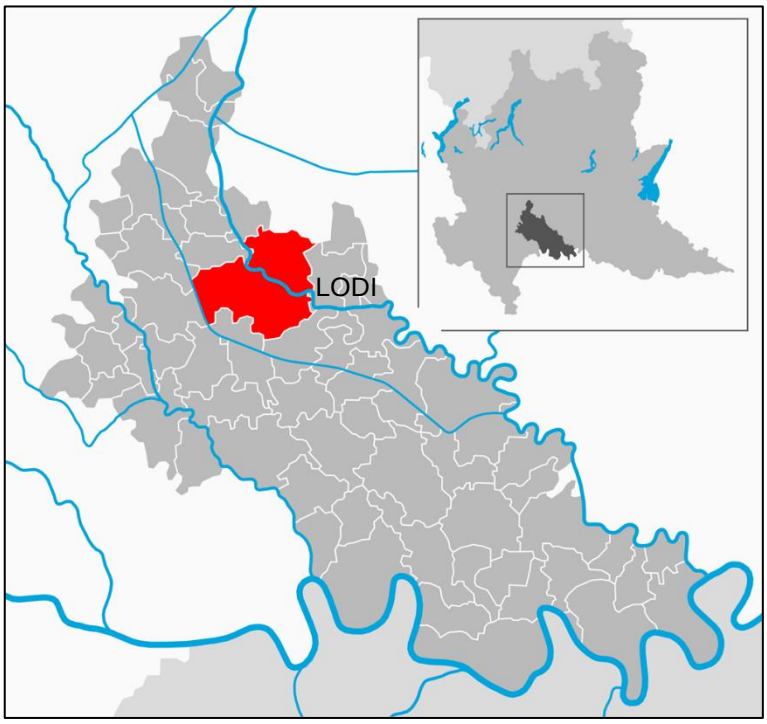

Figure 6 Detail of Lodi province

The old part of the city is located on the hydrographic right of the Adda river, on the trapezoidal-shaped *Eghezzone* hill. The rest of the city is partly built on the floodplain and on a morphologic terrace created by the river erosion. All the municipality territory is between 65 and 87 m.a.s.l.

The climate of the region is analogous to the rest of the Po Valley. The most intense precipitations occur during autumn and spring. The territory of the municipality is crossed by a lot of canals, the most important are the *Muzza* canal, which defines the west boundary of the city and the *Bertonica* and *Molina* ditches; the latter, which was tunnelled, is crossing the urban territory.

In this thesis, a hazard scenario for the hydrogeological risk in the city of Lodi is derived by considering the flood event occurred on 27 November 2002. In that occasion, due to the intense rainfall events occurred over the previous days, the city of Lodi was flooded by the main river that is crossing the city, Adda.

Figure 7 Aerial view, the river Adda

The Adda, whose name means "flowing water" from Celtic, is a main river located in North Italy (it is the second tributary of the Po river, after Ticino). It is the longest tributary of the Po river and the fourth longest Italian river. It entirely flows in the Lombardy region, passing through the provinces of Sondrio, Como, Lecco, Bergamo, Monza e Brianza, Milano, Cremona and Lodi.

Figure 8 The Adda catchment (Jaroslav Mysiak & Martina Gambaro, 2011)

The following table summarize the main characteristics of the Adda catchment:

Table 1 Summary of the main characteristics of the river Adda

Length	313 km
Average discharge (Q)	187 m^3/s
Catchment	7927 km^2 (11% of total Po Basins's surface)
Source	Monte del Ferro
Outflow	Po
Info	94% on Italian territory; 6% on Switzerland territory 79% mountain; 21% plain

The flow regime of the river is alpine and it is naturally controlled by the Lake of Como, where Adda is the main tributary and the only emissary. This behaviour is also modified by some dams located in the mountain area (Ardenno, San Giacomo di Frae, Cancano) and in the downstream part of the river (Olginate, Trezzo sull'Adda).

The average discharge is around 190 m^3/s, but during dry periods (i.e. 2003 summer) it can be even 18 m^3/s. The maximum discharge can be higher than 1000 m^3/s, as happened in 1987 and 2002 (1840 m^3/s) (Natale, 2003).

Historical catastrophic flood events of the Adda river occurred in 1520, 1987 and 2002.

Figure 9 An hystorical photo of the 2002 event

1.3 THE NOVEMBER 2002 EVENT

Before

18 November 2002: during the night between the 16th and 17th November, after an intense rainfall causing the flood of some farmland in the province of Lodi, the Italian National Civil Protection declared the alarm for hydrogeologic risk at Level 2 on a scale of 4[7]. In the afternoon of the same day. Water level which had been increased 1.5 meters under the Napoleone Bonaparte bridge, started to decrease and the emergency seemed as ended.

In the meantime, weather forecast gave unwelcome news: the big part of the storm was finished, however another and less strength perturbation could arrive within 3/4 days.

A newspaper article of the same day reported a declaration, made by Eng. Rossetti, the Mayor of the city and other municipality workers: they manifested discord about the lack of intervention after the last big hydrogeologic event (year 2000).

18 MARTEDÌ 26 NOVEMBRE 20

Il Cittadi

Speciale maltempo

A LODI RIUNITA IN PREFETTURA LA PROTEZIONE CIVILE, DISTRIBUITI SACCHETTI DI SABBIA AGLI ABITANTI, OGGI ANCORA ORE DI TENSIO

Giornata di grande paura per l'Add

Supera i 180 centimetri poi scende, sommerse alcune strad

LODI Occhi fissi sulla corrente grigiastra dell'Adda, che si spaccava contro i piloni del ponte napoleonico per andare a portare via altri pezzi all'isolotto Achilli, ormai assediato da giorni da gorghi e ritorni d'acqua che ne stanno decretando la fine, che appare sempre più vicina. La giornata di ieri a Lodi è trascorsa sotto una pioggia insistente, ma percolo vero e proprio non c'è mai stato, malgrado la regione avesse dichiarato lo stato di allarme anche per il territorio lodigiano. In mattinata nel municipio è stata allestita la sala comunale di protezione civile e funzionari, tecnici e operai si sono mossi al lavoro nelle loro rispettive competenze. Le notizie arrivavano in tempo reale, attraverso i terminali dei computer, via telefono o dalla viva voce di chi operava sul campo. Alle 11 venivano segnalati allagamenti nei pressi delle cascine Ciribina e Dordona e nella depressione che si trova dietro il tribunale, in questo caso a causa del sollevamento della falda: «Non si tratta però di fenomeni di esondazione del fiume - spiegava l'assessore alla protezione civile Francesco Marzorati - ma di situazioni legate all'ingrossamento delle rogge che non riescono a scaricare nell'Adda e si riversano nei campi».

Intanto il livello del fiume passava da 136 a 142 e poi ancora a 170 centimetri sopra lo zero idrometrico, ben al di sotto della soglia di 2 metri e 70 centimetri, il raggiungimento della quale avrebbe significato la tracimazione, con conseguente rischio per la stabilità del ponte.

Già verso mezzogiorno il livello veniva dato per calante, ma si si doveva aspettare la piena del Brembo, che entra nell'Adda a nord del Lodigiano, prevista per il pomeriggio. Nel frattempo, mentre i vigili del fuoco intervenivano in via del Capanno per alcune cantine allagate, il comune procedeva all'acquisto di mille sacchi di sabbia, che si aggiungevano ai circa trecento ancora nei magazzini, mentre un altro mi-

La minacciosa acqua marrone dell'Adda quasi lambisce le arcate del ponte di Lodi, ma ieri l'allarme è poi rientrato

Pescatori alla Piarda Ferrari mettono al sicuro le b

Il fiume quasi al livello delle sponde sul lungo Ad

to arrivavano le notizie da nord: dalla diga di Olginate al lago di Como de cui paratie sono costantemente aporte dal 15 novembre) venivano segnalati 570 metri cubi al secondo in uscita e 1.100 in afflusso da nord, mentre la portata del Brembo, passata senza danni l'ondata di piena, si attestava a 260 metri cubi d'acqua al secondo. Per portare a 3 metri il livello sopra lo zero idrometrico a Lodi, dal Brembo e da Olginate arrebbero dovuti arrivare tra i 1.800 e i 2.000 metri cubi di acqua al secondo. Dalla diga le piene impiega circa 6-8 ore per arrivare al ponte, mentre dalla Valle Brembana sono sufficienti 4 ore "di viaggio".

Il pomeriggio trascorreva in attesa, mentre dalla provincia di Bergamo arrivava la notizia che la pioggia aveva cessato di cadere. Lentamente il livello si attestava a 123 centimetri e cessava l'allarme nella sala di protezione civile della prefettura: volontari, operatori e forze dell'ordine lasciavano il campo, pur restando a disposizione, per rientrare in caso di riacutizzarsi del fe no pioveso. Oggi però si repli sto che le previsione meteo tutr'altro che incoraggianti tendono ulteriori precipitazio i 60 e i 70 millimetri.

Arrigo Bo

Figure 10 main page of a local newspaper

25 November 2002: after other intense rainfall events, even if the National Civil Protection was on alert, the alarm on the territory was low. On 25th of November, around 11 am, areas near the *Cascina Ciribina, Dordona* and on the depression near the courthouse were flooded by the water coming out from the ditches system.

[7] www.protezionecivile.gov.it/jcms/it/view_bcr.wp?contentId=BCR67598

Water levels were increasing from 136 cm to 142 cm, up to 170 cm, but they were far from 270 cm, fixed height for the overflow. The water level was 185 cm and 123 cm at 2 pm and at 6 pm, respectively (2*).

News came from the north of the river Adda: in Olginate (an important village from the hydrogeologic point of view because of the presence of a dam) the discharge was increasing around 1100 m^3/s and additional discharge of 360 m^3/s was flowing from Brembo (an affluent of Adda river). It was already known that to overpass the 3 meters level at the bridge, the discharge should have been around 1800 and 2000 m^3/s.

At the end of the day, due to the decrease of the water level, National Civil Protection stopped the alarm. The weather forecast was given as 60/70 mm of rain for the following hours.

Other newspapers articles complained about the uncontrolled urbanization of the last years with consequent impermeabilization of the soil. Others were against the elimination of floodplain area (*area golenare*), where in the past the river was able to expand without flooding the city.

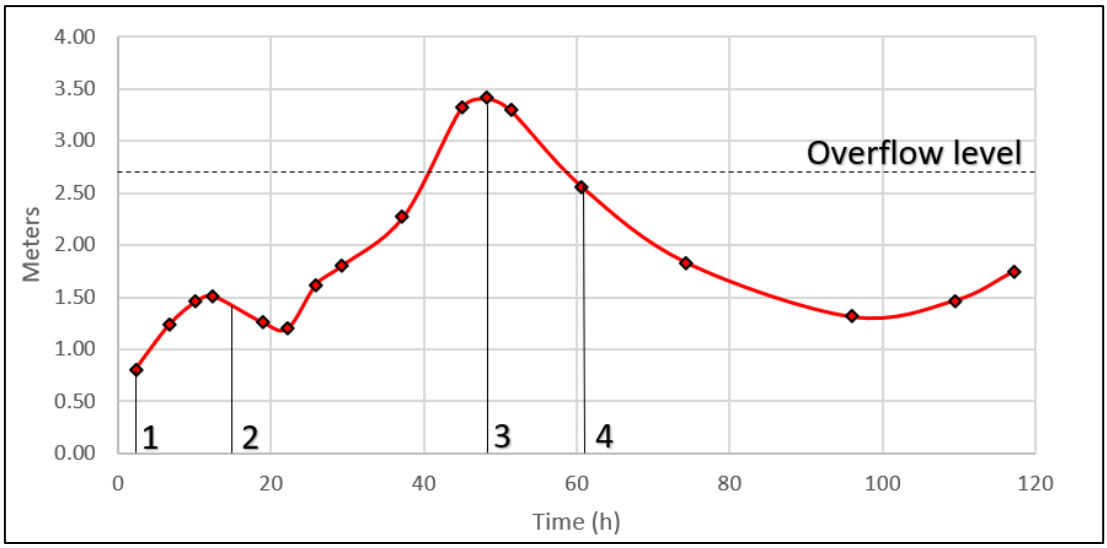

Figure 11 Measured levels at Napoleone Bonaparte Bridge

***1** 25-11-2002 (00 am)*

***2** Levels started to decrease*

***3** Maximum level 1.30 am 26-11*

***4** Level at the bridge is below the overflow level*

During

27 November: During the night between 25th and 26th Adda reached the record height of 3.43 m above the hydrometric 0 level (68.28m a.s.l), the flood was defined with return period of 200 years. The 25th November levels grew up of 15 cm/h and around 01.30 am of the 26th of November the historical level of 343 cm was reached (point **3** Figure 11).

The lower part of city (*la città bassa*) was underwater: 500 people were evacuated. It was reported that someone escaped from the window of his house.

Figure 12 Picture taken the morning after the flood

Houses, farms, farmhouses and offices were flooded. National Civil Protection, Firefighters, Red Cross and Police with boats, helicopter and others rescue vehicles were helping the people and saving animals. From 08.00 am, water levels started decreasing, at 13.30 pm they were under the 2.5 m (point **4** Figure 11). At 18.30 pm population was informed by telephone that water levels were decreasing, and that emergency was finished.

In the meantime, 98 evacuated people were accommodated in the shelters since their houses were full of mud and water.

A warning about the forecast of another flood was sent on the morning of the 29th, but fortunately nothing happened.

After

Following studies, performed by Eng. Natale and Studio Paoletti (taken as a references in this work) have highlighted in the next months the factors that determined the extraordinary event reported above. The summary of these researches is here reported.

Starting from the 14th of November, extreme rainfalls hit Lombardy and Piemont regions which caused a growth in the water level in the Lake of Como and, consequently the dam in Olginate was totally opened starting from the 15th November.

On 24th a second perturbation with rainfall less intensive but with a higher and concentrated peak was occurred. This event happened when the lake of Como was still full and summed with the wave of flood from Brembo river.

On 25th and 26th of November, water levels were already high due to the previous phenomena, and they were still rising.

Hydraulic regurgitation events started from the morning on the minor waterways (like the complex system of irrigation ditches present in Lodi area) provoking flood of some farmland.

During the entire day, water level rose and between 26th and 27th the lower part of the city was totally flooded.

1.4 AVAILABLE DATA

For the evaluation and the computation of the hydraulic model, secondary data[8] where used.

In the following all the secondary data collected are presented, which were obtained by the advisors of the project from previous researches, literature review, national agencies, governmental organizations and reports.

- past reports;
- river cross-sections;
- digital Surface Model (DSM);
- extension of the flooded area;
- observed water levels;
- hydrograph;
- photos;
- newspaper articles.

In the following sections all the reported data are described in detail.

Past reports:

Few reports from various studies, performed in Lodi and the flood event in 2002, were used to obtain the data and information. The main ones that were used are:

- *Disponibilità ed ottimizzazione nell'uso della risorsa idrica* (Paoletti, Bianchi et al., 1999);
- *Studio idrologico-Idraulico del tratto di F. Adda* (Rossetti & Cella, 2010a);
- *Delimitazione delle aree inondabili ad assegnati tempi di ritorno* (Natale, 2003);
- *Studio di fattibilità della sistemazione idraulica* (Autorità di bacino del fiume Po, 2003).

River cross-sections:

223 cross-sections of the river Adda were provided by the Po river basin authority (AdbPo). These sections represent the bathymetry of the river, which is not visible in the DTM due to the presence of the water. However, only 14 of the 223 available cross-sections were used to model the geometry of the area of interest. Examples of the sections are represented below.

[8] Secondary data refers to data that was collected by someone other than the user https://en.wikipedia.org/wiki/Secondary_data

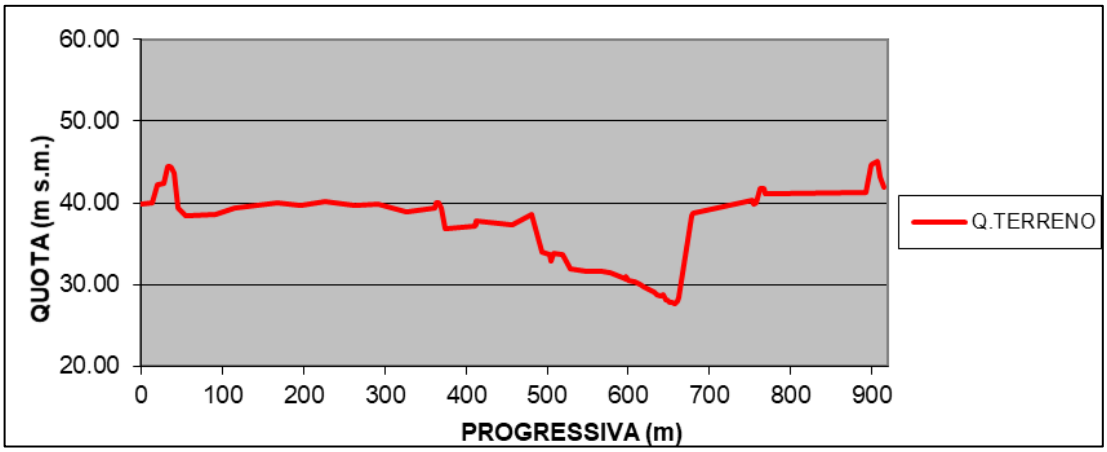

Figure 13 Example of Adda cross-section

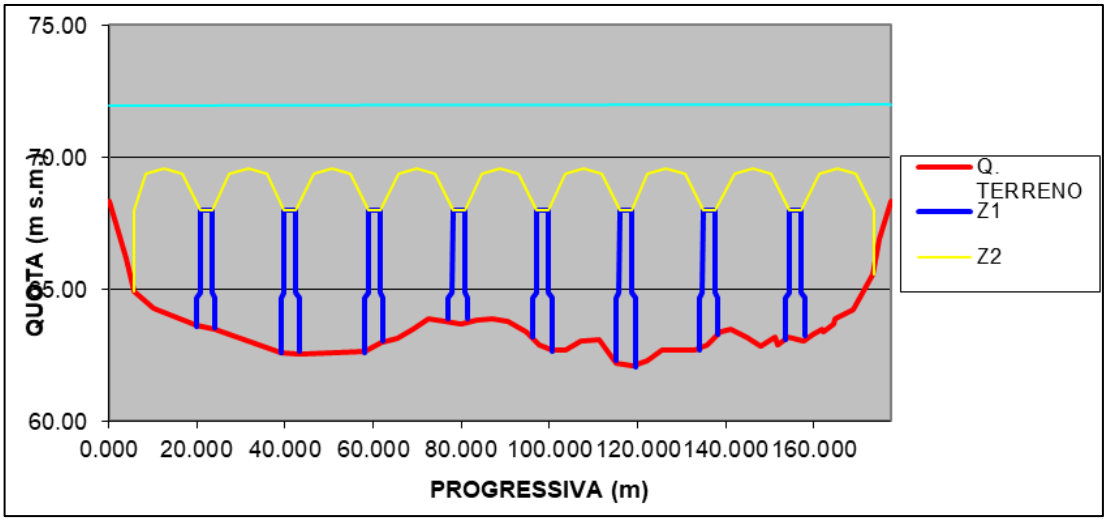

Figure 14 Cross section of the Napoleone Bonaparte bridge

DSM:

Digital Surface Model with the resolution of 10x10m is provided from AdbPo.

This data, after some modification that will be widely presented in chapter 3, it is used for modelling the terrain morphology of the study area.

Observed water levels:

Several water levels measured during the event are used in this work as reference for the computed results.

Available information consists of the combination of 3 different data sources:

- Observed water levels described in the damage compensation forms compiled by the citizens as well as reconstructions from photos taken during (or immediately after) the event; information on water depth are available for a total of № 260 georeferenced points.
- Water levels measured by the water gauge installed on the *Napoleone Bonaparte* bridge.

- Water levels reported in a previous study commissioned by the municipality of Lodi (№6) (Rossetti & Cella, 2010b).

In the following chapters it will be explained in detail why and how this data is useful for the calibration/validation of the hydraulic model.

Extension of the flooded area:

The flooded area of the event (Figure 15) is used as reference for the computed results of the hydraulic model developed in the work. This area was estimated in a previous hydrologic study (Rossetti & Cella, 2010b) of the event commissioned by the municipality of Lodi in 2005. This map includes additional information on water levels observed in 6 points inside the flooded area (yellow dots in Figure 15).

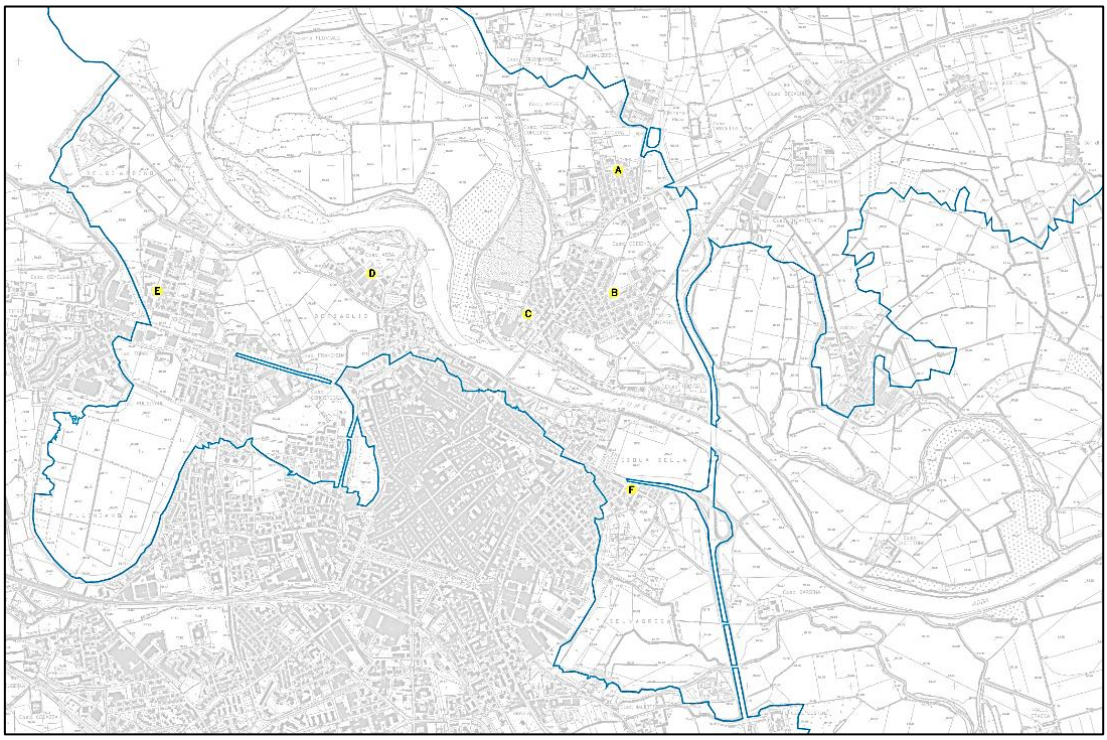

Figure 15 Estimation of the flooded area (Rossetti & Cella, 2010b)

Another area obtained from the municipality of Lodi is used as reference for the flooded area computed and to test the fast method. This area, commonly known as *fasce P.A.I.*, is provided by the AdbPo; this data, downloaded from the webgis site[9], is a shapefile representing the boundaries of a flood evaluated with a return period of 200 years.

[9] http://webgis.omnigis.it/omniwebgis/webapp.jsp?idUtente=comunale&codice_ente=E648 under the group "*Rischio idraulico"* (Hydraulic risk).

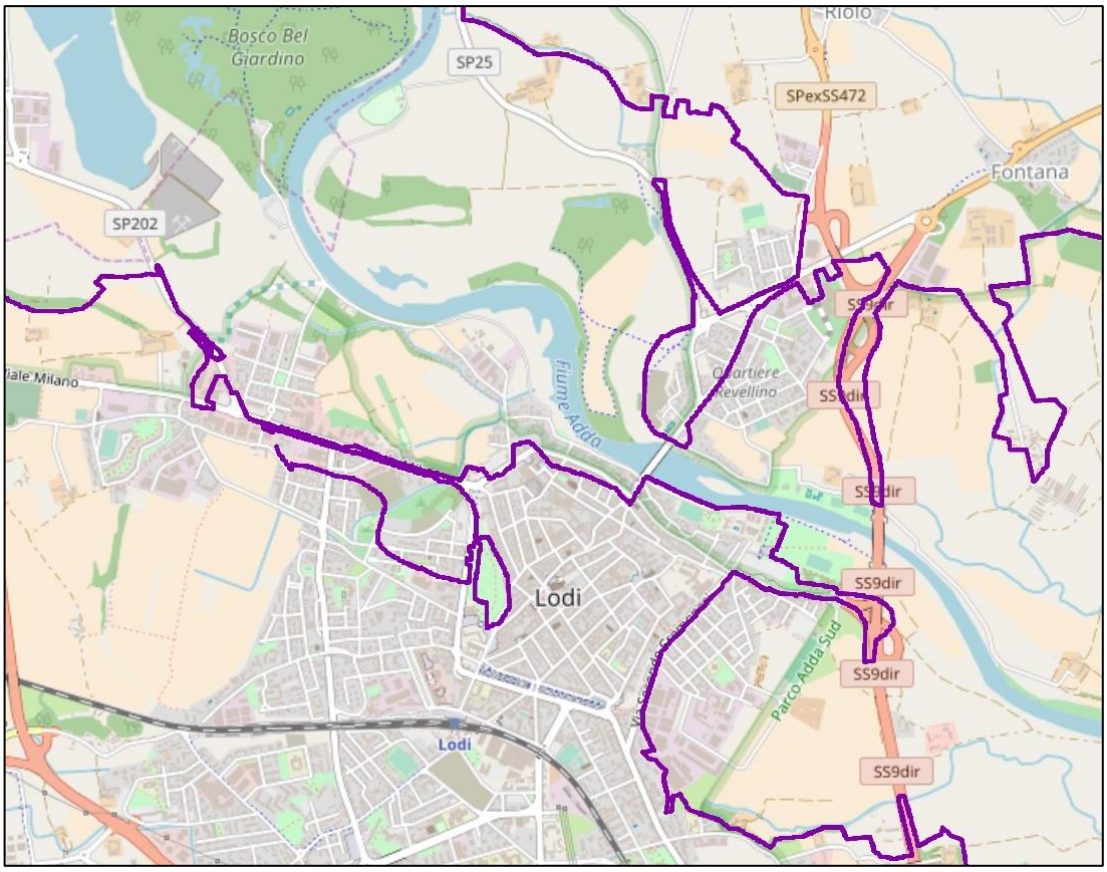

Figure 16 Fascia P.A.I. T=200 years

Hydrograph:

The 2002 flood hydrograph is provided by a former study (Natale, 2003) (Figure 17). In the first part of this work, the peak flow (1837 m^3/s) is considered to perform the steady analyses and the calibration of the model. Then, the whole hydrograph is used in the unsteady analyses.

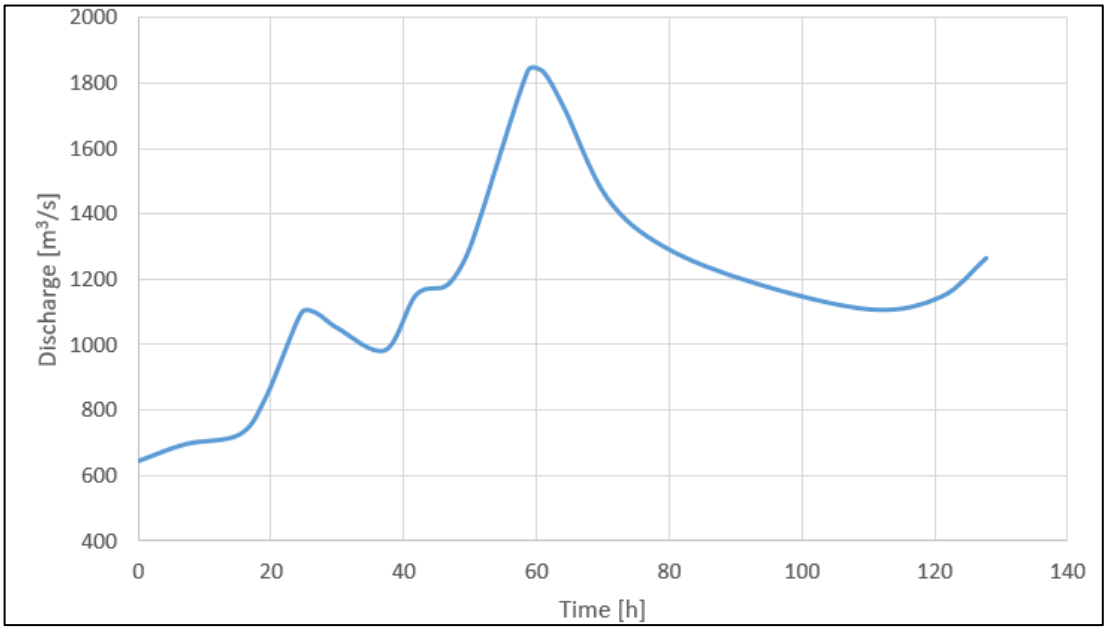

Figure 17 Discharge hydrograph

Photos:

Few photos of the event are collected from various sources (Civil Protection, Police, Municipality, Newspapers, etc). They are useful to extract, interpret data and to have a better overview of what happened.

Figure 18 Photo from the archive of the municipality

Other photos, videos, satellite images and orthophotos of current situation of case study area are collected with inspections and web research. All the collected data are useful in order to integrate incomplete or missing information.

Figure 19 Photo of drone survey

Newspapers:

Some articles are collected from the website of Flood-IMPAT+[10] project. These articles are useful to reconstruct what happened before, during and after the flood in case study area, also regarding to the point of view of the management of the emergency.

CHIUSE LE SCUOLE NEL CAPOLUOGO, PASTI CALDI AGLI SFOLLATI, SCONVOLGENTE SPETTACOLO IN CITTÀ BASSA CON CASE E CORTILI ALLAGATI

Lodigiano sconvolto dall'Adda

Cinquecento le persone evacuate in città, altre decine nella Bassa, danni ovunque
Ieri il livello è sceso dopo aver toccato la notte scorsa la quota record di 3,43 metri

Il giorno dopo la città ha colori grigi e il cielo che sembra voler concedere una piccola tregua a tutti quelli che stanno facendo i conti con la paura che non è ancora passata o con una casa allagata e una macchina che sembra una barchetta piantata in mezzo a un lago.
Il fiume ha toccato e superato la fatidica quota 800 (i tre metri di livello al ponte) che era considerata un limite quasi invalicabile, la soglia della "piena dei 200 anni": dopo una giornata passata con l'Adda che cresceva di 15 centimetri all'ora, all'1.30 di mercoledì, è stato raggiunto il livello storico di 343 centimetri. La città bassa è andata sott'acqua, le vie del Capannio, Lungadda, Ferrabini, Cavalletti, Massena, Borgo Adda e Defendente sono state evacuate, tremila le persone che sono state invitate a lasciare le abitazioni (cinquecento quelli che hanno dormito altrove, tra case di parenti o nel ricovero allestito dalla Croce rossa alla scuola media Spezzaferri dove erano stati preparati un centinaio di posti). Per tutta la giornata il numero degli sfollati è rimasto questo, anche se a disposizione per l'emergenza c'erano altre 800 brandine pronte per essere sistemate al palaCastellotti. Il fiume ha colpito duro anche nel resto del Lodigiano. Case devastate, argini abbattuti, corso del fiume modificato: si annunciano danni per milioni di euro.

Scatta l'evacuazione, a sinistra i gommoni dei vigili del fuoco in città bassa, a destra la gente che assiste ai soccorsi, proseguiti per tutta la notte, sopra un anziano portato in salvo

Figure 20 Article of a local newspape

[10] www.floodimpatproject.polimi.it

2 LITTERATURE REVIEW

The following chapter contains the literature review of the material that has been consulted and considered useful to develop the working procedure of the thesis. Different topics are discussed in each subchapter: after an introduction and a summary of the material available some useful conclusions are reported.

Analysed topics include:

- 2D flood modelling in urban areas;
- problem scale;
- sensitivity analysis of a hydraulic model;
- calibration of a hydraulic model;
- estimation of the water depth starting from the flooded area.

In the following parts, each topic is presented and analysed in detail.

2.1 2D FLOOD MODELLING IN URBAN AREAS

Introduction

The first article analysed (Alcrudo, 2004) regards the mathematical modelling techniques for flood propagation in urban areas, with the final aim to represent water depth and velocity distribution in the vicinity and around buildings.

In the second paper (Dottori et al., 2013), problems and precautions about 2D models are highlighted to aware modelers. In fact, it describes input datasets and model accuracy, two critical issues to understand the degree of precision of simulation outputs.

Literature review

The Navier-Stokes equations (NS) govern the 3D propagation of a flood. The determination of the solution can be compromised by turbulent flow, large size of the computational domain and long-time scale.

The problem of the turbulent flow is overcome by the introduction of the Reynolds-Averaged Navier-Stokes equations, which describe the mean flow by averaging the NS equations over time.

In any case, the resolution of 3D simulations is restricted to slow flow, that is a very different case from the one considered in this study.

The solution used to simplify the mathematical description consists in averaging the NS over depth, deriving the Shallow Water Equations (SWE). Another way to derive the SWE is the balance of the mass and the momentum on the flow direction.

The expression of the SWE is reported below:

$$\frac{\partial U}{\partial t} + \frac{\partial}{\partial x}(F + F_d) + \frac{\partial}{\partial y}(G + G_d) = H + I$$

where:

U is the variable vector;

F and F_d are the convective and diffusive vectors in the x-direction;

G and G_d are the convective and diffusive vectors in the y-direction;

H is the friction slope term, usually computed with empirical formulas (e.g. Manning's);

I is the infiltration source vector.

The simplification of the problem from 3D to 2D comes with the following approximations:

- velocity along the vertical direction is negligible;
- hydrostatic pressure field is considered;
- bed slope can be considered small enough to simplify the sinus of the angle with the angle itself;
- the velocity field in the horizontal direction is considered uniform;
- turbulence effects are negligible;
- friction formulations are taken from the uniform flow condition.

The resolution of the SWE equation is achieved with the methods of lines, where a space discretization is performed initially and then the ordinary differential equation is solved in time.

The space discretization can be completed in three ways: finite difference (FD), finite volume (FV), finite elements method (FEM). The second one is the most used strategy. The domain is subdivided in different finite volumes and the integral form of the SWE is applied to each one of them. One important gain of this method is that it assurances the conservation of the mass and momentum.

FV method can be applied on structured and unstructured grids. To get advantage of both grid types, the Quad-tree grid is used. The particularity of this grid type is that the initial layout is cartesian and, to reach the required resolution of some parts of the flow field, the grid refining procedure consists in the subdivision of only few cells.

To deal with urban flooding different techniques are proposed:

- 1D treatment of the city area, that can be represented as a channel network: this solution provides local flow information at low computational cost, but unfortunately it suffers from problems at junction nodes where the flow can be predominantly 2D. The expression of the SWE is $\frac{\partial U}{\partial t} + \frac{\partial F}{\partial x} = H + I$ where each term has the same meaning as the 2D case. The equation is solved numerically if boundary and initial conditions are provided.
- Local 2D friction-based representation of buildings and obstacles: the main difficulty of this model lies in the determination of the roughness coefficient to be used to properly represent obstacles. To use the most appropriate value, a calibration procedure must be performed. Another problem is that in this case the buildings are considered as storage tanks, which is in general not true.
  An example is presented below.

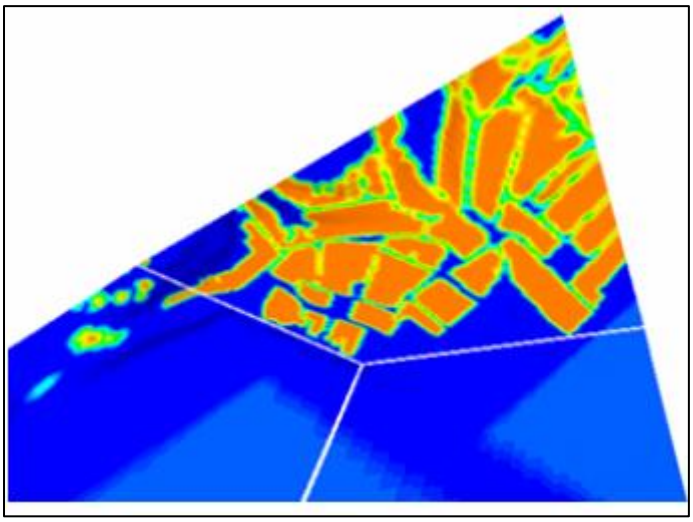

Figure 21 Example of friction-based representation of building (Alcrudo, 2004)

- 2D bottom elevation technique to represent buildings: this approach consists in increasing the height of the points that are inside a building area, with the adaptation of the mesh needed to have a clearer representation of the city. The main problem of this method is that it violates one of the above defined approximations of the SWE model, i.e. mild bed slope. However, this does not cause the model to fail, because the obstacle acts as an internal boundary causing water stagnation. Hence water around the obstacle can still be considered shallow. An example is presented below.

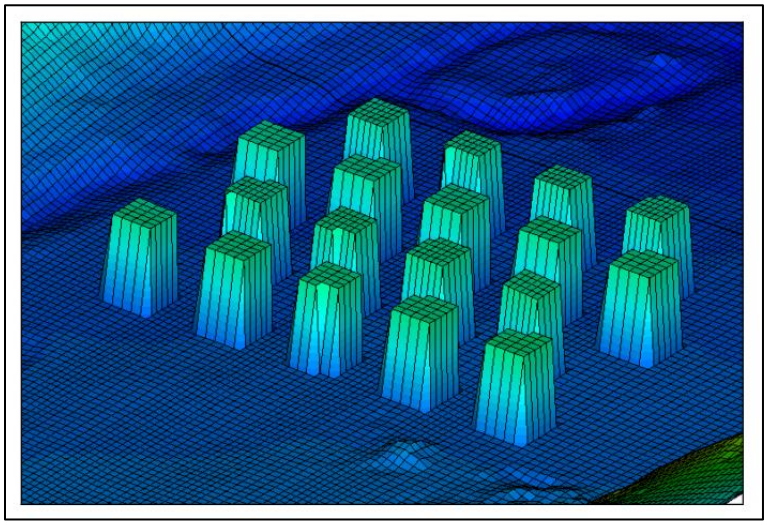

Figure 22 Example of bottom elevation technique to represent buildings (Alcrudo, 2004)

- 2D vertical wall representation of the buildings: this technique consists in excluding the buildings from the computational domain. Even though it is the most precise way to represent a city, this meshing procedure can be extremely complex, increasing significantly the computational cost. A mesh example is represented below.

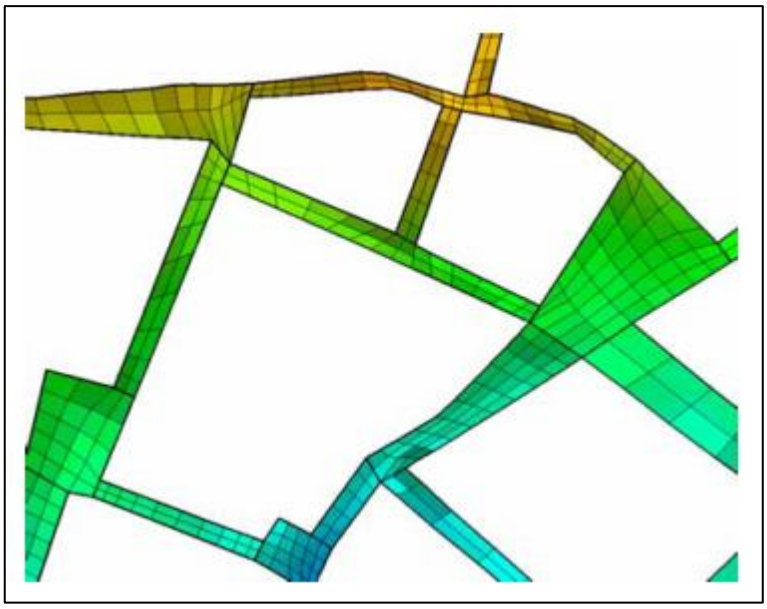

Figure 23 Example of 2D vertical wall representation (Alcrudo, 2004)

The second paper (F. Dottori et al., 2013) considered in this review presents several important topics related to flood modelling that should be taken in consideration by modelers.

In addition to internal uncertainty and weaknesses in model structure, uncertainty in model's input data can have important influence on the simulated dynamic of the flow. These include:

- topographic data, which can be the most relevant source of uncertainty;
- incorrectness or imprecision in boundary condition data (e.g. inflow magnitude and position);
- interaction with drainage systems (e.g. surface and underground drainage systems, often down during floods);
- interaction of smaller scale water flows;
- interaction of buildings with flow pattern;
- solid erosion and sediment transport, which can alter the morphology of the area under investigation and affect flow properties;
- digital surface model (DTM) errors.

These factors should be assessed, before and, in some cases, after running the simulations, that means performing a kind of sensitivity analysis.

Another problem for 2D modelling is the lack of consensus on the accuracy and reliability criteria.

Despite the increasing accuracy of the DTM resolution, observed datasets (e.g. direct flood depth measurements or satellite images about extension of the event) are usually affected by relevant uncertainties. These measurements, if available, can be very useful for the validation of the model or to assess its accuracy. An alternative can be the **measurement of high water marks,** but these are generally affected by a vertical **precision of 50 cm**. While flow velocity measurements during a specific event are almost impossible to find.

The optimal grid scale is still under discussion in the scientific community: several authors (Schubert et al., 2008; Fewtrell et al., 2011, Schubert and Sanders, 2012) agree that mesh size should be related to the average dimension of buildings and roads. In any case, the choice should accomplish the best compromise between:

- detail;
- maximum expected accuracy (it depends more on available input data than mesh resolution);
- computational efficiency.

Furthermore, extreme resolution of data and models may create false confidence in the precision of the model. Therefore, modelers should pay particular care in communicating the uncertainty, considering the different requirements of end users. About this topic, a series of methods are available which can be used to integrate high precision data into models with a good balance between reliability and efficiency. When doubling the grid resolution, the processing time may increase by a factor of about 10. In any case, availability of this high-resolution topography is still limited to specific areas in developed countries.

Conclusions

Form the literature review analysed above the equations used to model the flood propagation in urban areas have been presented in detail. Moreover, the available techniques used to represent buildings have been explained; all of them can provide a reasonable picture of the urban inundation process. The vertical wall method can provide the most accurate results, but the computational effort is considerably higher than that required by other methods. The bed friction approach is the easiest to use but the estimation of the roughness coefficient can be very complex.

In their work, modellers must deal with various problems that can affect the reliability of the results. A broad analysis of the case study should be done every time before choosing the input data and method to use, keeping in mind that result accuracy is not necessarily increased by higher resolution. Once the purpose of the work is completed, results should be provided with a measure of reliability, but it is difficult to describe accuracy and precision of a model without a comparison with real measurement.

2.2 SCALE OF THE PROBLEM

Introduction

Availability and quality of data is fundamental to obtain good and reliable results. Accuracy and computational time are a controversial topic. The method to represent reality may change depending on the scale of the problem and the precision required.

In literature, dozens of different approaches to model urban areas can be found varying from the micro to the macro scale, with different types of resolution.

Three different scales to model the scenario are analysed hereinafter, with their expected precision and associated problems.

Literature review

Firstly, it is examined an article (Bazin et al., 2017) whose aim is to model obstacles of a size smaller than that of a building, usually neglected. The authors believe that obstacles such as bus-stops, trees or parked cars may strongly modify the flow pattern. Consequently, they try to simulate the impact in the crossroad of obstacles and sidewalks using a 2D operational numerical model with a very simple turbulence model. The software used to model this single crossroad with a mesh of 3.5/5 cm is “Rubar20[11]”. The authors model few scenarios comparing the results to those obtained with a physical model performed in laboratory.

The results highlight the high accuracy of the method, with an error around 2% for the case without obstacles; the model can also predict the effects of an obstacle such as deflection, contraction accelerations and discharge distribution with an average error of 3%.

[11] www.irstea.fr/rubar20

In some experiments, when there is the formation of hydraulic jumps or when obstacles are positioned in the upstream part of the domain, errors may be larger. The problem can be solved increasing the mesh resolution, but this approach is too costly for large urban areas.

A key point highlighted by the authors is to take in consideration the uncertainty of other parameters such as hydrograph or rain in the computational domain; these inaccuracies can generate higher levels of errors.

In conclusion, in urban flood flow modelling, when obstacles of smaller dimensions are neglected errors should be smaller than 10%. The decision to choose a detailed approach or not depends on the order of magnitude of the other sources of uncertainty, i.e. the number, size and location of the obstacles and, finally, the data availability on obstacles. The **improvement of details is useless if the order of magnitude of other uncertainty sources is higher.**

Secondly, a mesoscale work is analysed (Ozdemir et al., 2013). In the paper, a new inertial formulation of the St. Venant equations is applied. This method is implemented within the LISFLOOD-FP[12] hydraulic model, using different high resolution terrestrial LiDAR data and roughness conditions in urban areas.

The case study is an inundation in Alcester, UK, where an entire neighbourhood is modelled with a terrestrial LiDAR with a 10 cm resolution.

In order to evaluate scale and roughness effects on urban surface flood modelling, different resolution DEMs produced from terrestrial LiDAR data and Manning's n data are prepared before applying the new inertial model. The resolution of DEMs are:

- 10 cm;
- 50 cm;
- 1 m.

The model prediction of water depths, flood extent and flow velocity are evaluated against the relevant benchmark high-resolution (10 cm terrestrial LiDAR DEM).

Results:

- The biggest differences in computed flooded area are registered among 1 m and 10 cm mesh with distributed roughness quantified on 10% of deviation.
- Maximum water depths and velocity are shown to increase by up to 37 and 32% respectively with increasing DEM resolution, whilst inundation extent is shown to decrease by approximately 6 %.
- Surface water inundation is more rapid with a composite friction and finer resolution models because the surface is smoother.
- Increasing the terrain resolution from 1m to 10 cm significantly affects modelled water depth, extent, arrival time and velocity.

Consequently, DTM resolution and different friction conditions affects:

- the water depth;
- inundation extent;
- arrival time;
- velocity;

On the contrary flood extent is less sensitive to surface friction configuration.

In conclusion, the micro scale terrain structures are relatively more important to flood wave development because they generate or stop the flow better than friction. Unluckily, simulation at 50 cm scales remains computationally expensive even using efficient software, so the authors suggest that future research should focus on increasing the efficiency of such models as well as developing techniques.

[12] www.bristol.ac.uk/geography/research/hydrology/models/lisflood

A last article, dealing with a macro-scale event (Beretta et al, 2018), has been chosen to complete this review.

In this work, authors analyse three different approaches to better model the flood in an urban area. The zone considered is near Olbia, hit by a severe flood in 2013.

Different methods to simulate the effects of buildings in an urban area during a flood are tested and compared to a scaled model in laboratory.

The crucial elements are the availability of complete and detailed information about the geometry of buildings and anthropic infrastructures in the domain. In this work diffusive wave equation and different methods to represent urban area are tested to make up for the lack of detailed DEM. In particular, the aim is to verify the precision of the roughness approach instead of the buildings insertion method.

HEC-RAS software and "FEST hydrological model[13]" have been used to model the experiments in laboratory and to reproduce the hydrographs of the real event.

In the laboratory experiment six bricks have been used to simulate the presence of a small urban area, while in the software model three different methods have been considered:

1. insertion of buildings using a high-resolution DEM (1 cm);
2. representation of buildings with a very high roughness (n=10 [$s/m^{1/3}$] - K_s=40[m]);
3. representation of the urban area by using a high roughness (n=0.15 [$s/m^{1/3}$] - K_s=15 [m]).

The results of the comparison between scaled-experiment and simulation show that the three methods are equivalent for the representation of water depth (max SD=0.11 cm), while method number 3 cannot represent velocity distribution in a plausible way, because it does not consider flow dynamics inside the urban area.

Finally, the real event occurred in Olbia is simulated using the approach 2 as the best compromise between errors and because approach 1 requires detailed topography that is not available for the case study. Method 3 is not used because it is considered more reliable for flood simulation with extended areas and with many urban zones, a different configuration from the case study.

Conclusions

The above literature review ranges from micro to macro scale with a resulting precision ranging from high (mm) to coarse (cm/dm), respectively. Availability of detailed data, required precision, efficiency and computational time are fundamental aspects influencing the choice of the approach and the software to use.

It is important to underline that is useless to improve details if the order of magnitude of other uncertainty sources is higher.

[13] www.fest.polimi.it

2.3 FLOOD MODELS CALIBRATION PROCEDURE

Introduction

The calibration of a model is the procedure that searches for the best possible representation of natural flow for a model. It also compensates for model insufficiencies and errors, which are unavoidable (Cunge, 2003).

The papers presented below are examples of multi-objective automatic calibration procedures for a large-scale model and the presents the most used objective functions.

Literature review

The first article (Dung et al., 2011) shows a 1-dimensional hydrodynamic model of the whole Mekong Delta, downstream of Kratie in Cambodia. The used flood model relies on the software MIKE 11[14]. The database used for the study includes water level time series from a network of gauging stations and some flood extent maps derived from ENVISAT ASAR satellite images.

The automatic calibration presented in the paper consists in automatically adjusting 5 different roughness parameters according to a specified procedure that optimises numerical measures of goodness-of-fit.

A multi-objective calibration problem is defined as an optimization problem over several objective functions. Its solution is not a single parameter but involves a set of Pareto-optimal solutions, which are the best solutions from a multi-objective prospective.

Generally, to solve the optimization process three approaches can be performed: the weighted sum approach, Pareto-ranking approach and genetic algorithms. In the study of Dung et al. (2011) the NSGA II algorithm is used. The stopping criteria used consist in setting a fixed number of loops, 30 in this case.

The objective functions are:

- F_1: it uses the Nash-Sutcliffe model efficiency coefficient, with a weight that indicates the importance given to a certain location of the network of gauging stations. This weight minimizes the effect of the ocean tides.
- F_2: it evaluates the spatial performance of the model in predicting flood maps utilizing a series of inundation extent maps.

$$F_i^M = \frac{P_i^{11}}{P_i^{11} + P_i^{01} + P_i^{10}}$$

where:

P_i^{11} is the number of pixels for which simulation and observation indicate “wet”;

P_i^{10} is the number of pixels for which observation indicates “wet” and simulation indicates “dry”;

$P_i^{01}$is the number of pixels for which simulation indicates “wet” and observation indicates “dry”.

One of the most important deficiencies of this indicator is the bias towards large inundation extent.

To calculate the second objective function, the F_i of the individual extent maps are combined with a weighted sum. In case of maps which cover partially the area of interest a lower weight is assigned.

[14] www.mikepoweredbydhi.com/products/mike-11

Since the objective functions have different scales, it is important to normalize their value. The whole calibration process lasted about 300 h.

The second article (Legates & McCabe Jr., 2005) discusses the topic of “goodness-of-fit” or relative error measurements, which are very important because they are useful to determine how a model fits the observed data.

Three basic methods are considered:

- Coefficient of determination (R^2): it describes the proportion of the total variance in the observed data that can be explained by the model. It ranges from 0.0 to 1.0 (higher value indicates a better agreement). Its expression is:

$$R^2 = \left\{ \frac{\sum_{i=1}^{N}(O_i - \bar{O}) \times (P_i - \bar{P})}{[\sum_{i=1}^{N}(O_i - \bar{O})^2]^{0.5}[\sum_{i=1}^{N}(P_i - \bar{P})^2]^{0.5}} \right\}^2$$

  where:

  - O_i are the observed values;
  - $\bar{O}$ is the average of the observed values;
  - P_i are the predicted values;
  - $\bar{P}$ is the average of the predicted values;
  - N is the total number of the values;

  The limitation of the R^2 parameter is that it standardizes for differences between the observed and predicted means and variance, because it only assesses linear relationship between variables.

  Large value of R^2 can be gained even with the model-simulated values very dissimilar in terms of magnitude and variability. In addition, correlation measures are more sensitive to outliers than to observations near the mean. This oversensitivity leads to a bias towards the extreme events if correlation-based measures are employed in model evaluation.

- Coefficient of efficiency (E): defined by *Nash and Sutcliffe [1970],* it varies from -∞ to 1.0, with higher values indicating better estimation of the predicted values. Its expression is:

$$E = 1.0 - \frac{\sum_{i=1}^{N}(O_i - P_i)^2}{\sum_{i=1}^{N}(O_i - \bar{O})^2}$$

  A value of 0.0 for the coefficient E indicates that the observed mean $\bar{O}$ is a good predictor as the model, while negative values indicate that the observed mean is a better predictor than the model.

  Because of the terms with squared differences, E is very sensitive to extreme values.

- Index of agreement (d): defined by *Willmott [1981],* it ranges from 0.0 to 1.0, with higher values indicating better agreement between the predicted values and the observed ones. Its expression is:

$$d = 1.0 - \frac{\sum_{i=1}^{N}(O_i - P_i)^2}{\sum_{i=1}^{N}(|P_i - \bar{O}| + |O_i - \bar{O}|)^2}$$

  The index of agreement is considered an improvement compared to the coefficient of determination, but it is sensitive to extreme values as well.

The over sensitivity of E and d results in high values of both statistics, thus a more generic index of agreement could be developed as:

$$d_j = 1.0 - \frac{\sum_{i=1}^{N}|(O_i - P_i)|^j}{\sum_{i=1}^{N}(|P_i - \bar{O}| + |O_i - \bar{O}|)^j}$$

Of interest is d_1 , known as modified index of agreement, whose benefit is that errors and differences are given their appropriate weighting, not magnified by their squared values.

The same adjustment can be done also on the coefficient of efficiency:

$$E_j = 1.0 - \frac{\sum_{i=1}^{N} |(O_i - P_i)|^j}{\sum_{i=1}^{N} |(O_i - \bar{O})|^j}$$

Instead of the average observed values, some methods define the baseline against which a model should be compared. Thus, both E_1 and d_1 can be rewritten in baseline adjustment form substituting $\bar{O}$ with $\bar{O}'$, defined as the baseline value of the time series against which the model is to be compared.

Even though the described indicators are dimensionless measures, the modellers should not rely completely on them. In fact, it is also suggested to quantify the error in terms of the units of the variable. These measures include the square root of the mean square error and the mean absolute error. Other procedures such as the slope and intercept of the predicted-versus observed regression line are pretty useful for this.

To conclude, a complete assessment of model performance should include at least one "goodness-of-fit" and at least one absolute error measure that provides supplementary information.

Conclusions

An example of calibration of flood model and some tools to assess the goodness-of-fit of the model to simulate reality have been reported in the above literature analysis.

The automatic calibration technique defines a methodology that can be exploited even manually in less complicated cases. It consists in the maximization of two objective functions, one regarding the depth and the other the flooded area.

However, the objective functions analysed have some drawbacks. The coefficient of efficiency (F_1 or E) is overly sensitive to extreme values, while the coefficient that evaluates the spatial performance of the model (F_2) bias towards large inundation extent.

A proposed solution to solve the problem of the coefficient of efficiency consists in the introduction of the modified coefficient of efficiency (E_1'). Unfortunately, the spatial extent indicator has no proposed corrections and it is still considered the basic measure used and recommended for deterministic calibration.

The last indication that can be deduced from the analysis is that the statistical coefficient should not be used exclusively in the calibration procedure. In fact, a quantification of the error in terms of units of the variable should be used.

2.4 SENSITIVITY ANALYSIS

Introduction

Sensitivity analysis (SA) is the procedure that determines how the uncertainties of the output of the model can be due to uncertainties in the input of the model (Lilburne & Tarantola, 2009).

The following literature review summarises the most common available approaches, focusing on the limitations arising during the sensitivity analysis of a spatial model.

Literature review

It is common knowledge that models are hindered by uncertainties, which may be related to input data, due to error in the measurements, unknown parameters or scaling errors. The SA can provide a wider understanding of how outputs of the model respond to variations in the inputs.

Before introducing the approaches, the difference between sensitivity and uncertainty analysis must be stated. The first one regards the study of how the uncertainty in the output of the model can be appointed to model inputs, meanwhile the latter one is about the quantification of the magnitude of the uncertainty in the outputs of the model, due to uncertainty in the inputs.

Most of the SA techniques consist in running the model many times in a Monte Carlo approach, but in case of temporal and spatial inputs, this procedure can become problematic because of the long computational time needed. Therefore, SA of spatial model is often ignored or relatively limited.

The possible methods for the SA are:

- Local sensitivity analysis: its aim is to determine the rate of change in the output of the model due to small variation in the uncertain input. This quantification is spatially dependent, therefore the result of the SA can be influenced.
- Global sensitivity analysis: it considers the full range of uncertainty of the input, which is characterised by its joint probability density function. In this method all the inputs are varied simultaneously, and multi-dimensional averaging technique is used to quantify interactions among them.
- Regression based approach: “a linear regression model linking the inputs to the outputs is fitted to the available points obtained from the Monte Carlo simulation” (Lilburne & Tarantola, 2009); to obtain the regression coefficients ordinary least squares is used.
- Variance-based methods: they compute the sensitivity indices regarding the assumptions on the intrinsic model. The total variance of the model V is decomposed in the share of variance V_i that is due by each model input.

  The Sobol’ method is a variance-based approach that provides a computational strategy to estimate V_i term used to compute:

  - the first-order sensitivity indices with the expression $\widehat{S_i} = \frac{\widehat{V_i}}{\widehat{V}}$;
  - the total-effect indices with the expression $\widehat{S_{Ti}}$

In case of models with spatially distributed outputs, an appropriate scalar objective function must be selected. The sensitivity analysis will be based on this number.

The approaches that can be used to simplify the spatial model sensitivity analysis are summarised in the next table (Figure 24), (Lilburne & Tarantola, 2009). It contains the technique name with the advantages and disadvantages related to the spatial sensitivity analysis.

Conclusions

From the literature review performed above it can be understood that between all the SA techniques, only some of them are suitable for the spatial models. In particular:

- the OAT (one at time) approach is the most common one even if it can lead to an unprecise SA;
- the Sobol' approach has the big advantage of making no assumptions about the model.

Having said that, it is clear that the model used to perform the SA must be chosen according the computational power available and the application scope.

Technique	Advantages	Disadvantages	Computational demand
OAT	Simple	Local SA only Results reliable only if the model is linear	Very low
Morris	Can work with large models Computationally cheap	Results are less accurate than the SA methods below Sample generation is not straightforward	Low
Regression	Simple and straightforward	Results depend on goodness of fit of linear response model Input parameters should be independent Does not handle spatially variable inputs	Moderate
Random balance design	Model independent	First-order effects only Not applicable when parameters have discontinuities Input parameters should be independent Does not handle spatially variable inputs	Moderate
Classic and extended FAST	Model independent Total-effect indices (only for extended FAST)	Not applicable when parameters have discontinuities Input parameters should be independent Does not handle spatially variable inputs	High
Winding stairs/Jansen	Model independent Total-effect indices High-order interactions Can have spatial input that is auto-correlated Spatial structure included in SA	Input parameters should be independent Specific sampling strategy required (usually winding stairs)	High
Sobol'	Model independent Total-effect indices High-order interactions Extension (using symmetries) makes this more efficient Can have spatial input that is auto-correlated Spatial structure included in SA	Input parameters should be independent Specific sampling strategy (usually quasi-random points)	High
Importance measure	Model independent Works with dependent inputs Can have spatial input that is auto-correlated Spatial structure included in SA	Specific sampling strategy (usually replicated Latin Hypercube) First-order effects only Computationally demanding	Very high

Figure 24 Summary of the approaches that can be used to simplify SA of spatial model

2.5 ESTIMATION OF WATER DEPTH IN A FLOOD EVENT WITH LOW DATA AVAILABILITY

Introduction

Nowadays, many organizations provide early flood information such as the extent of a flooded area given by satellite remote sensing. This near-real-time information do not provide floodwater depth, an important attribute for first responders, flood risk policymakers and damage assessment (Cohen et al., 2017).

Hydraulic models are commonly used to simulate flooding events, but to work properly this software require a lot and detailed information about the event (hydrograph) and riverine/floodplain morphology (DTM, roughness parameter, bridge geometry, etc…). Accurate simulation of a flood event is often time consuming and requires extensive data compilation and calibration.

Based on the following literature review, some authors proposed a solution for this problem with a new methodology based on GIS software. This method provides information about water depth in urban area based only on an inundation map and a digital elevation model.

The aim of the authors is to bypass the hydraulic modelling and compute, in a fast way, the water depth distribution (which is the most relevant factor for the damage estimation in an urban area), starting from *fasce P. A. I.* or from the observed inundation perimeter of a flood event.

All the studies performed by the authors are compared with a real event with a consequent discussion of the results.

Analysis of the literature

In the first two works (Gatti & Sterlacchini, 2016; Pastormerlo & Zazzeri, 2016) a new method called SWAM (*Surface Water Analysis Method*), is described in detail. This method is implemented in GIS environment, with the “Model Builder” tool (MB). The MB is a visual language of programming that uses the tools available in ArcGis, with the aim of automatizing the procedure and speed up the process.

The method is based on 2 fundamental hypotheses (HP):

- the external boundary of the flooded area represents the locus of points where the water depth is nil (i.e. *tirante idraulico =0*);
- the extreme symmetric points, positioned on the perpendicular line to the river, have comparable water surface elevation.

In an urban context, the first HP is not always verified. Because there are cases in which the perimeter is delimited by an artificial infrastructure like a wall. Therefore, the water depth at the boundary can be different from 0.

Also, the second HP can be not verified because of water deviation or channelling.

In the first work the authors start their method from the observed perimeter obtained with aerial photos taken during the event occurred in the Umbria region in 2012. They use 2 DTM, 20 m and 1 m resolution, respectively. Both of them are used to compare how the resolution of the DTM can influence the results. But firstly, to validate the model, a previous hydraulic model is used as reference.

Once the model is validated, to have an additional comparison, the results of the real case are computed using SWAM and a hybrid tool (1D and 2D) r.inund.fluv. available in the software GrassGis[15].

Before running the model, the boundary is manually corrected in order to fix evident errors.

The procedure followed in both validation and computation of the real event is here schematized.

- manual correction of some evident errors in the flood boundary;
- the elevation of the DTM is assigned to the polyline boundary with a GIS tool.
- using the 3D boundaries obtained before, a TIN (triangular irregular network) is created obtaining a surface (water surface elevation);
- the TIN is converted in a raster with two different methods: Linear interpolation and Natural neighbours;
- the surface obtained is clipped with the flood boundary;
- the DTM is subtracted to the water surface elevation (WSE) obtaining the water depth (WD).

From the second step the 20 m resolution DTM is abandoned due to evident errors and detailed comparison is performed between the different methods of interpolation.

The comparison between the SWAM method and the more complex and longer hydraulic one, gives back how this method has a low computational effort and a high accuracy for a non-urbanized area.

The second work is focused on the evaluation of the water depth for the assessment of exposure and damage.

The method used is called SWAM 2.0, a simple modification of the method explained before. The aim of this improvement is to avoid the appearance of triangular geometry characteristic of the TIN tool. Instead of creating the surface from a three-dimensional line, the lines are sampled into 3D points, and from this data an interpolation is directly performed.

In this situation the case study chosen is the flood occurred in Olbia (Sardinia region - Italy) in 2013.

Two different perimeters and different types of interpolation are used to compute the results.

Another major change is the introduction of measured water depth values. These are used to force the interpolation process and obtain more precise results.

The computational time needed is also exalted by the authors, a remarkable improvement is determined by adding the so called forcing points (*punti forzanti*).

The resulting best interpolation method is again “natural neighbour”.

In the last article, (Cohen et al., 2017) present another similar procedure *called Floodwater Depth Estimation Tool* (FwDET), based on the same hypothesis explained in the beginning of this section.

In this method instead of using 3D line or points, the boundaries of the flood event (coming from remote sensing) are transformed into a raster and the value of the DTM is assigned to each cell. The main difference is the type of method used to assign the boundary cells elevation to the domain cells: in order to do it, a tool called “focal statistic” is chosen. This tool

[15] GRASS GIS, commonly referred to as GRASS (Geographic Resources Analysis Support System), is a free and open source Geographic Information System (GIS) software suite used for geospatial data management and analysis, image processing, graphics and maps production, spatial modelling, and visualization. GRASS GIS is currently used in academic and commercial settings around the world, as well as by many governmental agencies and environmental consulting companies. It is a founding member of the Open Source Geospatial Foundation (OSGeo) - https://grass.osgeo.org/

assigns the elevation of the nearest boundary cell with a circular “focal statistic” neighbourhood to smooth the solution; A loop is used to fill all the domain. This is a sort of interpolation but more controlled.

As in the previous two methods, the raster representing the water surface elevation is clipped and subtracted to the DEM to obtain the water depth. In addition, this last raster is smoothed with the command Filter and with the option “low pass” selected.

The FwDET is applied on 2 different case studies in Texas and Colorado using respectively a 10 m and a 1 m DTM and compared to model-simulated water depth prediction.

While the method is applied on 2 different scales and with 2 different DTM, the results show that the main differences, evaluated with the RMSD are around 40 cm. In the work, authors describe how the most extreme overestimations calculated by FwDET method are along the banks of the main river channel; these are due to **the inability of this method to calculate fine-scale fluid dynamic effects**.

Conclusions

In all three works a manual quality control and correction of the data is necessary and an appropriate DTM resolution selection is needed to produce the best estimation; a calibration s often necessary.

For the moment SWAM and FwDET methods, due to the low quality of data, discrepancy between boundary and DSM and his primordial state, is not considered a valid replacement for the traditional hydraulic modelling procedure.

Anyway, due to the very low computational effort needed, this procedure seems to be a good tool to assess, immediately after the occurrence of a flood, the water depth and consequently obtain a first estimation of the damages occurred.

3 METHODS USED FOR THE FLOOD MODELLING

3.1 DEVELOPMENT OF THE DIGITAL TERRAIN MODEL

The starting point to create the digital terrain model to be used in the hydraulic simulations is a DTM provided at the beginning of the project; this one is already a modification of the DSM 10 m x 10 m provided from AdbPo[16].

The resolution of this “initial” DTM is 10 m X 10 m

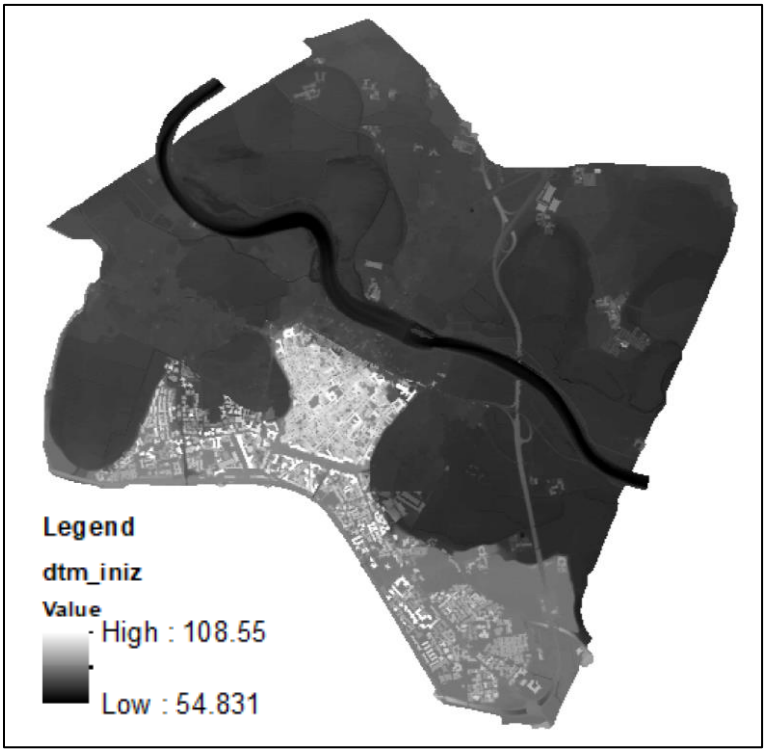

Figure 25 Initial DTM provided by AdbPo

Firstly, it is important to define what a DTM is and which are the differences between DTM and DSM. DTM is an abbreviation for digital terrain model, it describes the bare-earth terrain with uniformly-spaced Z values, as typical of a raster (Heideman, 2014a); meanwhile DSM, abbreviation for digital surface model, it similar to the DTM except that also elements above the terrain (houses, trees) are represented (Heideman, 2014b).

[16] www.adbpo.it/on-multi/ADBPO/Home.html

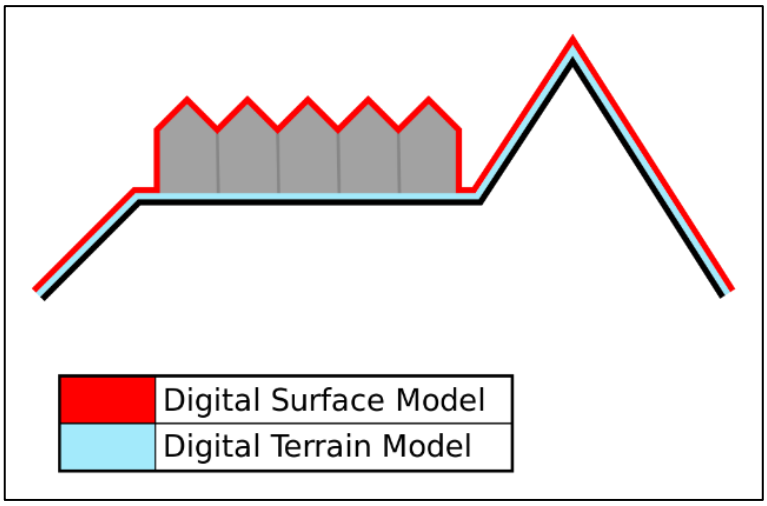

Figure 26 Difference between DSM and DTM

The given DSM in the beginning of the study contains many corrections regarding the height of the buildings, but some of them are still needed to be corrected.

To determine where the corrections must be applied, a 3D digital elevation model is created and placed in the following;

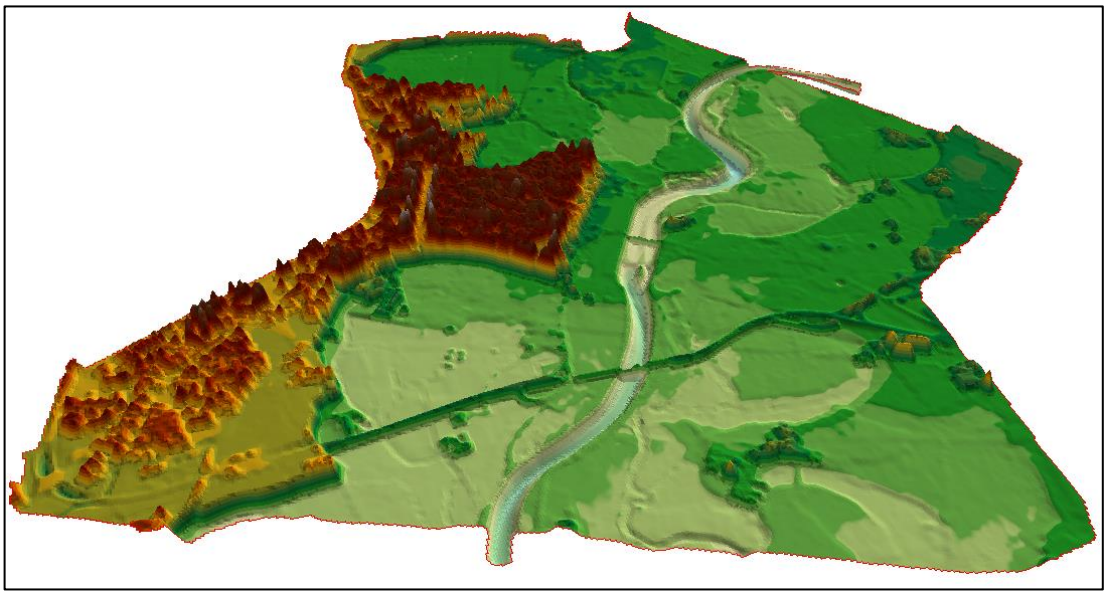

Figure 27 3D DTM of the city of Lodi

The 3D digital model and some ground surveys are useful to produce the map of the area that must be corrected. The following picture represents the DTM provided at the beginning of the work, where the highlighted regions represent where the most important modifications are performed.

Figure 28 Modification performed on the initial DTM

It is important to remember that the corrections are applied only inside the perimeter of the potentially flooded area of the 2002 event, because outside elements are irrelevant for the simulation.

The main changes that are introduced were located:

- **Near the highway bridge** (*ponte della nuova tangenziale di Lodi*): since the model of the terrain available is a DSM modified, some elements like bridges must be modified to allow water flowing under them, otherwise they would act as permeable wall.

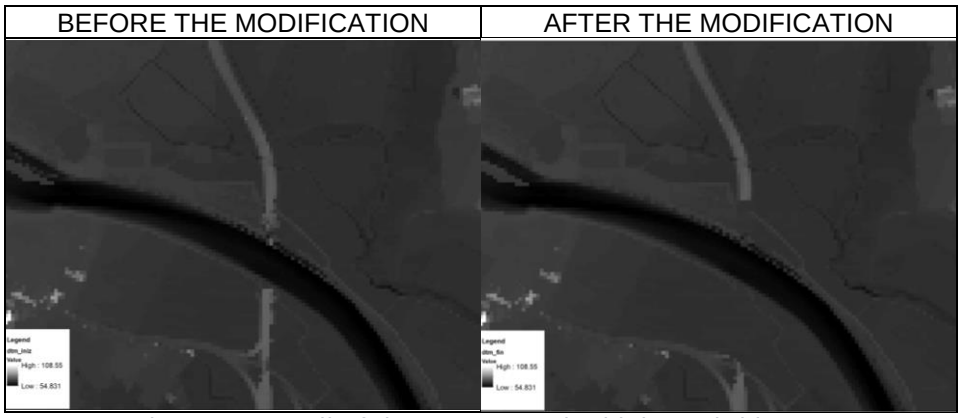

Figure 29 Detail of the DTM near the highway bridge

- **Area of Revellino district, between Via Lungo Adda Bonaparte and Via Borgo Adda and between Via Enrico Mattei and Via Defendente Lodi**: in this area the buildings are lowered to consider the altitude of the terrain. This is

accomplished considering the altitude of the roads near the buildings and performing a linear interpolation for the pixels between two roads.

Revellino district	
BEFORE THE MODIFICATION	AFTER THE MODIFICATION
	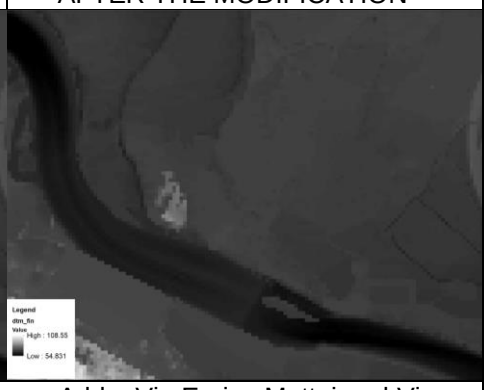
Via Lungo Adda Bonaparte and Via Borgo Adda, Via Enrico Mattei and Via Defendente Lodi	
BEFORE THE MODIFICATION	AFTER THE MODIFICATION
	

Figure 30 Up: detail of the DTM near the Revellino district. Down: detail of the DTM near the city

- **Ditches Gaetana and Gelata**: Lodi is characterized by an extensive network of ditches, with some of them tunnelled in the past. Reports explain that the inundation of some districts of the city was mainly due to water coming out from the ditches and not from a direct flooding of the Adda. To consider this, the most important ditches are "excavated" in the DTM in order to simulate their effect in the inundation process.

BEFORE THE MODIFICATION	AFTER THE MODIFICATION
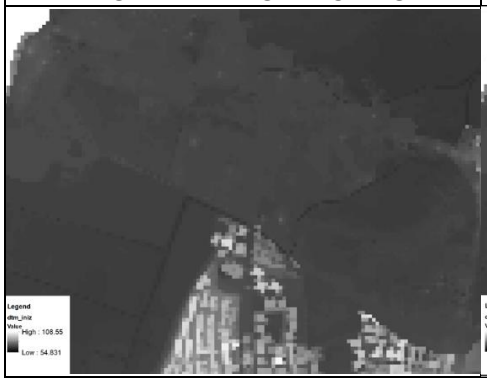	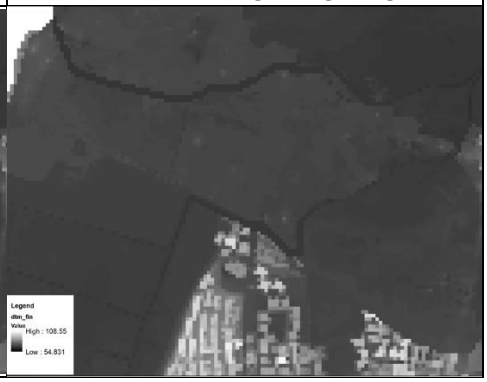

Figure 31 Detail of the DTM near the ditches Gaetana and Gelata

- **Piers of the bridge Napoleone Bonaparte and the highway bridge**: these elements are created as impermeable areas.

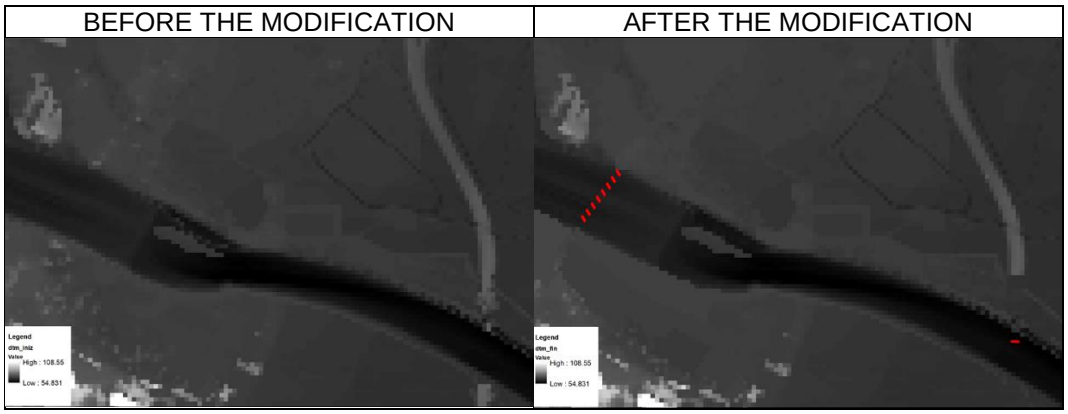

Figure 32 Insertion of impermeable areas as piers of the bridge

- **Tunnel on the highway near "Cascina Barbinetta".**

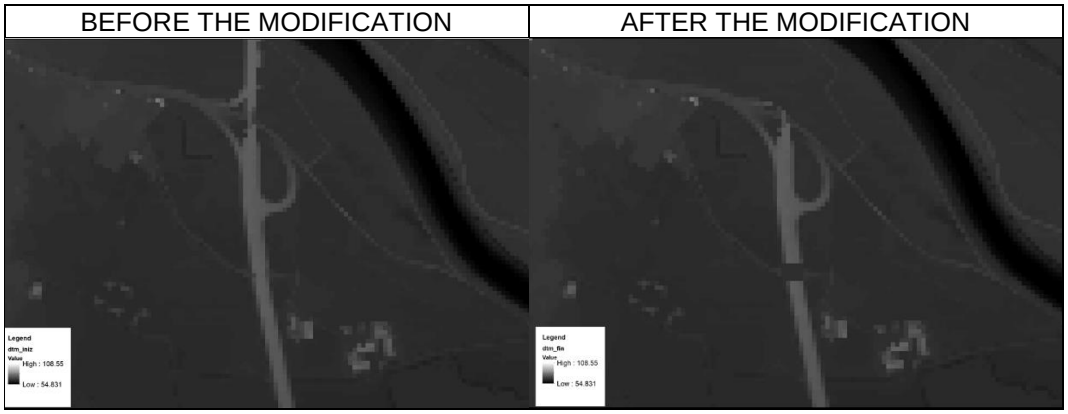

Figure 33 Manual insertion of the tunnel on the highway, not present in the DSM

The presence of the piers of the bridges and the ditches is analysed in detail with a sensitivity analysis that will be discussed in the following chapters.

To implement all the presented corrections the software ArcMap is used.

A point grid is geo-referenced on the map of the area of interest. Each point is characterised by its altitude and can be modified according to the corrections listed before. This grid is exported as an excel table and it is the main input for the 2D hydraulic simulations. The following picture shows the point grid just described.

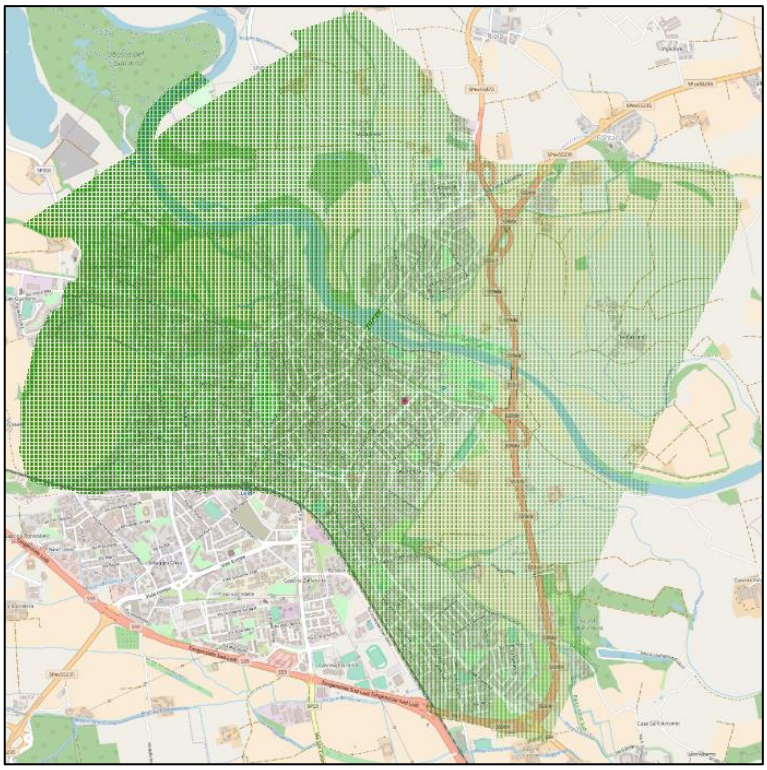

Figure 34 Computational grid used in R2D

Finally, in order to create the DTM, the points are interpolated by using the Kriging[17] technique. The following picture represents the final DTM that is produced.

[17] Kriging is an advanced geostatistical procedure that generates an estimated surface from a scattered set of points with z-values. Unlike other interpolation methods in the Interpolation toolset, to use the Kriging tool effectively involves an interactive investigation of the spatial behaviour of the phenomenon represented by the z-values before you select the best estimation method for generating the output surface. http://desktop.arcgis.com/en/arcmap/10.3/tools/3D-analyst-toolbox/how-kriging-works.htm

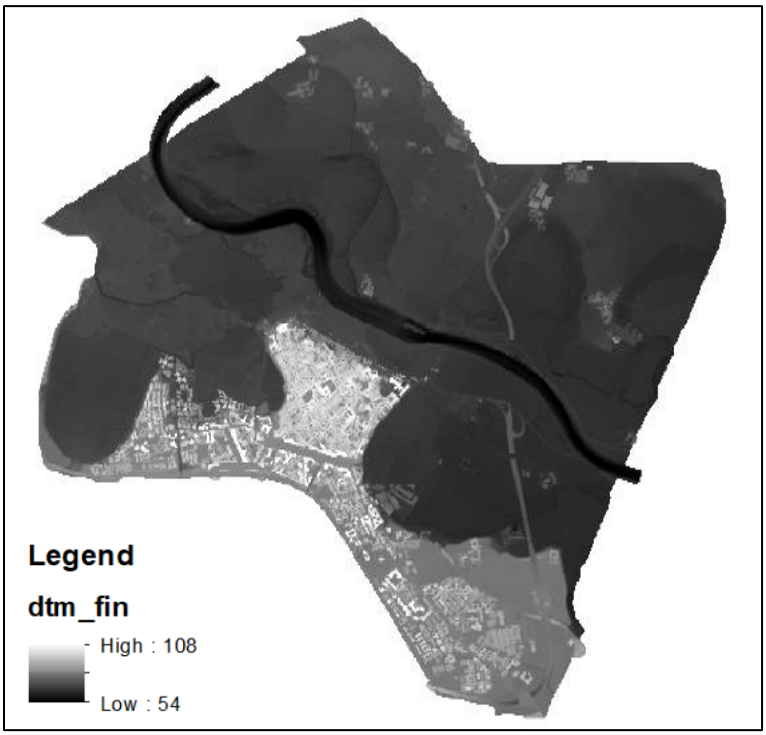

Figure 35 Final DTM

3.2 COMPUTATIONAL METHODS

This section is intended to be an explanation of the method that was developed in order to get the results of the flood model. The problem of the 2D flood simulation is approached in two different ways, firstly using a steady flow analysis, then an unsteady one.

To better understand why this approach is chosen, it can be useful to define what are steady and unsteady flow. A very trivial definition of steady flow is: “a flow which properties are not time depending”. Considering P as one of the properties of the flow (depth, velocity, pressure, etc.), the mathematical expression to define a steady flow is: $\frac{\partial P}{\partial t} = 0$

Instead, un-steady flow is defined as “a flow which properties are time depending”. In this case the mathematical expression is: $\frac{\partial P}{\partial t} \neq 0$

The choice of starting with the steady flow, instead of performing immediately an unsteady simulation, is driven by the fact that with the steady flow there is a better control of the parameters involved in the problem, like geometry, roughness and boundary conditions.

The framework that has been developed to perform each steady simulation is the following one:

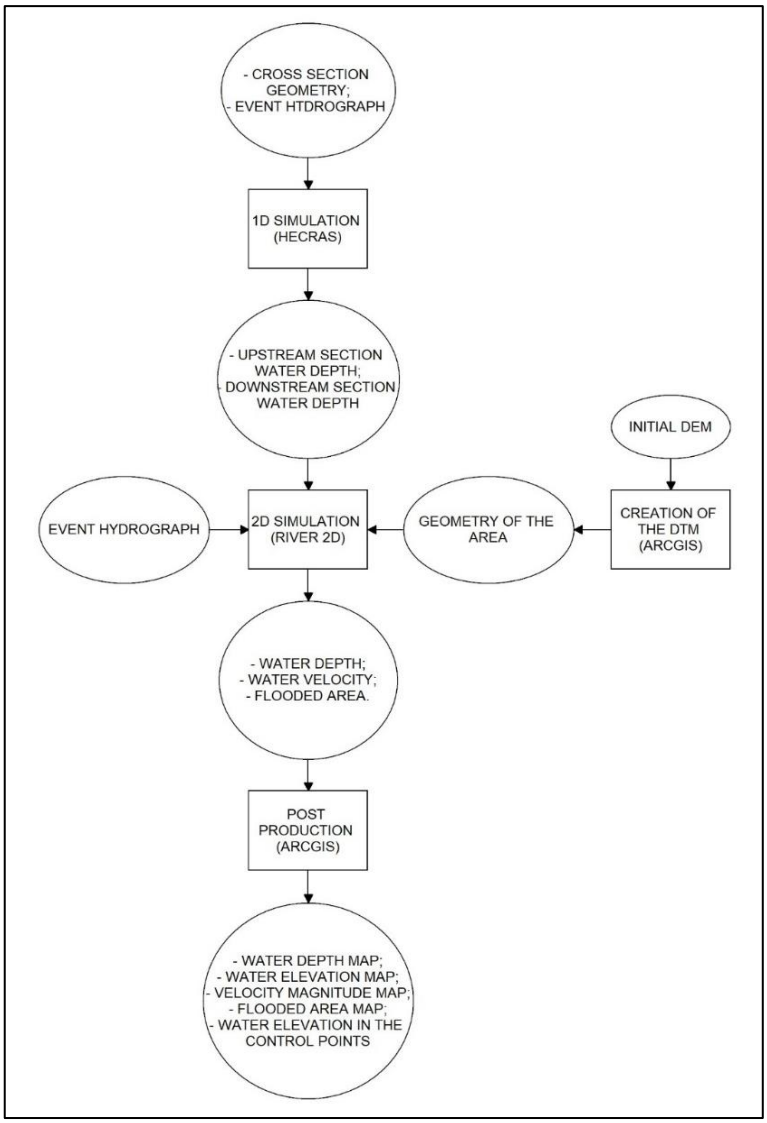

Figure 36 Framework used of the modelling procedure

From the sensitivity analysis it is possible to understand the impact of each parameter on the whole model. It is performed changing each time one of these parameters:

- **Roughness coefficient**: it is expressed with the Manning coefficient (n) or roughness height (K_s); in case of pipeline or an artificial channel the determination of the roughness coefficient is relatively simple, instead, for a natural channel or for an urban area, it is more difficult because the value depends on some characteristics, like the presence of trees, buildings or the aggregates dimension. The sensitivity analysis of this parameter shows if the model is affected (and how much) from a change in the roughness coefficient assumed as a base value.
  Initial trial values for the Manning coefficient for the rural area and the urban area are taken from a previous study (Rossetti & Cella, 2010a). Some initial trial values of the Manning coefficient for natural rivers can be seen in the table below (Chow, 1959).

Table 2 Common values of Manning coefficient (expressed in [s/m$^{1/3}$]) -(Chow, 1959)

tipo di superficie	Minimo	Normale	Massimo
ALVEI DI PIANURA			
non vegetati, rettilinei, corrente regolare	0.025	0.030	0.033
come sopra ma con pietre e alghe	0.030	0.035	0.040
non vegetati, tortuosi con mollenti e rapide	0.033	0.040	0.045
come sopra ma con pietre e alghe	0.035	0.045	0.050
come sopra, in magra	0.040	0.048	0.055
non vegetati, tortuosi, pietre, mollenti e rapide	0.045	0.050	0.060
molto irregolari e alghe molto fitte	0.075	0.100	0.150
ALVEI DI MONTAGNA (SPONDE CON ALBERI E CESPUGLI)			
sul fondo: ghiaia, ciotoli e massi radi	0.030	0.040	0.050
sul fondo: ciotoli e grandi massi	0.040	0.050	0.070
GOLENE E PIANE INONDABILI			
prato senza cespugli, erba bassa	0.025	0.030	0.035
prato senza cespugli, erba alta	0.030	0.035	0.050
campi incolti	0.020	0.030	0.040
coltivazioni a filari	0.025	0.035	0.045
colture di cereali in pieno sviluppo	0.030	0.040	0.050
aree con cespugli sparsi e erba alta	0.035	0.050	0.070
aree con cespugli bassi e alberi, in inverno	0.035	0.050	0.060
aree con cespugli bassi e alberi, in estate	0.040	0.060	0.080
cespugli fitti, in inverno	0.045	0.070	0.110
cespugli fitti, in estate	0.070	0.100	0.160

In the following it is reported, a brief explanation of the meaning and form of the roughness coefficient, in order to have a clearer understanding of the procedure:

The effective roughness height (K_s) is the resistance parameter to be specified at every node during the creation procedure of the 2D model. For the resistance due mainly to the roughness of the material of the bed, a first trial value of k_s can be taken as 1-3 times the largest grain diameter. The final value should be obtained by calibrating the model. (Steffler & Blackburn, 2002)

For the conversion from Manning to K_s it is used a tool available in the R2D_Bed software:

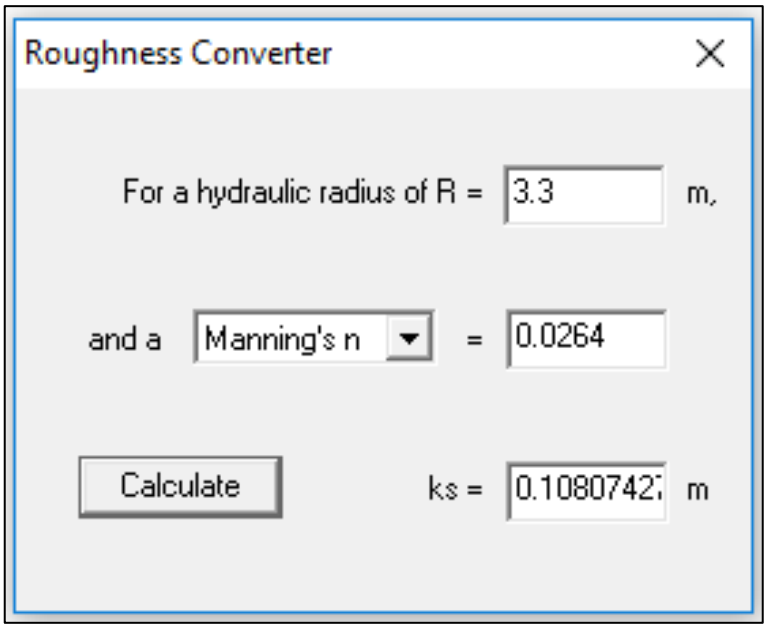

Figure 37 R2D bed software – Roughness Converter

This simple tool computes the roughness using the formula:

$$n = \frac{R^{\frac{1}{6}}}{2.5\sqrt{g}ln\left(\frac{12R}{k_s}\right)}$$

Where:

- R is the hydraulic radius that can be approximated by the depth of flow to the free surface that is: $R = \frac{A}{P}$;
- A is the cross-section area of the channel;
- P is the wetted perimeter of the channel at A.

For this work is chosen R = 3.3 [m], that is a mean value for this type of channel.

- **Cross section geometry for the 1D model:** the geometry of the 1D model is highly influencing the result because from the one-dimensional simulation, the boundary conditions for the two-dimensional model are retrieved.
  The cross sections of the Adda river are available in two different forms: one without the floodplains, provided by the AdbPo and another with the floodplains, extracted by the DTM created. The difference between the two options are evident in the pictures below.

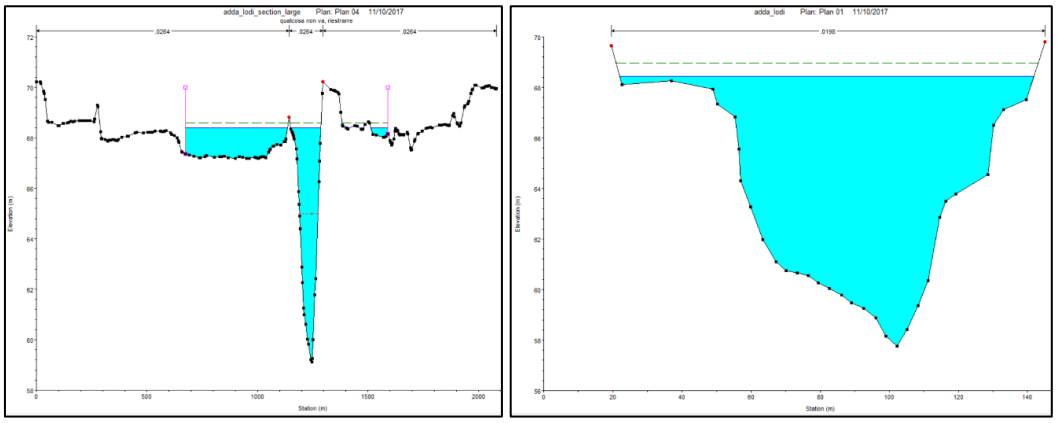

Figure 38 Left: large cross-section. Right: narrow cross-section

- **Inflow and outflow dimension for the 2D model:** in the 2D model the boundary conditions are provided as segments where the water is flowing inside and outside the model, respectively for the upstream condition and for the downstream condition. The length of these segments is one of the parameters that must be inserted as information, with the discharge and the water height (respectively for the upstream and downstream boundary condition).
  It is not known a priori the length of the segments; therefore, it is assumed that can vary between three values named: N (narrow), M (medium) and L (large). Then, the effects of the variation are studied.
  The next picture is showing one of the possibilities that are analysed during the sensitivity analysis.

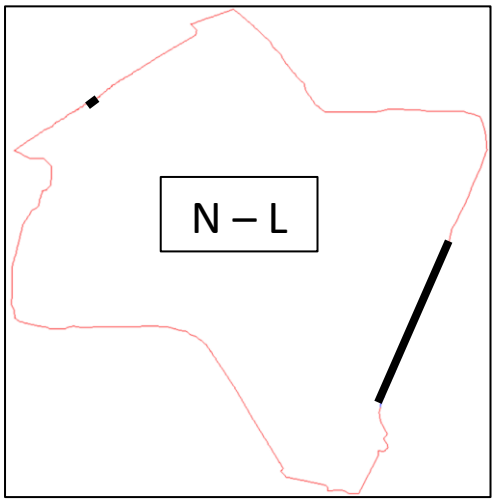

Figure 39 Dimension of the boundary conditions

- **Geometry of the area in the 2D model**: some modifications of the DTM are gradually inserted in order to understand the importance of them on the whole model.
  They include: “excavation” of diches, addition of the piers of the bridges and lowering of the height where obstacles not related with the terrain are present (buildings or trees).

To understand where the change of the parameter is more relevant, the zone under investigation is subdivided in three sectors (upstream, centre, downstream) as it is presented in the picture below.

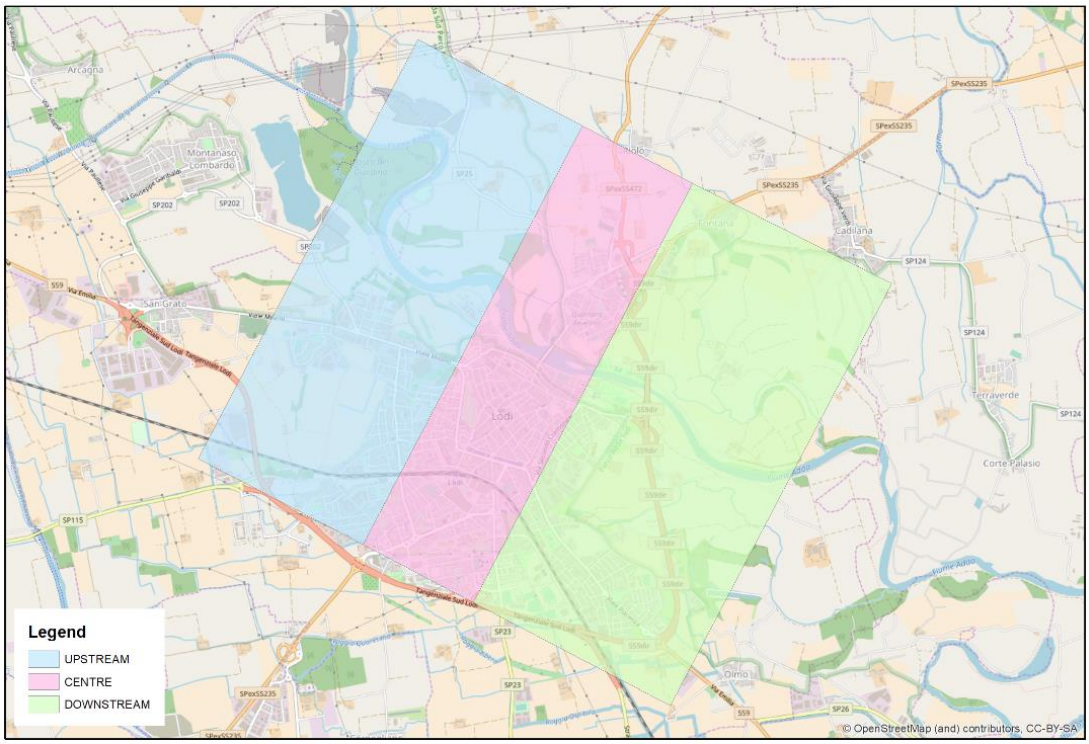

Figure 40 Sector subdivision of the interested area

In these three sectors two parameters are computed to quantify the sensitivity of the model with respect to a selected parameter:

- **Areal parameter**: $F_{area} = \frac{flooded\ area\ reference\ case}{flooded\ area\ i-case}$

  Where:
  $flooded\ area\ reference\ case$: it is the measure of the area of the flooded zone in the case assumed as reference;
  $floded\ area\ i - case$ = is the measure of the area of the flooded zone in the case where the k-parameter varies.

  The range of the F_{area} varies between 0 and +∞; when it is smaller than 1, it means that after changing the parameter the flooded area is increased, instead if it is bigger than 1, it means that the flooded area is decreased.
  To evaluate the value of F_{area}, a function, that can be used with the software ArcMap, is developed.
  The logical framework of the function can be understood by the following graph.

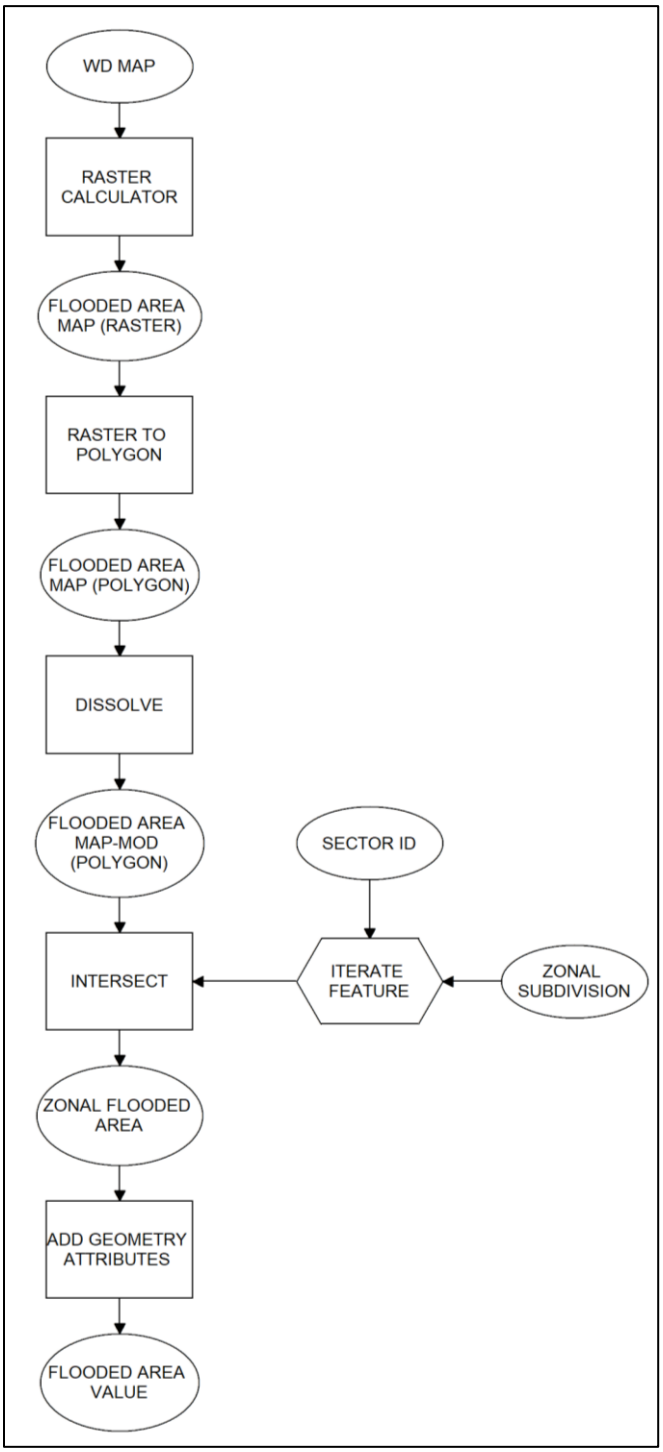

Figure 41 Framework of the function that produces the value F_{area}

The code used to create the function and explanation of all the sub functions can be found in the Appendix B.

Depth parameter: $F_d = \frac{1}{N}\sum_{j=1}^{N} \frac{depth\ in\ the\ reference\ case}{depth\ in\ the\ i-case}$

Where:

N = is the number of control points zones present in this sector;

$depth\ in\ the\ reference\ case$ = is the average depth in the j-control point zone in the reference case;

$depth\ in\ the\ i-case$ = is the average depth in the j-control point zone in the i-case.

The range of F_d varies between 0 and +∞; when it is smaller than 1, it means that after changing the parameter the average water depth is increased, instead if it is bigger than 1, it means that the average water depth is decreased.
To evaluate the value of the function F_d a function, that can be used with the software ArcMap, is developed.
The logical framework of the function can be understood by the following graph.

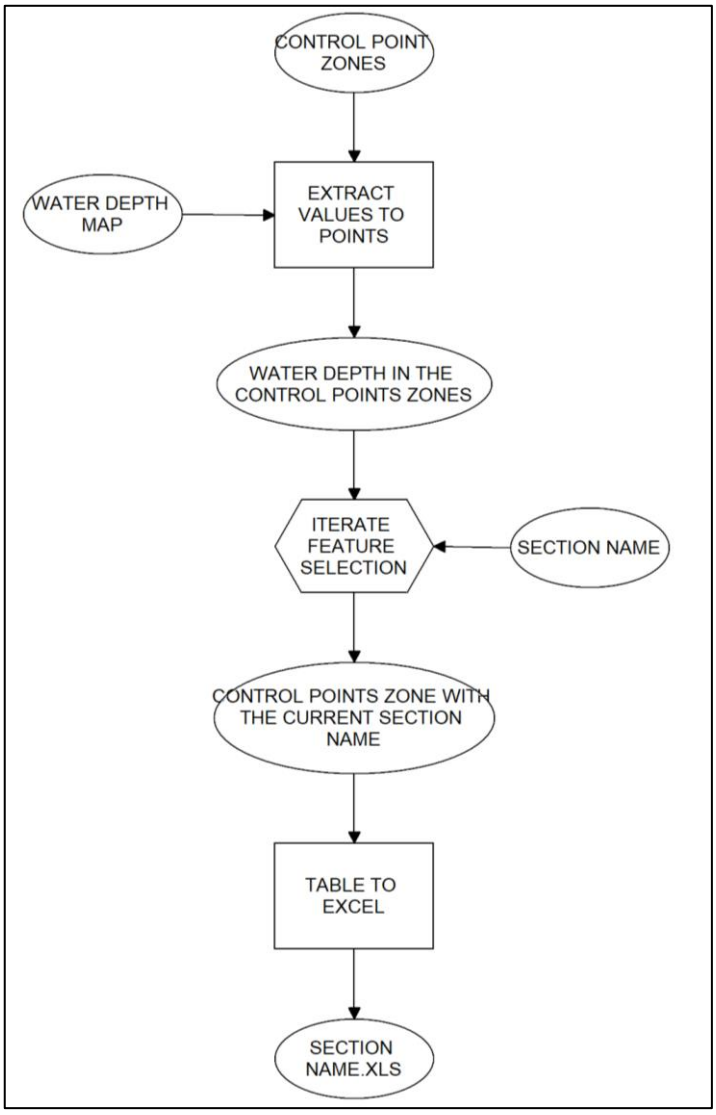

Figure 42 Framework of the function that produces the value F_{depth}

The code used to create the function and explanation of all the sub functions can be found in the Appendix A.

With this information the steady flow calibration of the model is performed.

To carry out it, two data are used as reference:

- **Control points:** a large data set of points is used, including points for which water depth is derived from image interpretation, damage claims and data available from previous studies (Rossetti & Cella, 2010a). The control points are widely distributed along the city, therefore, in order to have a more accurate calibration, they are grouped in 8 zones, as shown in the picture below.

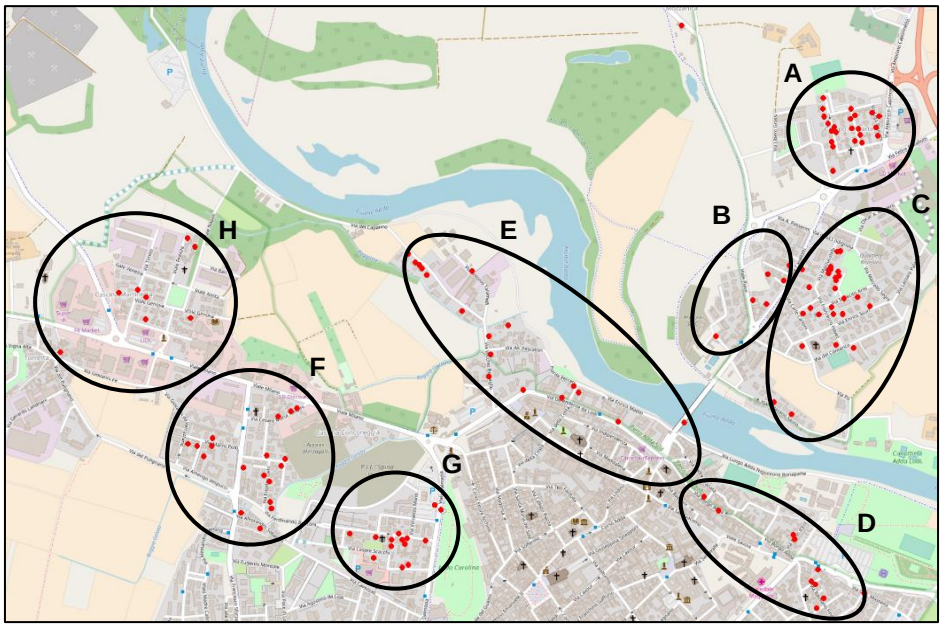

Figure 43 Zonal subdivision of the control points

- **The flooded area:** the extension of the flooded area is available only as a description of the event (text format) and with some images taken after the event. To have a map of the flooded area, the extent produced in a previous study (Rossetti & Cella, 2010a) is considered; this one, compared with the written reports, produces the following result.

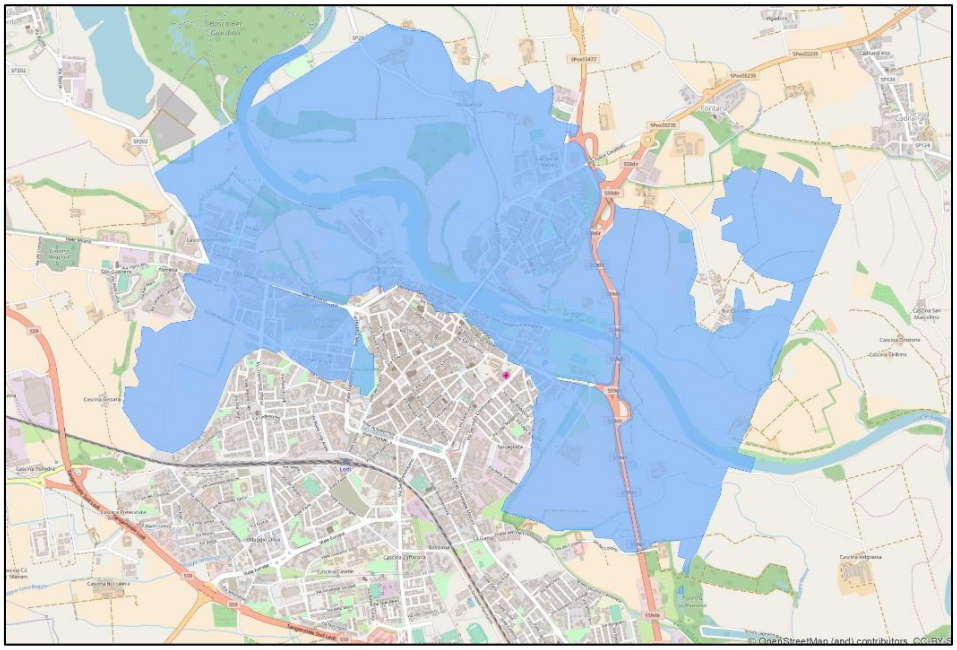

Figure 44 Flooded area

To perform the calibration, simulated and measured values are compared. Four indicators are introduced to estimate the quality of a simulation:

- **1st objective function**: defined as the Nash-Sutcliffe efficiency (E) (Krause, Boyle, & Bäse, 2005):

$$F_1 = E = 1 - \frac{\sum_{i=1}^{n}(O_i - P_i)^2}{\sum_{i=1}^{n}(O_i - \bar{O})^2}$$

Where:
O_i = is the value of the observed quantity in the i-position;
P_i= is the value of the quantity that is predicted by the model;
$\bar{O}$ = is the value of the average observed quantity.
F_1 may range between 1, goal value, and -∞.
Citing Krause et al. (2005) : “the largest disadvantage of the Nash-Sutcliffe efficiency is the fact that the differences between the observed and predicted values are calculated as squared values” (Krause et al., 2005).
Due to this, larger results in a simulation are strongly overestimated, meanwhile lower values are neglected.
In order to derive the F_1, a function that creates all the necessary maps, extracts the values to the control points and exports them into an excel file, where the value of the F_1 is calculated for each zone, is created.
The logical framework of the function can be understood by the following graph.

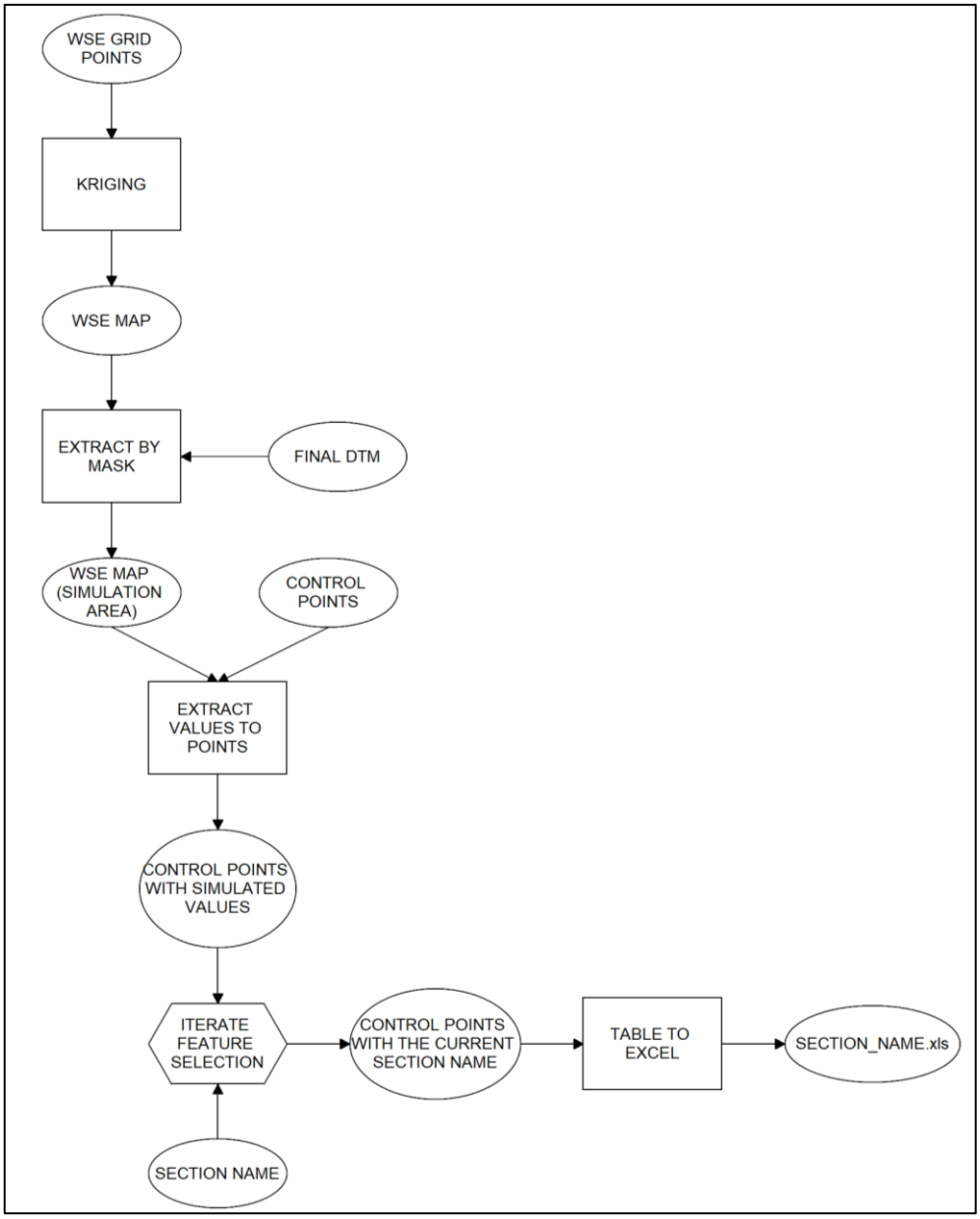

Figure 45 Framework of the function that produces the depth value in the control points

The code that is developed to create the function and the explanation of all the sub functions can be found in the Appendix C.
Another code (MACRO), developed with excel, is also used to automatize all the tasks.
2nd objective function, defined as the flood area index F_2^M, is a function that defines the performance of the model predicting inundating extent (Dung et al., 2011):

$$F_2^M = \frac{P^{11}}{P^{11} + P^{01} + P^{10}}$$

Where:
P^{11} = is the area where the simulated and observed flood extension maps give the result "wet";
P^{01} = is the area where the simulated flood extension map gives the result "wet" and the observed flood extension map "dry";
P^{10} = is the area where the simulated flood extension map gives the result "dry" and the observed flood extension map "wet".

The range of F_2^M may range between 1, goal value, and 0.
To evaluate the value of the function F_2^M a function, that can be used with the software ArcMap, is developed.
The logical framework of the function can be understood by the following graph.

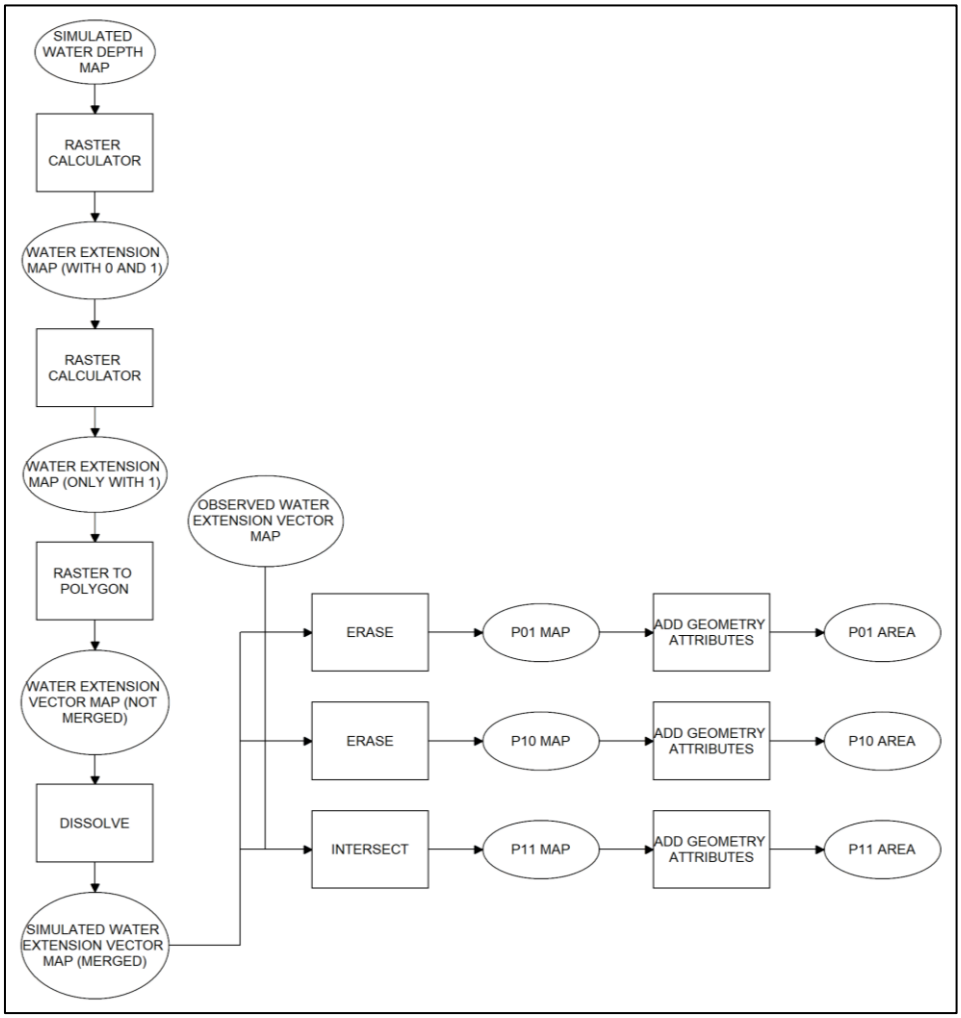

Figure 46 Framework of the function that calculates the terms for the F_2^M

The code used to create the function and explanation of all the sub functions can be found in the Appendix D.

The excel code used to manage the tasks is the same as the one introduced before.

- **Average of the difference:** It is the difference between the simulated and estimated water surface elevation**.**
  The goal value of this indicator is defined to 0, an average of the difference lower than zero indicates that there is a lack of water in the model.
  This parameter is computed by using the same function which is useful to compute the parameter F_1, because in the output files of the defined function there are values of simulated and observed water surface elevation.
- **Average absolute difference:** It is the absolute difference between the simulated and estimated water surface elevation**.**
  The goal value of this indicator is defined to 0.
  As before, also this parameter is computed with the function used to compute the parameter F_1.

To calibrate the steady model, it is considered the best combination produced of the four parameters just explained. This is obtained normalising the indicators and computing a weighted average. The calibrated simulation chosen is the one with the highest value of the weighted average.

All the details regarding the results of the steady simulations are presented in Chapter 4.3.

After the steady modelling, the unsteady model is performed. The parameters chosen to perform the simulations are the ones obtained from the calibration of the steady model.

Results of the unsteady model are:

- **Flooded area in each time step**: the dynamic of the flooded area shows the progression of the inundation during the considered event. To have a further validation of the model, this outcome is compared with the descriptions of the real event which are available in reports and newspapers.
- **Water depth in each time step**: the dynamic of the water depth in the area is collected as an input for the damage evaluation model, not object of the current thesis.
- **Water velocity in each time step**: the dynamic of the water velocity in the area is collected as an input for the damage evaluation model, a simple approach can be applied to understand if the velocity can provoke additional damages.

The resultant hazard map of the event, which is characterised by 200 years return period, will be the map representing the water depth and the flooded area in the peak of the hydrograph.

All the software used to develop the described working method are presented in the following section.

3.3 SOFTWARE USED

The principal software used in this work are: HEC-RAS, River 2D and ArcMap.

Others secondary software used are: Excel, ArcScene, Google Earth and Notepad.

HEC-RAS[18] (VER. 4.1.0). 

This one-dimensional software is provided by the US Army Corps of Engineers and its distribution is unlimited.

[18] www.hec.usace.army.mil/software/hec-ras

The River Analysis System software allows to perform one-dimensional steady and unsteady flow river hydraulics calculations. (Brunner, 2010)

It is a very fast (in terms of time of computation) and simple software to compute water surface profiles.

The data required as input are:

- river geometry (cross-sections, bridges and Manning's coefficients);
- discharge (Q);
- type of flow regime.

The software is founded on the Saint-Venant Equations and it is based on some 1D hypothesis:

- single bulk value of velocity for each section;
- assigned flow direction;
- sections are independent (not linked each other).

Due to the complexity of the case of study, this type of approach is limited, because it is not able to consider:

- complex section shape;
- different directions of velocity;
- lateral dissipation and lateral mass exchange (sediments and water infiltration). (Radice & Crotti, 2016b)

Considering all the characteristics and the limitations, this freeware is used only to compute the B.C. In order to obtain the results (flooded area and water levels) R2D is chosen.

RIVER 2D[19] (VER. 0.95A) 

This software is developed and distributed by the University of Alberta (Canada).

"Two-Dimensional Depth Averaged Model of River Hydrodynamics and Fish Habitat. In channel and river engineering, two-dimensional (2D), depth averaged models are beginning to join one-dimensional models in common practice. These models are useful in studies where local details of velocity and depth distributions are important." (Steffler & Blackburn, 2002)

This software is widely used in the current thesis for the computation of the results, therefore it can be considered as the most used program.

R2D is provided as a suite of 4 software: Bed, Ice (not used), Mesh and River2D. Bed is used for the creation of geometry, Mesh to create the computational grid and River2D to compute the solution (Radice & Crotti, 2016a).

"The hydrodynamic component of the River2D model is based on the two-dimensional, depth averaged St. Venant Equations expressed in conservative form. These three equations represent the conservation of water mass and of the two components of the momentum vector. The dependent variables actually solved for are the depth and discharge intensities in the two respective coordinate directions."(Steffler & Blackburn, 2002)

[19] www.river2d.ca

The conservation of mass is expressed with:

$$\frac{\partial H}{\partial t} + \frac{\partial q_x}{\partial x} + \frac{\partial q_y}{\partial y} = 0$$

The conservation of x-direction momentum has the expression:

$$\frac{\partial q_x}{\partial t} + \frac{\partial}{\partial x}(Uq_x) + \frac{\partial}{\partial y}(Vq_x) + \frac{g}{2}\frac{\partial}{\partial x}H^2 = gH(S_{0x} - S_{fx}) + \frac{1}{\rho}\left(\frac{\partial}{\partial x}(H\tau_{xx})\right) + \frac{1}{\rho}\left(\frac{\partial}{\partial y}(H\tau_{xy})\right)$$

The conservation of y-direction momentum has the expression:

$$\frac{\partial q_y}{\partial t} + \frac{\partial}{\partial x}(Uq_y) + \frac{\partial}{\partial y}(Vq_y) + \frac{g}{2}\frac{\partial}{\partial y}H^2 = gH(S_{0y} - S_{fy}) + \frac{1}{\rho}\left(\frac{\partial}{\partial x}(H\tau_{yx})\right) + \frac{1}{\rho}\left(\frac{\partial}{\partial y}(H\tau_{yy})\right)$$

Where:

H is the depth of flow;

U and *V* are the depth averaged velocities in the *x* and *y* coordinate directions;

q_x and q_y are the respective discharge intensities which are related to the velocity components through:

$q_x = HU$

and

$q_y = HV$

g is the acceleration due to gravity;

ρ is the density of water;

S_{0x} and S_{0y} are the bed slopes in the *x* and *y* directions;

S_{fx} and S_{fy} are the corresponding friction slopes;

τ_{xx}, τ_{xy}, τ_{yx} and τ_{yy} are the components of the horizontal turbulent stress tensor.

The software, when an unsteady flow simulation is performed, considers also other two parameters:

- Transmissivity: The rate at which groundwater flows horizontally through an aquifer.
- Storativity: “The storativity is defined as the volume of water the ground will release from storage per unit surface area of the ground per unit decline in the water table.”(Steffler & Blackburn, 2002)

The main input data required are: the geometry of the area of interest (coordinates X, Y and Z, and roughness coefficient), the inflowing discharge and the two boundaries conditions (in-outflow height).

Computational time can increase rapidly from some minutes to some days, depending on the resolution and complexity of the geometry.

The main problem in using this software (as others[20] for this purpose) is the determination of some parameters: the roughness coefficients, the inflow and outflow area, and how to model urban areas and other impervious areas. Therefore, as it is stated in the chapter regarding the working method (Chapter 3.2), sensitivity analysis and calibration were performed.

The results are stated in terms of: flooded area, waters depth, velocity (expressed with magnitude and direction) and other properties which will not be used for the case of study.

ARCGIS[21] (VER. 10.3.1) 

"ArcGIS provides contextual tools for mapping and spatial reasoning, so you can explore data and share location-based insights. ArcGIS creates deeper understanding, allowing you to quickly see where things are happening and how information is connected"

ArcGis is produced by ESRI and is under license. Other programs with the same functionality are available as freeware (e.g. QGis, partially used for the creation of DTM and measured points).

ArcMap

"ArcMap is where you display and explore GIS datasets for your study area, where you assign symbols, and where you create map layouts for printing or publication. ArcMap is also the application you use to create and edit datasets. ArcMap represents geographic information as a collection of layers and other elements in a map."[22]

This is a worldwide used and complete program, useful for many applications based on geographic information system(GIS).

This program is used for the creation of DTM (Chapter 3.1), the post production of the output data coming from R2D and the implementation of the SWAM method.

ArcScene

"ArcScene is a 3D viewer that is well suited to generating perspective scenes that allow you to navigate and interact with your 3D feature and raster data."[23]

ArcScene is provided with ArcGIS suite, thanks to the 3D visualization of the DSM/DEM (in ArcMap is in 2D) it is used to have a better overview of the area of interest and to identify place were modify the DSM.

[20] Other similar SW (2D and 1D): Basement, FESWMS, TELEMAC-2D, Mike11, Sobek etc.

[21] www.esri.com

[22] ArcGis help searching "What is ArcMap"

[23] ArcGis helper searching "Working with ArcScene"

4 FLOOD MODELLING

The following chapter is intended to present the detailed procedure that is developed to create the hazard scenario, which will be used for the hydrological risk assessment in the city of Lodi, considering the event happened in November 2002.

The 1D model used to retrieve the boundary conditions for the 2D model is firstly described, with a full explanation of all the decisions and assumptions that are considered. Secondly, the results of the sensitivity analysis are discussed with the explanation of all the parameters considered and all the process used to identify the most critical ones; then, at the end of the section, the parameters are presented which are used for the first trial simulation (i.e., first set of inputs for the following section).

The third section regards the 2D modelling of the event. In the first part, the procedure for the calibration of the steady model is presented with the complete description of the results. Then, the final used parameters are summarized and the flood hazard maps for the steady conditions are shown. The second part of this section reports the results of the unsteady analysis, with the discussion of all time-depending parameters and the presentation of the flood hazard maps deriving from the unsteady simulation.

The last section contains the conclusions about the 2D modelling with a summary of the results and the presentation of the final hazard maps.

4.1 COMPUTATION OF BOUNDARY CONDITIONS WITH HEC-RAS (STEADY AND UNSTEADY CASES)

HEC-RAS is used to model the Adda river over a 4.58 km long reach in the city of Lodi. As introduced in Chapter 3.3, HEC-RAS is a one-dimensional software which is able to calculate water surface profiles, starting from the geometry, the type of flow regime and at least two boundary conditions. Due to its limitations (Chapter 3.3), this software is used only to compute the upstream and downstream water levels needed for the 2D modelling with the software R2D.

First of all, the geometry of the model is created starting from the river cross sections and later also with the dimensions of the two bridges (Bridge *Napoleone Bonaparte* and Highway Bridge, Figure 47), both provided by AdbPo. The sections are oriented with an orthophoto, this orientation process is not very useful under the computation point of view, since flow direction is always taken perpendicular to section. However, it displays a more realistic view of the model and the results.

In the first attempts, only the sections defined as “narrow” are used; however, under high flow conditions, this geometry is not sufficient for a proper representation of water behaviour. To solve this problem, the defined “large” sections are extracted from the DTM. Besides, due to the big distance among available cross sections, additional interpolated sections are included using the HEC-RAS interpolation tool, increasing their number from 14 to 107.

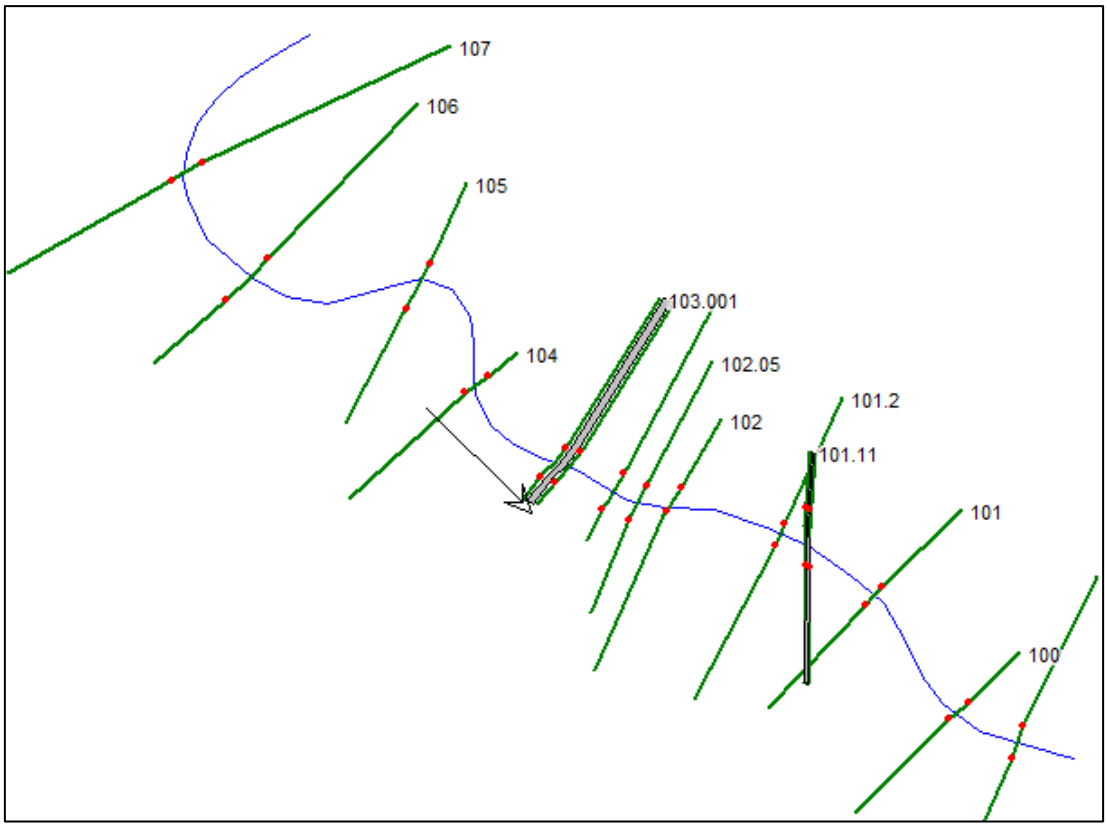

Figure 47 Visualization of the available cross sections used in HEC-RAS

Beyond river's bathymetry, the computation of a water surface profile requires information on roughness coefficients to be assigned to the channel and overbanks (OBs). The hydraulic roughness is a measure of the amount of frictional resistance that water experiences when passing over land and channels. An increase in this parameter will cause a decrease in the velocity of water. A distinction between the roughness of the channel and the two OBs is necessary to obtain a more suitable result.

In HEC-RAS the roughness parameter is requested as Manning's coefficient [$s/m^{1/3}$], instead River2D software requires K_s, defined as the "roughness height" [m]. Manning's coefficients are one of the unknown parameters that must be determined with the calibration of the model. Therefore, for the initial attempts, a standard coefficient (0.0264 $s/m^{1/3}$) is assigned based on tables available from literature (Table 2). Afterwards, its value is changed according to the results obtained.

Once the geometry is defined, HEC-RAS requires the definition of the flow regime and the discharge (Q) magnitude. Since the area of Lodi is predominantly flat, the flow regime is set to sub-critical. Consequently, flow is controlled by the downstream section, where a boundary condition should be known.

A distinction between the steady case and the unsteady one is necessary for the choice of the boundary condition typology:

- Steady: normal depth calculated for the peak flow (Saltelli, 2002) of the event (1837 [m^3/s]) and a slope set to 0.6% are used as fixed downstream boundary condition.
- Unsteady: similar to the steady case for the downstream condition, while the upstream condition is defined by the hydrograph of the event[24].

Due to its stability and reduced computation time, the steady condition is preferred for the sensitivity analysis and calibration, which require some attempts. Then, once the unknown

[24] See former study (Natale, 2003)

parameters are computed, an unsteady simulation can be performed. It must be remembered that the results obtained from the one-dimensional modelling are used as input for the two-dimensional computation.

Hereinafter, the steady cases are listed and analysed in detail. The different cases are identified by changing:

- roughness coefficient;
- use of “narrow” to “large” cross sections;
- boundary condition size;
- adding bridges.

The results are organized in tables, which show:

ID	The conditions that are changed	The resulting computed heights

Below, there is presented the résumé regarding the HEC-RAS models used to compute the BCs needed for the 2D **sensitivity analysis**:

Table 3 Summary of the sensitivity analysis, the corresponding conversion in Ks (for R2D) and the HEC-RAS results.

	Roughness coefficient with narrow sections		Height results m a.s.l.	
	n [s/m$^{1/3}$]	Ks [m]	Upstream	Downstrem
1	**0.0264**	**0.108**	69.19	66.54
2	0.033	0.352	69.92	67.44
3	0.0198	0.015	68.44	63.55

	Boundary condition size with n = 0.0264 [s/m$^{1/3}$]		Height results m a.s.l.	
	Upstream	Downstream	Upstream	Downstrem
4	Large	Narrow	68.4	63.55
5	Medium	Narrow	68.4	63.55
6	Narrow	Narrow	68.26	63.55
7	Narrow	Large	68.26	65.45
8	Narrow	Medium	68.3	65.91

	Adding Bridges with n=0.0264 [s/m$^{1/3}$]		Height results m a.s.l.	
	Upstream	Downstream	Upstream	Downstrem
9	Narrow	Narrow	68.29	63.55

From the height results obtained it can be noticed that

- increasing the roughness coefficient, the downstream levels are higher. On the contrary the upstream levels are not significantly influenced;
- changing the BC size, the downstream levels are slightly influenced. On the contrary the upstream levels are not significantly influenced;
- adding bridges, the levels here are not influenced.

Below is presented the résumé of the main HEC-RAS models used to compute the BCs needed for the 2D **calibration** phase:

Table 4 Summary of the n coefficients used, the corresponding conversion in Ks (for R2D) and the HEC-RAS results.

	Channel		Overbank		Height results m a.s.l.	
	n [s/m$^{1/3}$]	Ks [m]	n [s/m$^{1/3}$]	Ks [m]	Upstream	Downstrem
1	0.025	0.0776	0.09	7	68.46	**66.08**
2 -25% Overbank	0.025	0.0776	**0.0675**	**3.93**	68.42	**65.96**
3 -25% Channel	**0.01875**	**0.0097**	0.09	7	67.94	**65.3**
4 -15% O.B. -8%Ch.	**0.023**	**0.05**	**0.0765**	**5.16**	68.45	**66.01**
5	**0.02645**	**0.11**	0.0765	5.16	68.55	**66.07**
6	0.02645	0.11	**0.0826**	**6**	68.56	66.1
7	0.025	0.0776	0.0765	5.16	68.45	**66.01**

From the height results gained it can be observed that, changing the roughness parameter from the reference value, levels at the inflow and outflow are not influenced, except in the run 3, where the manning of the cannel is extremely different from the reference one defined before.

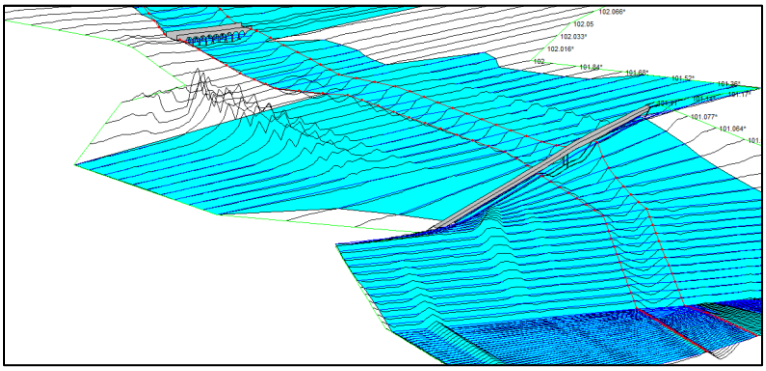

Figure 48 Quasi-3D visualization of one result of a steady simulation.

Once the roughness parameters for the calibration are chosen, the unsteady simulation can be performed using them. The main motivation to use an unsteady one-dimensional simulation is that for a 2D transient simulation the use of only one downstream level is not enough, due to the evolution of the water profile with the time. Therefore, the “Time Varying Elevation” (called “stage hydrograph” in HEC-RAS software) should be given as downstream BC to R2D.

For the unsteady simulation, it is used the same geometry with the same roughness coefficient corresponding to the best calibration resulting from the 2D simulation (explained in the next chapter).

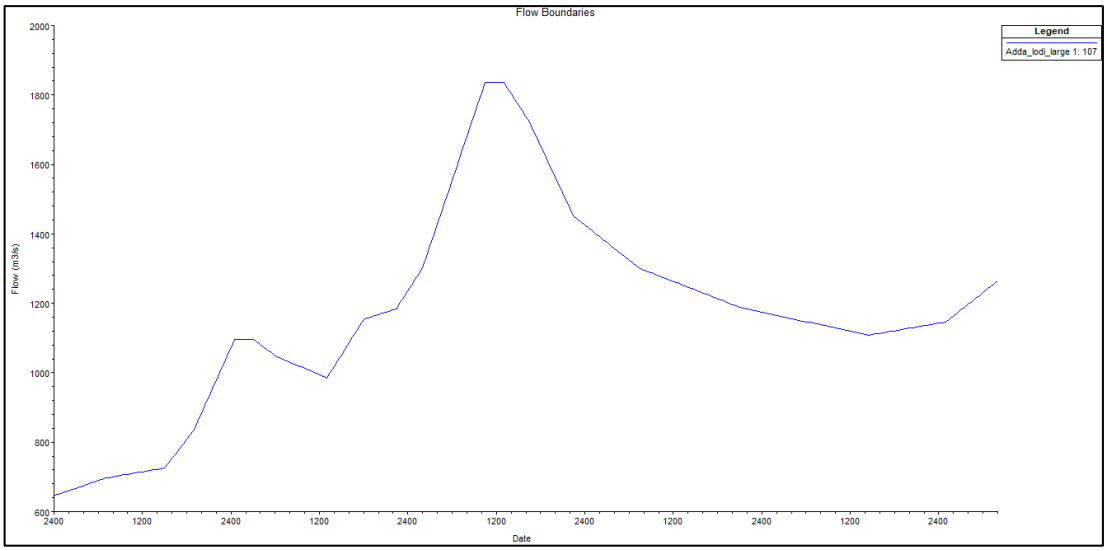

Figure 49 Discharge hydrograph inserted in HEC-RAS

For the downstream BC it is chosen again the normal depth, using the same slope of the previous cases.

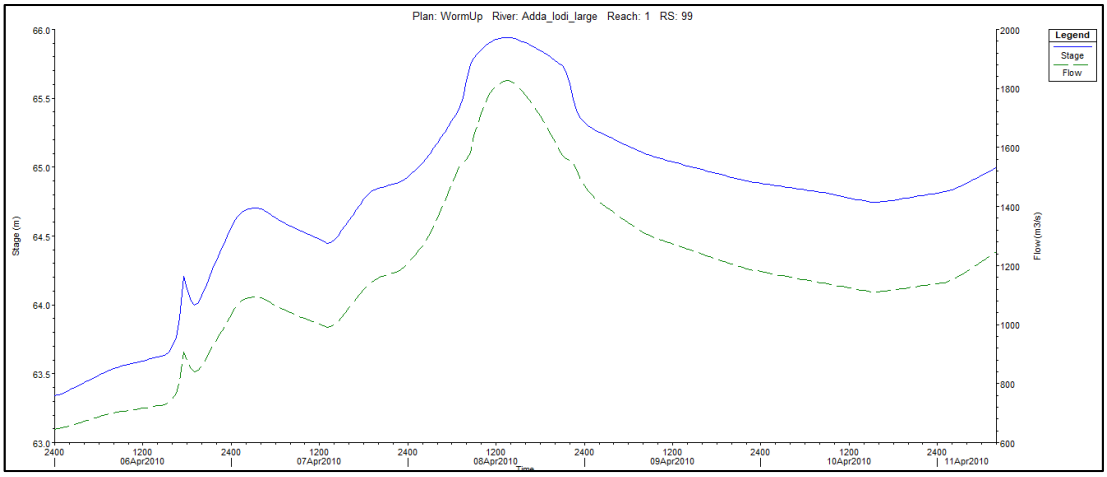

Figure 50 Unsteady 1D simulation output: The blue line is the water surface elevation for the downstream section

As it can be understood from the foregoing graph, HEC-RAS output gives the stage hydrograph, for each section. Only the hydrograph of the last section is reported since it is the crucial one for the thesis purpose.

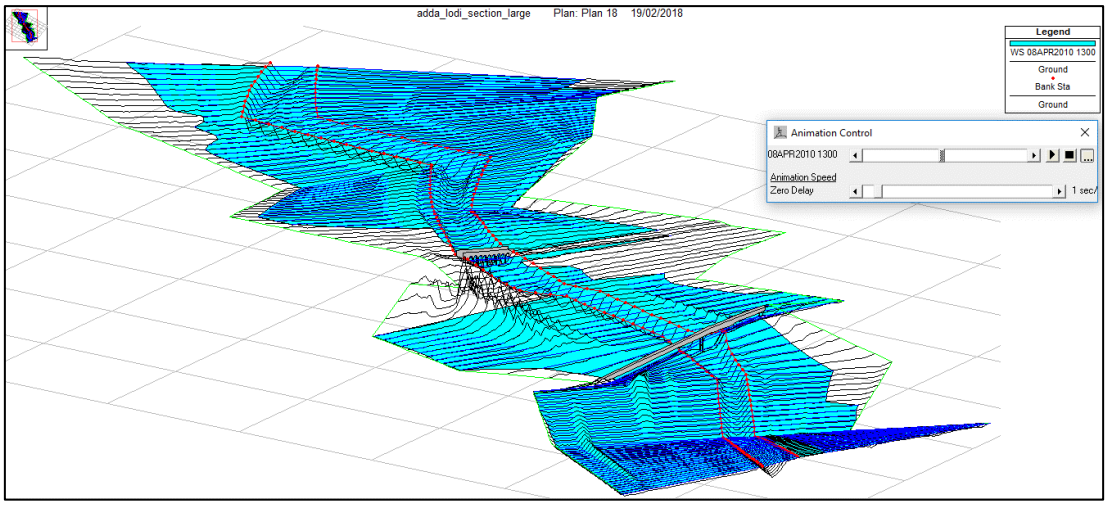

Figure 51 Quasi 3D visualization of the peak instant.

Another output of the software is a quasi-3D animation of the flood event. Although the limitations of the software and the reliability of the consequent animation, this solution, with a more quantitative result, can be an interesting comparison between the one-dimensional and the two-dimensional models.

4.2 SENSITIVITY ANALYSIS

In the current available literature, sensitivity analysis (SA) is defined as “the study of how the uncertainty in the output of a model can be apportioned to different sources of uncertainty in the model input” (Saltelli, 2002). In fact, it can be easily considered as a starting point for the creation of the model.

Therefore, the performed SA is used to determine the parameters influencing the model from a qualitative and quantitative points of view.

As it is introduced in Chapter 3, the parameters that are analysed in the current SA are:

- roughness coefficients;
- cross section geometry for the 1D model, which is used to determine the BC for the 2D model;
- BCs size for the 2D model;
- geometry of the area in the 2D model.

The approach used in the current SA is to change one parameter at the time, in order to determine its importance on the results of the model.

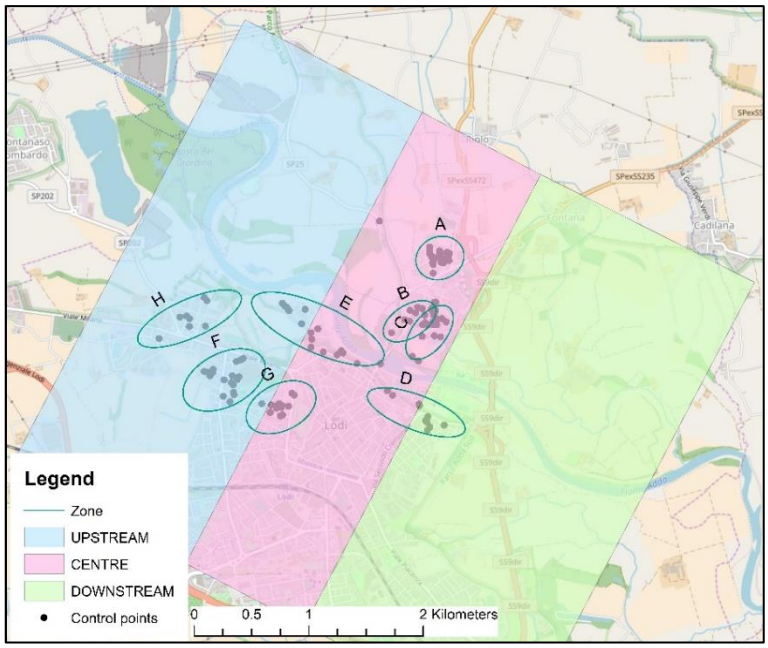

Figure 52 subdivision of the flooded domain in 3 sectors and subdivision of the control points in 8 zones

Regarding the quantification of the influence of a parameter, a comparison with a "base case" is performed, which gives as results the coefficients F_{area} and F_d (Chapter 3). From the obtained values, is defined the sensitivity of the model, in terms of depth or flooded area, with 4 classes:

- Not sensitive: the difference between 1 and the value of the coefficient is equal to 0.
- Slightly sensitive: the difference between 1 and the value of the coefficient ranges from 0 to 0.2.
- Moderately sensitive: the difference between 1 and the value of the coefficient ranges from 0.2 to 0.7.
- Highly sensitive: the difference between 1 and the value of the coefficient is higher than 0.7

In the following section all the results of the SA are presented and analysed in detail.

4.2.1 CASES CONSIDERED FOR THE SENSITIVITY ANALYSIS

During the SA, the following cases are performed:

- **Roughness coefficient**: the following table lists all the runs performed for the selected parameter; the first column shows the chosen values of K_s, while the others report the flooded area in the 3 sectors and the average water depth in the zones in which the control points are subdivided in (Figure 52).

Table 5 Runs performed during the SA for the roughness coefficient

K_s [m]	Area sector 1 [km²]	Area sector 2 [km²]	Area sector 3 [km²]	A [m]	B [m]	C [m]	D [m]	E [m]	F [m]	G [m]	H [m]
0.108	2.574	1.689	4.197	0.139	0.291	0.225	0.297	0.620	0.006	0.016	0.030
0.352	3.281	2.126	4.428	0.495	0.594	0.852	0.960	0.944	0.303	0.611	0.155
0.015	1.800	1.014	3.787	0	0.069	0.002	0.013	0.398	0	0	0.001

Considering as the "base case" the one marked in blue in the table, the main characteristics of this simulation are can be summarized as follows:

- roughness coefficient (K_s) = 0.108 m;
- mesh dimension = 20 m;
- discharge (Q) = 1840 m^3/s;
- section dimension in the 1D model = narrow;
- BC (upstream and downstream) = 69.19 m - 66.54 m.

The following picture shows the resulting flooded area and water depths.

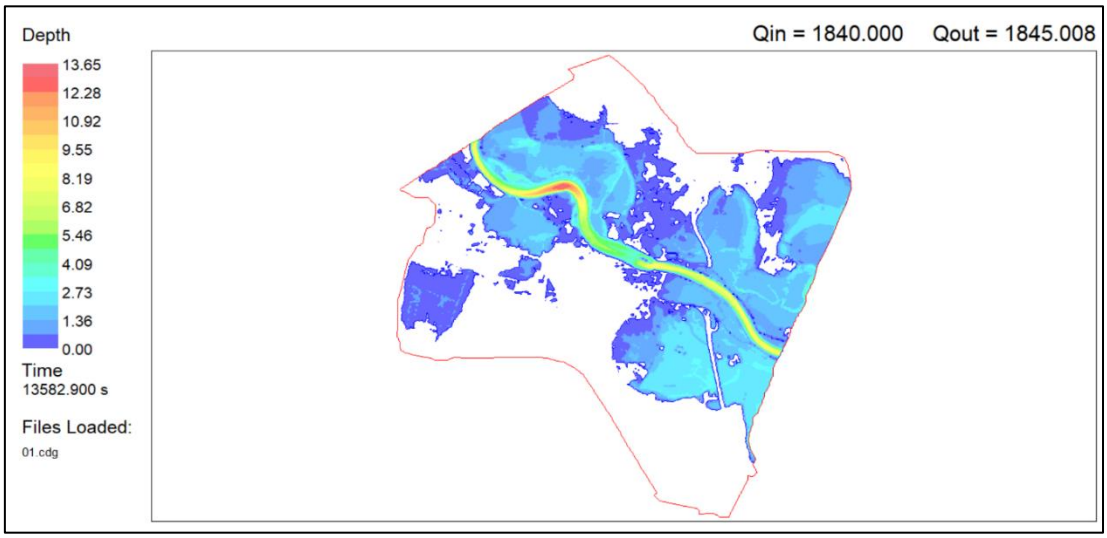

Figure 53 SA roughness coefficient- hazard map for the "base case"

From the comparison of the simulations with the "base case" it is possible to compute the areal parameter (F_{area}) and the depth parameter (F_d), as it is explained in the Chapter 3.2.

The results of the SA about the roughness coefficient are described in the graphs presented below.

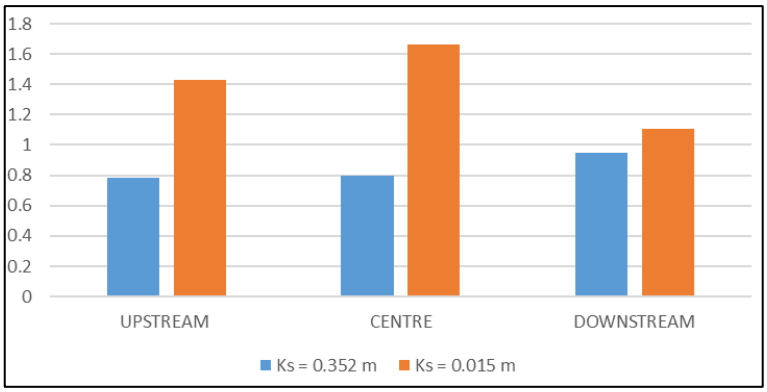

Figure 54 SA roughness coefficient – areal coefficient

If F_{area} > 1, the considered run gives smaller flooded area than that computed in the "base case" in the studied sector.

If F_{area} < 1, the considered run, gives larger flooded area than that computed in the "base case" in the studied sector.

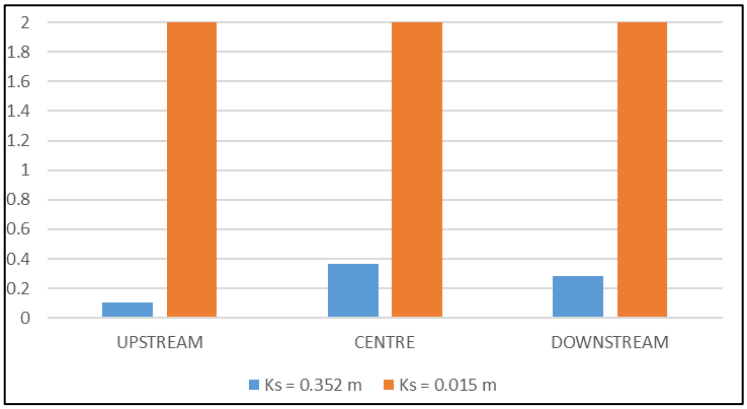

Figure 55 SA roughness coefficient – depth coefficient

If F_d > 1, the considered run gives lower average depth means than that computed in the "base case" in the studied sector.

If F_d < 1 the considered run gives higher average depth means than that computed in the "base case" in the studied sector.

Considering the two parameters presented above, it can be understood that:

- The model is moderately sensitive in the "upstream" and "centre" sectors, while it is slightly sensitive in the "downstream" one, in terms of flooded area.
- The model is highly sensitive in all the sectors, in terms of water depth.

Therefore, it can be deduced that the roughness coefficient has a key role on the output of the model.

- **Cross section geometry for the 1D model**: the following table lists all the cases performed for the selected parameter.

Table 6 Runs performed during the SA for the cross-section dimension

Cross section	Area sector 1 [km²]	Area sector 2 [km²]	Area sector 3 [km²]	A [m]	B [m]	C [m]	D [m]	E [m]	F [m]	G [m]	H [m]
Narrow	2.574	1.689	4.197	0.139	0.291	0.225	0.297	0.620	0.006	0.016	0.030
Large	1.762	1.124	2.550	0	0.198	0.081	0	0.526	0	0	0

The “base case” for this SA, which is “narrow sections” and marked in blue in the table, shows the same characteristics as in previous SA analysis. Therefore, it is not presented again.

The results of the SA on the cross sections’ dimensions are described in the graphs presented below.

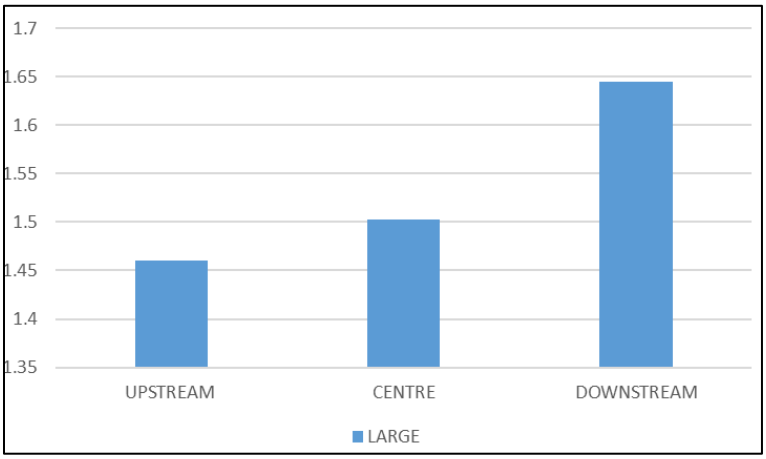

Figure 56 SA cross section dimension – areal coefficient

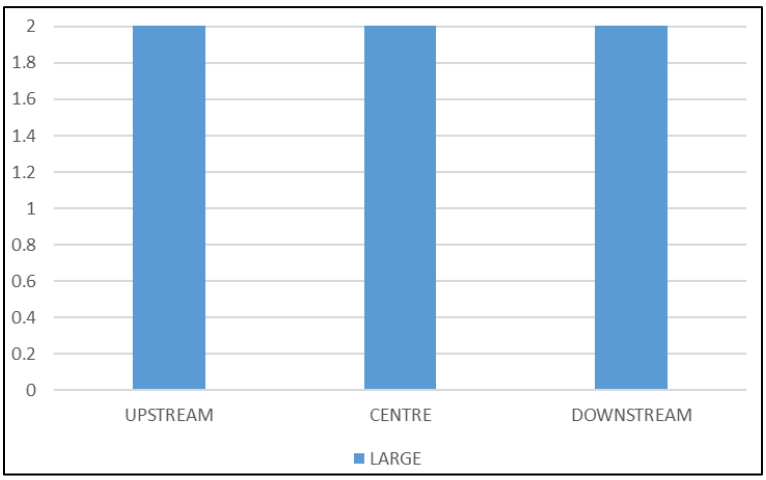

Figure 57 SA cross section dimension – depth coefficient

Considering the two parameters presented above, it can be understood that:

- the model is moderately sensitive, in all the sectors, in terms of flooded area;
- the model is highly sensitive, in all the sectors, in terms of water depth.

Therefore, it can be deduced that the cross-section geometry for the 1D model has a key role on the behaviour of the 2D model.

The SA is not suggesting which cross section dimension is more suitable for the purpose of the model under development, but it is only quantifying the sensitivity of the model regarding this parameter. Consequently, an alternative between the case “Narrow” and the case “Large” must be selected carefully.

- **Inflow and outflow boundary condition dimensions for the 2D model**: the following table lists all the cases performed for the selected conditions.

Table 7 Runs performed during the SA for the BC dimension

BC dimension	Area sector 1 [m²]	Area sector 2 [m²]	Area sector 3 [m²]	A [m]	B [m]	C [m]	D [m]	E [m]	F [m]	G [m]	H [m]
L-N	4.197	1.314	3.525	0.003	0.226	0.157	0	0.541	0	0	0.009
M-N	2.058	1.281	3.335	0	0.216	0.143	0	0.537	0	0	0.007
N-N	1.762	1.124	2.550	0	0.198	0.081	0	0.526	0	0	0
N-L	1.826	1.285	3.148	0	0.210	0.147	0	0.546	0	0	0
N-M	1.900	1.299	3.584	0	0.224	0.151	0	0.542	0	0	0

Considering as the “base case” the one marked in blue in the table, the main characteristics of this simulation can be summarized as follows:

- roughness coefficient (K_s) = 0.108 m;
- mesh dimension = 20 m;
- discharge (Q) = 1840 m^3/s;
- section dimension in the 1D model = large;
- BC (upstream and downstream) = 68.29 m - 63.55 m.

The following picture shows the resulting flooded area with water depths.

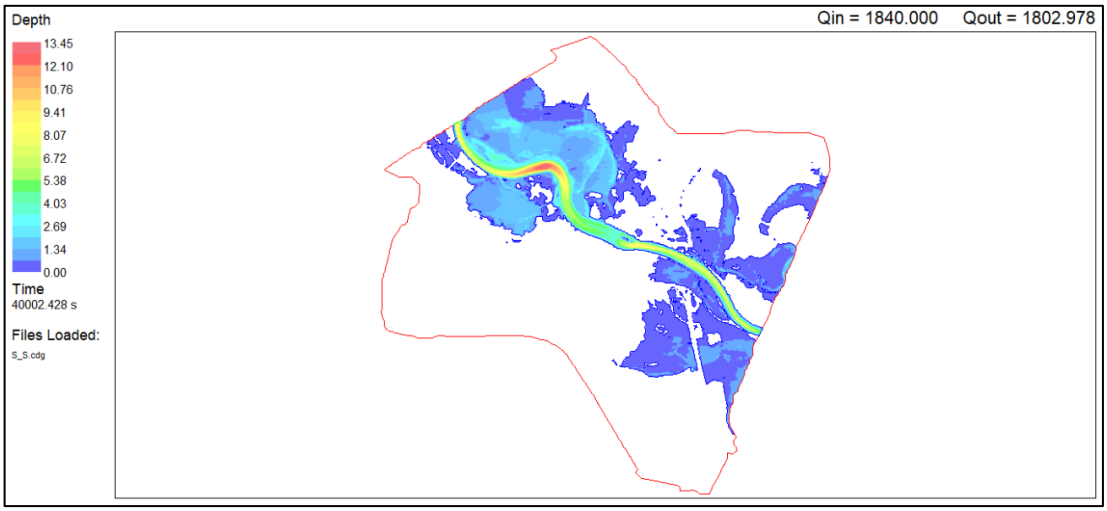

Figure 58 SA BC dimension- hazard map for the “base case”

The results of the SA on the cross sections dimensions are described in the graphs presented below.

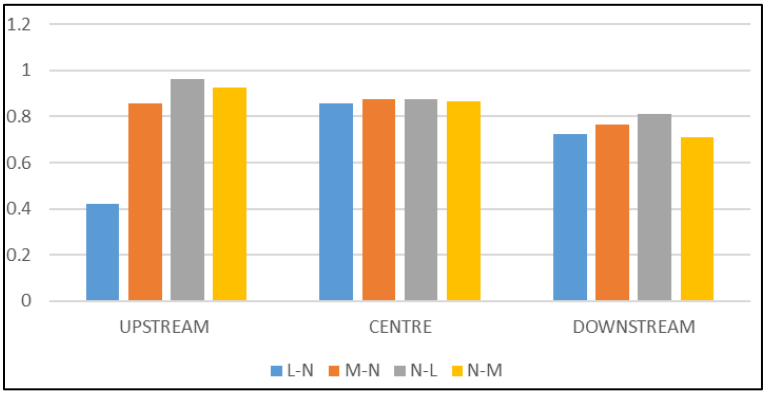

Figure 59 SA BC dimension – areal coefficient

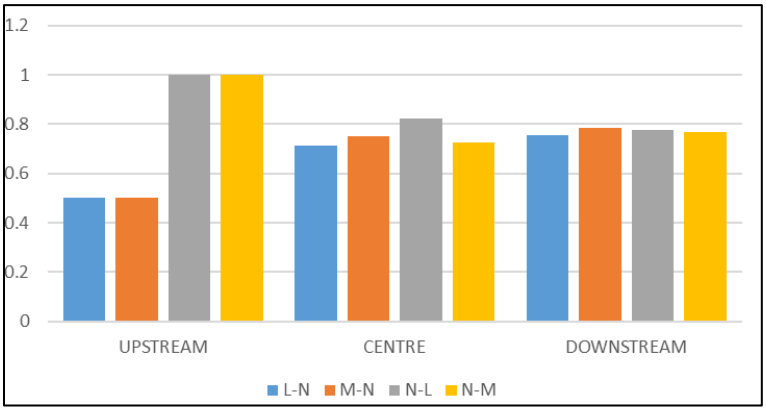

Figure 60 SA BC dimension – depth coefficient

Considering the two parameters presented above, it can be understood that:

- the model is always moderately sensitive in the "downstream" sector in terms of flooded area, while it is mainly slightly sensitive in the other sectors;
- the model is always slightly sensitive in all the "centre" and "downstream" sectors, in terms of water depth. In the "upstream" sector, in two cases the model is moderately sensitive and not sensitive in the other two cases

Therefore, it can be deduced that inflow and outflow dimensions for the 2D model are not a key parameter for the behaviour of the model. In fact, it is affecting the "upstream" sector.

- **Geometry of the area in the 2D model**: the following table shows all the cases performed for the selected geometry.
  The description of the geometrical features for each case is presented in detail in Chapter 3, therefore it will not be repeated in this chapter.
  The terminology used to name each case is the following:
  - In presence of ditches, the case is identified as *YES.D.* (*NO.D.* in the opposite case).
  - In presence of bridge piers, the case is identified as *YES.B.* (*NO.D.* in the opposite case).
  - In presence of discharge coming from the network of ditches, the case is identified as *Q.* in the name (in the opposite case the Q. is not present).
  - In presence of a highway underpass hole on the highway, which connects flooded zones, the case is identified as *H.* (in the opposite case the H. is not present).

Table 8 Runs performed during the SA for the geometry of the area in the 2D model

Case	Area sector 1 [km^2]	Area sector 2 [km^2]	Area sector 3 [km^2]	A [m]	B [m]	C [m]	D [m]	E [m]	F [m]	G [m]	H [m]
NO.D.-NO.B.	1.875	1.364	3.434	0.07	0.35	0.27	0	0.60	0	0	0
YES.D.-NO.B.	2.017	1.374	3.265	0.08	0.30	0.22	0	0.58	0.05	0	0.02
YES.D.-YES.B.	2.893	1.858	3.357	0.50	0.57	0.57	0.07	0.89	0.36	0.56	0.11
YES.D.-YES.B.-Q.	3.104	1.960	3.678	0.49	0.59	0.60	0.08	0.94	0.36	0.60	0.16
YES.D.-YES.B.-H.	2.713	1.847	3.369	0.47	0.61	0.60	0.07	0.84	0.33	0.51	0.08

This SA is implemented in a slightly different way than the ones performed before, in fact the "base case" is not unique. Considering the "i-case" in the computation of the sensitivity parameters, the "base case" is the "i-1 case".

Each "i case" is, in fact, comprehensive of the geometrical modifications introduced in the "i-1 case". Therefore, the SA for the considered parameter is performed firstly in relative terms.

The results of the SA on the cross sections dimensions are described in the graphs presented below.

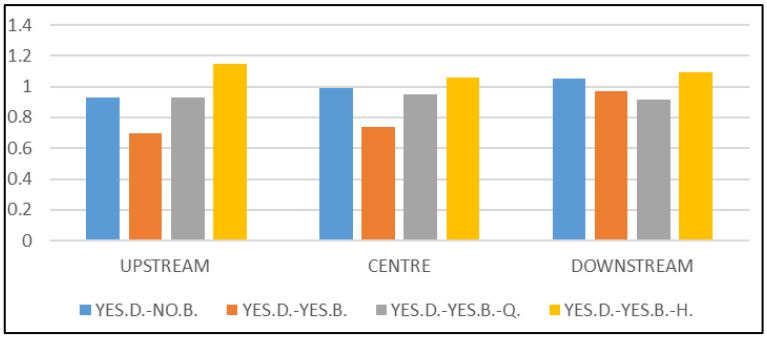

Figure 61 SA geometry of the area in the 2D model – areal coefficient

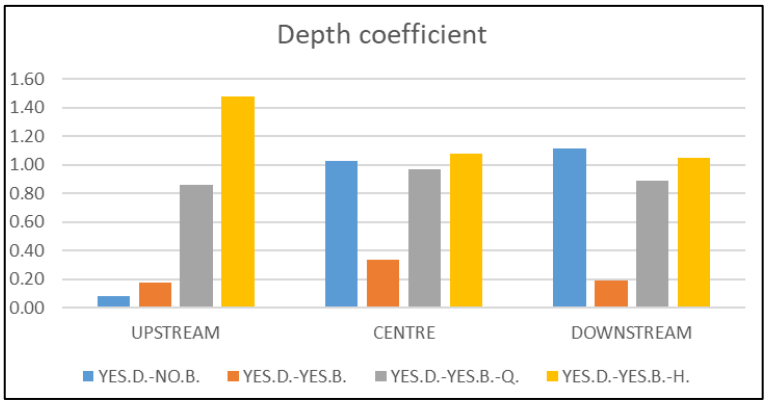

Figure 62 SA geometry of the area in the 2D model – depth coefficient

Considering the two parameters presented above, it can be understood that:

- The model is generally slightly sensitive, in all the sectors, in terms of flooded area. The only geometrical modification that causes moderate differences in the “centre” and “upstream” sectors, is the introduction of the bridges’ piers.
- The model is moderately-high sensitive (excluding the YES.D.-YES.B.-Q. case, where it is slightly sensitive), in terms of water depth, in the “upstream” sector. Instead, in the “centre” and “downstream” sector it is slightly sensitive or not sensitive (excluding the YES.D.-YES.B. case, where it is moderately sensitive).

Therefore, it can be deduced that the only geometrical parameters that are influencing the model, from a relative point of view, are the inclusion of ditches and bridges’ piers in the geometry of the 2D model. On the contrary, the introduction of discharge coming from the ditches has a negligible influence on model’s results, thus it can be ignored. The introduction of the highway underpass is needed to connect two flooded zones, although it is not influencing the model.

In a second step are introduced two other geometrical modifications of the area in the 2D model, but they cannot be compared in relative terms, because they are based on two different approaches. The first one divides the model area in zones where the roughness coefficient is increased in the urban areas; the second one has a uniform roughness coefficient, but the urban areas are modelled as impermeable blocks. Unfortunately, the latter approach has two major drawbacks:

- a very low computation velocity, due to the high complexity of the geometry of the urban area;
- a poor ratio $\frac{Q_{in}}{Q_{out}}$, which means a lower convergence of the steady model.

These two are important factors that must be considered, in case of similar effect, in the choice of the best solution.

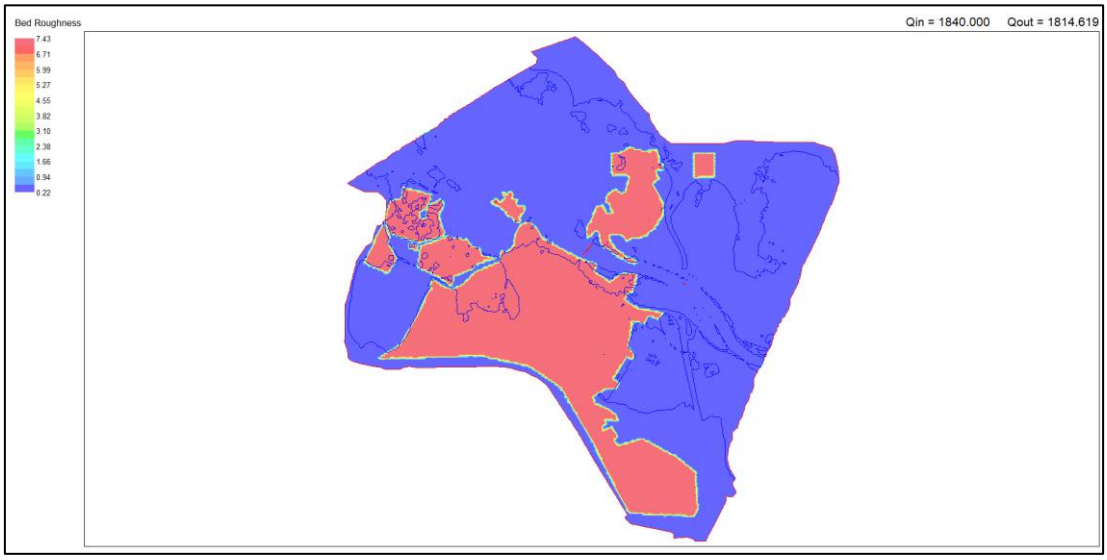

Figure 63 Map of the zonal Manning parameter

Figure 64 Map of the computational domain with building as impermeable areas

Furthermore, the last case of the SA just presented (*YES.D.-YES.B.-H.*) is defined as the "base case". The comparison is performed with this simulation run in order to understand the influence of the two last parameters.

The following table shows all the cases performed for the selected geometry;

Table 9 Runs performed during the SA for the representation of buildings in the 2D model

Case	Area sector 1 [km^2]	Area sector 2 [km^2]	Area sector 3 [km^2]	A [m]	B [m]	C [m]	D [m]	E [m]	F [m]	G [m]	H [m]
YES.D.-YES.B.-H.	2.713	1.847	3.369	0.47	0.61	0.60	0.07	0.84	0.33	0.51	0.08
ZONAL M.	3.209	1.954	3.476	0.66	0.82	0.84	0.09	0.96	0.43	0.67	0.26
BLOCKS	3.139	1.851	3.493	0.68	0.65	0.61	0.09	0.95	0.42	0.63	0.12

Considering as the "base case" the one marked in blue in the table, the main characteristics of this simulation are:

- roughness coefficient (K_s) = 0.219 m;
- mesh dimension = 20 m;
- discharge (Q) = 1840 m^3/s;
- section dimension in the 1D model = large;
- BC (upstream and downstream) = 68.51 m - 63.55 m.

The following picture shows the flooded area with the water depth.

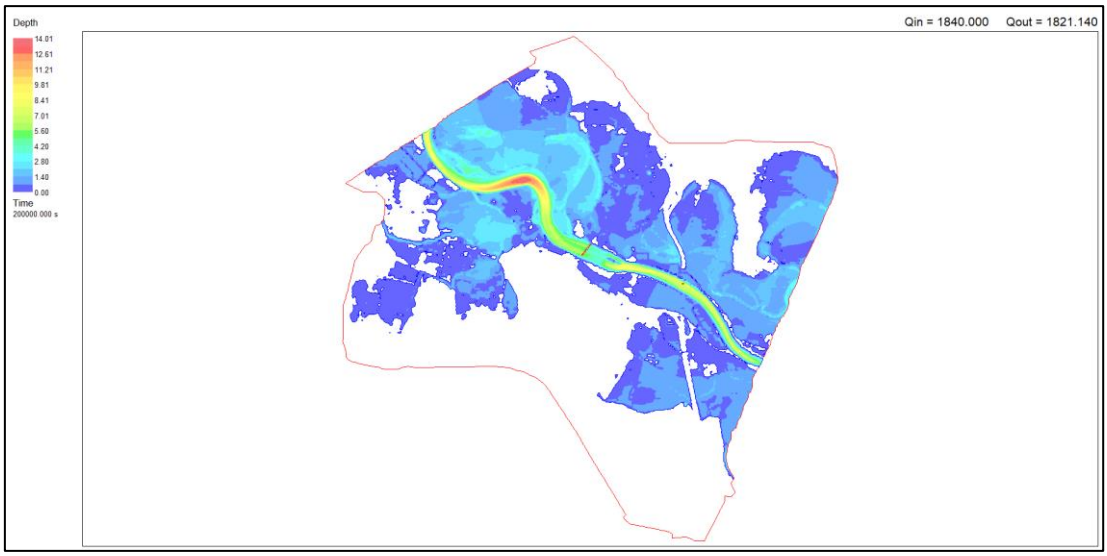

Figure 65 SA representation of buildings in the 2D model- hazard map for the "base case"

The results of the SA on cross sections dimensions are described in the graphs presented below.

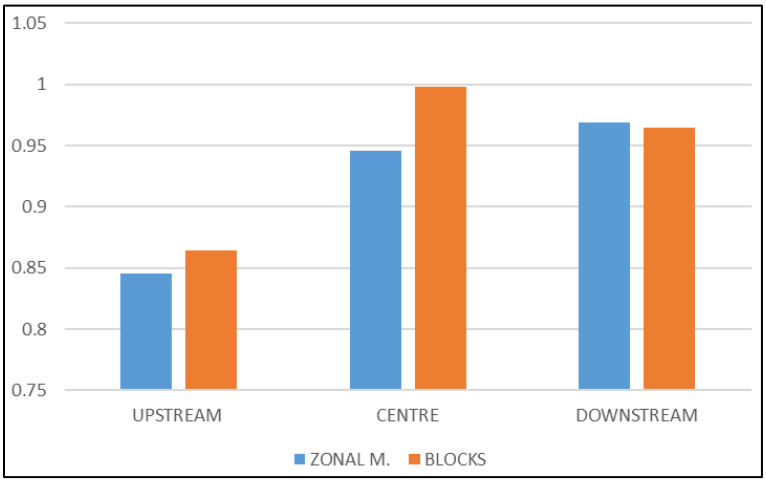

Figure 66 SA representation of buildings in the 2D model – areal coefficient

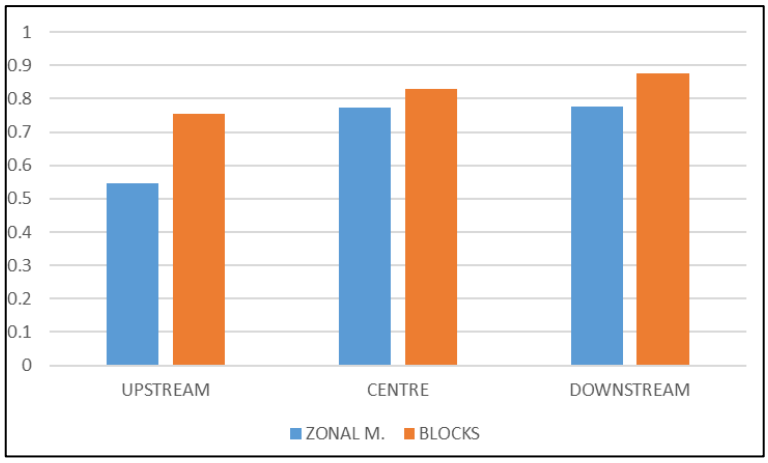

Figure 67 SA representation of buildings in the 2D model – depth coefficient

Considering the two parameters presented above, it can be found that:

- the model is slightly sensitive in the "upstream" sector, in terms of flooded area, while it is mainly not sensitive in the other sectors;
- the model is always moderately sensitive in the "upstream" sector, while it is slightly sensitive in terms of water depth in the other sectors.

Therefore, it can be deduced that the geometry of the area in the 2D model is a key parameter for the behaviour of the model, even if it is affecting mainly the "upstream" sector, where most of the geometrical elements are placed.

Considering all the parameters analysed during the SA, to start the calibration procedure it is chosen:

- Geometry of the area in the 2D model: introduction of ditches, bridges' piers and zonal Manning (3 different roughness zones)

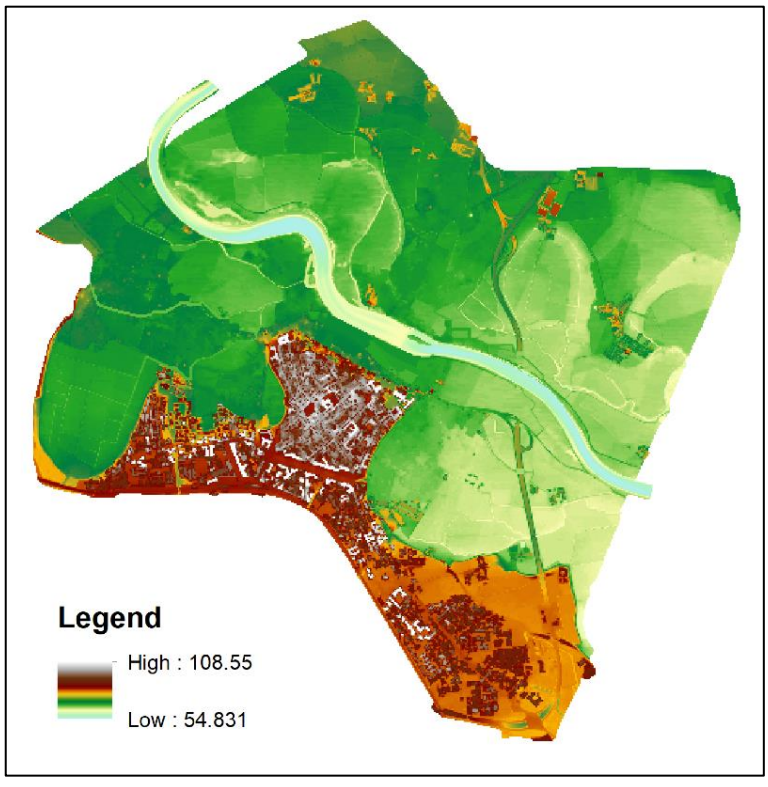

Figure 68 Geometry in the DTM to start the calibration procedure

- Section dimension in the 1D model = large, the choice of this configuration for the 1D geometry is driven by the fact that the BCs derived from the 1D model are higher. This choice results in a wider flooded area in the 2D, almost equivalent to the one that is used for the calibration procedure.
- Roughness coefficient (K_s)
  - bed roughness = 0.0776 m;
  - roughness for rural areas = 7 m;
  - roughness for urban areas = 20 m;

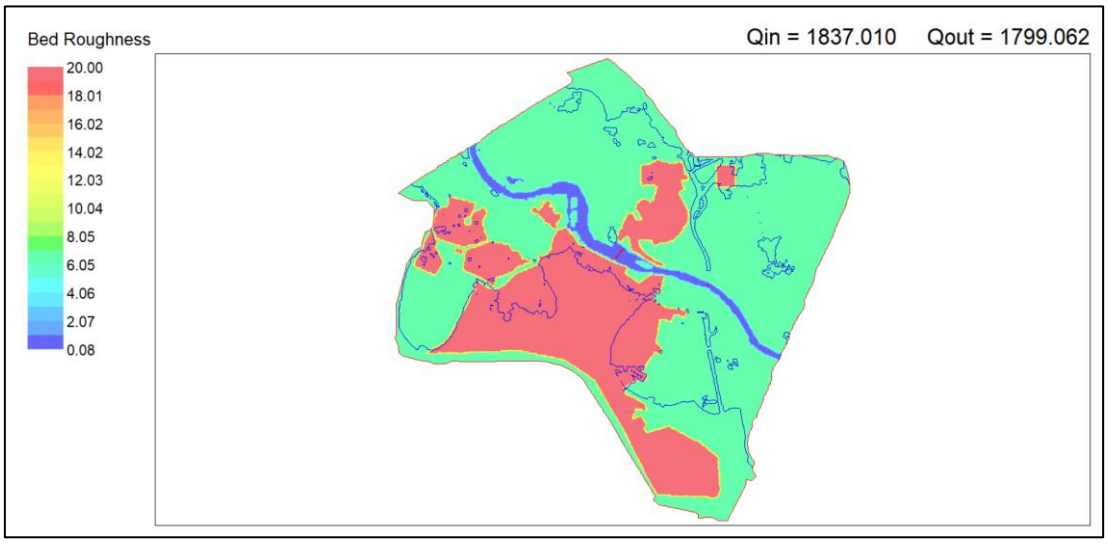

Figure 69 zonal manning to start the calibration procedure

- mesh dimension = 20 m;
- discharge (Q) = 1837 m^3/s;
- BCs size for the 2D model
  - Upstream = narrow;
  - Downstream = narrow;

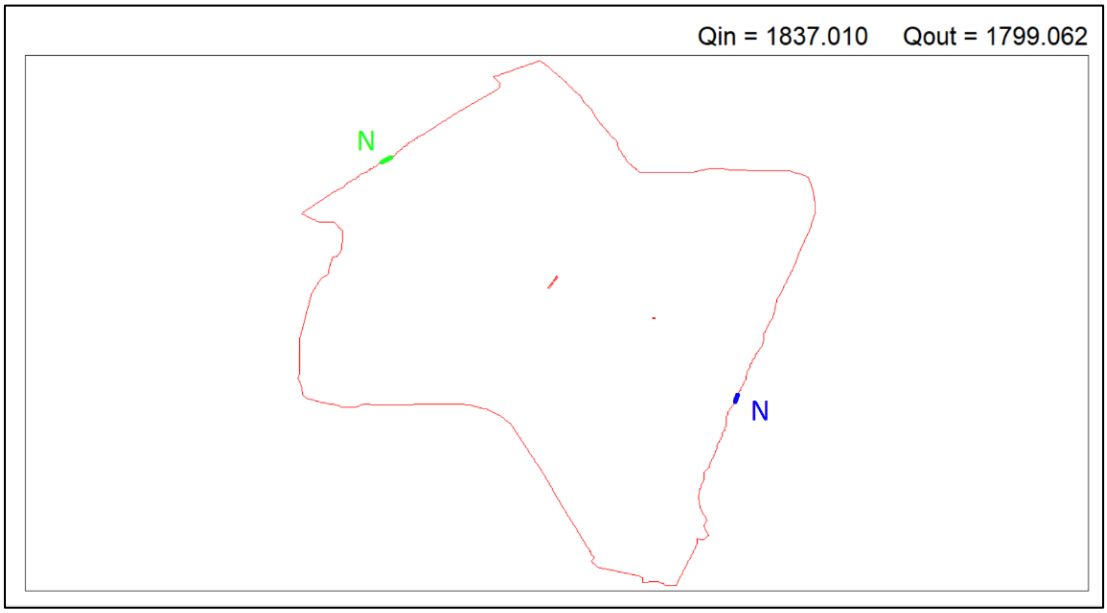

Figure 70 BC dimension to start the calibration procedure

- BC (upstream and downstream) = 68.43 m - 63.78 m;

The result of the initial simulation is presented in the following picture. In the next chapter the problem of model calibration will be explained and analysed in detail.

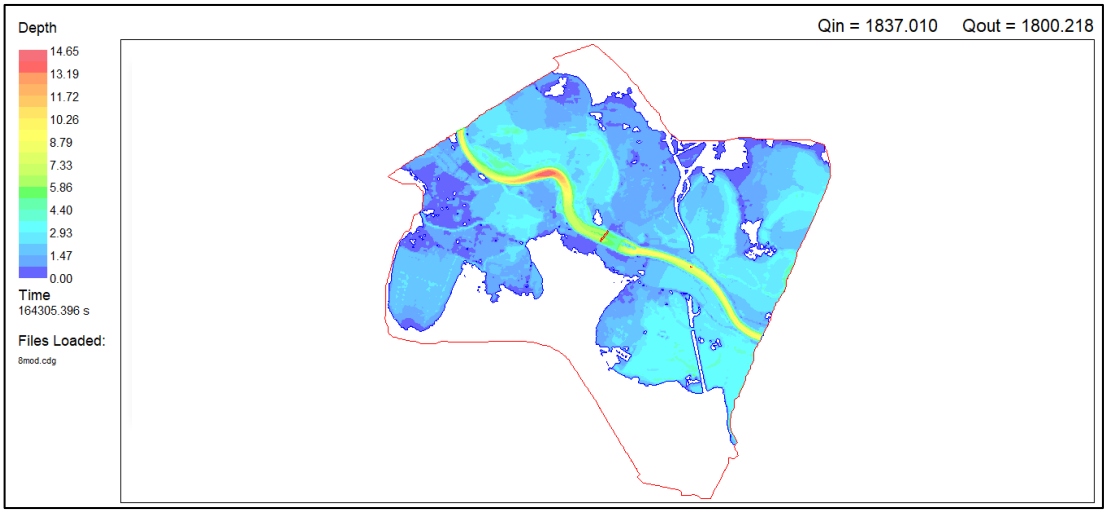

Figure 71 Resultant hazard map to start the calibration procedure

4.3 2D MODELING OF THE FLOOD EVENT

4.3.1 STEADY MODEL

As it is introduced in the chapter 3, a steady model is a condition in which the time dependency is neglected. In this simulation, discharge is constant and its magnitude is equal to the correspondent peak of the hydrograph. For river floods, a steady model with the peak discharge may return depths that are similar to maximum ones for an unsteady model (Steffler & Blackburn, 2002).

The unsteady case, on the other hand, gives an accurate dynamic of the events, but requires a very high computational effort (6/14 days for the case analysed).

Therefore, the calibration part is performed in steady conditions, due to the minor computation time and the no interest in the evolution of the flow parameters.

As introduced before, for all the steady calibration models performed in R2D, the most achieved geometry is chosen.

Although the architecture of R2D is actually an unsteady model, it can be used either to perform a transient analysis and to obtain a steady state solution. For steady state results, an accelerated convergence procedure speeds up the process to final completion by systematically increasing the time increment (Steffler & Blackburn, 2002).

Anyway, due to its unsteady nature, in steady mode the software requires the insertion of a final time used to end the simulation. This parameter should be the real final time for the unsteady case, but for the steady case is inserted as a random value, high enough to permit the convergence of the final result. The convergence is measured such as the ratio between the outflow and the inflow discharge and, to consider the simulation completed.

In the steady simulation the retarding effect does not occur, therefore, to have a complete convergence of the solution, the inflow should be equal to the outflow. The convergence value of 95% is chosen as a good compromise in terms of cost-benefits (time-precision).

4.3.2 CALIBRATION OF THE MODEL

To simulate water flow along rivers over floodplains and in urban surface water accumulation zones, simulations are often combined with Geographic Information System (GIS) techniques to build flood maps. This ideally requires substantial observed data for model **calibration** and validation. For fluvial floods, hydraulic models can use time series of historical river flows, historical rainfalls or time series of synthetic design rainfall events.(Steffler & Blackburn, 2002).

As seen in chapter 1 “Available data”, for the case under investigation, model calibration is possible, given the availability of information on the extension of the flooded area, on water stage at the bridge *Napoleone Bonaparte* and on the 266 observed water levels in different various places of Lodi.

After the complete definition of the geometrical characteristics of the model, the only parameters that must be accurately evaluated are the values of the roughness coefficients and section dimension in the 1D model

The calibration procedure of the latter parameter is not performed because the most suitable solution for this parameter is already selected.

The method to reach the best combination of coefficients is recursive: the first simulation is performed starting with the roughness values determined in the sensitivity analysis. At the end of each simulation, a postprocessing of the results is done based on the quality indicators, as explained in the “Methodology” section (Chapter 3). The values of Manning’s coefficients are changed according to the behaviour of the water depth (WD) of the control points in each zone. At the end of each attempt, another simulation is prepared to run with the new configuration.

The following flow diagram synthesizes the entire recursive process.

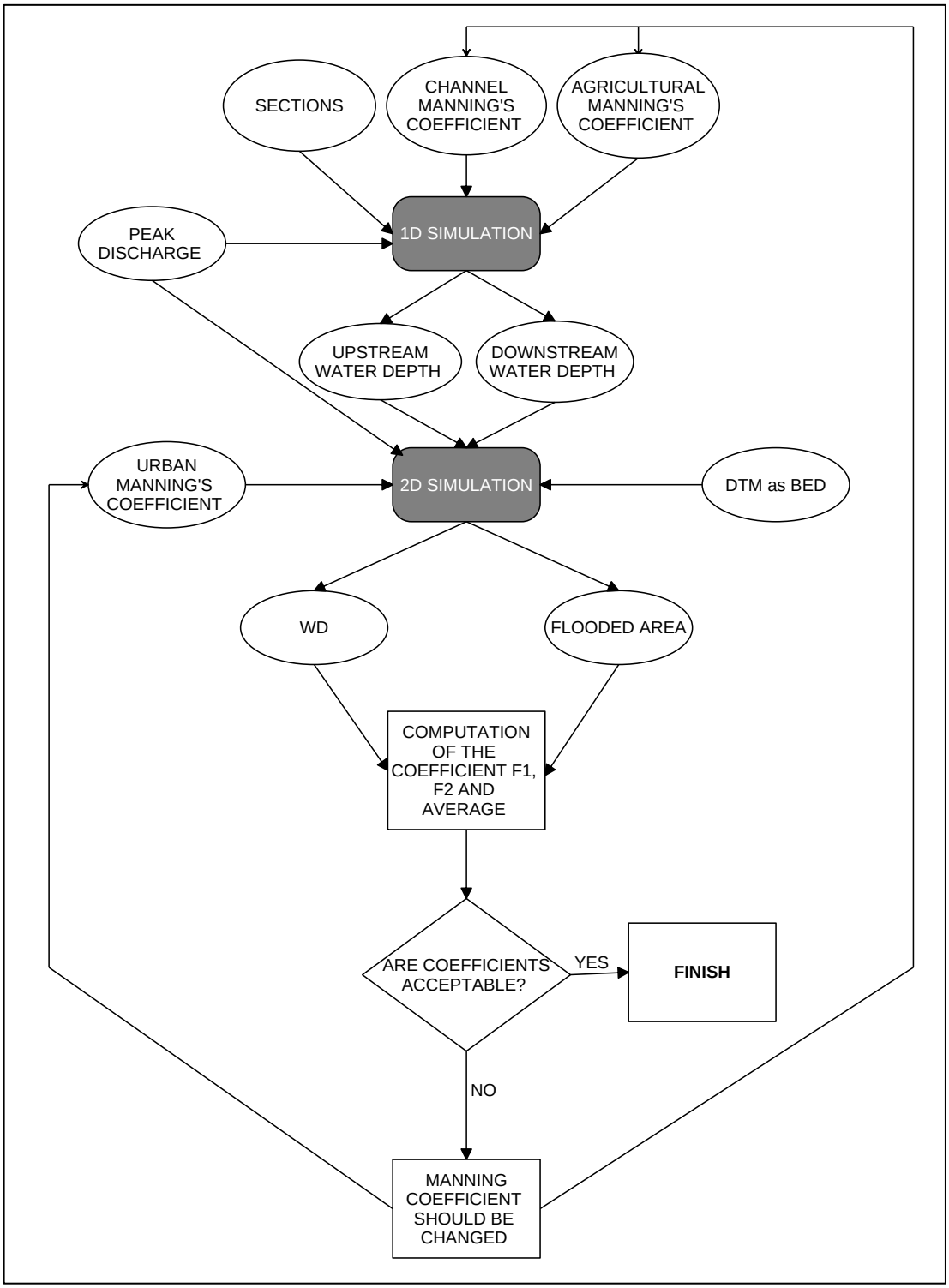

Figure 72 Recursive process to find the best simulation

A résumé of all the calibration runs is illustrated below:

Table 10 The parameters highlighted in bold are the main changes made with respect to the previous calibration run

	Channel		Rural		Urbam		B.C. from 1D simulation [m a.s.l.]	
	n [s/m1/3]	Ks [m]	n [s/m1/3]	Ks [m]	n [s/m1/3]	Ks [m]	Upstream	Downstrem
1	0.025	0.0776	0.09	7	0.228	20	68.43	66.78
2	0.025	0.0776	0.09	7	0.228	20	68.46	66.08
3 -25% Overbank	0.025	0.0776	**0.0675**	**3.93**	0.228	20	68.42	65.96
4 (Urban - 0.25%)	0.025	0.0776	0.09	7	**0.171**	**15.9**	68.46	66.08
5 -25% Channel	**0.0187**	**0.0097**	0.09	7	0.228	20	67.94	65.3
6 -15% O.B. - 8%Ch.	**0.023**	**0.05**	**0.0765**	**5.16**	0.228	20	68.45	66.01
7	**0.0264**	**0.11**	0.0765	5.16	0.228	20	68.55	66.07
8	0.0264	0.11	**0.0826**	**6**	0.228	20	68.56	66.1
9	**0.025**	**0.0776**	**0.0765**	**5.16**	0.228	20	68.45	66.01

At the end of each 2D computation, data are imported in GIS environment and consequently the water surface elevation (WSE) in each control point is extracted. Values are exported in Excel and the quality coefficients for each zone are automatically computed.

Quality indicators used are described in detail in chapter 3.2:

- F1: Nash-Sutcliffe efficiency may range between 1, goal value, and -∞.
- F2: Flood area index defines the performance of the model predicting inundation extent; the goal value is 1.
- Average of the difference (AD): difference between the simulated and estimated water surface elevation; the goal value is 0.
- Average Absolute difference (AAD): absolute difference between the simulated and estimated water surface elevation; the goal value is 0.

The quality indicators are separately analysed for each zone in order to decide how and where an increase or decrease of the Manning's coefficient is necessary.

Afterwards, to evaluate which is the best calibration attempt, an average value for each coefficient is calculated in the different zones, obtaining 4 total indicators for each calibration attempt.

The following figures show the trend of each coefficient computed in the different attempts.

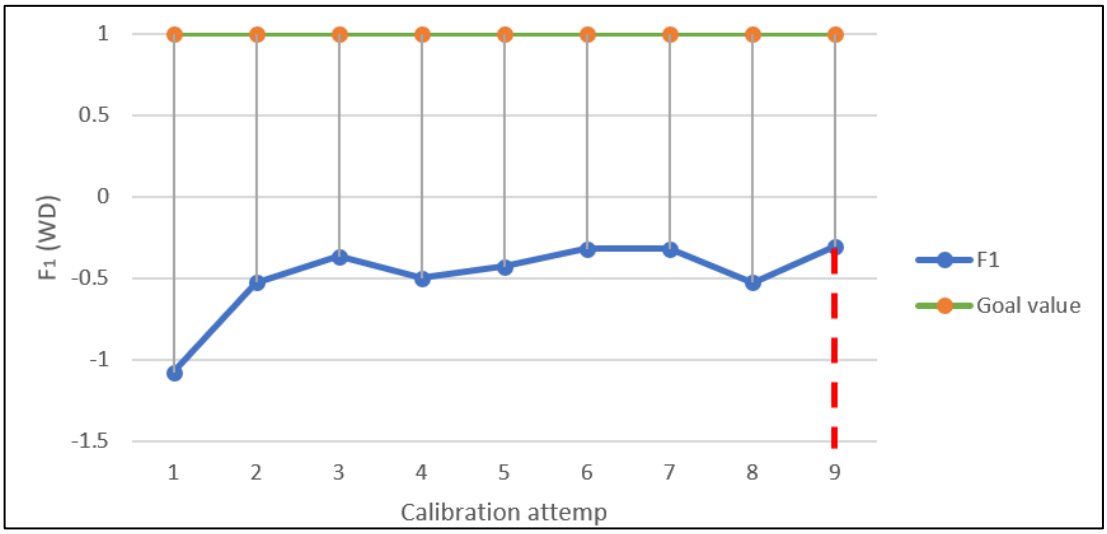

Figure 73 F1 indicator trend for the different calibration attempts. The best one is the 9th.

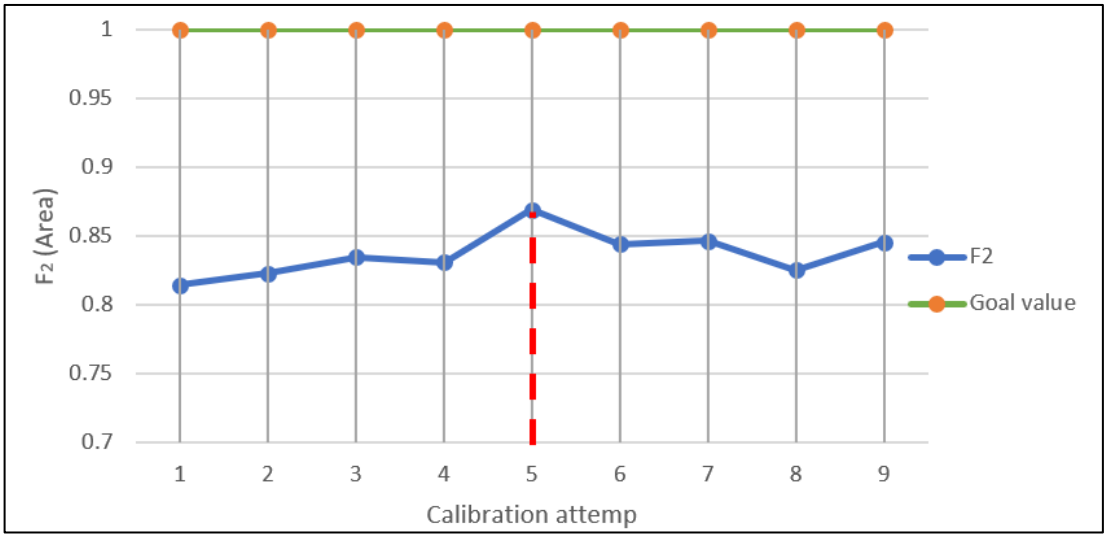

Figure 74 F2 indicator trend for the different calibration attempts. The best one is the 5th

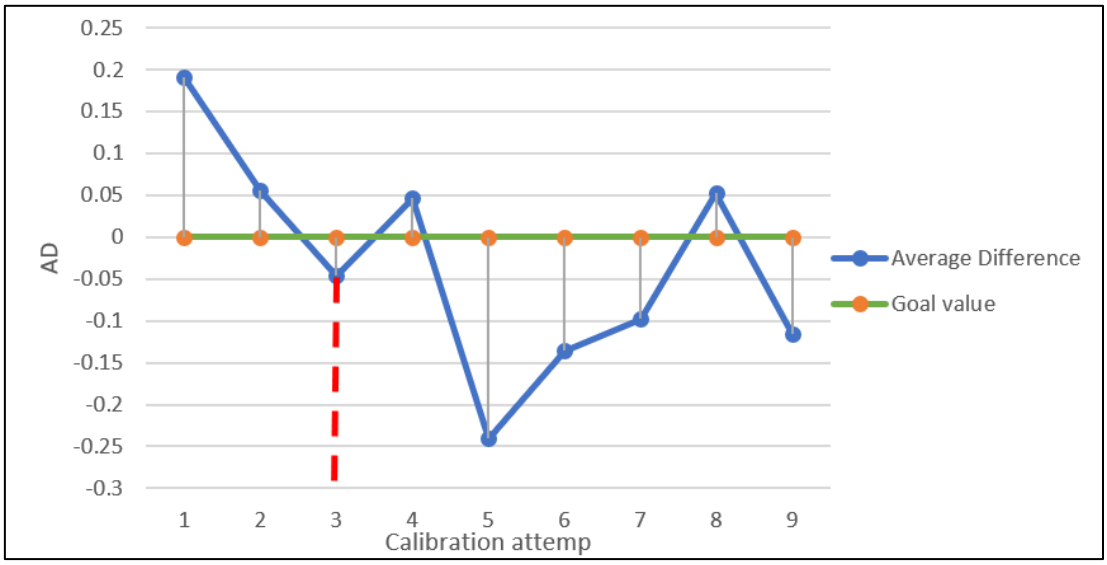

Figure 75 The average of the difference indicator trend on the different calibration. The best one is the 3th.

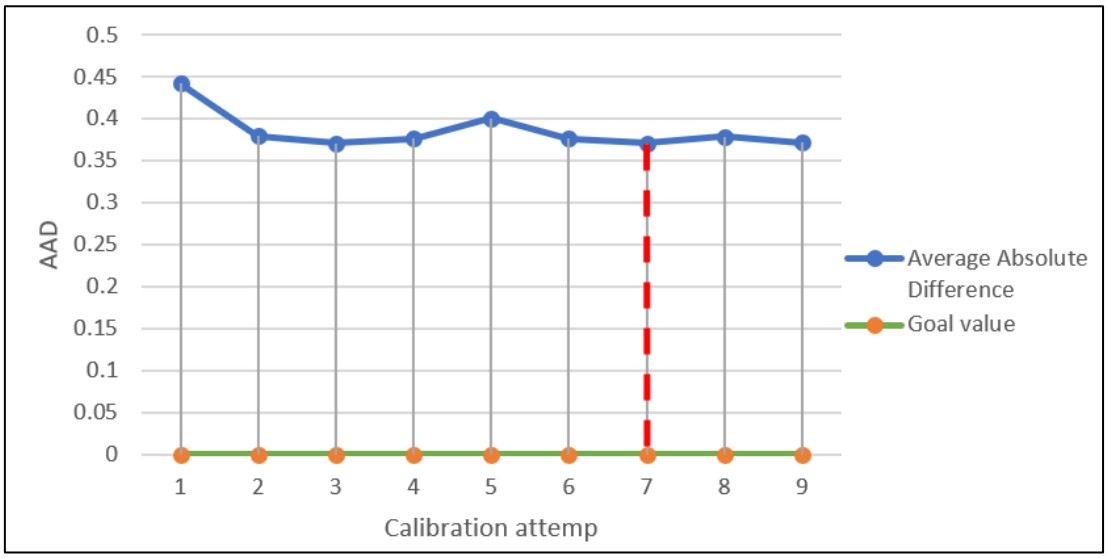

Figure 76 The Absolute Average Difference indicator trend on the different calibration. The best one is the 7th.

Considering that there is not a unanimous best run as results of the quality indicators, another final indicator is created, defined as the average of the aforementioned ones.

This final indicator shows which calibration fulfil the best compromise among the quality indicators.

The following Table, reporting the final indicator values, shows that the calibration run 3 is the best compromise of quality.

Table 11 Final indicator for the calibration procedure

Simulation	1	2	3	4	5	6	7	8	9
Score [0-1]	0.25	0.61	0.68	0.63	0.54	0.60	0.64	0.61	0.63

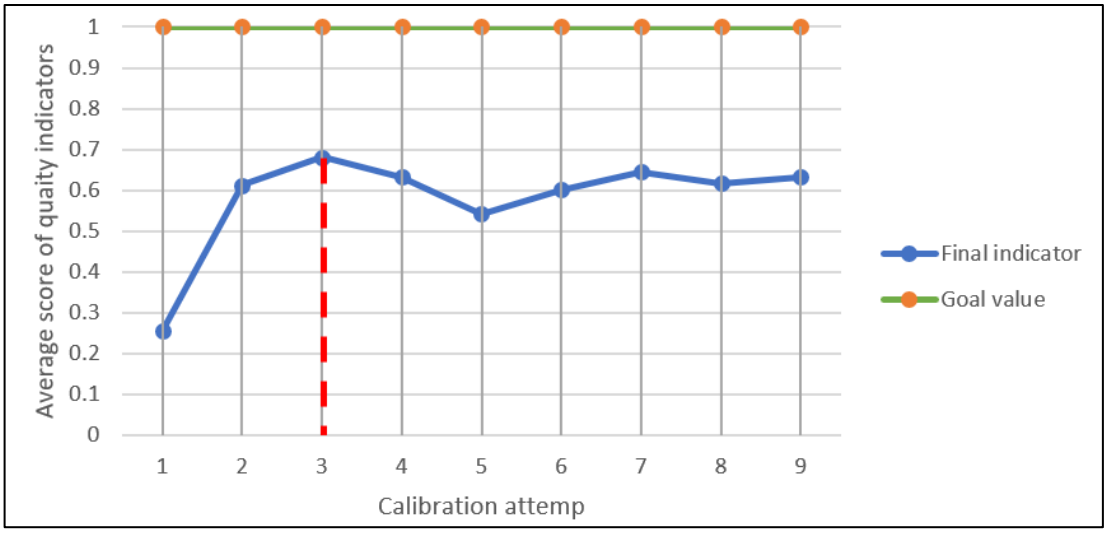

Figure 77 The trend of the Average score quality indicator in the calibration attempts

The detailed values of the quality indicators for the calibration number 3 (divided by zones), taken as the best one, are shown hereinafter.

In the column “average of the difference (AD)”:

- If the value is negative, it means that in the corresponding area, we have an underestimation of the water depth computed compared to the measured one.
- At the contrary, if it is positive, we have an overestimation.

Table 12 indicators results for the best steady run

CALIBRATION 3 (-25% Agric) KS Channel:0.0776 m; Agric.:3.96 m; Urb:20m				
ZONE	**Average of the diff.**	**Average absolute diff.**	**F_1**	**F_2**
A	0.094	0.209	-0.245	**0.835**
B	-0.006	0.292	0.052	
C	0.341	0.422	-2.481	
D	0.176	0.331	0.392	
E	-0.390	0.571	-0.045	
F	-0.184	0.359	-0.188	
G	-0.161	0.376	-0.106	
H	-0.235	0.408	-0.310	
Total	**-0.046**	**0.371**	**-0.366**	

As it can be observed from the Table 12, calibration 3 is realized with the following roughness coefficient:

- channel: n=0.025 [s/m$^{1/3}$] / Ks=0.0776 [m];
- rural: 0.0675 [s/m$^{1/3}$] / Ks=3.93 [m];
- urban: 0.228 [s/m$^{1/3}$] / Ks=20 [m].

This combination will be used for the final unsteady simulation.

4.3.3 RESULTS OF THE CALIBRATION RUN 3

The results of this computation can represent, with a good reliability, the extension of the flooded area, water depth, flow direction and velocity of the real event at its peak. Unsteady analysis will give the same type of results, but for each moment of the event. In the following some results are shown:

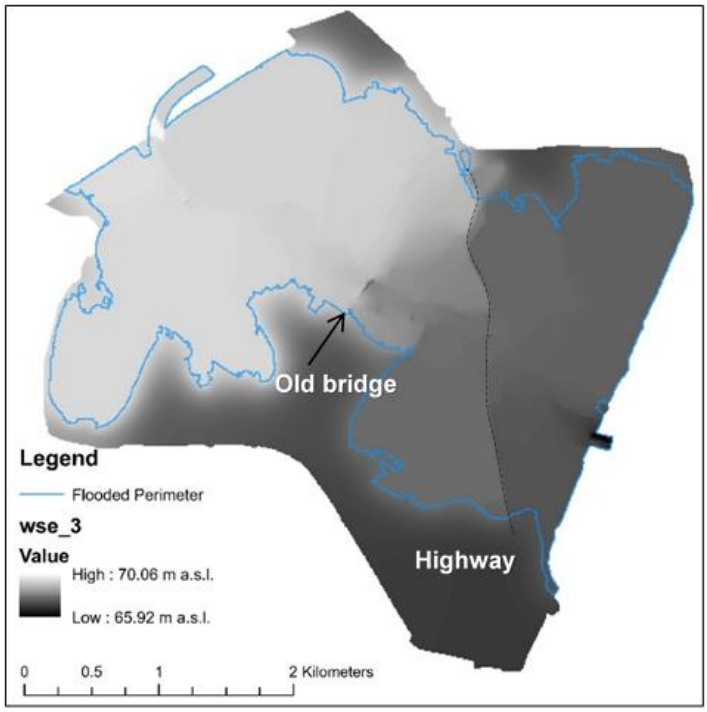

Figure 78 WSE map and some infrastructure highlighted

Figure 78 shows the result coming from the run 3. As we can see, the water level in the upstream part is approximately uniform, while we have an abrupt decrease of WSE downstream from the bridge, despite the bed elevation does not change significantly. The reason can be found to the dam effect caused by Napoleone's bridge and to the presence of a little weir downstream of it (*briglia*). Another difference in the WSE levels is evident between the left and right side of the highway. In this case, the embankment triggers a dam effect that corresponds in an extension of the flooded area

The presence of water outside the observed flooded perimeter, is due to the fact that R2D considers also the infiltration process. Therefore, inside the perimeter, the water level is higher than the bed elevation and outside, on the contrary, the liquid is underground.

To obtain the map of the WD, is necessary a subtraction between WSE and bed elevation. This computation is easily executed by the "raster calculator tool" in GIS. Since the WSE map and the bed map are both raster files with same cell size, a simple subtraction is done obtaining the water levels in each point.

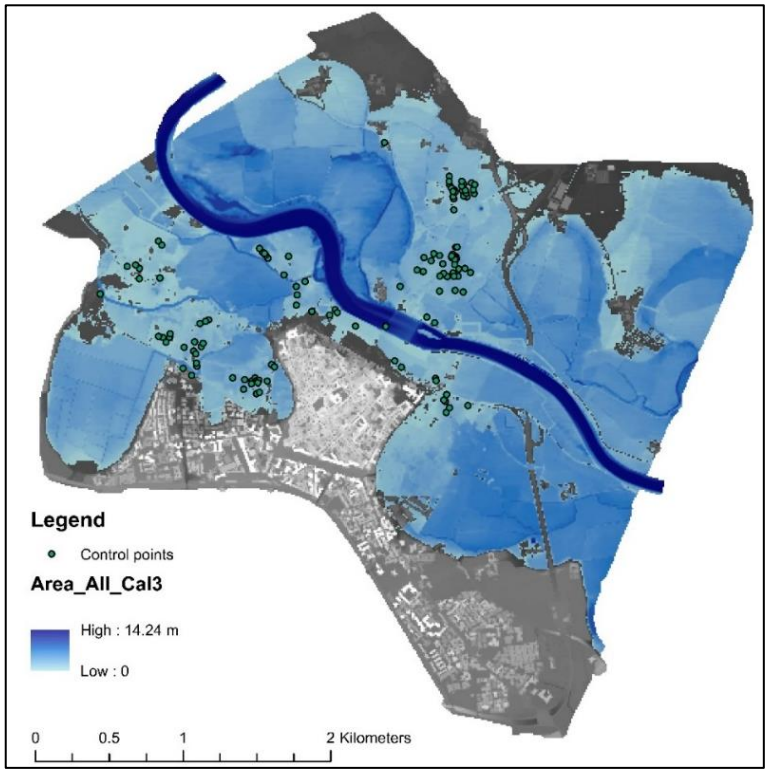

Figure 79 Hazard map: WD map of the calibration 3 with the control points

From this map, still using GIS, the values of WD in each control point are extracted and the value of the flooded area is computed (9.38 km^2). These values are compared with the reference values obtaining the difference and the quality indicators described before.

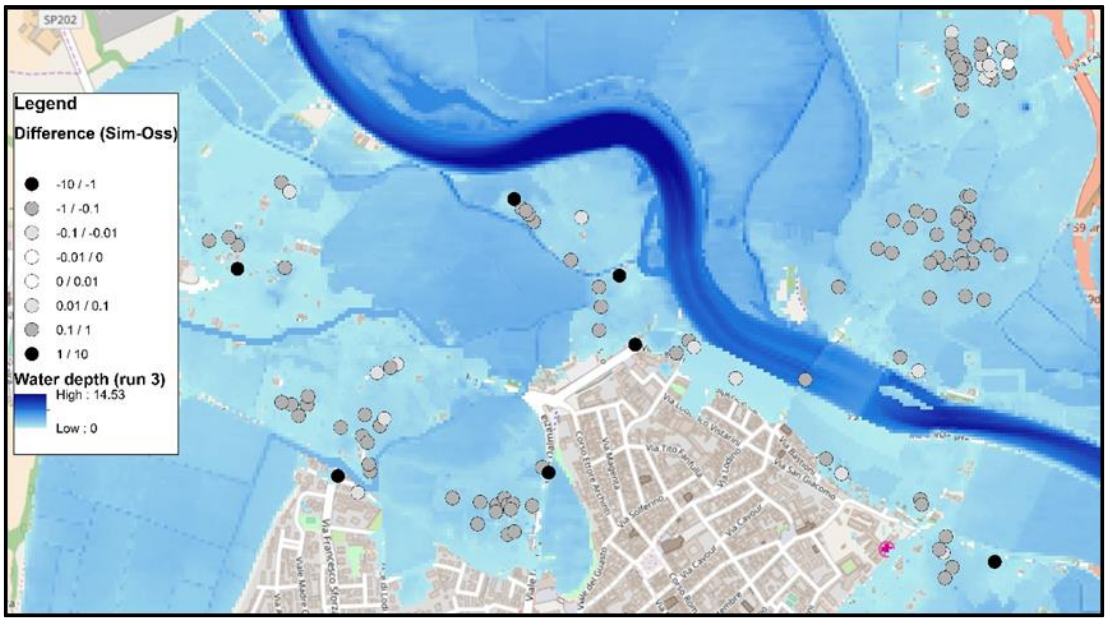

Figure 80 Difference between simulate and observed depth (logarithmic scale)

Considering the calibration attempt under analysis, the following graphs can be produced based on the depth values extracted in the control points.

The graphs are produced during the calibration phase of the steady analysis also for the other runs, which are not reported here because they are considered not useful for the purposes of the thesis.

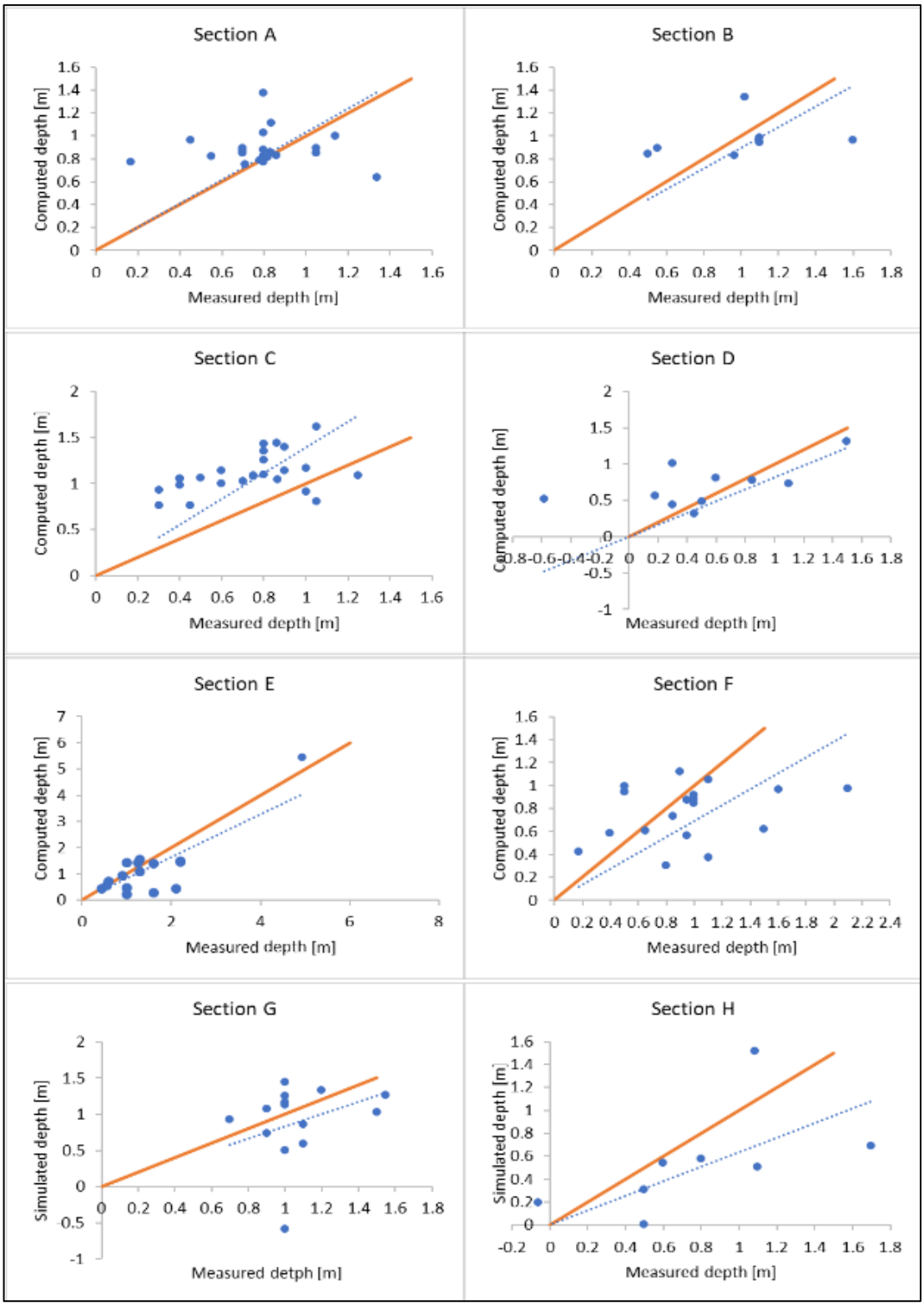

Figure 81 Scatter (dispersion) plots of measured vs simulated depths in the different zones (calibration 3)

The scatter plots in Figure 81 show a comparison between simulated and the observed water depths.

If the computed value is equal to the measured one, the point will overlap the bisector (orange line). The further the point deviates from the bisector line, the more the computed value is far from the one measured. In each graph is also present the trend line passing from the axis origin (dotted line), that shows the general behaviour of the data compared to the bisector line. The more the dotted line is close to the orange one, the more the computed measures are similar to the observed ones. With this approach it is possible to understand in a qualitative way, by checking the graph, the behaviour of results in the corresponding zone.

Analysing the graphs is possible to understand that there is a general underestimation of the depth in the zones, in particular the zones:

- B, D, E, F, G, H have computed water depths underestimated respect to the measured ones;
- A, C have computed water depths overestimated respect to the measured ones.

Even if this result is already deduced by the parameter “average of the difference”, this graphical visualization is helpful to understand the presence of possible geometrical singularities of the terrain that are influencing the results of the simulation

The two set of graphs below (Figure 83Figure 84 and Figure 84) shows another technique to represent the distribution of the measured points compared to the computed solution.

In each zone a perpendicular and a parallel line to the direction of the flow are drawn. Subsequently, on the two lines a projection of the points is done, resulting in two graphs: the first one contains the projection of the data on the direction parallel to the flow, the second one comprises the projection of data on the direction perpendicular to the flow.

The big advantage of using these representations is that the possible change in WSE is described in more detail.

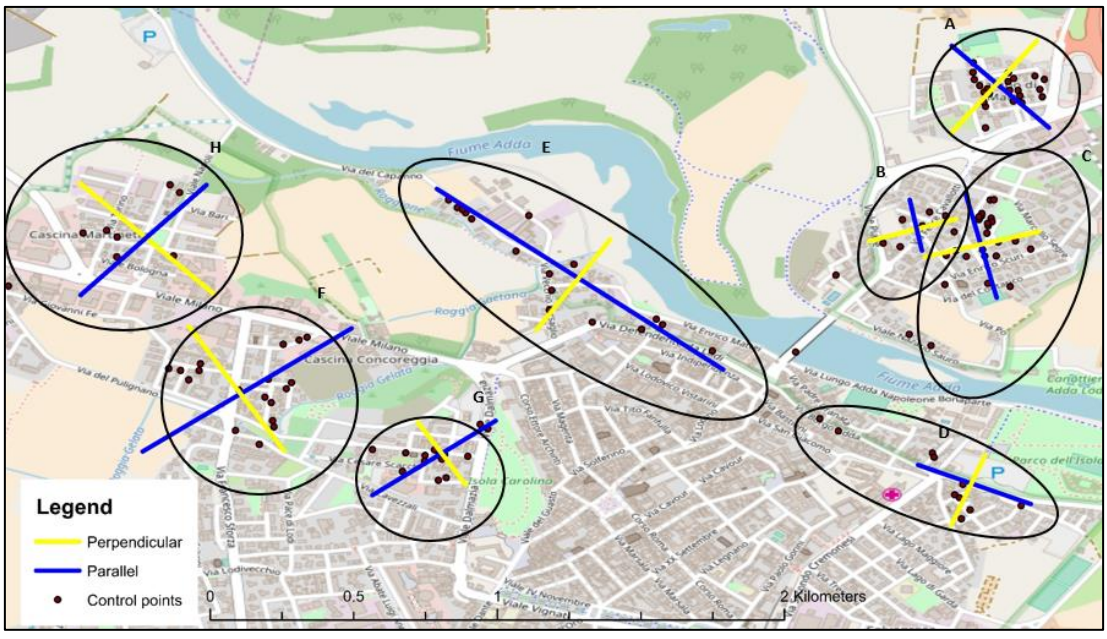

Figure 82 Perpendicular and parallel section used to draw the projection

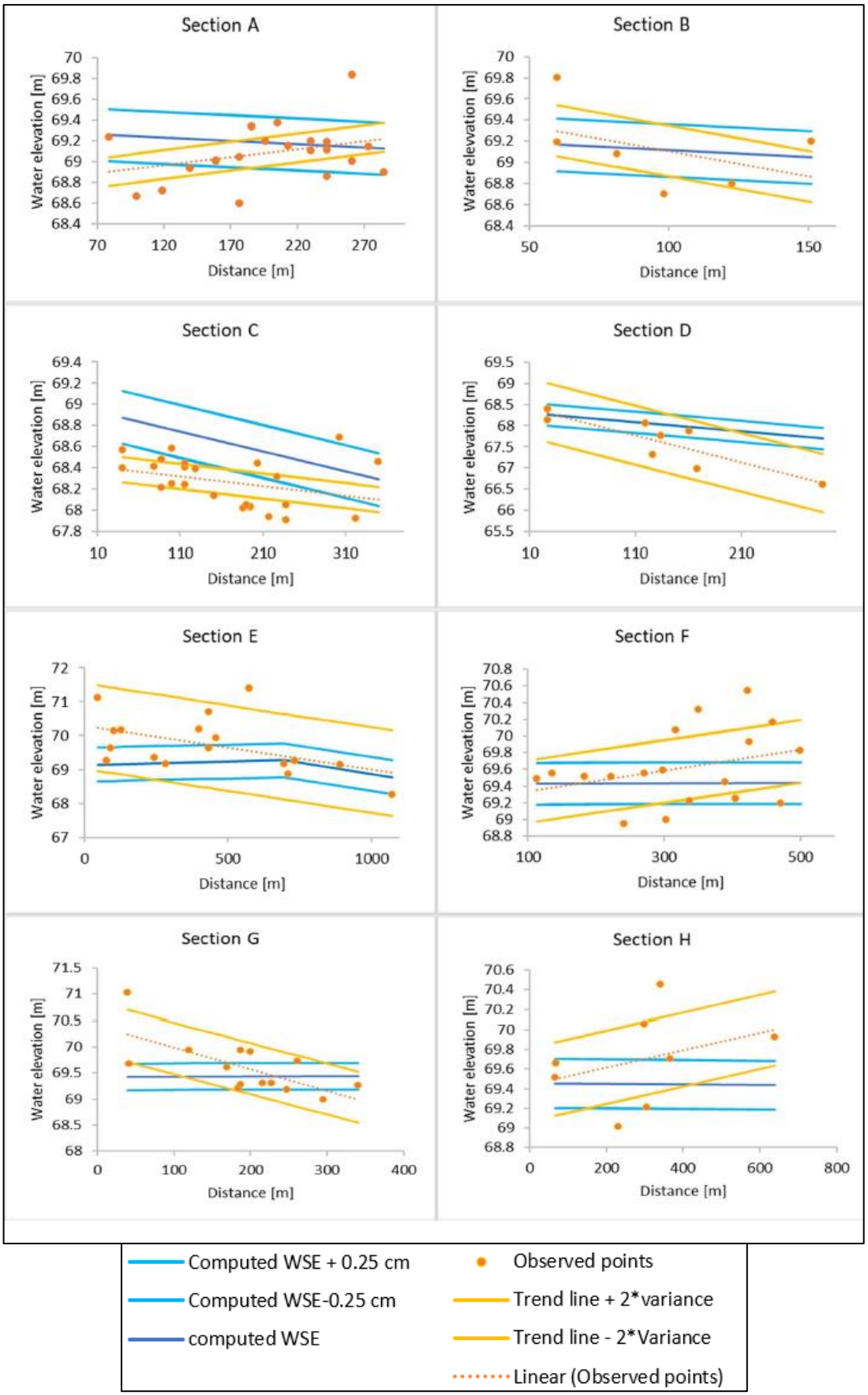

Figure 83 the distribution of the measured points compared to the computed solution - parallel projection

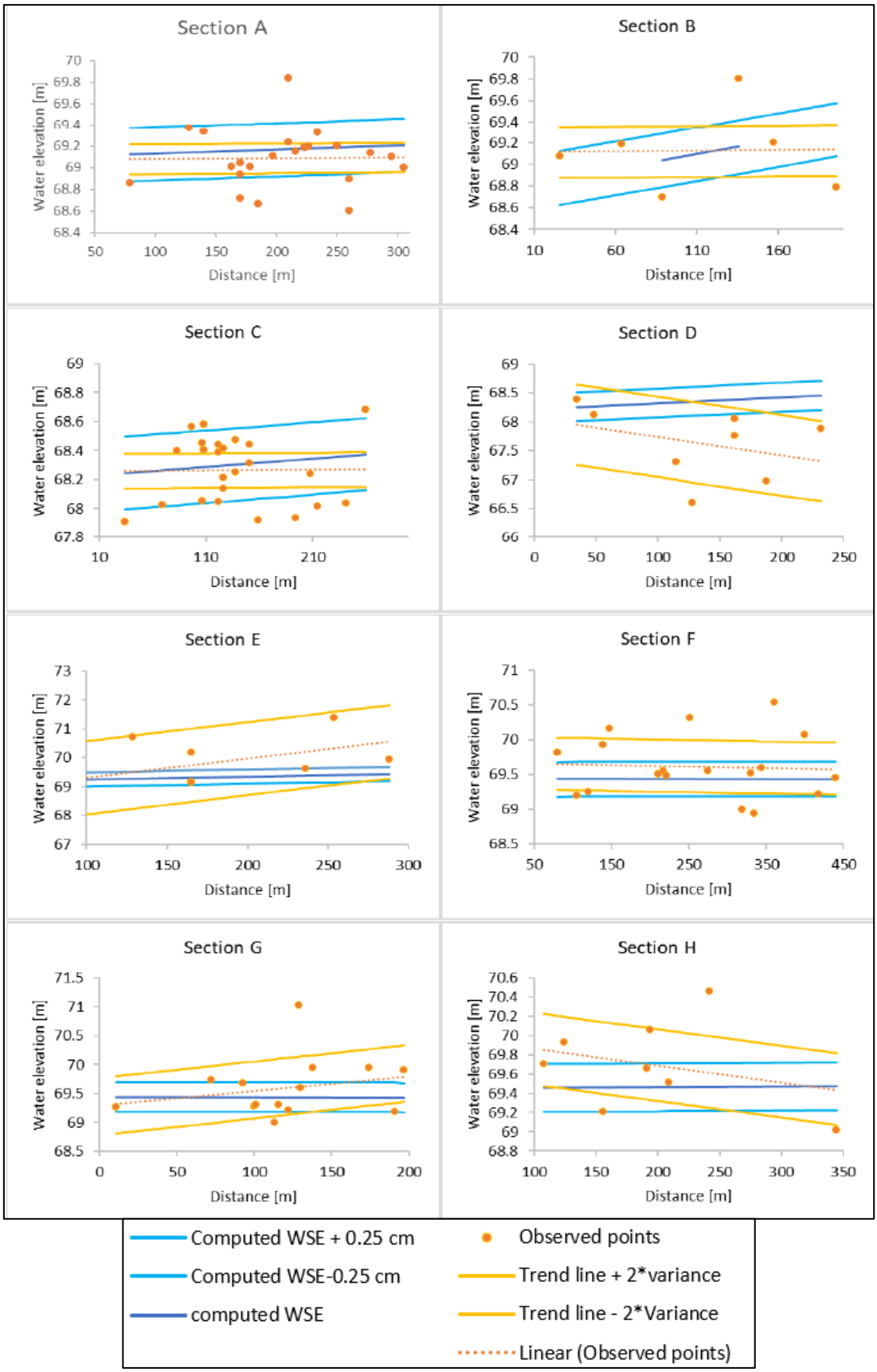

Figure 84 the distribution of the measured points compared to the computed solution - perpendicular projection

From the above graphs it can be deduced, that some outcasts are present in the group of data that are used in the calibration phase.

The number of these points is generally low respect to the total number of points available, thus it is not influencing the quality indicators in a significative way. Nevertheless, with the dispersion graphs presented before, it can be verified that the result of the quality indicator is still reliable even with some outcasts in the data.

More insights can be derived from the analysis of the velocity distribution map.

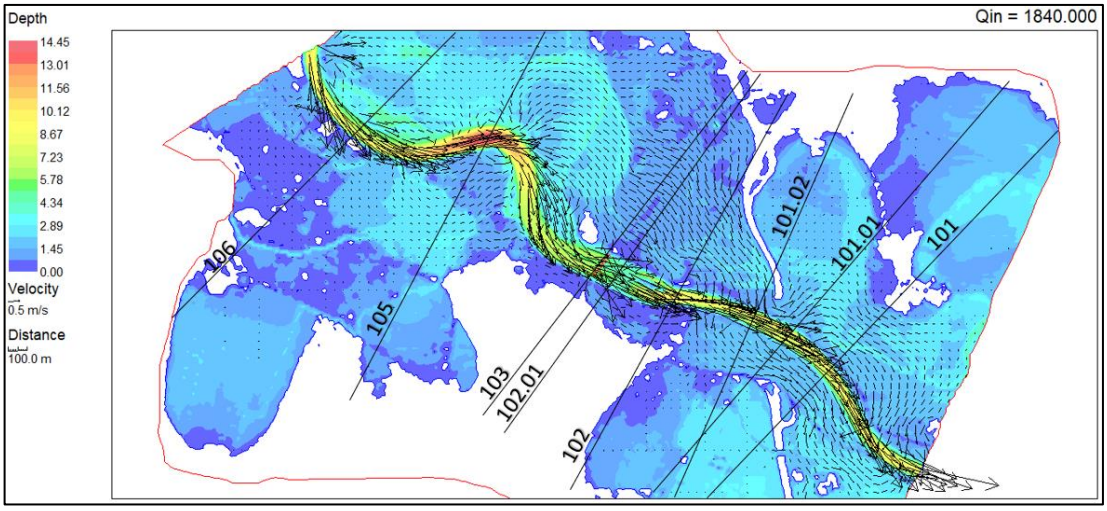

Figure 85 Flow direction and velocity magnitude overlapped to the WD

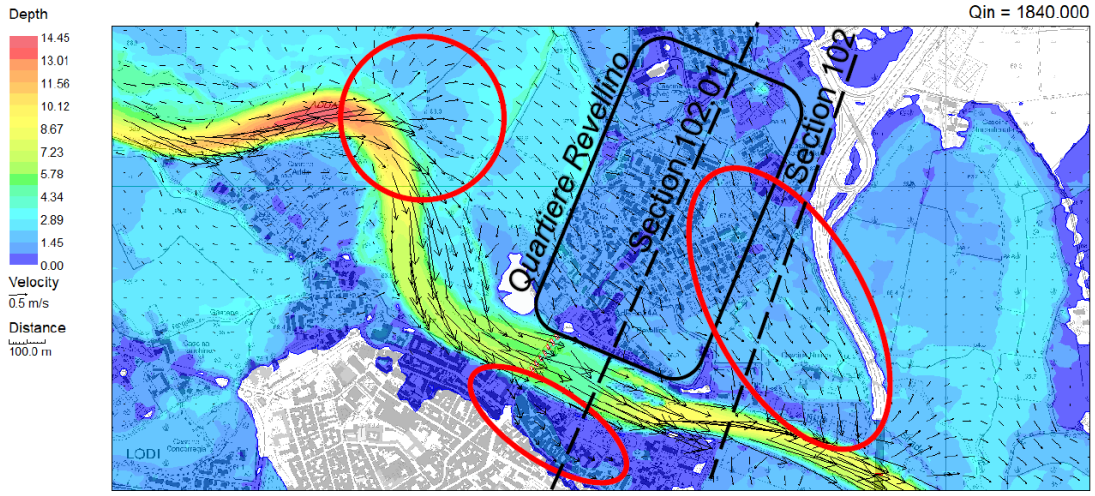

Figure 86 Detail of flow direction and intensity near the old bridge and the Revellino neighbourhood

Figure 85 provides a detailed representation of the flow direction and magnitude resulting from the R2D simulation. From this type of analysis, it is possible to investigate and understand if the features of the flood inundation obtained with the steady simulation are coherent with those illustrated in the reports and newspapers describing the event. Figure 86 clearly confirms that the model can also correctly describe the dynamic of the event: in fact, the *quartiere Revellino* is flooded by the water overflowing from the upstream curve, as it is presented in the available records.

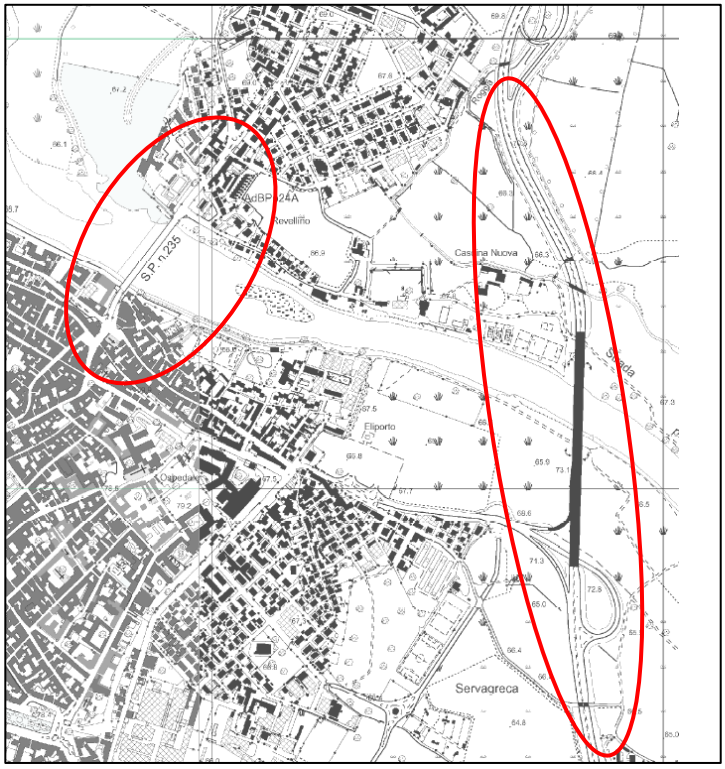

Figure 87 Infrastructures that affects the flow direction

The effect of artificial infrastructures is now analysed (Figure 87); in fact, the highway (tangenziale) and the bridge Napoleone Bonaparte, can create a dam effect and deviate the flow of water with a consecutive increment of WD.

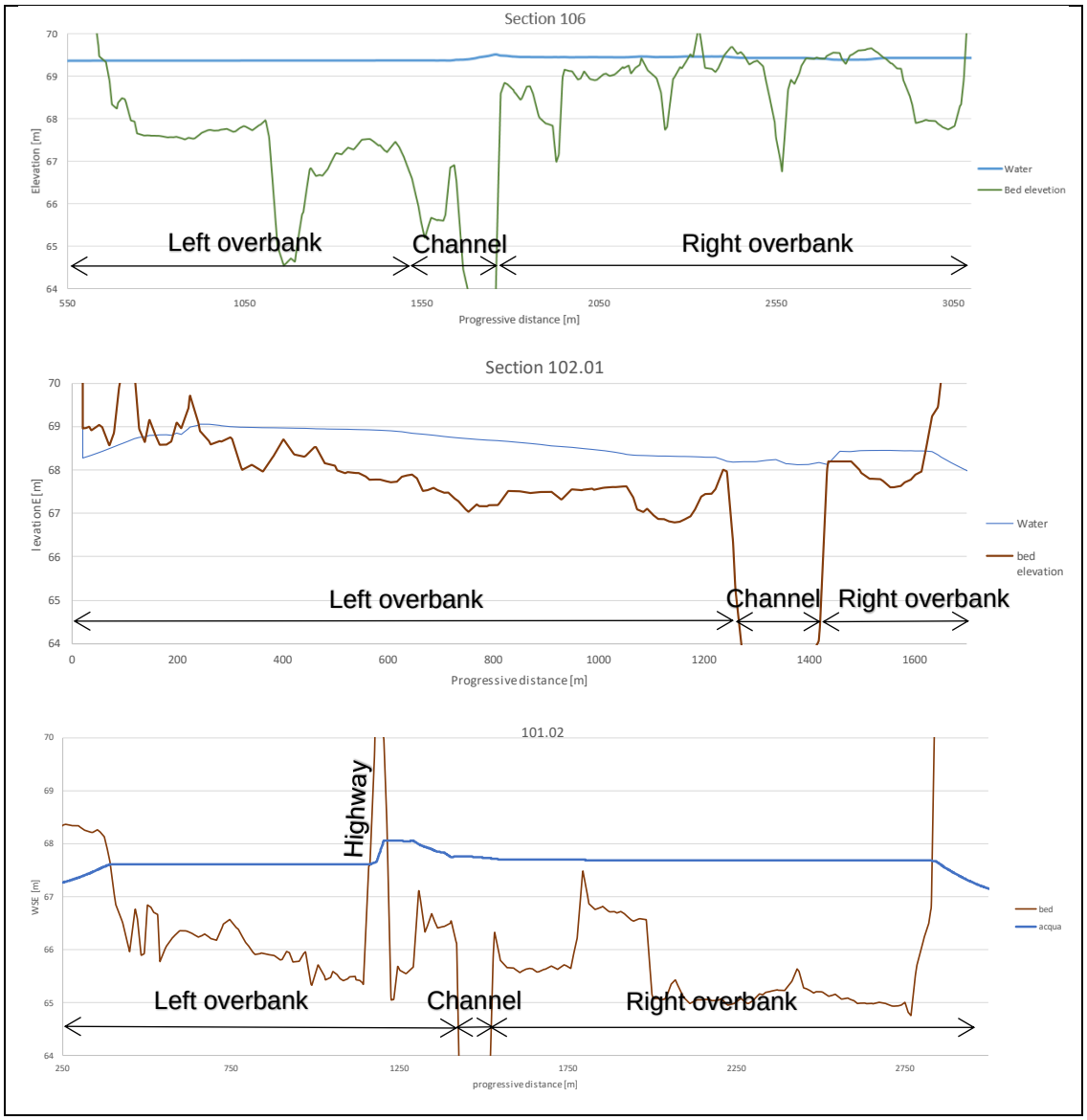

Figure 88 Sections extracted from R2D where flow direction does not influence WD (section 106) and where flow direction influence WD (section 102.01 and 101.02)

(To better understand the above figures and the following explanation, it is suggested to see the position of these sections looking Figure 85)

Figure 88 shows the effect of flow direction on WD. In the left overbank, water levels are higher than those in the channel because of the inflow coming from the curve: as a consequence, lateral flow occurs. This effect is also evident in the right overbank of the section 102.01, but in this case, higher levels are due to the dam effect of the upstream bridge.

All the observations described above are more evident with the unsteady simulation, thanks to which is possible to follow the dynamic of the flood event with time.

4.3.4 UNSTEADY MODELLING

In a transient simulation, the objective is to obtain accurate spatial results throughout the duration of a specific temporal event (Steffler & Blackburn, 2002). This means that it is possible to obtain the entire dynamic of the flood event, in terms of flow path, water levels and flooded area.

The unsteady simulation is performed considering the geometry parameters of the most reliable simulation obtained in the steady regime (4.3.2).

For unsteady modelling:

- the BC are expressed as a discharge hydrograph (graph of discharge versus time) and stage hydrograph (graph of levels versus time) obtained from the 1D unsteady computation (Steffler & Blackburn, 2002);
- initial condition must be specified at every point in the computation domain and should reflect the flow conditions prior to the simulation event. (Bettiga, 2016).

To initialise the process, a warm up phase is needed. Practically, the discharge and the stage hydrograph are modified adding a series of 10'000 time steps with a constant value equal to the first one of the correspondent original graph (Figure 49 Discharge hydrograph inserted in HEC-RAS).

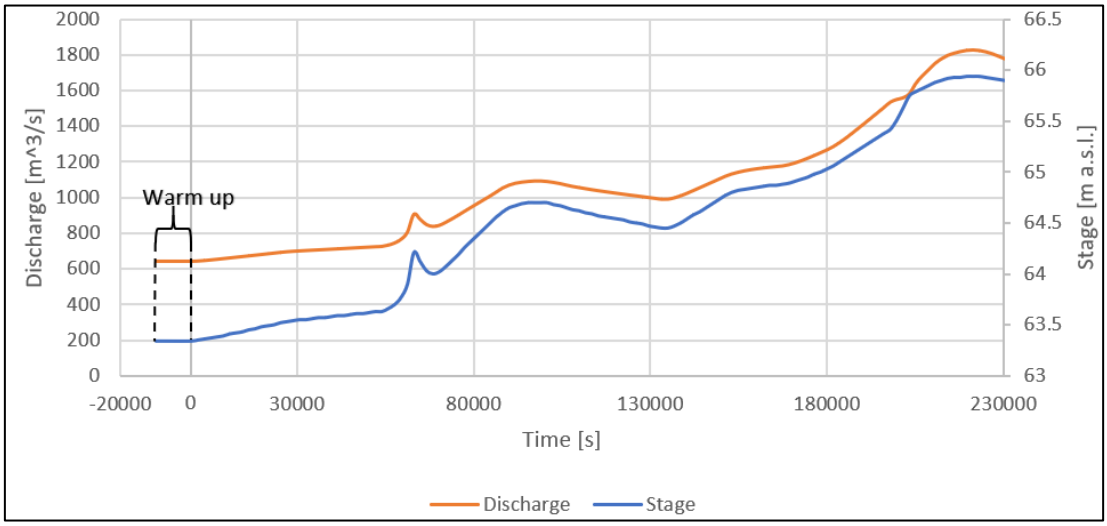

Figure 89 Stage and discharge graphs, with the 10'000 sec warm up highlighted

Other two important parameters should be set before running the simulation: Groundwater Transmissivity and Groundwater Storativity. As defined in 3.3, these two parameters are chosen based on calibration tests performed in others works regarding urban flood modelling (Bettiga, 2016).

The Groundwater Transmissivity, responsible for the rate at which groundwater flows horizontally through an aquifer, is set to 0.1.

The Groundwater Storativity, responsible for the quantity of release storage water, is set to 0.01.

Initial and final time should be set equal to 0 and to duration of the event (in our case 460'800 seconds, i.e. 128 hours), respectively. The software, in case of unsteady simulation, allows to choose three types of output:

- video output: to obtain a direct dynamic of the flooded area (set at 1800 sec);

- point output: to have the entire dynamic of WD and WSE of each control points (set at 1800 sec);
- R2D file output: to have the full set of information in the case of necessity of some more detailed analysis in a specific time step (set at 5000 sec).

The time required to execute the model depends on the time necessary for the phenomenon to propagate through the domain and on the size of the time step increment.

In this specific case, computational time for completing the unsteady simulation is about 14 days (336 hours), with the peak flow, which occurred after 65 hours in the real time scale, computed in 144 hours.[25]

The following figures show some output snapshots taken in the most interesting time steps.

[25] The computer characteristics are: Intel Core i7-4790 4-core CPU with 3.60Ghz, 8 GB DDR3 RAM. But due to the limitations of the SW, only the 31/35% of the computing power is used.

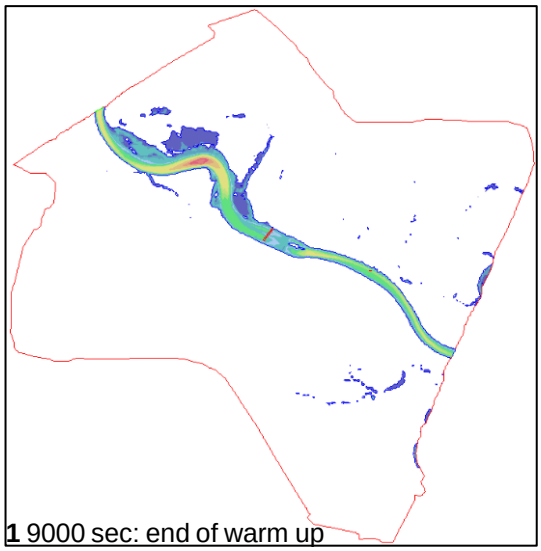

1 9000 sec: end of warm up

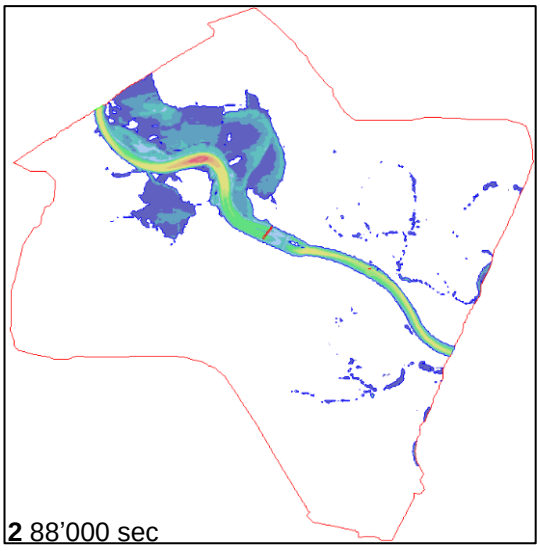

2 88’000 sec

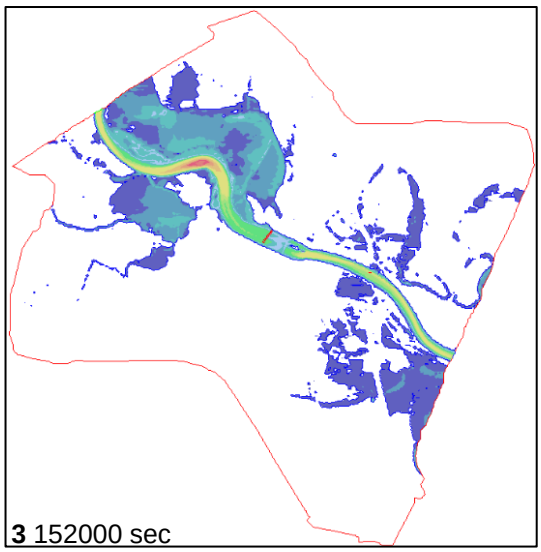

3 152000 sec

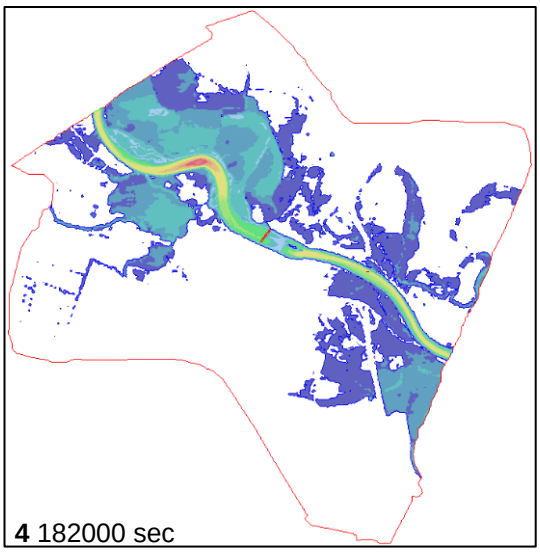

4 182000 sec

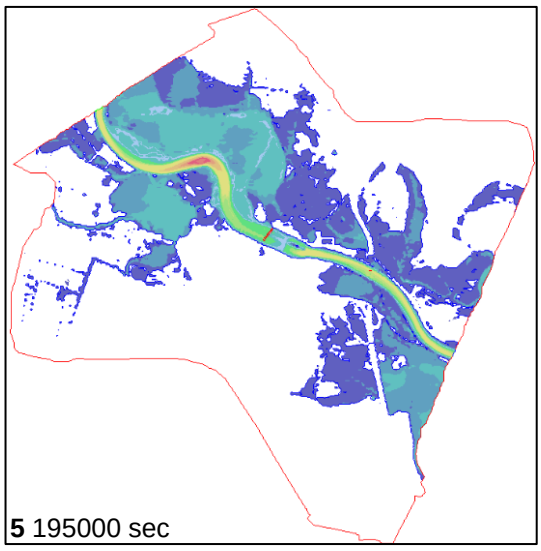

5 195000 sec

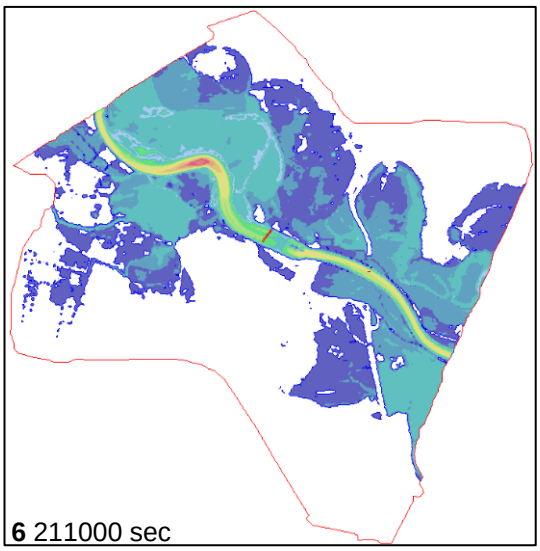

6 211000 sec

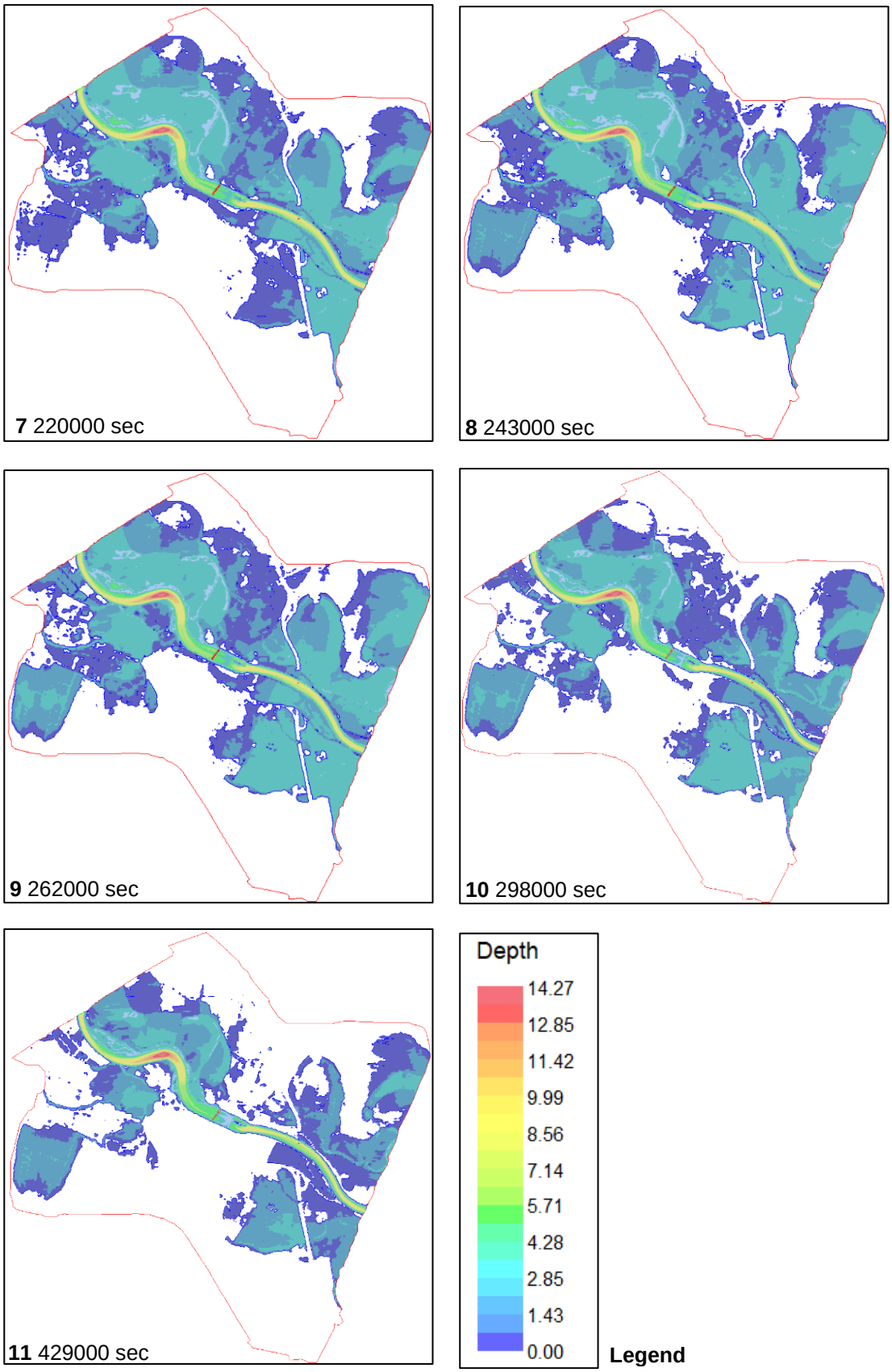

Figure 90 Output snapshots taken in the most interesting time steps

The table below reports, as it is done for the steady simulation, depth and areal coefficients, computed using the maximum WSE reached in each control point.

Table 13 indicators results for the unsteady case

UNSTEADY KS = 7 & 20 & 0.219 [m]				
ZONE	**Average of the diff.**	**Average absolute diff.**	**F_1**	**F_2**
A	0.046	0.201	-0.150	0.849
B	-0.058	0.300	0.017	
C	0.285	0.381	-1.873	
D	-0.300	0.470	-0.177	
E	-0.434	0.559	-0.057	
F	-0.235	0.383	-0.364	
G	-0.193	0.376	-0.152	
H	-0.253	0.419	-0.385	
Total	**-0.143**	**0.386**	**-0.393**	

It can be observed that:

- the coefficients are very similar to those computed in the steady calibration case number 3 (Table 12);
- the average of the difference in relative terms is lower than the -0.04 [m] obtained in the steady calibration case number 3.

This difference is supposed to be due to convergence problems. In fact, the steady case has the time necessary to reach the convergence, whereas in the unsteady one, the convergence is not reached at each time step.

In addition, the following graph, representing the dynamic of the inundated area with time, is used to compare the flooded area calculated with the unsteady analysis to the one computed in steady condition.

It shows that the flooded area increases linearly with Q until the peak flow is reached After the peak, the area continues to increase for approximately 6 hours, then it starts to decrease

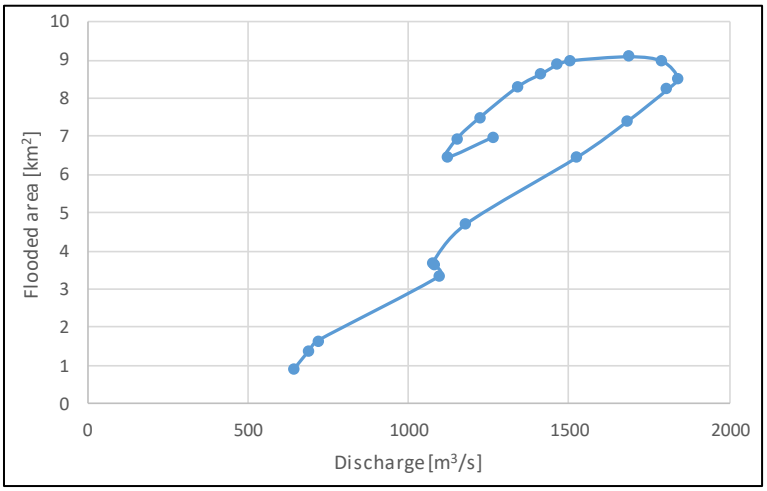

Figure 91 Flooded area versus discharge graph

A process similar to that used for the evaluation of the maximum water depth is used to evaluate the velocity.

Maximum velocity in a point may also occur when the discharge is not at the peak. Therefore, in order to have a unique maximum velocity map, 10 time steps were chosen. For each point the maximum velocity value is selected among the 10 available.

The graph below shows that the majority of the maximum velocity values are observed in the time step 63.9 h, corresponding to a discharge of 1828 m^3/s, very close to the peak of the hydrograph.

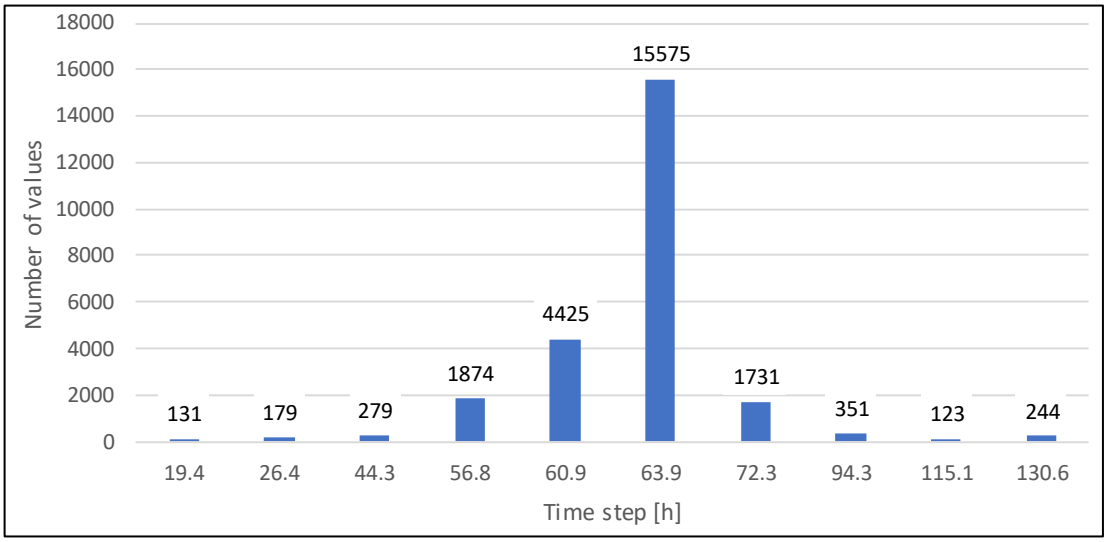

Figure 92 Distribution of the maximum reached velocity in the in the selected time steps

The flow velocity map in Figure 93 shows quite low flow velocities in the floodplain area, with maximum values around 0.8/2 [m/s] registered in the *Revellino* district.

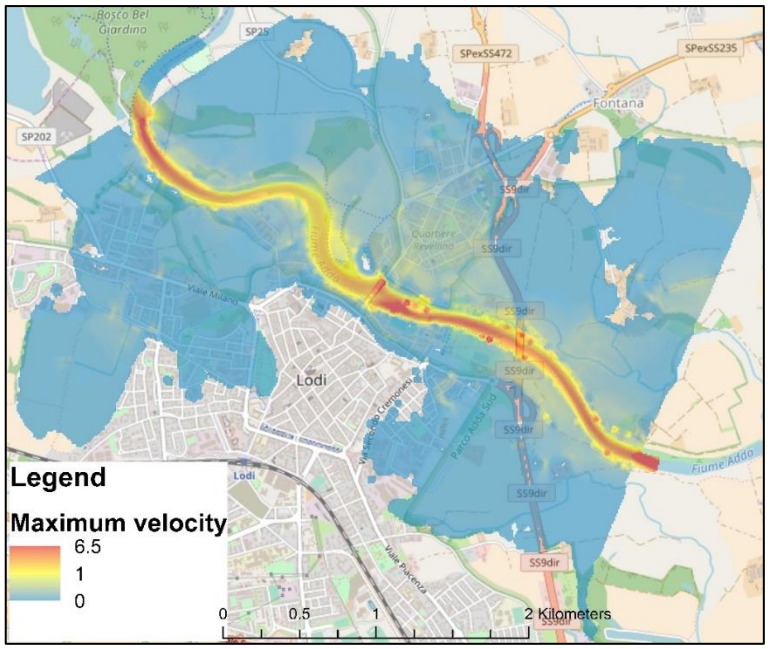

Figure 93 Maximum velocity in each point

Depending on the damage model used, velocity of the water can influence and increase the damages on buildings.

According to the probabilistic approach proposed by Clausen and Clark (1990), Partial damage on structures due to the velocity occurs when velocity (V) is higher than 2 [m/s] and the product between V and WD gives a result higher than 3 [m^2/s] (Cohen et al., 2017). In the following picture the fragility function is reported:

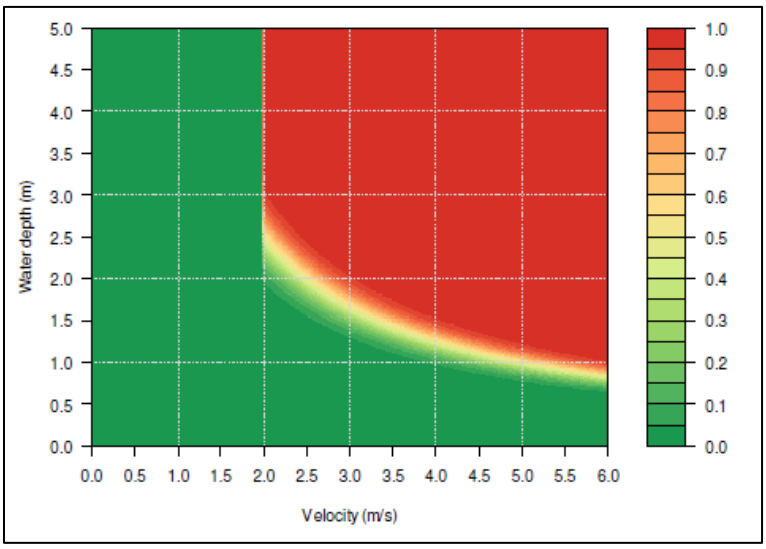

Figure 94 Fragility function WD/V

Considering the worst condition, in the following is reported the maximum velocity reached for the unsteady case.

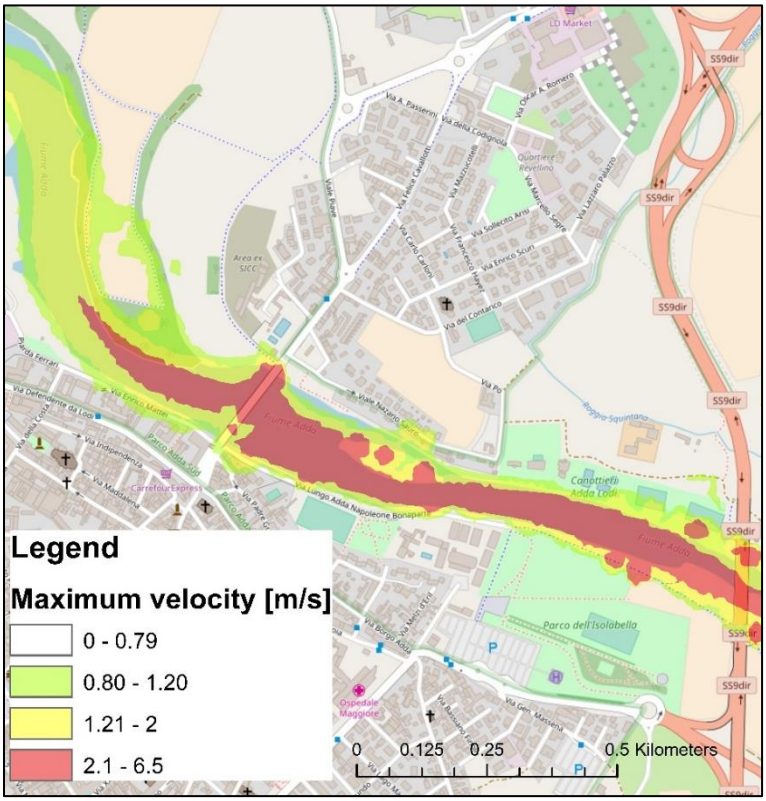

Figure 95 Detail of the velocity hazard map near the bridge Napoleone Bonaparte (unsteady case)

Looking this map it is possible to notice that the only zone affected by high velocity (v>0.8 m/s) are some urban areas near to the river, where velocity locally reaches 0.8-2 m/s.

With the “raster calculator” tool, is computed the product between the velocity and the maximum water depth and the resultant map is here reported:

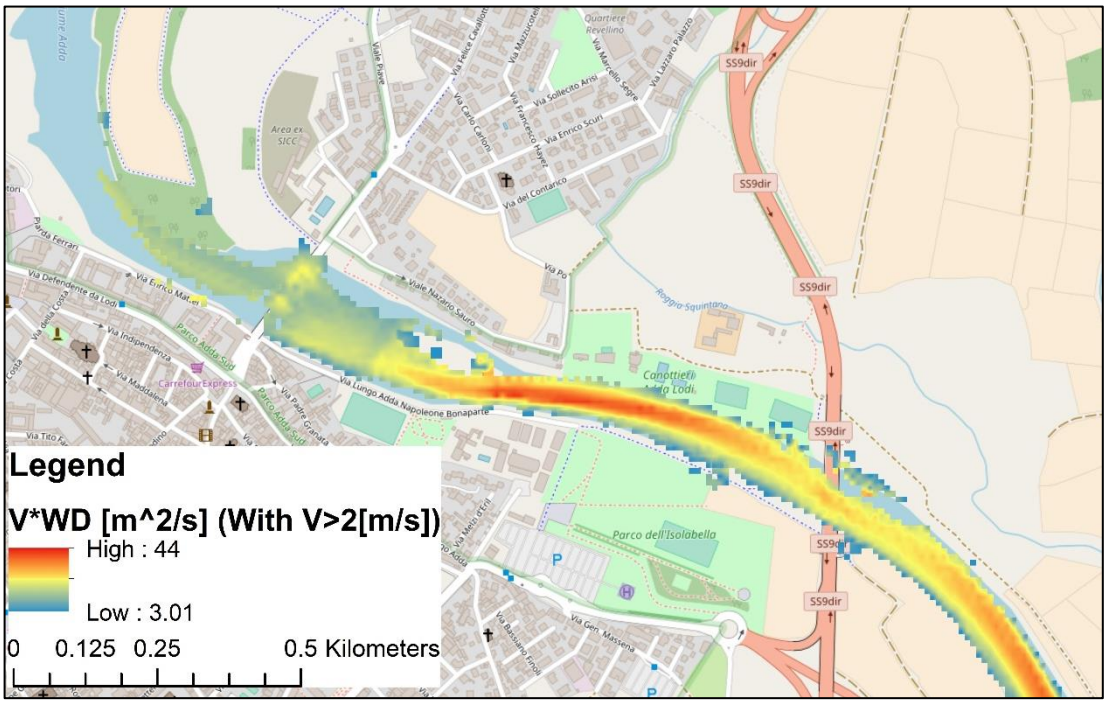

Figure 96 Product between Velocity and Water Depth taking only the velocities higher than 2 [m/s]

The number of building, that according the probabilistic law, register partially damage due to the velocity is very low (2/3). It can be concluded that for the event considered the velocity is negligible for the computation of the damage. Therefore, the WD is the most influential parameter.

4.4 CONCLUSIONS

In the above chapter are presented the results of the simulations used to create the hazard scenario, which will be used for the hydrological risk assessment in the city of Lodi, considering the event happened on November 2002.

From the SA the following conclusions can be obtained

Table 14 Summary of the results of the sensitivity analysis

PARAMETER	SECTOR	FLOODED AREA	AVERAGE WATER DEPTH
Roughness coefficient	UPSTREAM	M.S	H.S
	CENTRE	M.S	M.S
	DOWNSTREAM	S.S	H.S
Cross section geometry for the 1D model	UPSTREAM	M.S	H.S
	CENTRE	M.S	H.S
	DOWNSTREAM	M.S	H.S
BCs size for the 2D model	UPSTREAM	S.S	M.S
	CENTRE	S.S	S.S
	DOWNSTREAM	M.S	S.S
Geometry of the area in the 2D model	UPSTREAM	M.S	M.S
	CENTRE	N.S	S.S
	DOWNSTREAM	N.S	S.S

The chromatic scale used in the above table is useful to understand the importance of the parameter on the behaviour of the model. It can be noticed that the key parameters which must be calibrated with more attention are the roughness coefficient and the cross-section geometry for the 1D model.

From a cost-benefit analysis between the geometry “BLOCKS” and “ZONAL M.” the latter one is preferred because it has a better convergence and computation speed.

Once the importance of each parameter is defined through the SA, the values of the parameters chosen to start the calibration procedure are:

Table 15 Parameters used to start the calibration procedure

PARAMETER	CHARACTERISTICS
Geometry of the area in the 2D model	introduced ditches, bridges’ piers and zonal manning (3 different roughness zones)
Section dimension in the 1D model	Large
Roughness coefficient (K_s)	Bed roughness = 0.0776 m; Rural roughness = 7 m; Urban roughness = 20 m;
Mesh dimension	20 m
Discharge (Q)	1837 m^3/s;
BCs size for the 2D model	Upstream = narrow; Downstream = narrow
BC (upstream and downstream)	68.43 m - 63.78 m;

Starting from the above values many attempts are performed in order to calibrate the value of the roughness coefficient.

The calibration procedure of the section dimension in the 1D model is not performed because the most suitable solution for this parameter is already selected.

The calibration can be defined as the procedure in which, for each attempt, a parameter is changed in order to have simulated results as similar as possible with the measured ones.

In each attempt, are computed 4 quality indicators regarding the depth and the flooded area. Furthermore, to decide where and how a change in the roughness value is needed, 3 types of graph are produced: dispersion, perpendicular projection and parallel projection.

The final indicator used to evaluate the best attempt is the average of the quality indicator.

The best calibration attempt resulted is “run 3”, realized with the following roughness coefficients:

- channel: n=0.025 [s/m$^{1/3}$] / Ks=0.0776 [m];
- rural: 0.0675 [s/m$^{1/3}$] / Ks=3.93 [m];
- urban: 0.228 [s/m$^{1/3}$] / Ks=20 [m]

From this model is produced the hazard map of the depth and velocity. (Figure 79)

Using the same data of the steady simulation, it is performed an unsteady model with the real hydrograph of the event.

The calibration part is not performed, because of the time needed to compute the unsteady model.

The results produced with this type of analysis are:

- 4 quality indicators;
- a video of the progression of the flood (Figure 90) presented as some snapshots taken in the most interesting time steps;
- the hazard map of the maximum velocity magnitude reached in each point (Figure 93);
- the dynamic of the flooded area with the discharge (graph area versus discharge) (Figure 91).

From the results, it can be deduced that the model crated can simulate the event considered with a good approximation even if are needed a lot of observed data, many calibrations attempts and long computation time.

The last part of the conclusion about the modelling, regards the comparison between the unsteady and steady results:

- From the **quality indicators**, represented below it is clear how the steady results are very similar to the ones obtained with the unsteady simulation.

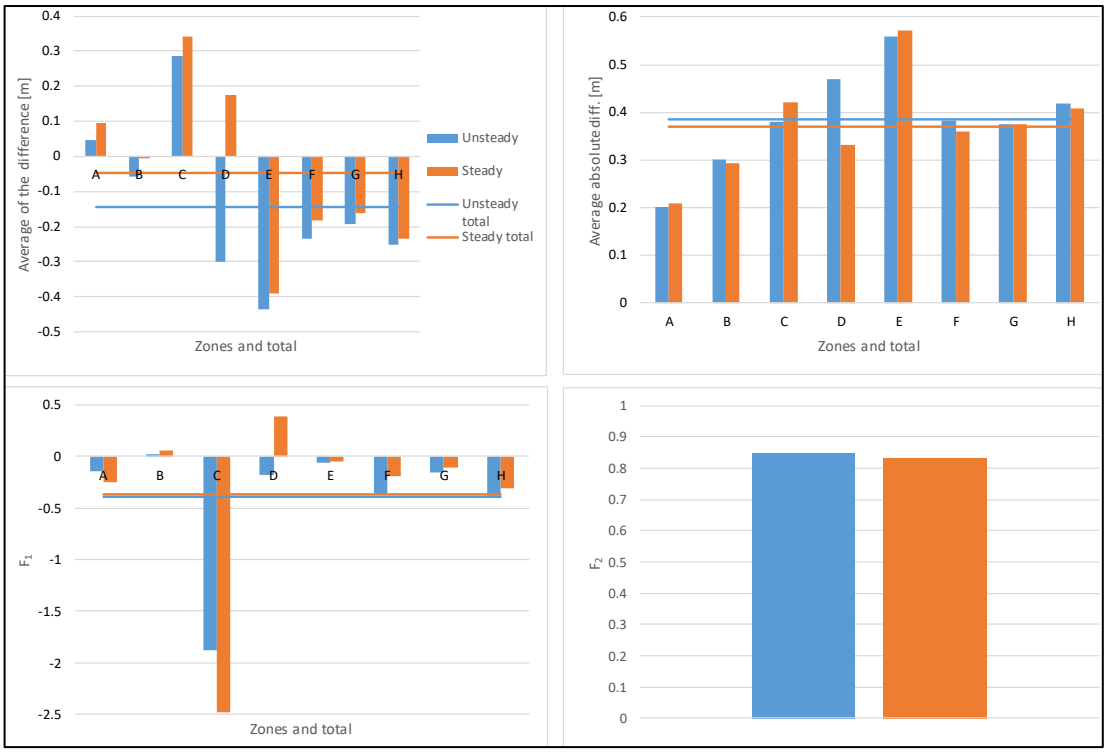

Figure 97 Comparison of the quality parameters between steady run 3 and unsteady.

- The **video,** obtained as output of the unsteady simulation, depicts with high precision the dynamic of the event. Instead, the result of the steady dynamic is only a map, due to the lack of the time variable in the model.
- The **hazard map of the maximum depth** reached is very similar between the steady case and the unsteady one.

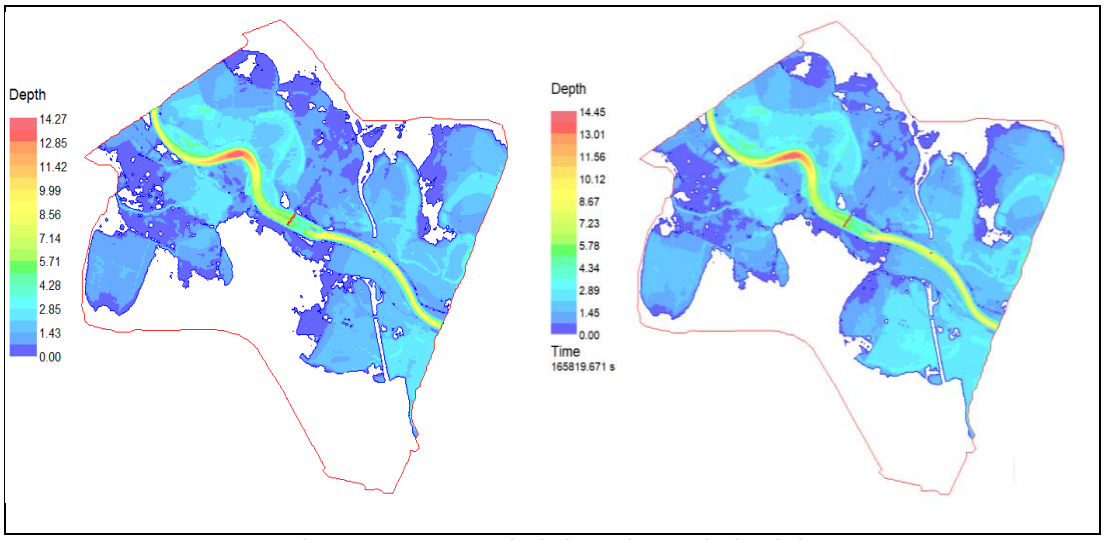

Figure 98 Unsteady left and steady in right

- The **hazard maps of the maximum velocity and direction** are very similar to the one obtained in the steady condition

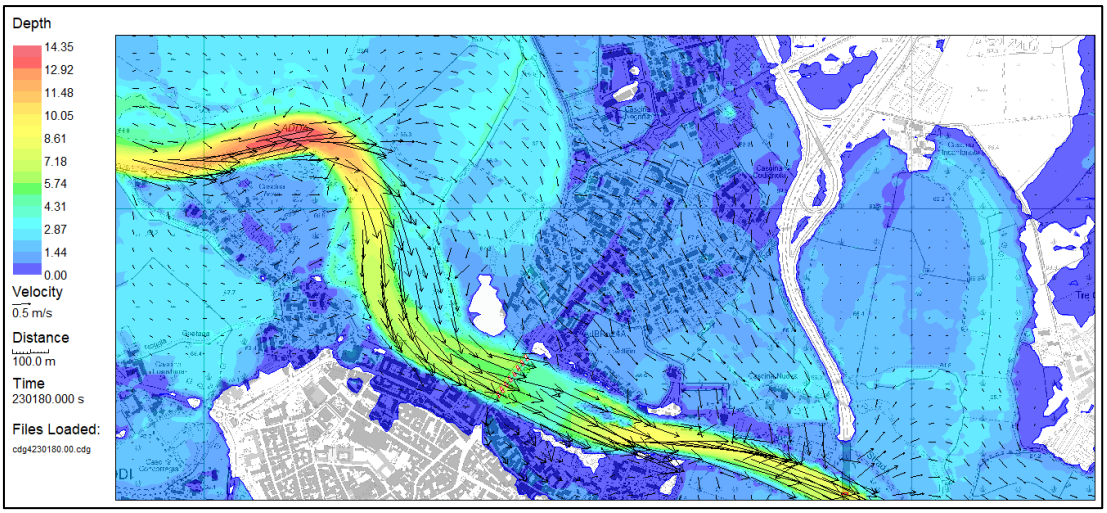

*Figure 99 Velocity magnitude and direction for the **unsteady** case*

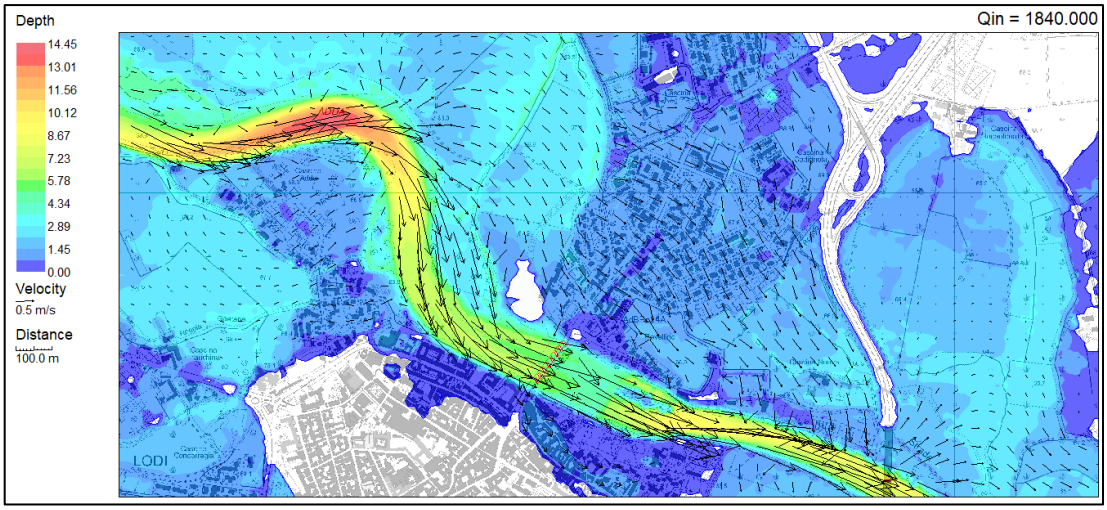

*Figure 100 Velocity magnitude and direction for the **unsteady** case*

In both cases, the results are undoubtedly influenced by singularity in the geometry and by artificial infrastructures that can obstruct and deviate the flow of the water.

- The **dynamic of the flooded area** represents that the area increases linearly with the discharge, until the peak discharge. After this moment the behaviour of the flooded area is unpredictable, and it depends on the characteristics and on the morphology of the terrain. The maximum flooded area is registered some hours after the peak (retarding effect) and it is well approximated by the steady computation. As it can be seen from the following graph, in the steady case the extent is generally larger do to the higher convergence rate of the solution.

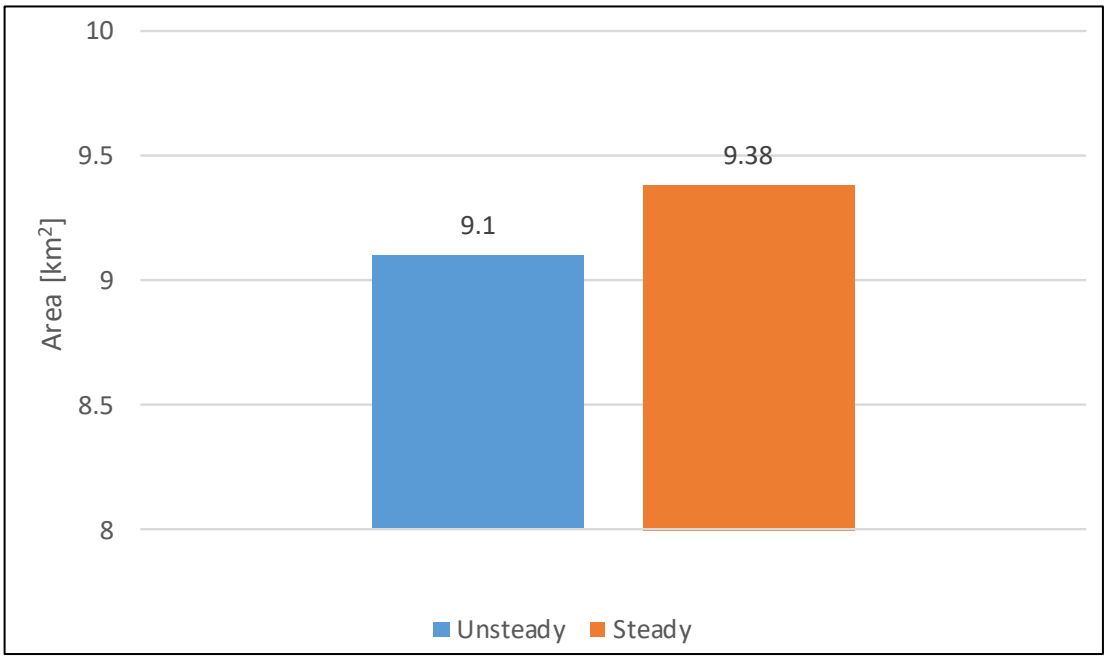

Figure 101 Comparison between the flooded area computed in the unsteady and the steady simulation

To conclude, in the table below are schematized the advantages and disadvantages of the two methods.

Table 16 Results on the comparison between steady and unsteady simulation

	Best simulation method [steady – unsteady]
Max WD	No difference between the two methods
Max velocity	No difference between the two methods
Dynamic of WD	Unsteady
Dynamic of the flooded area	Unsteady
Time computation	Steady

5 HAZARD MAPPING FROM FLOOD EXTENT

5.1 INTRODUCTION

Traditional hydraulic modelling, as shown in previous chapters, requires a long procedure involving numerous and accurate data to properly model a flood event. Despite that, a calibration of the model is always necessary, given that a number of parameters can still remain unknown. Moreover, depending on the extension of the interested area and on the software used, computational time can vary from some minutes to some hours.

In the recent years, the number of organizations that provide flood inundation maps based on satellite remote sensing at high quality is increased. These services do not provide floodwater depth (Cohen et al., 2017), an important attribute for first responders and damage assessment. As a consequence, few researchers have started to develop tools to integrate the traditional approach and compute local water depths from the areal extent of a flood event.

5.1.1 OBJECTIVE

The aim of the new method, known as *Surface Water Analysis Method* (SWAM) or *Floodwater Depth Estimation Tool* (FwDET), is to compute water depths starting only from the **areal extent of a flood event** and a **DTM**.

To reduce efforts and to be able to produce a hazard map in less time, this new method, still under development, is here explained, implemented and improved on the Lodi 2002 flood case study. Afterwards, it is tested using boundary data provided from AdbPo.

The objective is to develop and improve the accuracy of this method in GIS environment using the Model Builder, a very useful tool already exploited within this thesis.

5.1.2 HYPOTHESIS OF THE MODEL

The method is based on two fundamental hypotheses:

- the external boundary of the flooded area represents the locus of points where the water depth is nil (i.e. *tirante idraulico =0*);
- the extreme symmetric points, positioned on the perpendicular line to the river, have comparable water surface elevation.

Taking advantage from the first hypothesis, knowing the boundary of a flood event and having a good DTM it is possible to assign to that points the elevation of the terrain. The resulting point will represent the water surface elevation.

The second hypothesis gives the possibility to connect one point to the opposite one with a line that approximates the water elevation over its length.

The simplified steps of the method are reported below.

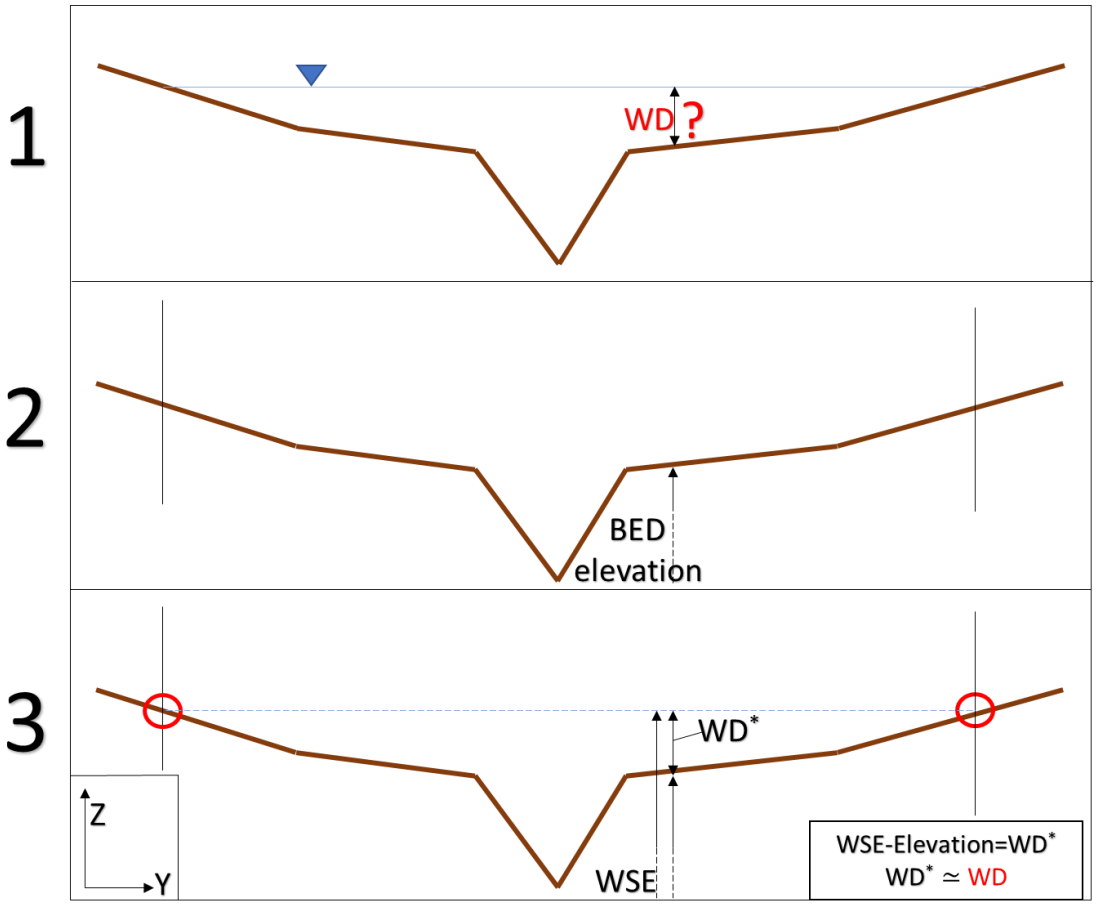

Figure 102 Semplified scheme of the method

1 Flood occurs / **2** Boundary of the flood are drawn on the DTM / **3** The intersection of the boundary with the terrain are connected and with a simple subtraction the approximation of the WD in each point is obtained.

Translating the approach from 2 to 3D, it is possible to represent the WSE over the entire domain (Figure 103).

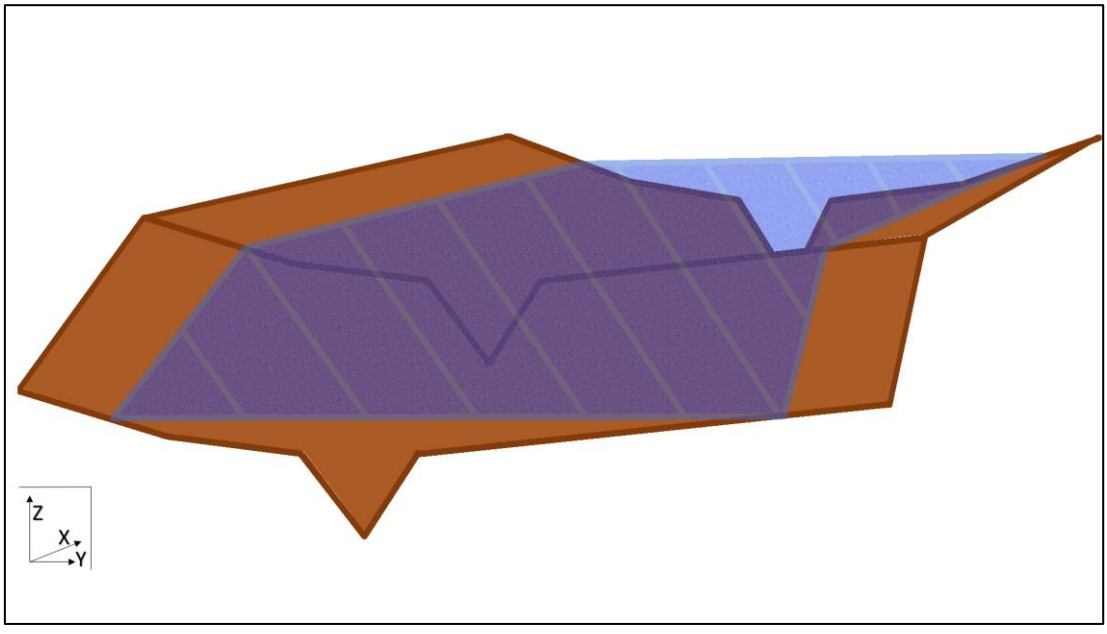

Figure 103 3D solution of the problem

Due to its simplicity, the method has some important limitations. In fact, if the water is obstructed by an anthropic structure, as it happens in urban areas, the first hypothesis fails. Moreover, if the external limit is determined by a vertical anthropic structure (like a wall or an elevated road) the WD in that point will be different from 0. Examples of such issues are reported in the following figures.

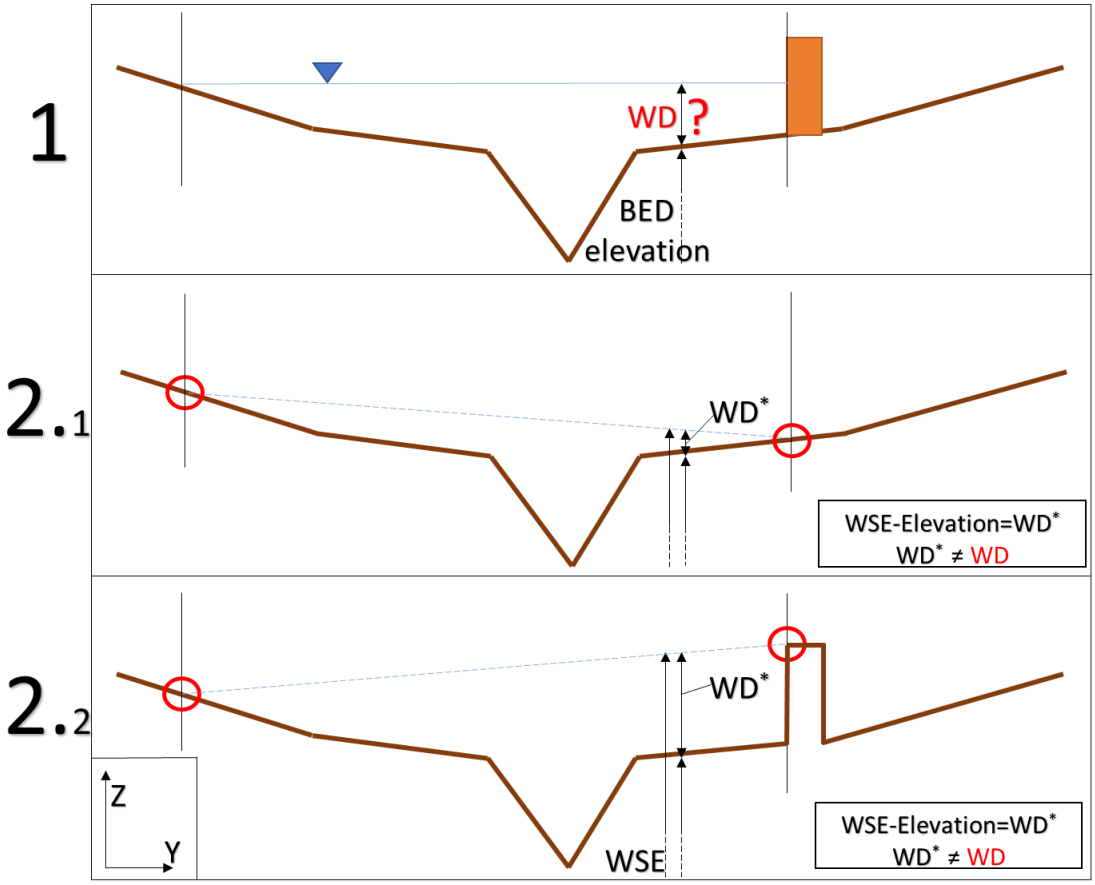

Figure 104 Simplified scheme of the limitations

1 The flood extension is influenced by a vertical structure / **2.1** if the vertical structure is not present in the DTM the solution is underestimated / **2.2** if the structure is represented also in the DTM, the solution could be overestimated

Therefore, in case of an urbanised area, also the second hypothesis is not always verified.

Due to the evident limitations of the method, in the following sections an improvement on the method is proposed in order to minimise errors.

5.2 CROSS-SECTIONS PROFILE INTERPOLATION STARTING FROM FLOODED PERIMETER

5.2.1 METHODS

Before introducing the GIS-model, some attempts have been made applying the method directly on the flooded perimeter (obtained from the R2D-model). As expected, the points of that perimeter close or inside the urban area are 3/10 meters higher than the WSE used as reference.

To fix the problem, all the points falling near the urbanized area are excluded from the computation. Without these points, the solution is improved, but large errors are still present. This is because of the interpolation method used.

The literature on the method (Gatti et al., 2016; Pastormerlo et al., 2016) suggests to interpolate the boundary points with the natural neighbour tool. However, it has been noticed that this interpolation method is “uncontrolled”, because also “distant” points are used for the computation of the solution, whereas only the nearest and symmetric points (with respect to the river, in perpendicular direction) should be used.

To adjust this problem, the interpolation direction is forced through a specified direction using lines that introduce additional points to the interpolation method. These lines must be defined perpendicular to the axis of the river.

In this work, the lines used to force the interpolation direction are represented the cross-sections provided by the AdbPo, already used for the 1D computation in the chapter 4.1. These sections, generally fulfil the perpendicular requirement introduced above (except for one that is then modified).

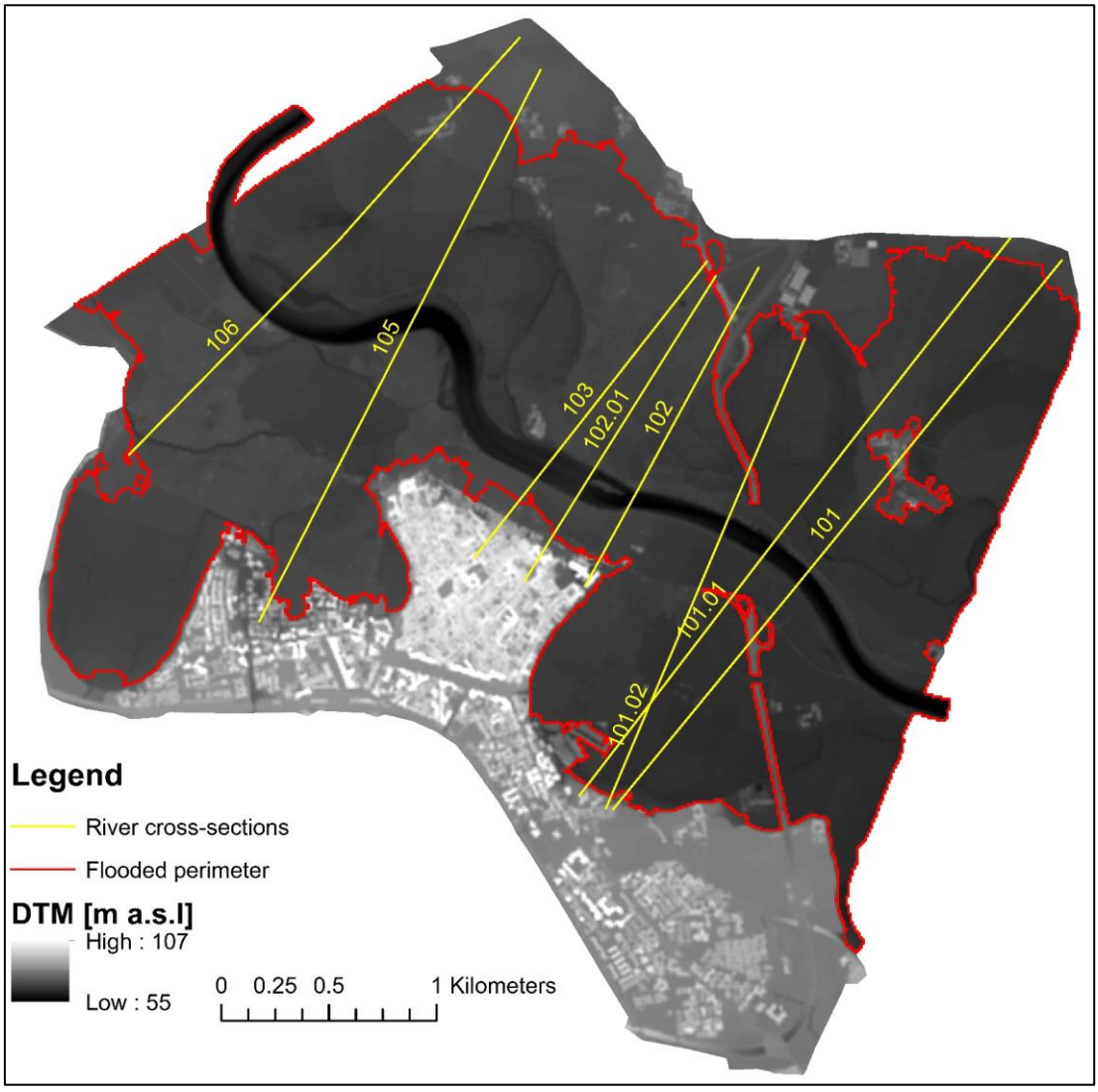

Figure 105 Flooded perimeter and cross sections

The purpose of this part is to compare for each section the reference WSE to the WSE obtained with a linear interpolation between 2 extreme points of the section, obtained by intersecting the cross-section line and the flooded perimeter (see Figure 104).

The resulting interpolated points will be used, in addition to the ones obtained from the perimeter, for the interpolation over the entire domain.

Firstly, an analysis on the singular sections has been performed to choose which method should be used to perform the interpolation and to quantify the quality of this type of approximation.

A first attempt is done manually using both ArcMap and Excel:

- (ArcMap) a series of points with 1 m spacing has been generated for each cross section;
- (ArcMap) it has been assigned to these points the correspondent value of:
  - bed elevation;
  - WSE of the best hydraulic result from R2D (see Chapter 4);
  - roughness value;
  - longitude and latitude coordinates;
- (ArcMap) the attribute table for these points has been exported to excel;
- (Excel) for each section, the points where the WSE is higher than the bed elevation have been defined;
- (Excel) between the 2 points a linear interpolation is applied assigning all the intermediate elevation values;
- differences between the obtained points and the reference WSE are computed and represented in a graph with its CDF (Cumulative Distribution Function).

Examples of the outputs of the procedure described above are presented in the following pictures.

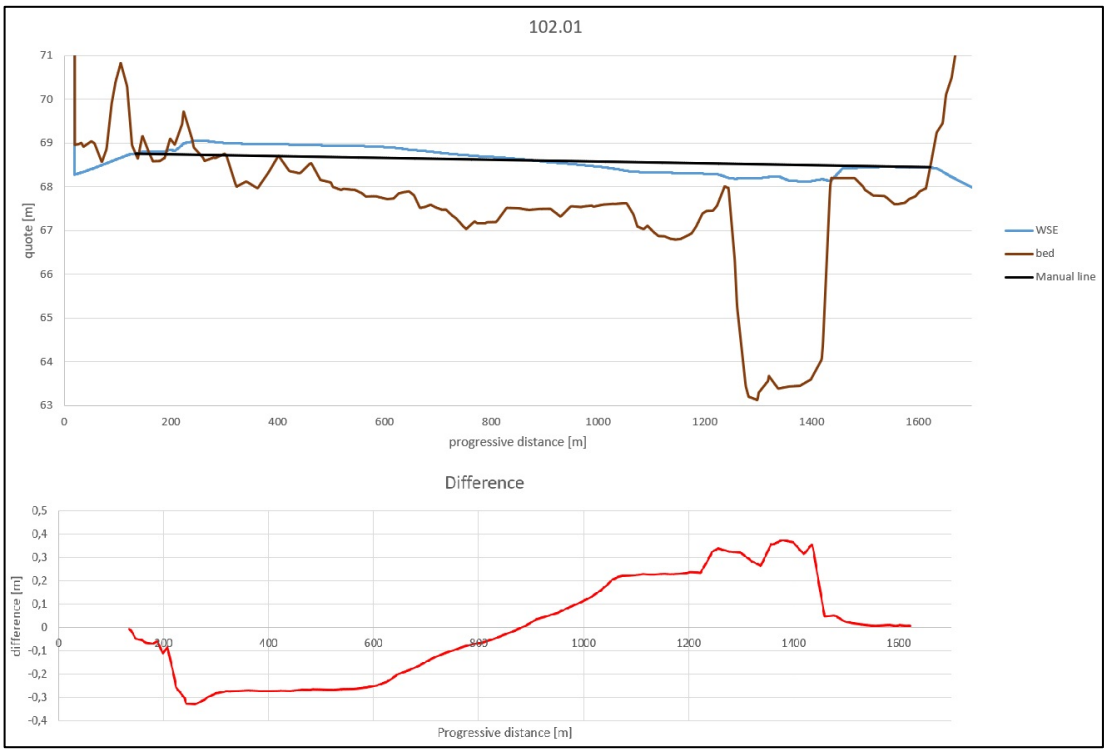

Figure 106 Above: the comparison between WSE and the manual line computed / Below: the computed differences

As the procedure applied is quite long, an automatic process is implemented to speed and standardize the process. A code, is written expressly for this purpose with the “Model Builder” (MB). The following flow chart summarises the framework created with the MB.

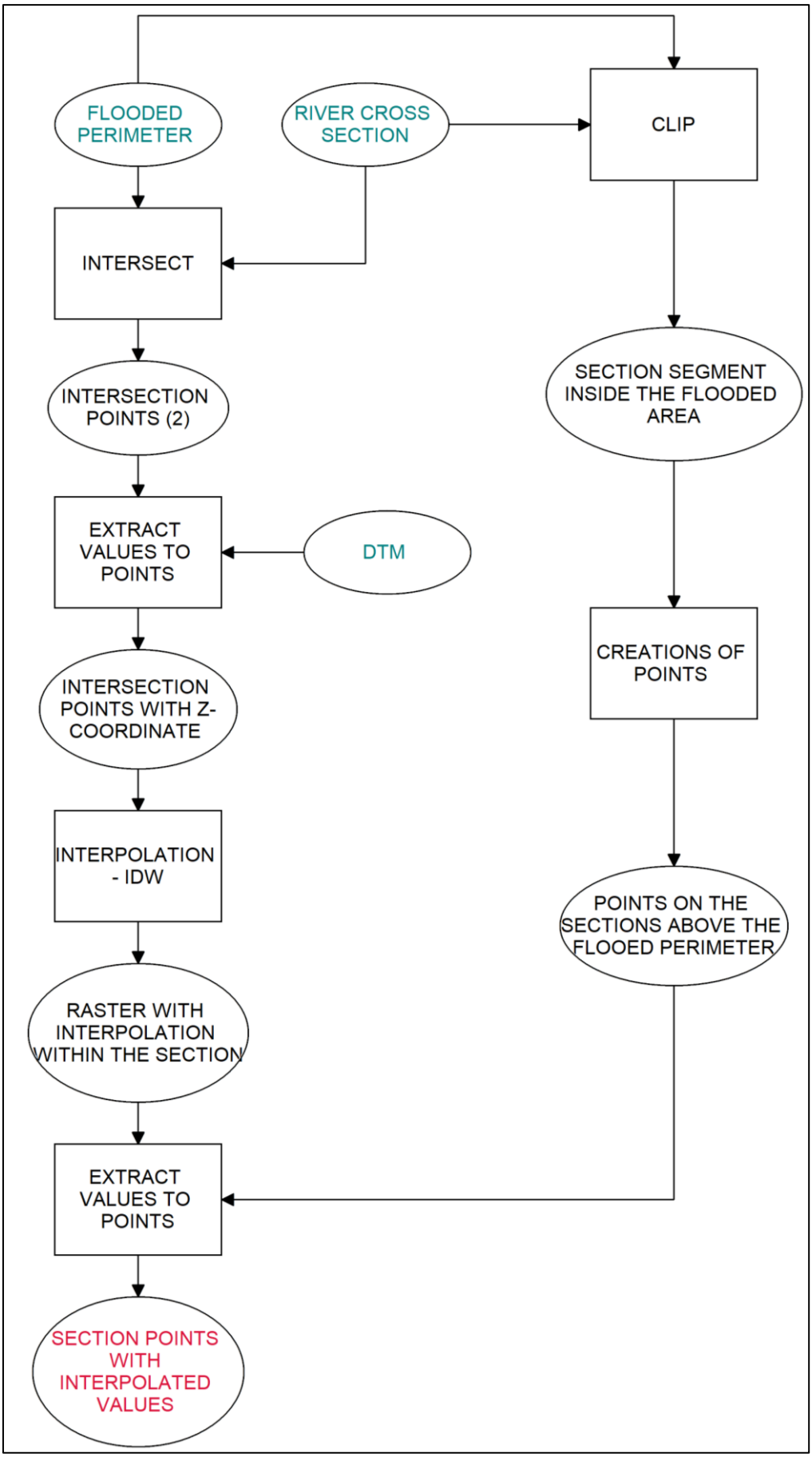

Figure 107 Scheme of the method written in the MB for a single section

The necessary inputs are:

- FLOOD PERIMETER;
- RIVER CROSS SECTIONS;
- DTM.

Once implemented, the process presented above takes only **1** section at time, therefore a cycle has been applied for the N sections used. The flow chart representing this iteration is presented below.

The output produced consists of SECTION POINTS WITH INTERPOLATED VALUES.

As shown in the scheme above, the interpolation of the points among the 2 extreme points are performed using the IDW[26] tool. So, the resulting line is not straight, as with the manual procedure, but it is a spline.

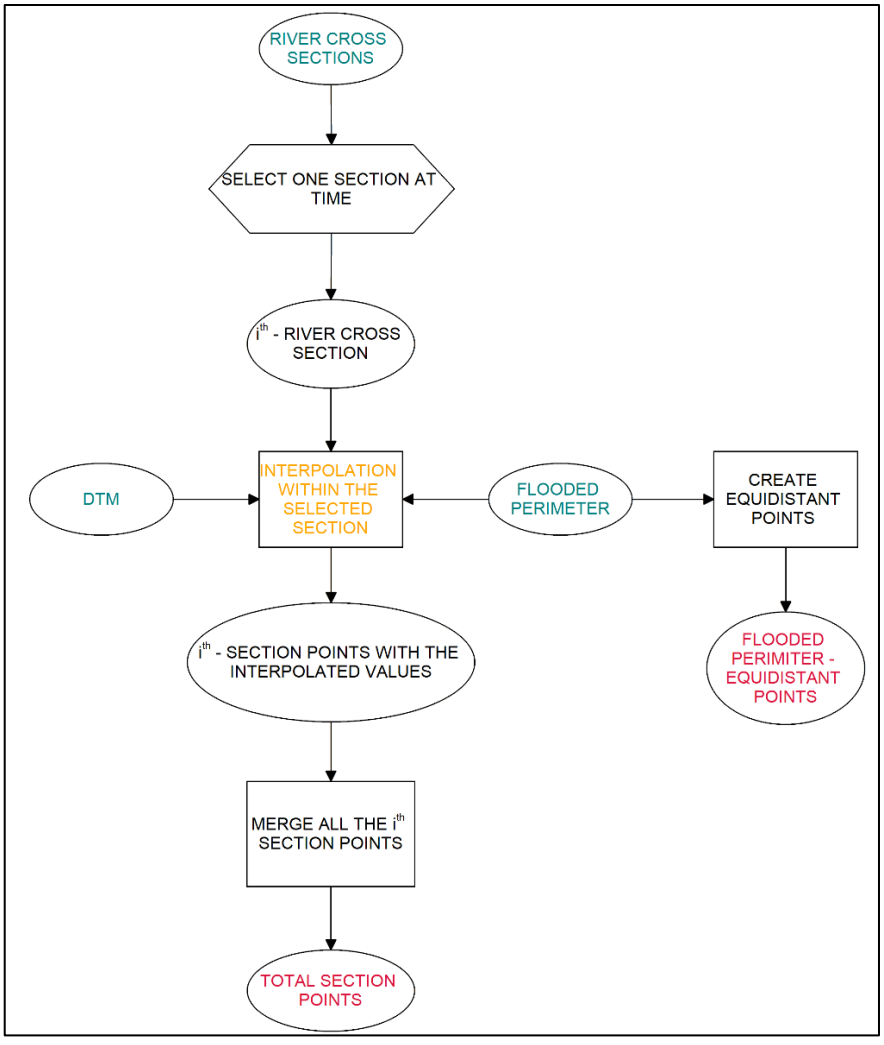

Figure 108 Scheme of the method written in the MB for n sections

[26] Inverse distance weighted (IDW) interpolation determines cell values using a linearly weighted combination of a set of sample points. The weight is a function of inverse distance. The surface being interpolated should be that of a locationally dependent variable. This method assumes that the variable being mapped decreases in influence with distance from its sampled location. (http://desktop.arcgis.com/en/arcmap/10.3/tools/3d-analyst-toolbox/how-idw-works.htm)

The outputs are:

- TOTAL SECTION POINTS;
- FLOODED PERIMETER EQUIDISTANT POINTS (this output is not employed in this section, but it will be used in the following parts).

Once again, to test and to estimate the precision of this method, it is decided to draw the profile and compute the differences of the points obtained with this automatic computation: “GIS interpolation”. An example is presented below.

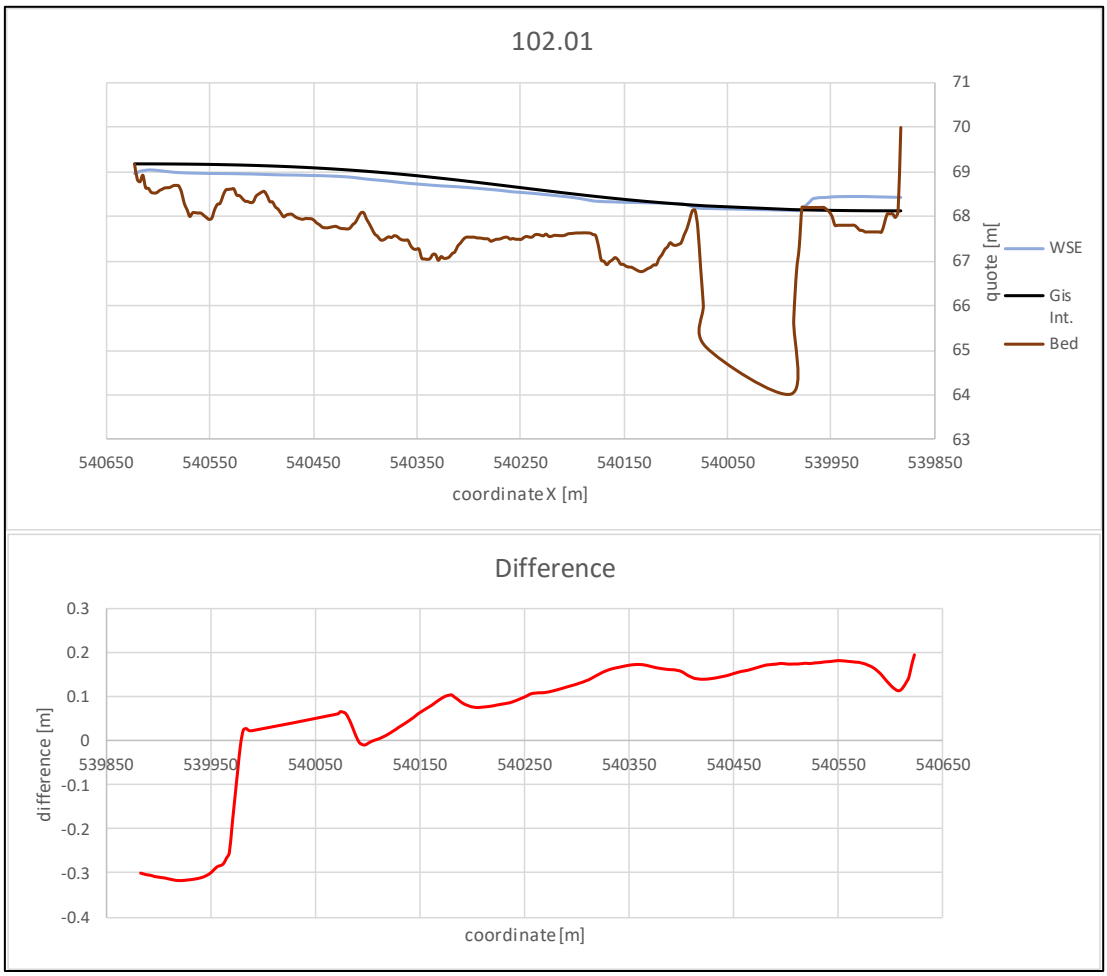

Figure 109 Above: the comparison between WSE and the GIS line computed / Below: the computed differences

5.2.2 RESULTS

The differences between reference WSE and the one calculated with the two different methods are computed for all the sections: “Tot” case. Then, for both methods, they are classified according to:

- their roughness coefficient:
  - Ks=20 [m]: “Urban” case;
  - Ks=3.93 [m]: “Rural” case;
  - Ks=0.077 [m]: “Channel” case;
- the presence of lateral flow: “Lateral Flow” case.

Finally, a comparison between the two cases is done to understand which case performed better. The following statistical parameters are considered:

- average of the differences: computed for each point on the section inside the flooded perimeter.
- absolute average: useful to evaluate the mean value, excluding the “balance effect” due to the presence of values with opposite sign.
- standard deviation of the differences: useful to evaluate how much the differences deviate from the average value.
- CDF representation: Possible analysis of the impact of the Manning’s parameter.

The parameters of the **manual case** are summarised hereinafter:

Table 17 Statistical parameters - manual case

Differences (manual line -WSE)	Average [m]	Absolute Average [m]	Standard deviation [m]
Total	-0.09	0.10	0.15
Urban	-0.11	0.13	0.15
Rural	-0.08	0.09	0.15
Channel	0.33	0.33	0.03
Lateral flow	-0.15	0.88	0.22

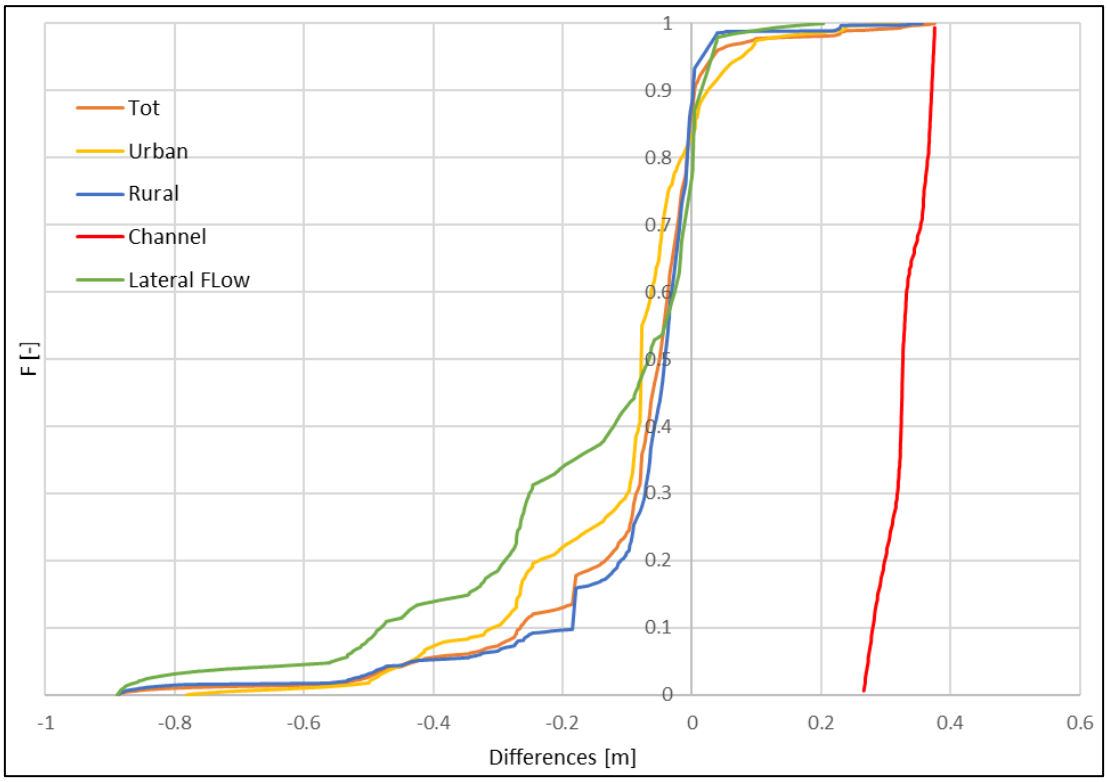

*Figure 110 Superimposition of the CDFs for the **manual method***

If the differences are negative, the solution is underestimated, vice versa if they are positive.

For the case “Tot it can be noticed an underestimation of around 10 cm. The CDF of the rural case is very similar to the trend of the total, probably because most of the total points includes the rural values.

The urban part is underestimated, more than the rural part, probably due to the higher roughness parameter that affects the elevation, indeed the roughness element is not considered by the method.

From the graph and the values in the table above, it is clear that the method does not provide good results for lateral flow. In fact, they are clearly underestimated. This indicates that the method is not able to compute the 2D aspect of the flow that determines a localised increase on the WSE.

Similarly, the parameters of the **automatic GIS case** are listed below:

Table 18 Statistical parameter - GIS-case

Differences (manual line -WSE)	Average [m]	Absolute Average [m]	Standard deviation [m]
Total	-0.04	0.13	0.15
Urban	-0.04	0.14	0.16
Rural	-0.04	0.12	0.15
Channel	-0.001	0.12	0.15
Lateral flow	-0.03	0.18	0.21

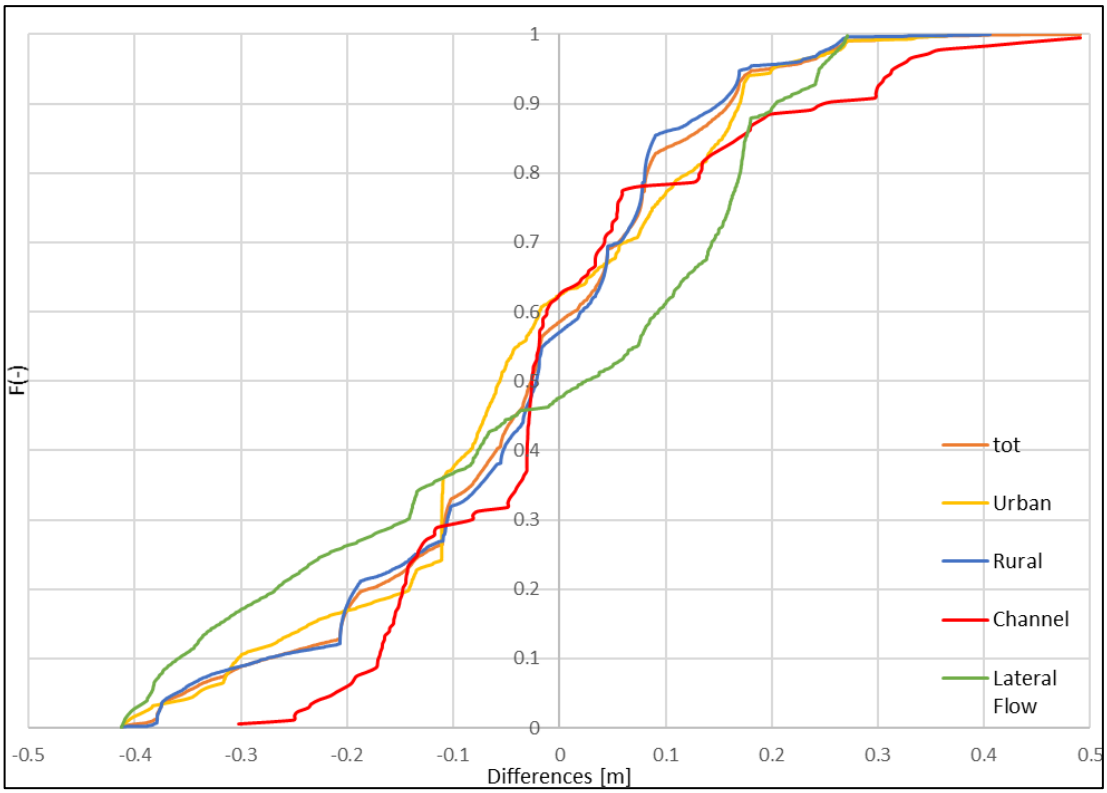

*Figure 111 Superimposition of the CDFs for the **GIS case***

The graphical comparison between the manual results and those computed with GIS are shown in the following figure:

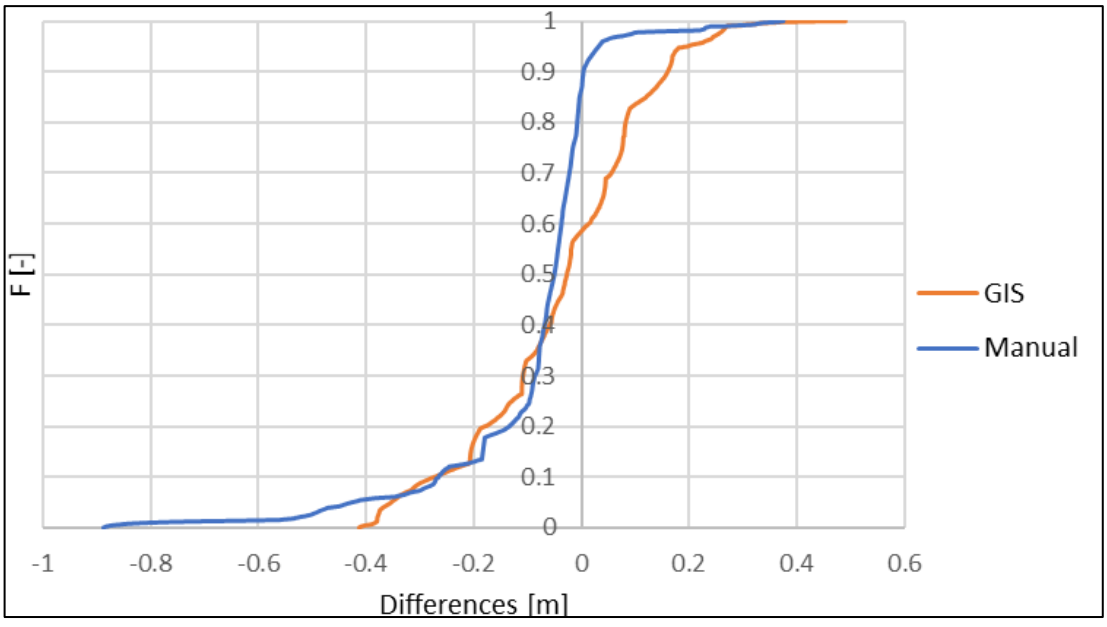

*Figure 112 Superimposition of the CDFs for the **GIS case** and **manual case** - total*

From the CDF, that represents the distribution of the differences in all the points of the computational domain, it can be understood that:

- the left tail is shorter in “GIS” case;
- the right tail is slightly shorter in the “Manual” case;

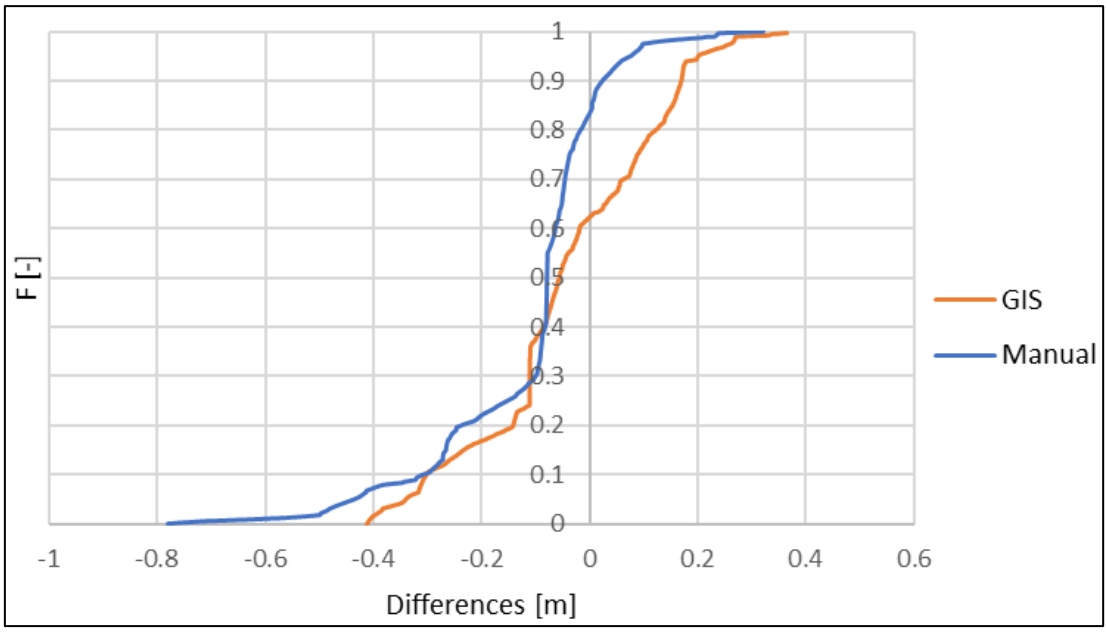

*Figure 113 Superimposition of the CDFs for the **GIS case** and **manual case** - urban*

The CDF curve for the urban value of the Manning parameter is showing that:

- the left tail is shorter in the “GIS” case;
- the right tail is slightly shorter in the “Manual” case;

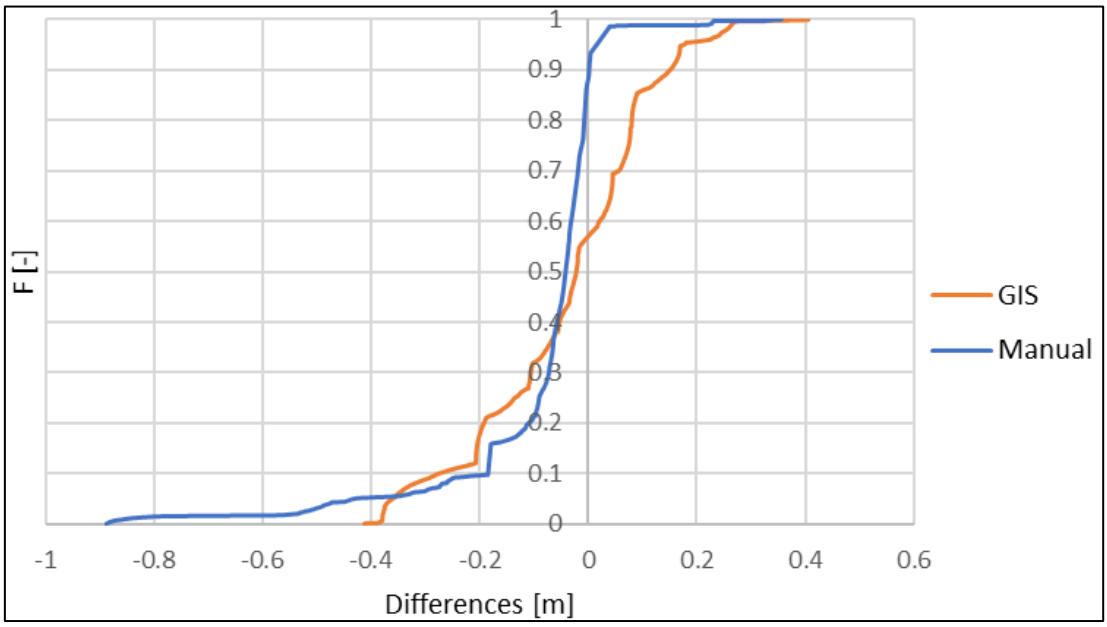

*Figure 114 Superimposition of the CDFs for the **GIS case** and **manual case** - rural*

The CDF just presented has the same characteristics of the “CDF total”, therefore the conclusions are not repeated.

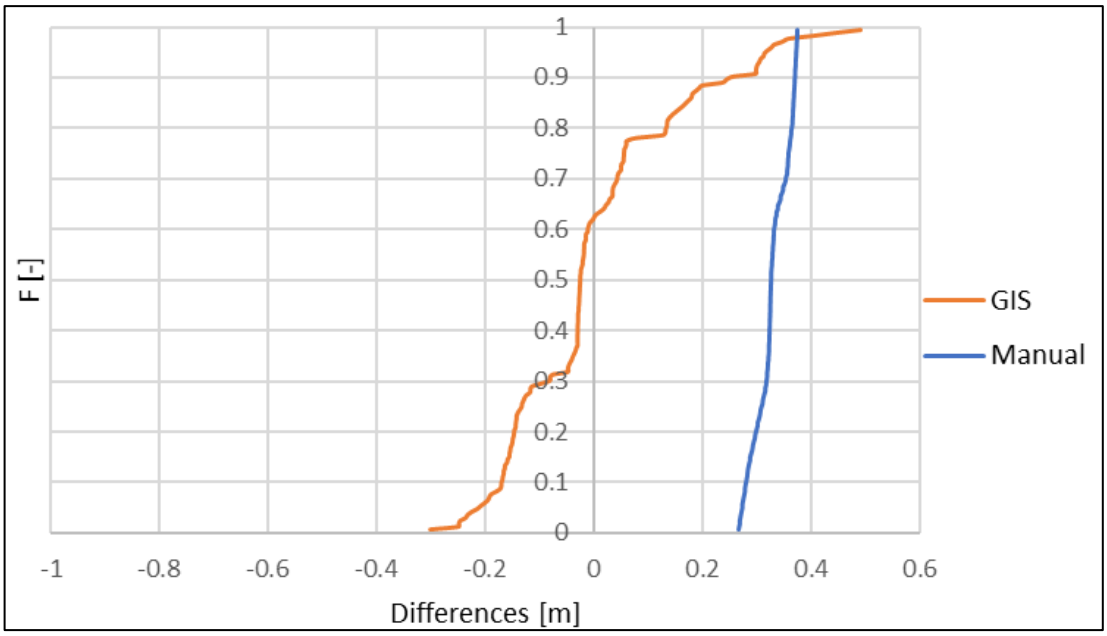

*Figure 115 Superimposition of the CDFs for the **GIS case** and **manual case** - channel*

By analysing the CDF representing points that are in the computational domain characterised by the "channel" value of the Manning coefficient, it is clear that:

- the tails are both shorter in the "Manual" case;
- the best one is the "GIS" case, whose shape anticipates a lower average value, but probably a higher standard deviation.

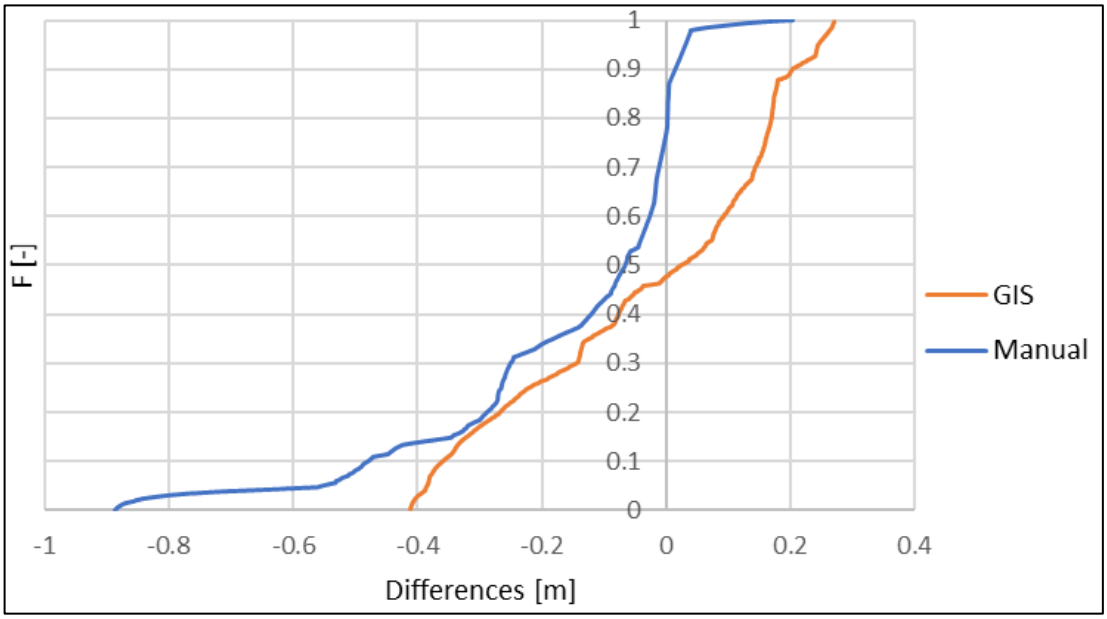

*Figure 116 Superimposition of the CDFs for the **GIS** and **manual case** - lateral flow*

With the CDF representing points that are in the computational domain characterised by the "Lateral Flow", it is clear that:

- the left tail is shorter in the "GIS" case;
- the right tail is slightly shorter in the "Manual" case;
- the maximum differences in the Manual case are much higher;

Finally, in the following tables the average, absolute average and standard deviation are compared, and the best alternative is highlighted in green.

*Table 19 Comparison **manual case** vs **GIS case** - average*

	AVERAGE [m]	
CDF	MANUAL CASE	GIS CASE
Total	-0.09	-0.04
Urban	-0.11	-0.04
Rural	-0.08	-0.04
Channel	0.33	-0.001
Lateral flow	-0.15	-0.03

*Table 20 Comparison **manual case** vs **GIS case** – absolute average*

	ABSOLUTE AVERAGE [m]	
CDF	MANUAL CASE	GIS CASE
Total	0.10	0.13
Urban	0.13	0.14
Rural	0.09	0.12
Channel	0.33	0.12
Lateral flow	0.88	0.18

*Table 21 Comparison **manual case** vs **GIS case** – standard deviation*

	STANDARD DEVIATION [m]	
CDF	MANUAL CASE	GIS CASE
Total	0.15	0.15
Urban	0.15	0.16
Rural	0.15	0.15
Channel	0.03	0.15
Lateral flow	0.22	0.21

Except for the channel (better in the GIS case), the results are very similar.

From the CDF it is possible to notice that the medians of the GIS curves are closer to the vertical axis, then the mean values are closer to 0.

This comparison proves that this automatic GIS elaboration, without using the WSE to determine the extreme points, can better approximate the flood depths.

For these reasons, the GIS procedure to interpolate water behaviour in the sections is preferred over the manual one and it is selected to be used in the validation analysis.

5.3 INTERPOLATION FROM THE FLOODED AREA

5.3.1 METHODS

The framework of the GIS-model developed to compute the water depth is subdivided in 2 steps:

1. computation of the cross-sections water profile: this step is devoted to the computation of the water profile of the defined river cross-sections and to the creation of the equidistant points on the flooded perimeter. This procedure is introduced and explained in chapter 5.2, therefore it will not be repeated;
2. interpolation within the flooded domain: its aim is to compute the final outputs of the GIS-model, the water surface elevation and water depth. This step needs as input:

- flooded perimeter: it is the contour of the inundated area; in the case of validation, this is selected as the output coming from the 2D flood model produced with R2D. It is presented in the Figure 105;
- the flooded perimeter – equidistant points: it is a point shapefile that contains a series of equidistant points drawn over the flooded perimeter. It is produced at the end of step 1;

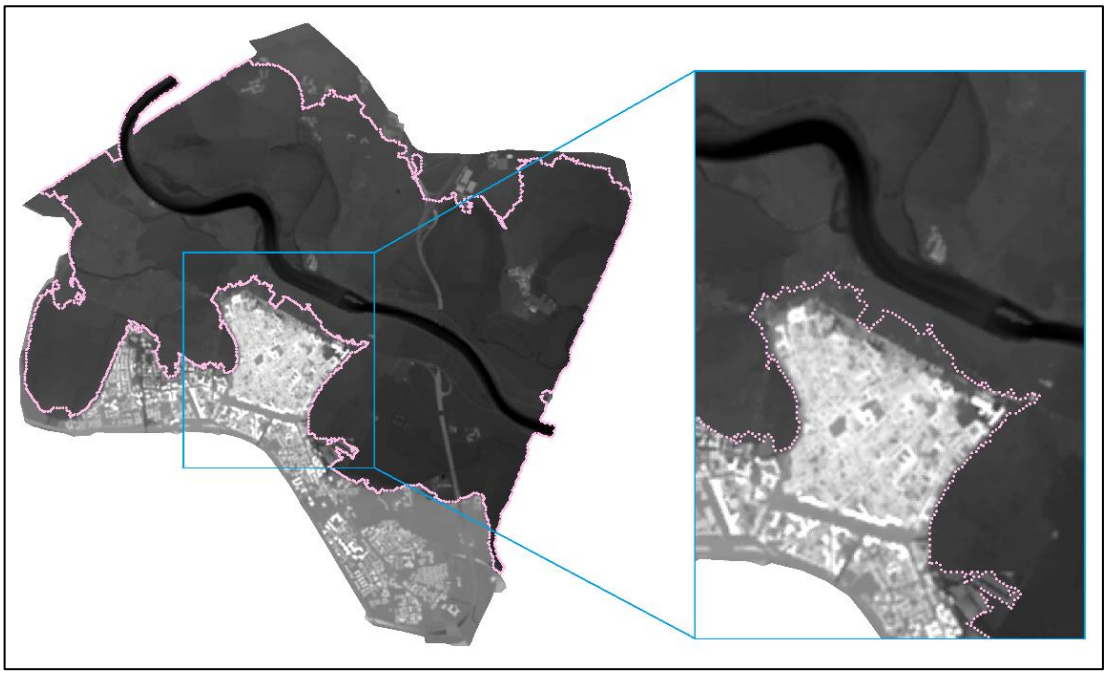

Figure 117 Flooded perimeter from steady simulation with a zoom on the urban area

- polygons mask: it is a polygon shapefile that is used to delete the entities from the shapefile "flooded perimeter – equidistant points" which are against the hypothesis of the model as stated in chapter 5.1. The one used in the validation procedure is presented here below;

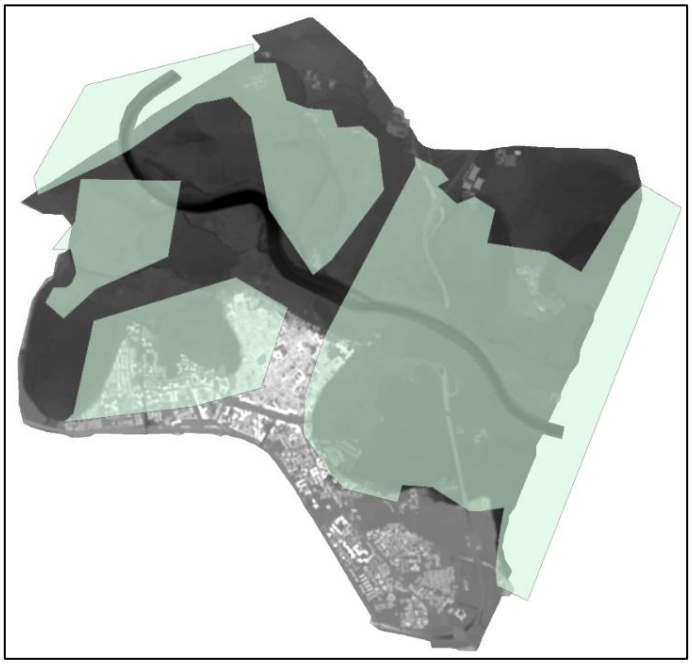

Figure 118 Polygon mask

- DTM: it is a raster file that represents the surface of the terrain. It is created from elevation data of the territory under study. The DTM used for the GIS-model is created with the same procedure described in chapter 3.1, the only difference is that as output of kriging interpolation method, a 1m resolution is selected[27] to have better results. Practically, the DTM is the same as the one presented at the end of the chapter 3.1;
- total section points: it is a punctual shapefile that contains the interpolated water surface elevation in the river cross-sections. It is produced at the end of step 1; the river-cross sections used during the validation procedure are the same presented in the picture Figure 105.

After defining the input parameters of this step, the model framework is presented. The code used to create the function and explanation of all the sub functions can be found in the Appendix E The framework itself is shown in the next page (Figure 119).

From the shapefile "FLOODED PERIMETER – EQUIDISTANT POINTS", using the "POLYGONS MASK", the points that do not fulfil the first hypothesis of the model (i.e. points in the urban zone and near the highway bridge) are deleted. Then the height value is assigned from the DTM to the remaining points. These are merged with the "TOTAL SECTION POINTS", a point shapefile resulting from the step 1, to have the "TOTAL POINTS".

The last shapefile produced contains all the points that are used during the interpolation phase. This one is performed using the natural neighbour[28] interpolation method and its result is the "WSE2 map". Considering that the natural behaviour of the water does not have sharp peaks in its elevation, a filter that removes extremes points is applied. This results in a smoother and more realistic WSE map named "WSE-FILTERED".

The last part of the GIS-model is dedicated to the calculation of the water depth map, by means of a subtraction between WSE and DTM. Finally, to present only positive values of the WD, a clip on the flooded area is performed.

[27] instead, in the 2D simulation performed with the R2D, 10 m is used because the software cannot process a DTM with that resolution.

[28] The algorithm used by the Natural Neighbor interpolation tool finds the closest subset of input samples to a query point and applies weights to them based on proportionate areas to interpolate a value (Sibson 1981). It is also known as Sibson or "area-stealing" interpolation. Its basic properties are that it is local, using only a subset of samples that surround a query point, and interpolated heights are guaranteed to be within the range of the samples used. It does not infer trends and will not produce peaks, pits, ridges, or valleys that are not already represented by the input samples. The surface passes through the input samples and is smooth everywhere except at locations of the input samples. The natural neighbors of any point are those associated with neighboring Voronoi (Thiessen) polygons. Initially, a Voronoi diagram is constructed of all the given points. A new Voronoi polygon is then created around the interpolation point. The proportion of overlap between this new polygon and the initial polygons is then used as the weights. (http://desktop.arcgis.com/en/arcmap/10.3/tools/spatial-analyst-toolbox/how-natural-neighbor-works.htm)

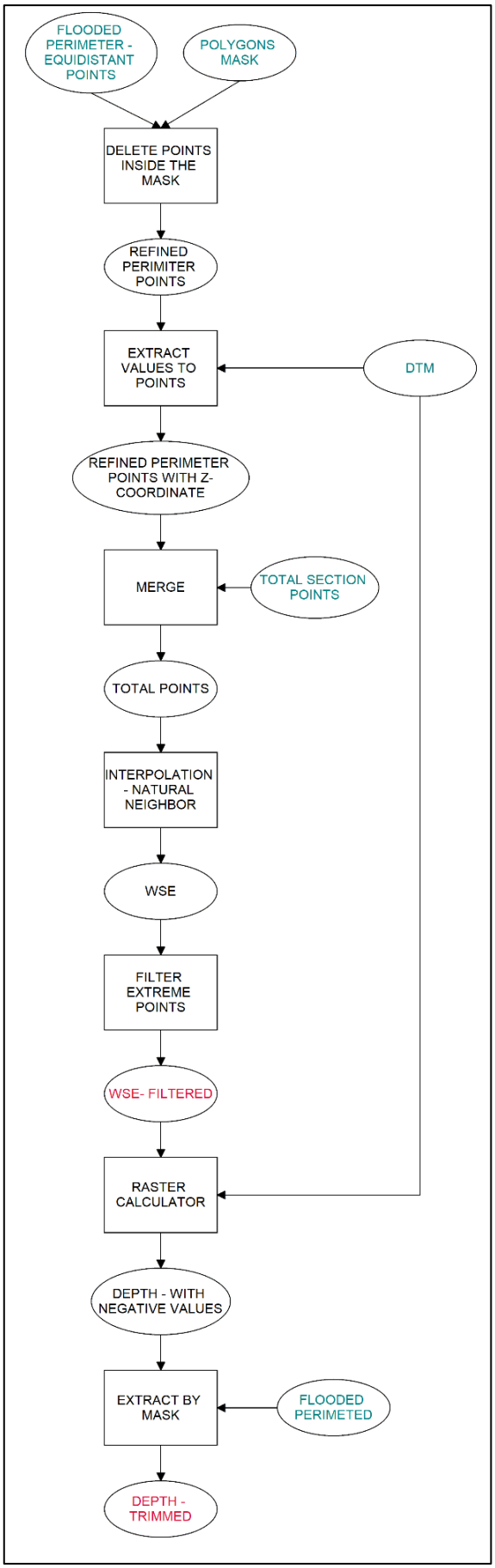

Figure 119 Framework of the GIS-method to compute the WD

The validation process for the developed GIS-model consists in comparing the results obtained with the output of the bi-dimensional flood modelling analysed in chapter 4. If the proposed method provides comparable results to those obtained with the 2D model, it can be stated that the simplified procedure can be employed in the damage evaluation process without affecting significantly the overall damage value.

As it is introduced in chapter 5.3, some additional points are used to force the interpolation procedure to avoid incorrect behaviour in the water profile. To understand the effect of the river cross-sections, two cases are compared:

1. “isotropic” case: it uses as punctual input only the “flooded perimeter – equidistant points” without “total section points”;
2. “sections” case: it uses as punctual inputs the “flooded perimeter – equidistant points” and “total section points”.

In both cases all the other inputs described above remain unchanged. Moreover, the framework used in both cases is the same, in fact to create the section case 1 it is sufficient to set as input an empty “total section points” shapefile.

From the WSE computed for both cases, the maps of the differences between the WSE computed with the GIS-model and the one calculated with the R2D-model can be produced. This is needed to understand from a qualitative point of view how the 2 cases are performing compared to the simulation computed with R2D.

To understand how the values of the differences are distributed along the flooded domain, cumulative distribution functions (CDF) are computed. For each case 4 CDF curves are presented:

- total CDF: one curve is computed for all the points inside the computational domain;
- CDFs for each value of the Manning parameter: this subdivision is used to understand in qualitative and quantitative terms if the Manning is influencing the WSE resulting from the GIS-model. The classes of Manning’s value considered are the same as shown in 5.2.2 (rural, urban and channel).

Finally, to understand which case is performing better, a comparison between the two cases is done, using the following statistical parameters: average of the differences, absolute average and standard deviation of the differences (see section 5.2.2).

The best case is the one that minimises these statistical parameters.

5.3.2 RESULTS

The results of the validation process are presented hereinafter, and conclusion are derived.

5.3.2.1 ISOTROPIC CASE

The following pictures represent the outputs of the GIS-model described in the previous section. They are the “WSE – FILTERED” trimmed on the flooded perimeter (Figure 120) and the “DEPTH -TRIMMED” (Figure 121), respectively.

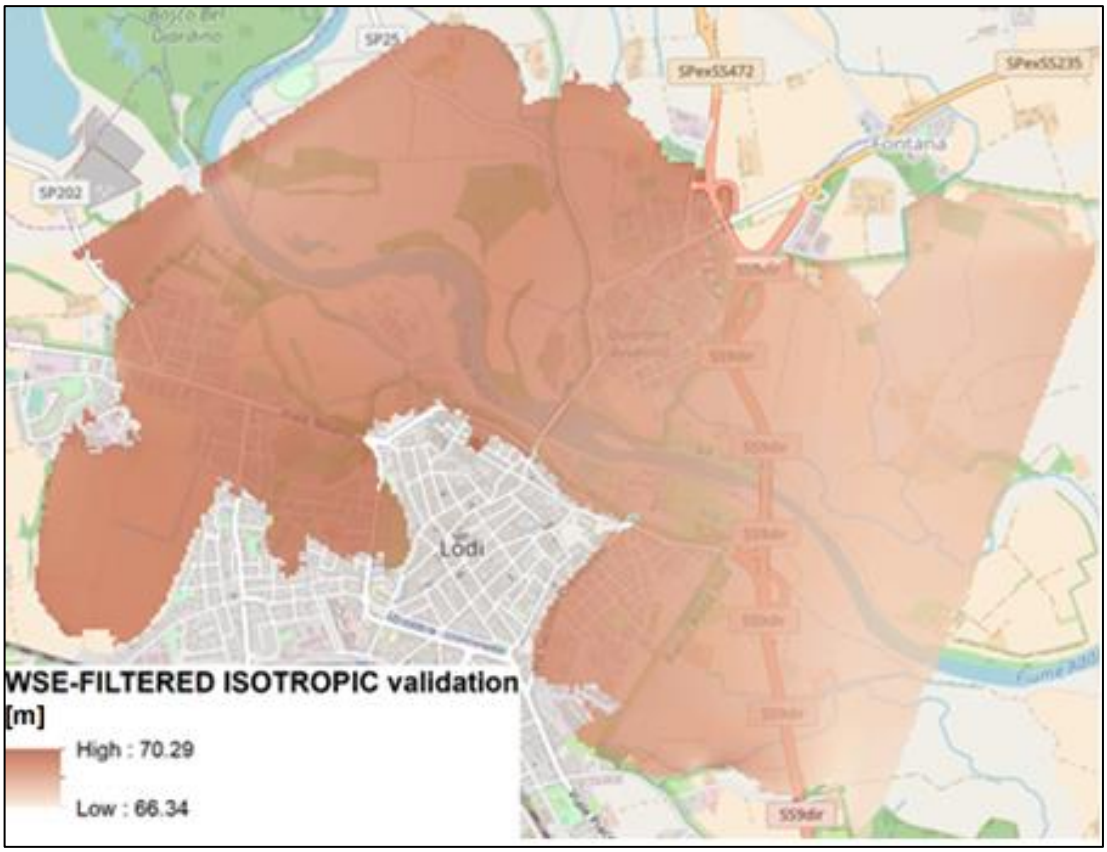

Figure 120 WSE map ISOTROPIC

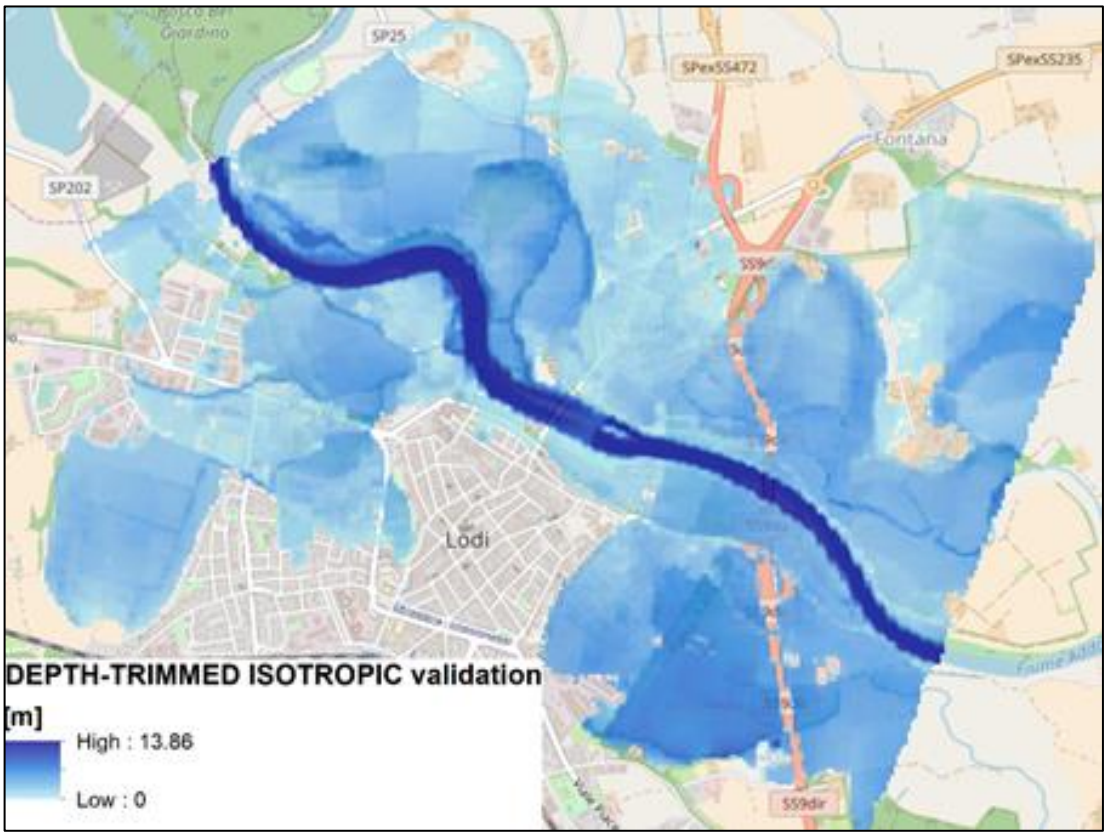

Figure 121 WD map ISOTROPIC

The following picture represents the computed difference between the “WSE-FILTERED” and the “R2D-WSE”.

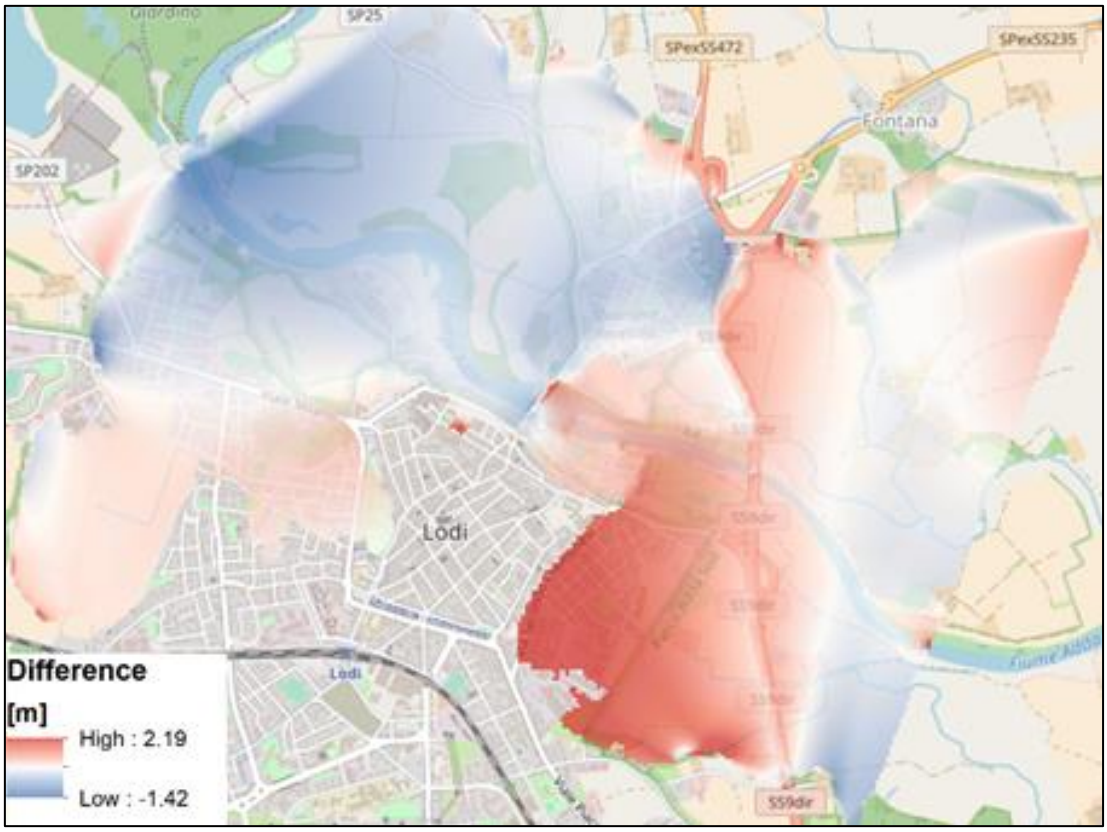

Figure 122 Difference map ISOTROPIC

The CDFs derived from the previous maps are shown in the following graph.

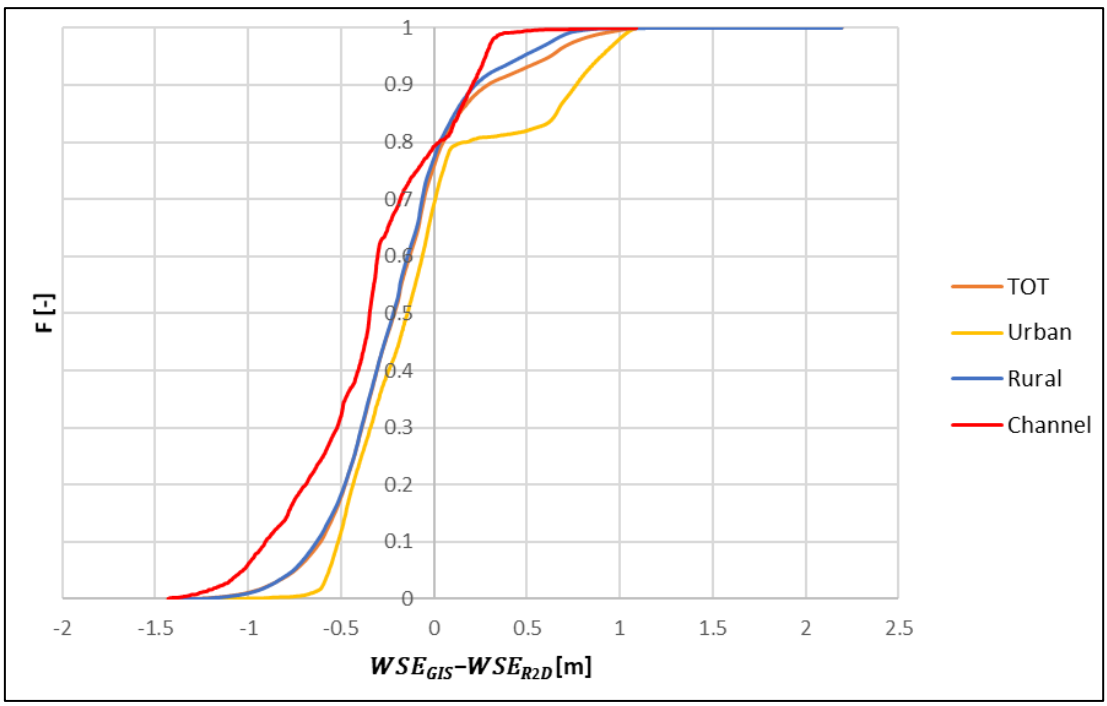

Figure 123 Superimposition of CDFs curves ISOTROPIC

The “TOT” distribution, that is computed considering all the points in the domain without subdivision, is very similar to the “Rural” one; probably because most of the points in the computational domain are characterised by rural value of the Manning’s coefficient.

The CDF related to the “Channel” case clearly shows that the water surface elevation is mostly underestimated. In the other cases there is a similar behaviour: they are all shifted on the negative part of the graph, meaning that there is a general underestimation of the water surface elevation, but less evident than the “Channel” one.

All the curves have the left tail with values higher than the right one (except for the “Rural” one where there are some outliers protracting the curve)

The other parameters produced are listed in the table below:

Table 22 Statistical parameter - ISOTROPIC

CASE	AVERAGE [m]	ABSOLUTE AVERAGE [m]	STANDARD DEVIATION [m]
Total	-0.19	0.34	0.38
Urban	-0.05	0.36	0.45
Rural	-0.20	0.33	0.35
Channel	-0.35	0.44	0.39

5.3.2.2 SECTION CASE

As in the previous case, the following pictures depict the output of the GIS-model.

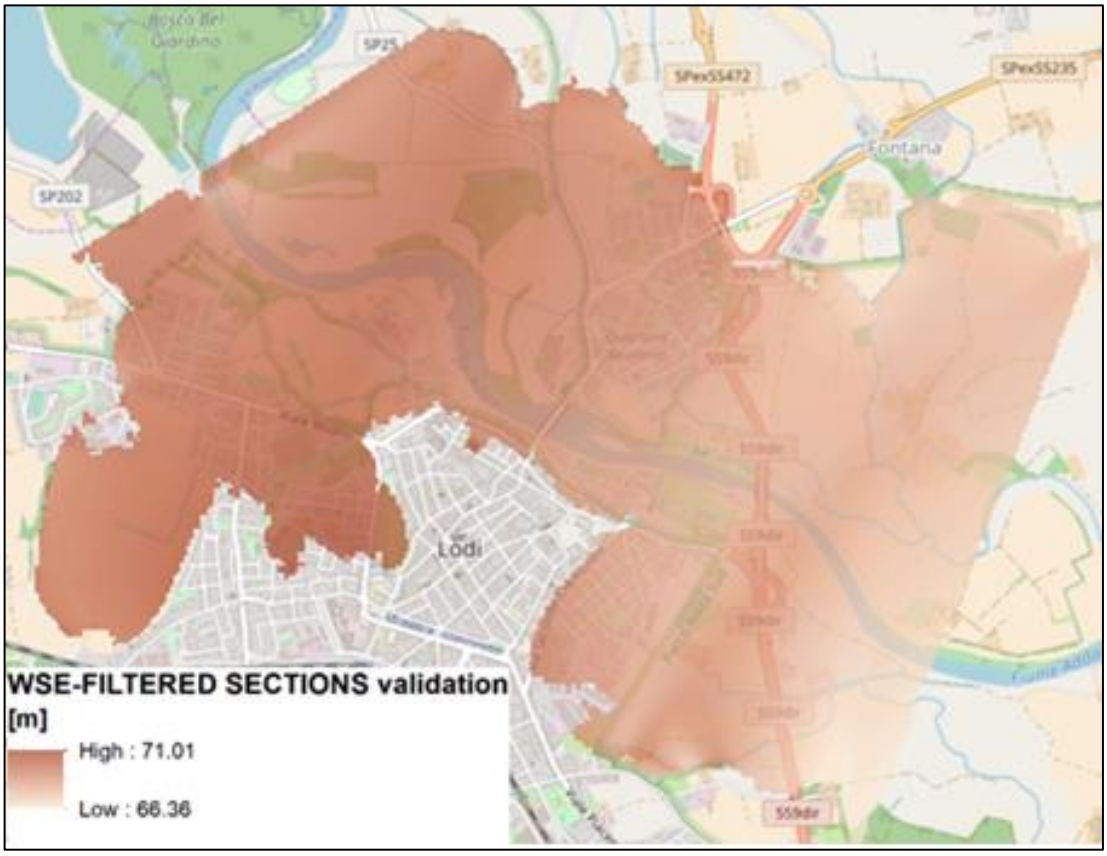

Figure 124 WSE map SECTIONS

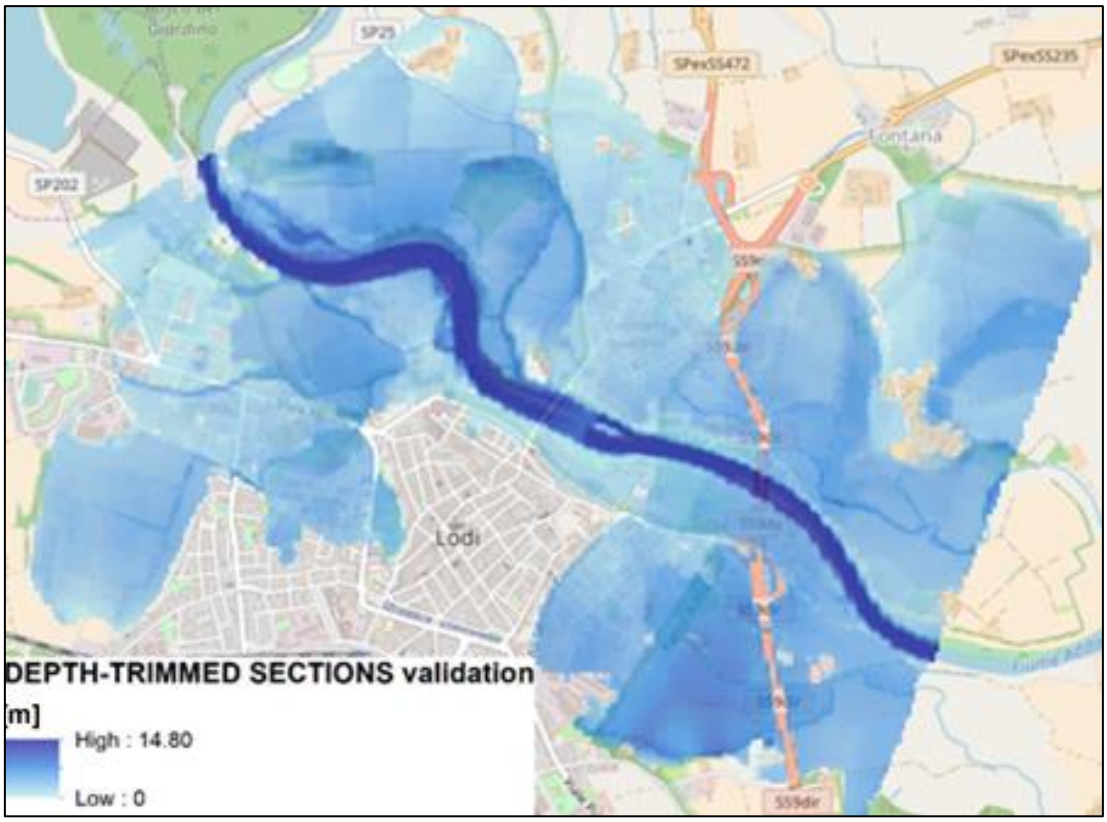

Figure 125 WD map SECTIONS

The following picture represents the computed difference between the “WSE-FILTERED” and the “R2D-WSE”.

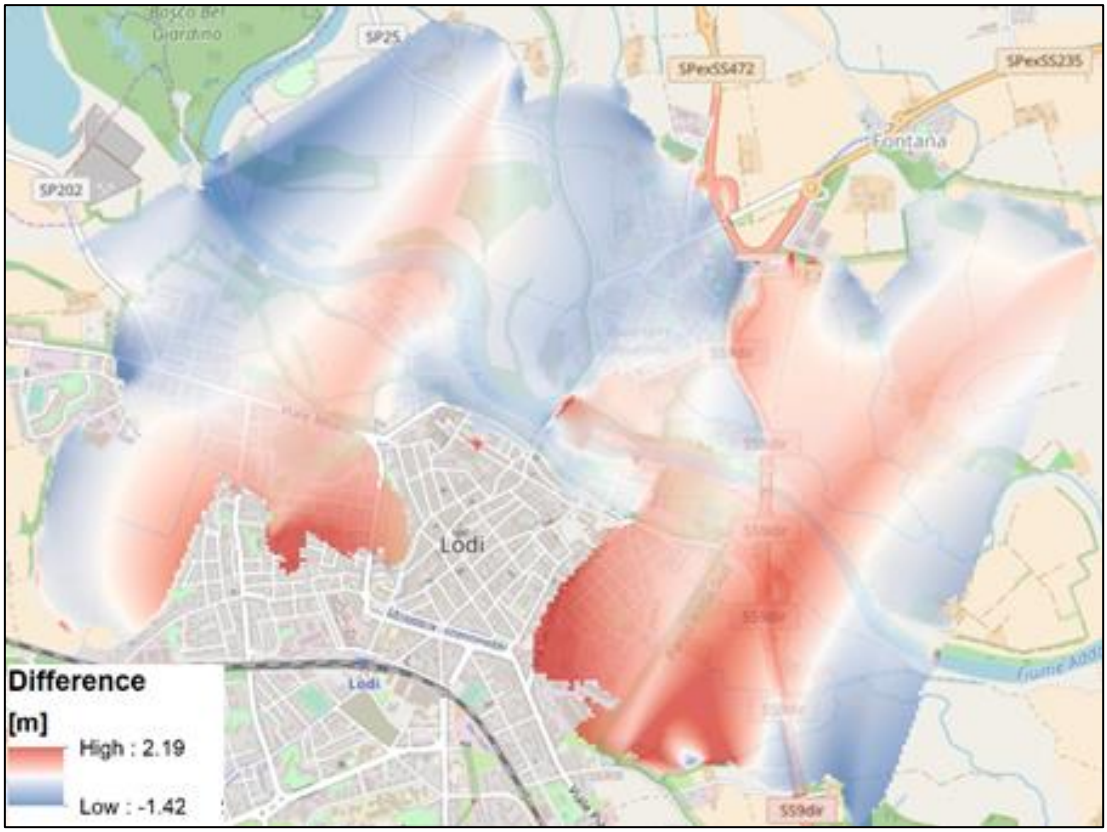

Figure 126 Difference map SECTIONS

The CDF produced starting from the previous picture are listed below.

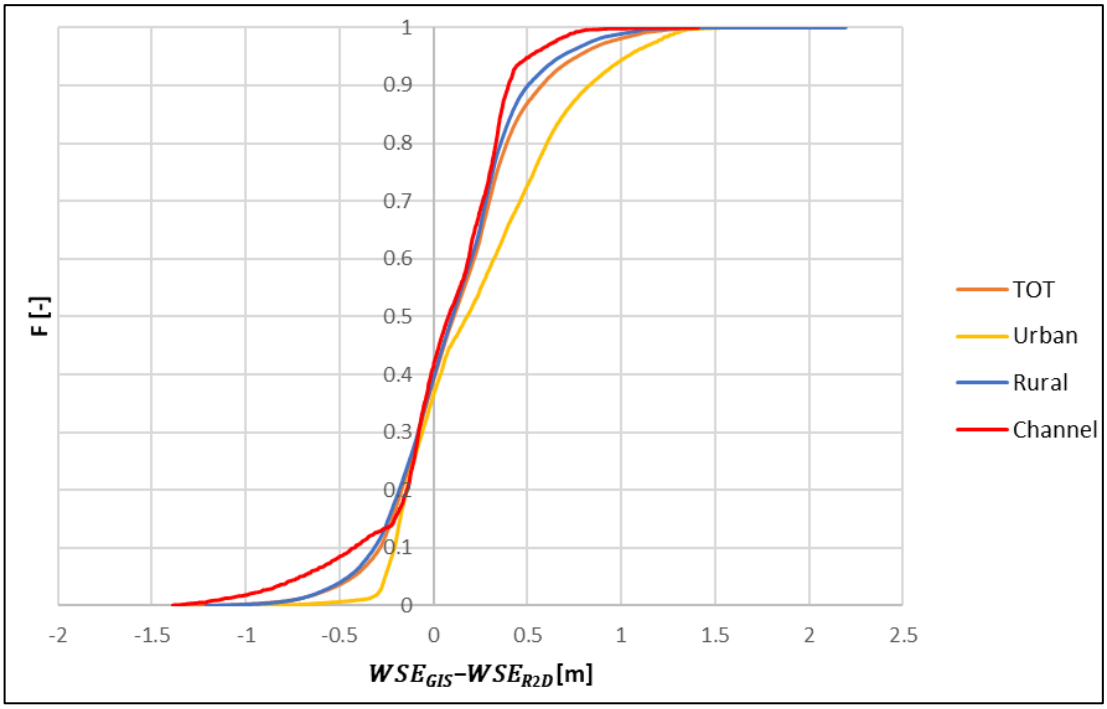

Figure 127 Superimposition of CDFs curves SECTIONS

Similarly, to the “isotropic” case, the “TOT” CDF is very similar to the “Rural” curve. But it can be easily noticed that in this case all the distributions have a behaviour more similar than the one presented for the “isotropic” case.

The CDF related to the “Urban” case is showing that the water surface elevation is overestimated. In the other cases the behaviour is almost equal, with a slight shift on the positive part of the graph, meaning that in general there is an overestimation of the water surface elevation. It can be noticed that the absolute shift is small than that observed in the previous case.

All the curves have the left tail with values higher than the right one (except the “Rural” one where, also in this case, there are some outliers modifying the curve)

The other parameters produced are listed in the table below:

Table 23 Statistical parameter - SECTIONS

CASE	AVERAGE [m]	ABSOLUTE AVERAGE [m]	STANDARD DEVIATION [m]
Total	0.12	0.29	0.36
Urban	0.24	0.36	0.41
Rural	0.10	0.28	0.34
Channel	0.04	0.27	0.36

5.3.3 MODEL VALIDATION

Firstly, the CDF curves are compared to understand how the resulting WSE is influenced by introducing cross-sections in the interpolation procedure. The following figure shows the superimposition of the CDFs for all the points in the computational domain.

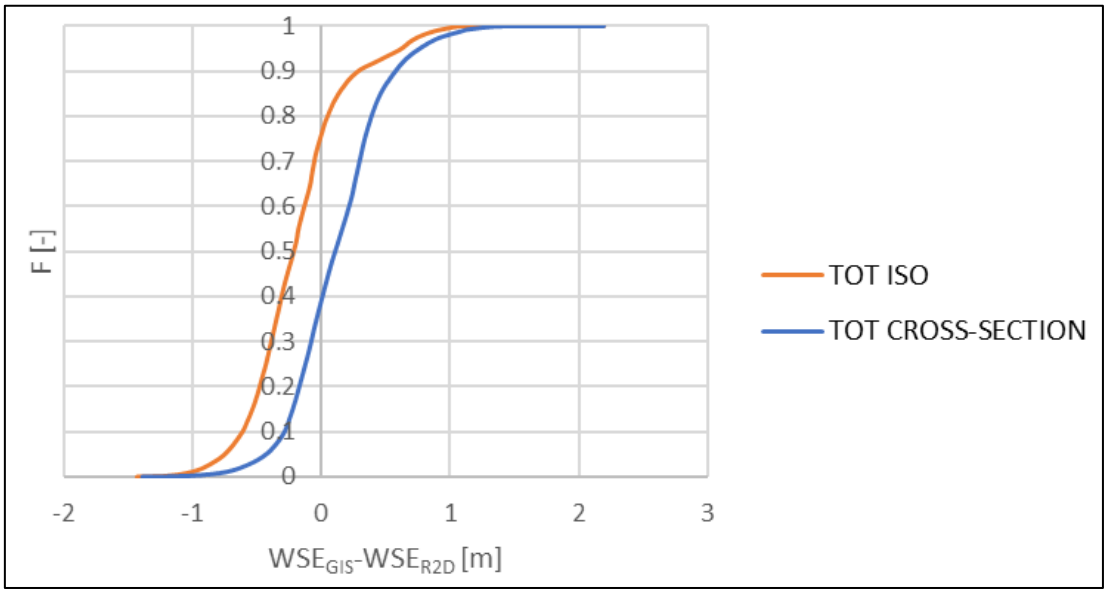

*Figure 128 Superimposition of the CDFs for the **sections case** and **isotropic case** – total*

From this CDF it can be understood that:

- the left tai, is shorter in the “TOT CROSS-SECTION” case;
- the right tails are equal for both cases;
- the introduction of the cross sections is shifting the CDF on the right, meaning that it leads from underestimated WSE to an overestimated WSE;

With the CDF representing points that are in the computational domain characterised by the “channel” value of the Manning’s coefficient (below), it is clear that:

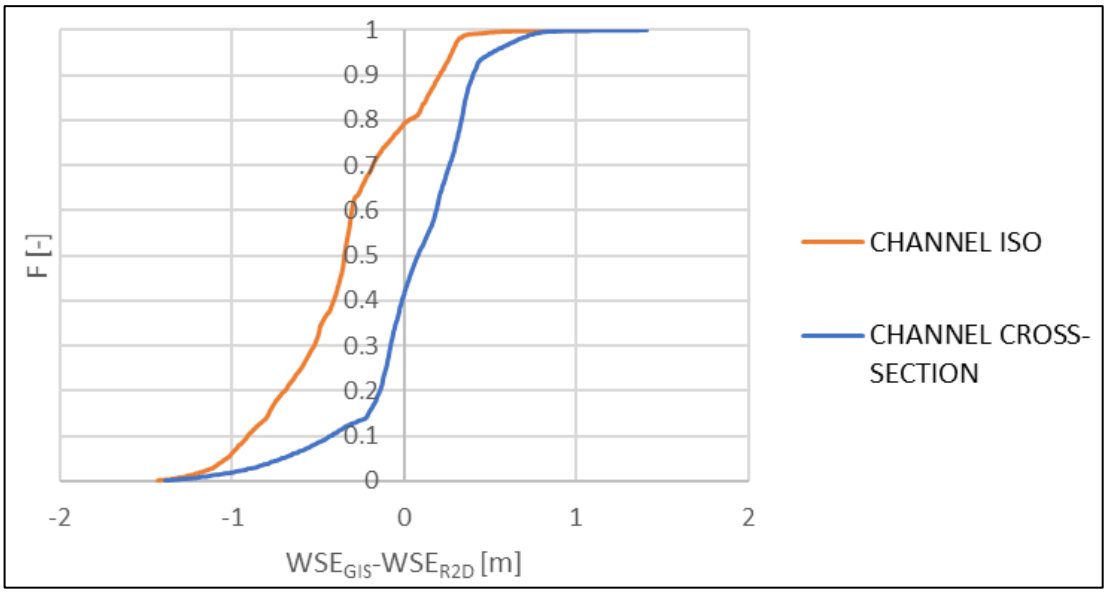

*Figure 129 Superimposition of the CDFs for the **sections case** and **isotropic case** – channel*

- the left tail is slightly shorter in the “CHANNEL CROSS-SECTION” case;
- the right tails are similar for both cases;
- the introduction of the cross sections is changing the shape of the CDF curve: clearly the best one is the “CHANNEL CROSS-SECTION” case, whose shape anticipates a lower average value and a lower standard deviation.

The CDF representing points that are in the computational domain characterised by the “rural” value of the Manning’s coefficient (below) has the same characteristics of the “CDF total”, therefore the conclusions are not repeated.

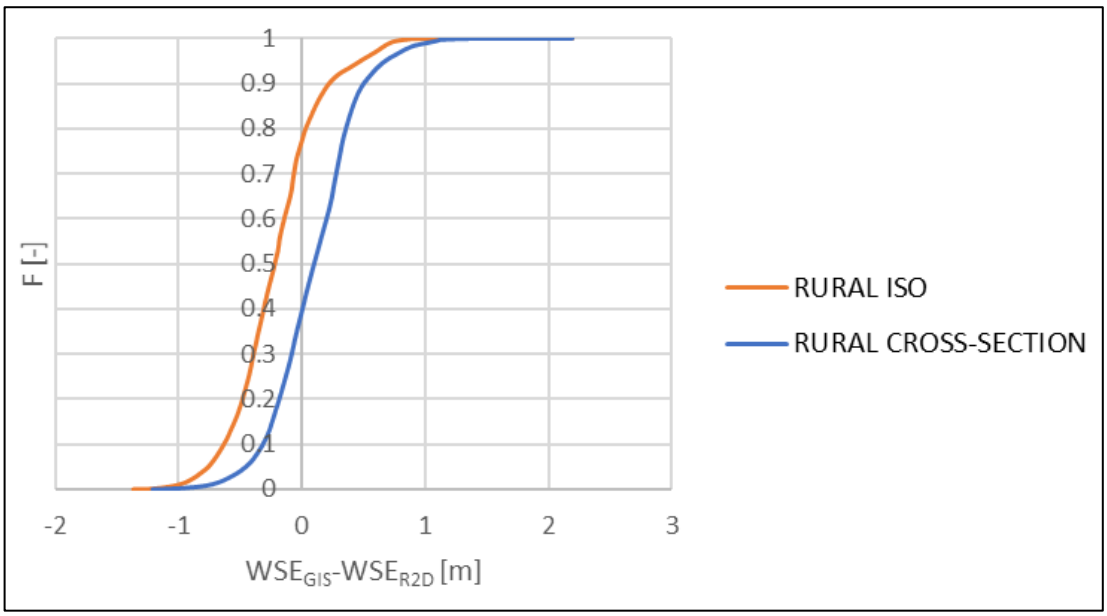

*Figure 130 Superimposition of the CDFs for the **sections case** and **isotropic case** – rural*

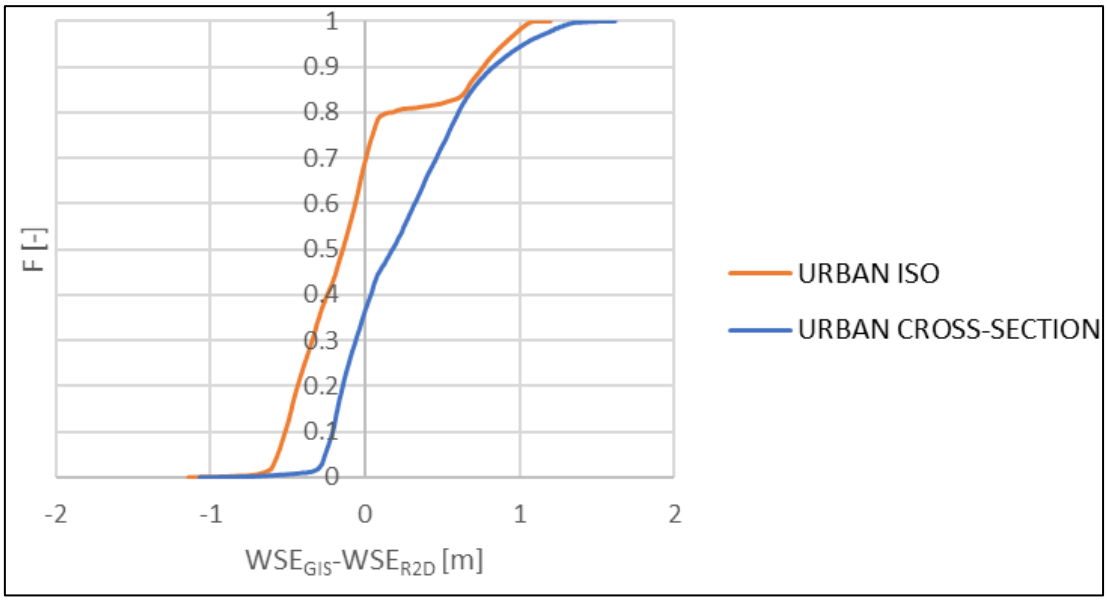

*Figure 131 Superimposition of the CDFs for the **sections case** and **isotropic case** – urban*

The CDF curve for the urban value of the Manning parameter is showing that:

- both cases have deficiencies in representing the WSE in the urban area;
- the left tail, is shorter in the "URBAN CROSS-SECTION" case;
- the right tail is shorter in the "URBAN ISO" case;
- the introduction of the cross sections is shifting the CDF on the right, meaning that it leads from underestimated WSE to an overestimated WSE.

Finally, in the following table the average, absolute average and standard deviation are compared and, the best alternative is highlighted in green.

Table 24 Comparison isotropic case vs sections case - average

	AVERAGE [m]	
CDF	**ISOTROPIC CASE**	**SECTIONS CASE**
Total	-0.19	0.12
Urban	-0.05	0.24
Rural	-0.20	0.10
Channel	-0.35	0.04

Table 25 Comparison isotropic case vs sections case – absolute average

	ABSOLUTE AVERAGE [m]	
CDF	**ISOTROPIC CASE**	**SECTIONS CASE**
Total	0.34	0.29
Urban	0.36	0.36
Rural	0.33	0.28
Channel	0.44	0.27

Table 26 Comparison isotropic case vs sections case – standard deviation

	STANDARD DEVIATION [m]	
CDF	**ISOTROPIC CASE**	**SECTIONS CASE**
Total	0.38	0.36
Urban	0.45	0.41
Rural	0.35	0.34
Channel	0.39	0.36

From this comparison, the “SECTION CASE”, providing better results, can be considered as the most reliable one.

5.3.4 ACCURACY AND LIMITATIONS OF THE MODEL

In this section, the maximum precision of the developed method is estimated. This aim is reached introducing the following modification in the input of the GIS-model:

- the flooded perimeter – equidistant points: instead of extracting the values of the DTM, the “ideal” values of the WSE-R2D are used. In this way it is assumed that the hypothesis WSE = DTM along the flooded perimeter is perfectly fulfilled.

As before, the outputs of the GIS-model are:

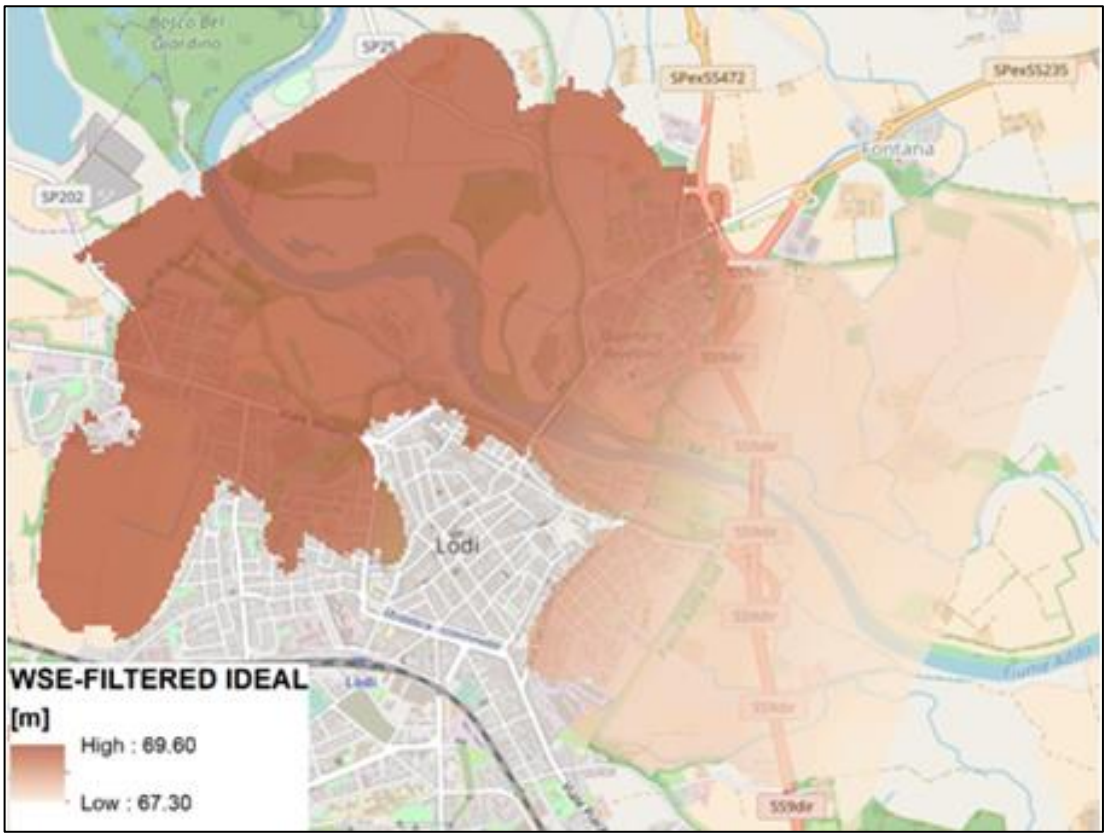

Figure 132 WSE map - IDEAL

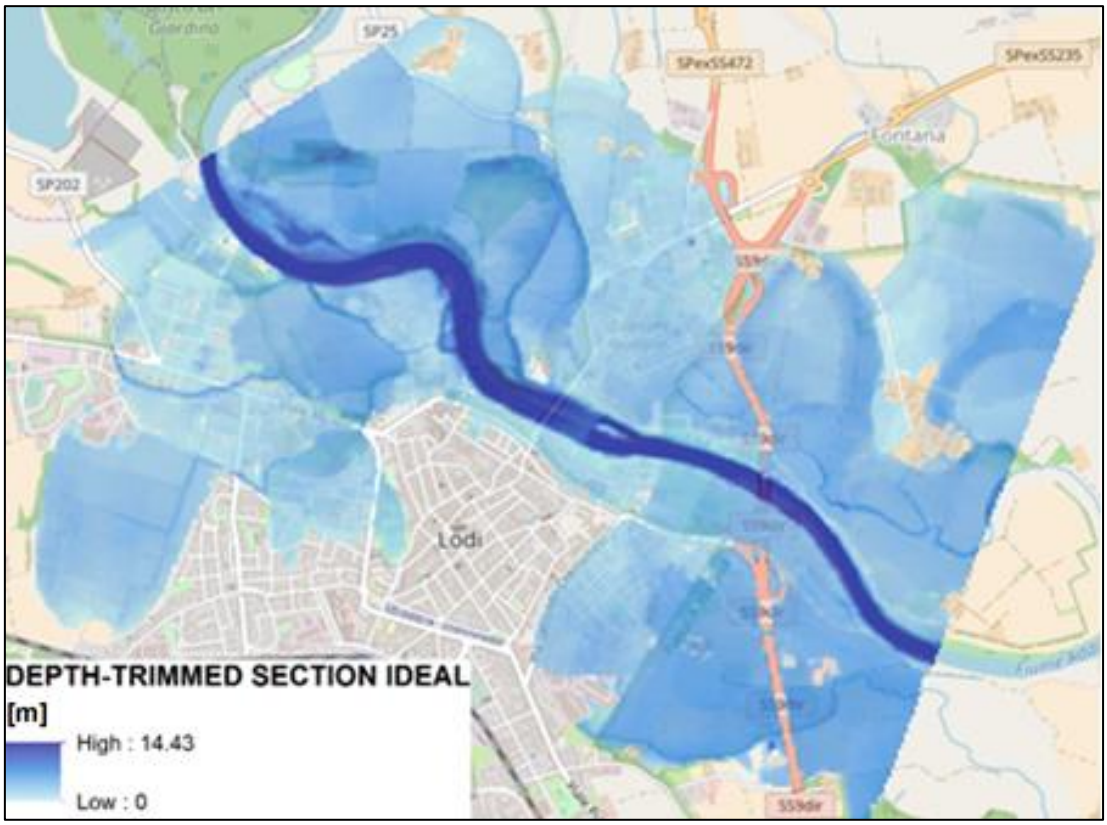

Figure 133 WD map IDEAL

In addition, the map of the differences between WSE_{GIS} and WSE_{R2D} is presented below.

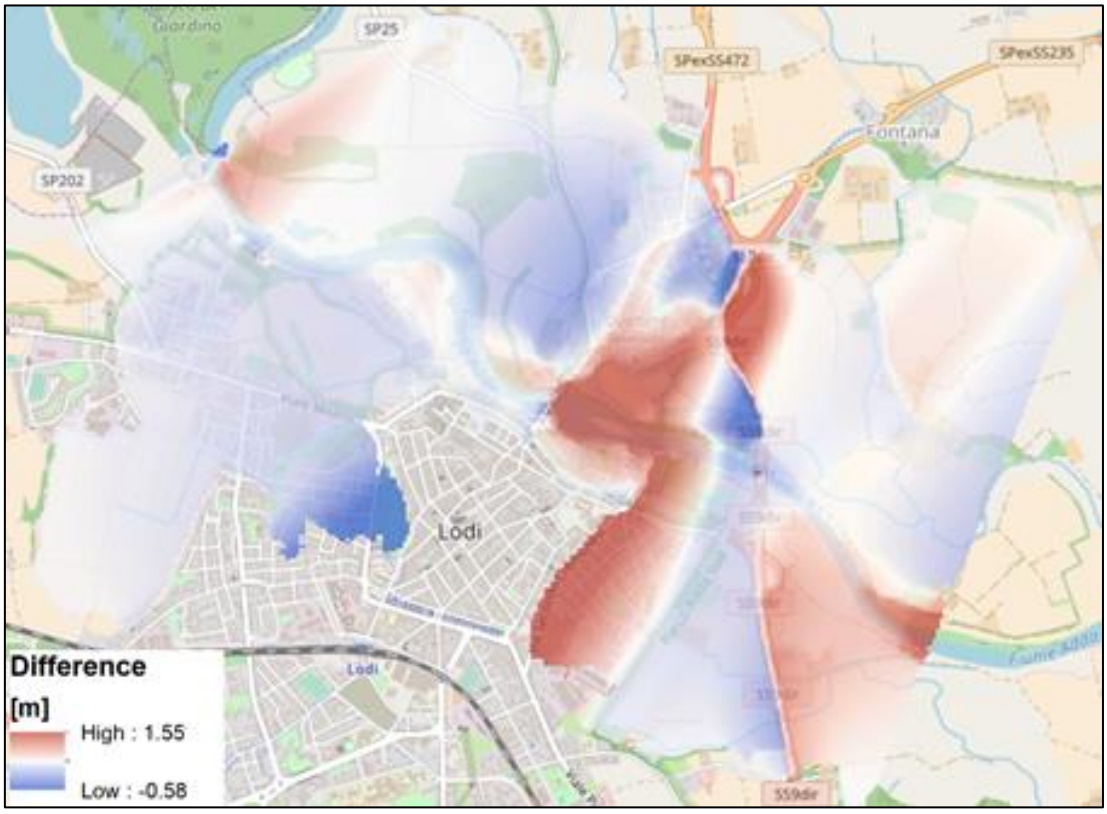

Figure 134 Difference map IDEAL

From the map of the differences the following statistics can be derived:

- the average difference = 0.012 m;
- standard deviation = 0.125 m.

These two values are very important, because they represent the maximum precision that the GIS-model can attain. In fact, working with an “ideal” input where DTM = WSE, it means that 0.012 m is the error due only to the interpolation along the cross-sections and between cross-sections points and perimeter points. Moreover, higher differences are located where the effect of the anthropic structures is present. A clear example occurs near the highway embankment, where the water depth is strongly influenced by the tangential fluxes, which, as presented in the chapter 5.2, are not well predicted by the GIS-model.

5.4 APPLICATION OF THE MODEL ON P.A.I. CASE

5.4.1 METHODS

The last aim of the developed GIS-method is to derive a flood depth map starting from the *fasce P.A.I.,* which represent the inundated area related to a given return period (T) flood event.

For the case study, the flooded perimeter of the 200-years flood is chosen.

A comparison between the GIS-method and the R2D-method is again possible because:

- T is equal to the one estimated in the study by (Natale, 2003), considered as reference for the input on the discharge used in the R2D-model;
- The discharge (Q) between the GIS-method and R2D-method is very similar.

As before, the comparison is proposed considering the cases:

3. “isotropic” case;
4. “sections” case.

Their explanation is already present in chapter 5.3, therefore it is not repeated.

In this application the input parameters used for the GIS-model are:

- The flooded perimeter: it is the polygon shapefile representing the *fascia P.A.I.* with T = 200 years. This one is slightly modified in order to:
    - correct transformation errors from the reference system (R.S.) used for the *fascia P.A.I*. (Rome Montemario) to the default R.S. used to create the GIS-model (WGS 84);
    - correct inconsistencies between the flooded perimeter and the DTM used, since the *fascia P.A.I.* is calculated with a 1D model and with a different DTM from the one used in this model.

  The picture below shows the input just explained.

Figure 135 Fascia P.A.I T=200 years

- Polygon mask: to eliminate entities from the shapefile “flooded perimeter – equidistant points” which are do not fulfil the hypothesis of the model.

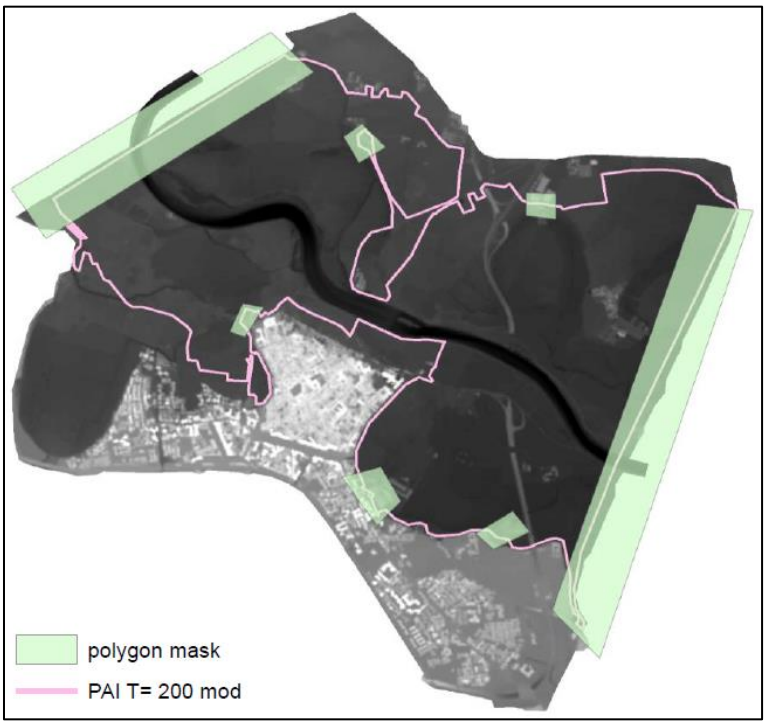

Figure 136 Polygon mask

- DTM: the same DTM used in the chapter 5.3 is considered;

- Total section points: this point shapefile is produced with the procedure described in the chapter 5.2; moreover, the river-cross sections used are the same that are employed for the validation procedure in chapter 5.3.

As in chapter 5.3, the results produced are:

- “WSE-FILTERED” map;
- “DEPTH-TRIMMED” map;
- map of the differences between the “WSE-FILTERED” and the “R2D-WSE”;
- CDFs derived from the map of the differences, respectively for total, urban, rural and channel points;
- statistical parameters.

5.4.2 RESULTS

The outputs listed above are presented hereinafter. They are subdivided between the “isotropic” and “sections” case.

5.4.2.1 “ISOTROPIC” CASE

The results are:

- “WSE-FILTERED” map

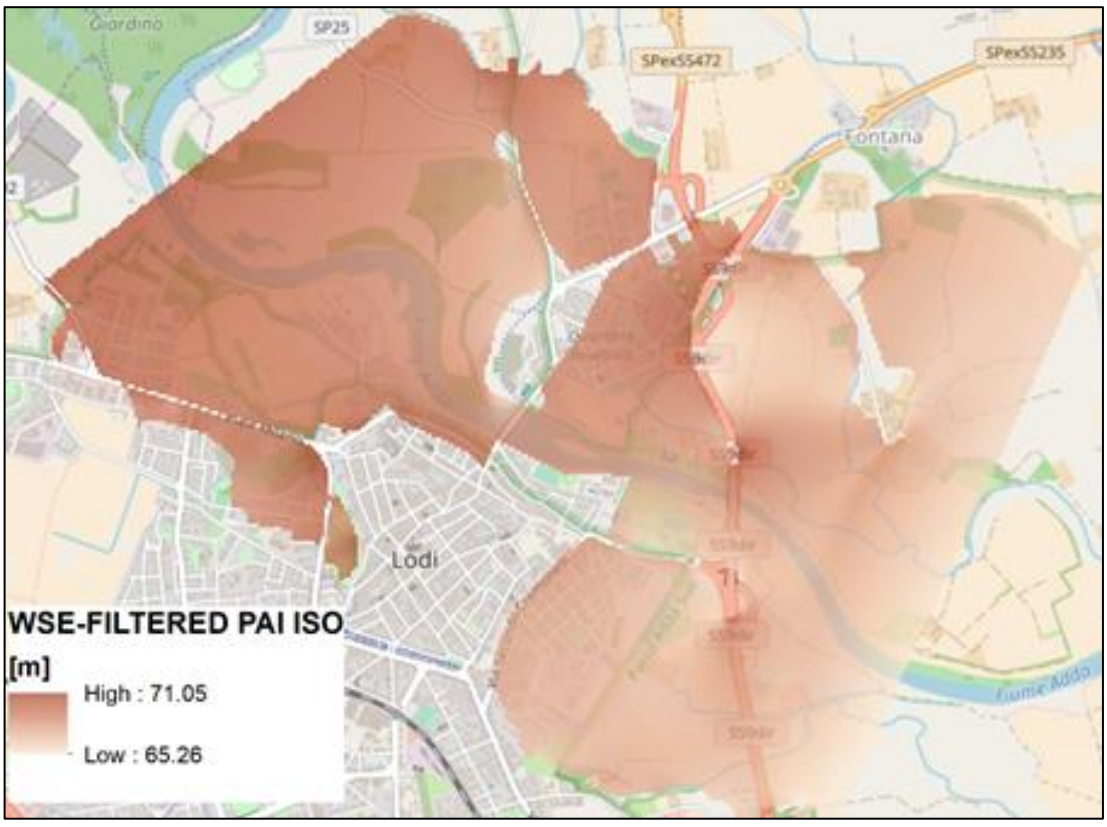

Figure 137 WSE map P.A.I. ISOTROPIC

- “DEPTH-TRIMMED” map

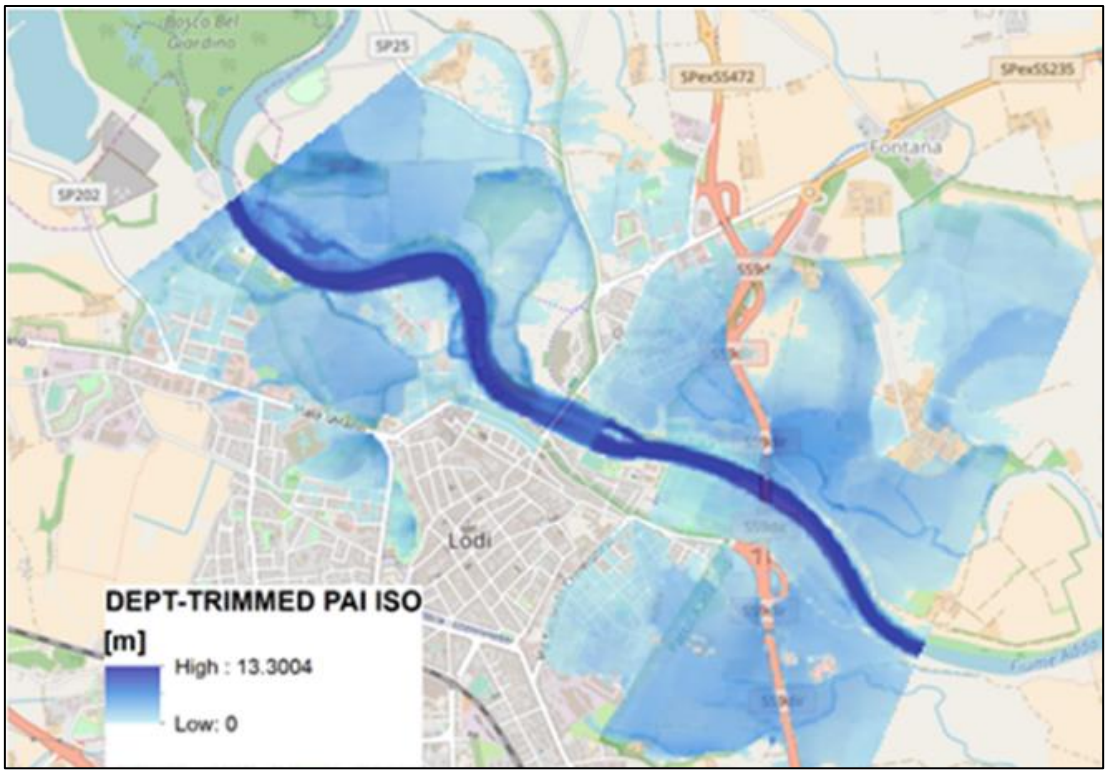

Figure 138 WD map P.A.I. ISOTROPIC

- Map of the differences

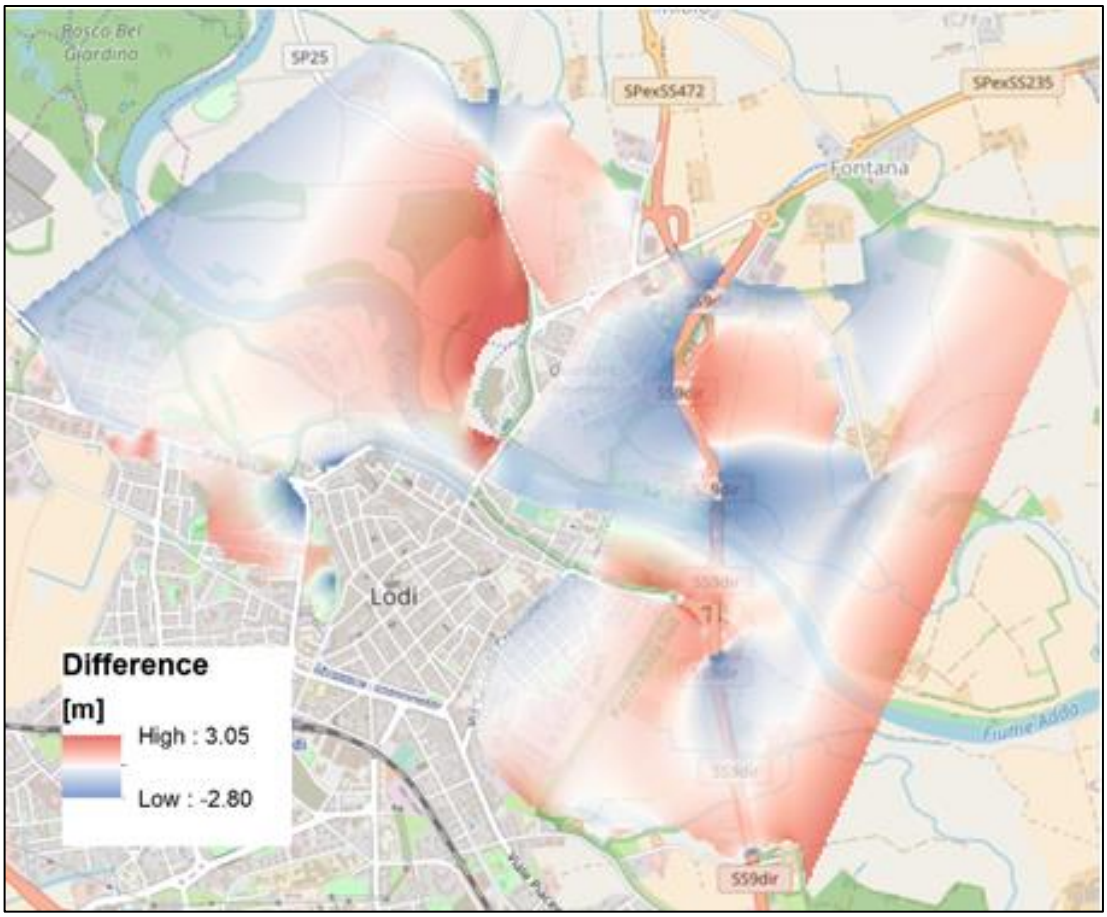

Figure 139 Difference map P.A.I. ISOTROPIC

- CDFs graphs

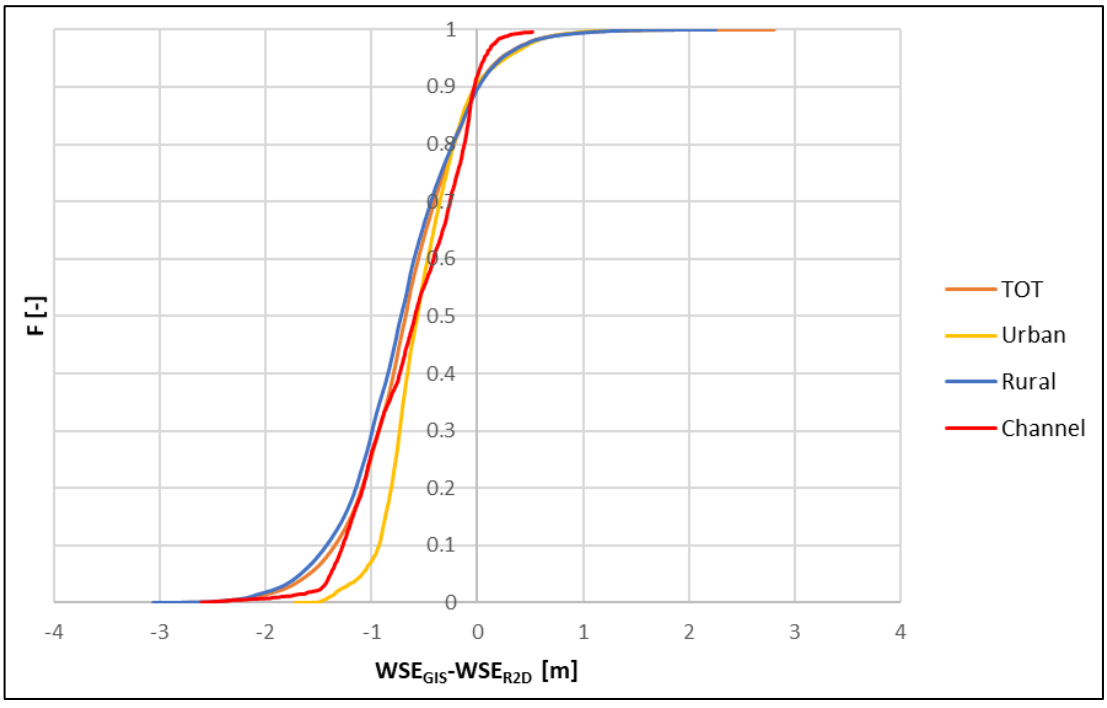

Figure 140 Superimposition of CDFs curves P.A.I. ISOTROPIC

Again, the “TOT” CDF is very similar to the “Rural” curve. But it can be easily noticed that in this case all the distributions have a similar shape.

The CDF related to the “Urban” case shows an underestimation of the water surface elevation. In the other cases the behaviour is almost equal, with a slight shift on the negative part of the graph, meaning that in general there is an underestimation of the water surface elevation.

All the curves have the left tail with values higher than the right one (except for the “Channel” one where the right tail is much shorter than the left one).

Statistical parameters:

Table 27 Statistical parameter – P.A.I. ISOTROPIC

CASE	AVERAGE [m]	ABSOLUTE AVERAGE [m]	STANDARD DEVIATION [m]
Total	-0.66	0.73	0.55
Urban	-0.51	0.57	0.41
Rural	-0.70	0.77	0.58
Channel	-0.61	0.63	0.49

5.4.2.2 “SECTION” CASE

The results are:

- “WSE-FILTERED” map

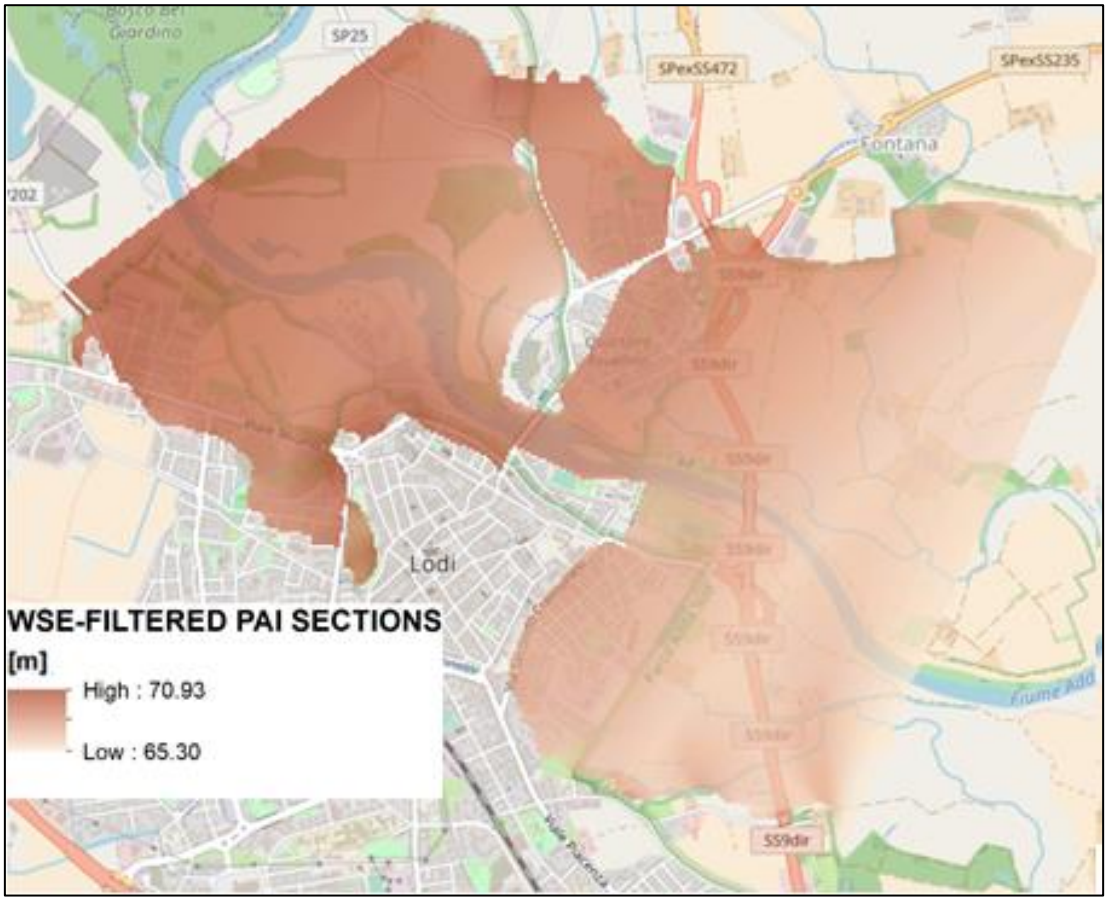

Figure 141 WD map P.A.I. SECTIONS

- “DEPTH-TRIMMED” map

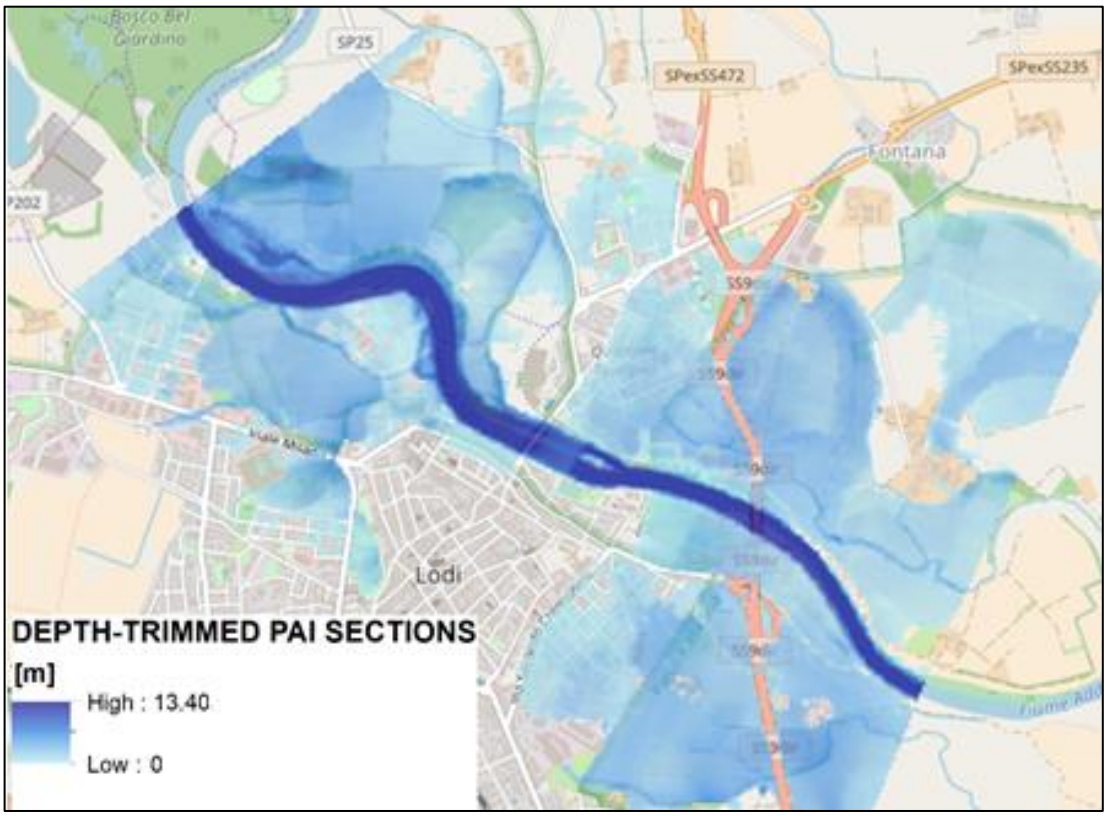

Figure 142 WD map P.A.I. SECTIONS

- Map of the differences

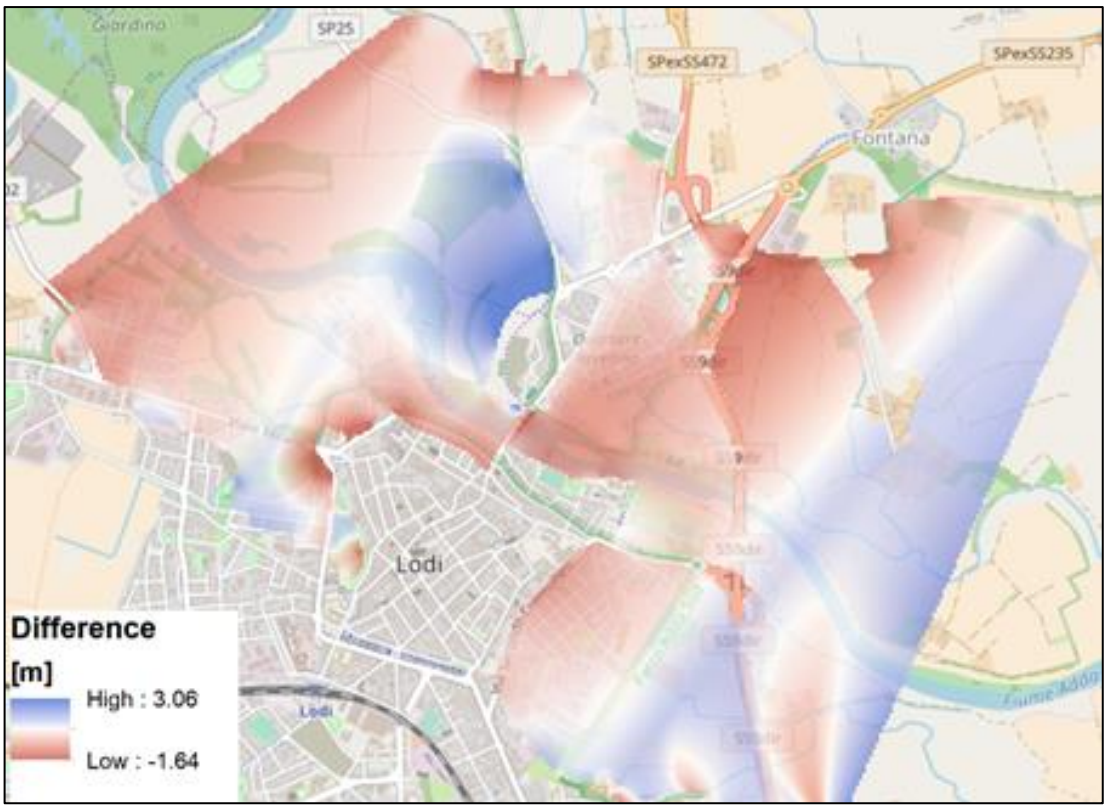

Figure 143 Difference map P.A.I. SECTIONS

- CFDs graphs

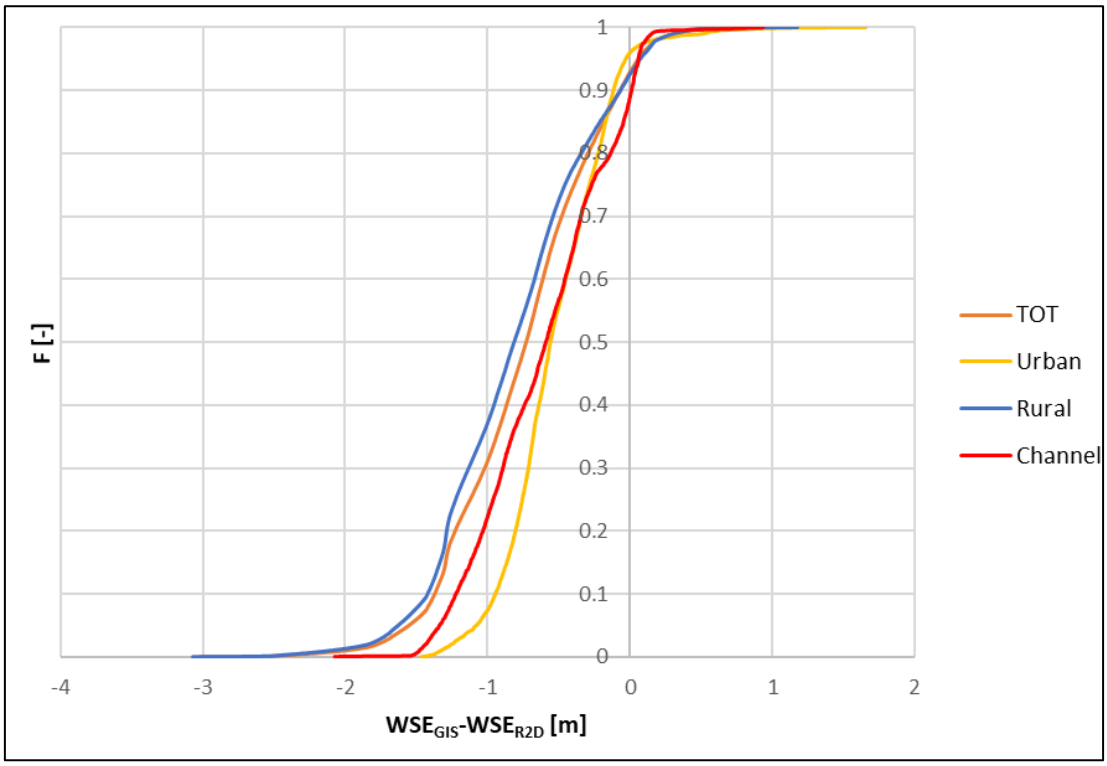

Figure 144 Superimposition of CDFs curves P.A.I. SECTIONS

For this case, the same conclusions drawn for the previous one can be repeated.

- Statistical parameters

Table 28 Statistical parameter – P.A.I. SECTIONS

CASE	AVERAGE [m]	ABSOLUTE AVERAGE [m]	STANDARD DEVIATION [m]
Total	-0.74	0.77	0.51
Urban	-0.53	0.55	0.34
Rural	-0.80	0.83	0.52
Channel	-0.60	0.62	0.44

Finally, in the following table the average, absolute average and standard deviation are compared and, the best alternative is highlighted in green.

Table 29 Comparison isotropic case vs sections case – P.A.I. average

	AVERAGE [m]	
CDF	ISOTROPIC CASE	SECTION CASE
Total	-0.66	-0.74
Urban	-0.51	-0.53
Rural	-0.70	-0.80
Channel	-0.61	-0.60

Table 30 Comparison isotropic case vs sections case – P.A.I. absolute average

	ABSOLUTE AVERAGE [m]	
CDF	**ISOTROPIC CASE**	**SECTION CASE**
Total	0.73	0.77
Urban	0.57	0.55
Rural	0.77	0.83
Channel	0.63	0.62

Table 31 Comparison isotropic case vs sections case – P.A.I. standard deviation

	STANDARD DEVIATION [m]	
CDF	**ISOTROPIC CASE**	**SECTION CASE**
Total	0.55	0.51
Urban	0.41	0.34
Rural	0.58	0.52
Channel	0.49	0.44

From the above comparison, it can be noticed that the "SECTION CASE" gives better results in terms of standard deviation, meanwhile the "ISOTROPIC" one is better for the average and absolute average. Both cases underestimate the water depth in the computational domain.

As it can be noticed, the errors are higher compared to the ones computed in Chapter 5.3. This could be explained as follows:

- The *fascia P.A.I.* is very different from the one resultant from the R2D-model. In particular, some zones, that are flooded in the R2D-model, are not inundated in case of the *fascia P.A.I.*; this is due to the fact that the latter is computed starting from a 1D simulation, that does not consider the lateral flow. In the picture below, the differences are highlighted in red.

Figure 145 Main differences between the P.A.I. perimeter and the perimeter obtained by the steady simulation with R2D

- The discharge used to calculate the *fascia P.A.I.* is lower than the one used to perform the simulation with R2D. In fact, as it can be noticed from the following graph (Figure 146) the discharge used to compute fascia P.A.I. for a return period of 200 years is around 1500 m^3/s.

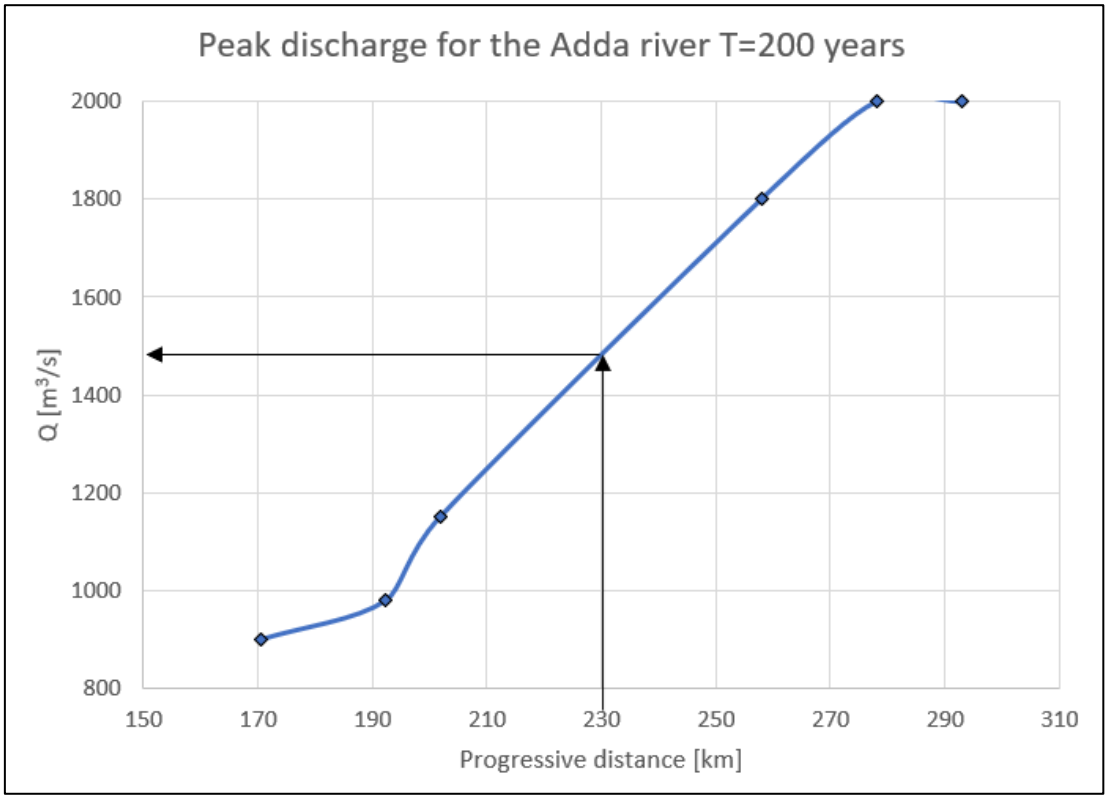

Figure 146 Progressive distance VS discharge (from AdbPo[29])

(230 km is the progressive distance of the section 107)

5.5 CONCLUSIONS OF THE HAZARD MAPPING FROM FLOOD EXTENT

In the above chapter a new GIS-model to derive flood hazard maps is presented. It is based on an interpolation between a series of points along the flooded perimeter and some user-defined cross-sections.

The two main hypotheses are:

- WD = 0 m along the flooded perimeter;
- specular perimeter points have comparable WSE.

The input parameters needed are:

- flood perimeter;
- cross-sections;
- DTM;

[29] http://www.adbpo.it/PAI/7%20-%20Norme%20di%20attuazione/7.2%20-%20Direttive%20di%20Piano/Direttiva2/Direttiva2.htm

- polygon mask.

The outputs of the model are:

- WSE map;
- WD map;

The validation process is performed using as a reference the results of the R2D model explained in the previous chapters. It shows that the GIS-model produces quite good results. In fact, the considered statistical parameters have:

- Average of the differences: 12 cm;
- Absolute Average of the differences: 29 cm;
- Standard deviation: 36 cm.

The most extreme errors by the model (red and blue values in Figure 126) are near the urban area, where there is a lack of perimeter points. This is because these points are against the first hypothesis of the model. To reduce them the introduction of additional cross-section is highly recommended.

These error estimations are due also to the chosen interpolation method. In fact, the maximum precision that the model can attain, for the case study considered, has an average of the difference and a standard deviation around 2 cm and 13 cm, respectively.

In conclusion, this can be considered a quite good improvement compared to other proposals available in the literature that have a value of the “average of the differences” of about 40 cm.

At the end of the chapter the application with the *fascia P.A.I.* T =200 years is computed to show one of the possible application fields of the method. The GIS-model is applied using the “isotropic” interpolation procedure, which is based only on the perimeter points, and the “section” interpolation procedure, which is based on the perimeter points and the cross-sections points. In this application the comparison with the R2D-model is still performed because the return period is also in that case 200 years. The resulting errors are quite high with both the procedures. Possible explanations for this error are:

- the huge difference between the fascia P.A.I. (based on a 1D model) and the flooded perimeter resulting from the R2D model;
- the difference between the discharge used for the computation of the fascia P.A.I. and the discharge used in the R2D-model.

6 CONCLUSIONS

According to recent studies, every year floods are among the most dangerous natural disasters. Their impact has grown steadily due to the increase of population living in the floodplains. The assessment of the impact of future floods has therefore an important role to develop hydrogeological risk management. The main scope of this thesis consisted in the development of a hazard scenario for the city of Lodi, considering the event happened in November 2002.

Two different ways were used to fulfil this task:

- traditional hydraulic modelling;
- fast modelling based on GIS software.

Traditional hydraulic modelling

The starting point for this procedure was the creation of the DTM, by modifying the DSM provided by the Po river basin authority. All the pixels that represent the built environment (bridges, houses, roads above ditches) were modified in order to represent only the terrain.

HEC-RAS and River2D were the software adopted to model the case study, for the 1D and 2D models respectively. The output produced were the hazard maps representing water depths and flow velocities in the flooded area.

A sensitivity analysis (SA) was performed to understand the impact of each input parameter on the model's performance. The parameters considered were: the roughness coefficient, the cross-section geometry for the 1D model, the inflow and outflow dimension for the 2D model as well as the geometry of the area in the 2D model. From the SA, it was deduced that the key parameters for the model under study were the roughness coefficient and the cross-section geometry for the 1D model. These two parameters were subjected to the calibration procedure for the steady model.

Since, there were only two possible values for the section dimension in the 1D model, the most suitable one was selected immediately after the sensitivity analysis. Therefore, only the roughness coefficient was calibrated with a procedure that maximise the so called "final indicator". The results in terms of water depth and velocity were shown in Figure 79 and Figure 85.

The following step was the development of an unsteady model, using the hydrograph of the event. The main output of the unsteady analysis was the dynamic of the event for each time-step of the hydrograph. In the Figure 90 the most influential snapshots were displayed. Comparing the results with the real data of the event, it was observed that the model can simulate the considered event with a good approximation. The main drawback of the unsteady analysis performed was that it required a long computation time. Comparing the steady and the unsteady analysis, it was noticed that the results were quite similar, therefore if the objective of study was only the worst-case scenario, the steady one was recommended to perform the simulation.

Fast modelling based on GIS software

To reduce efforts required by the traditional hydraulic modelling, the new procedure based on GIS software was implemented and improved. To have a comparison between the results obtained from the previous method, the same case study was used. The products of this process were the water surface elevation map and the water depth map.

This method consisted of an interpolation procedure between the points above the flooded perimeter. The fundamental hypotheses were:

- the external boundary of the flooded area represents the locations of points where the water depth is equal to zero;
- the extreme symmetric points, positioned on the perpendicular line to the river, have comparable water surface elevation.

The main limitations introduced by the previous hypotheses were:

- if the water is obstructed by an anthropic structure, as it happens in urban areas, the first hypothesis fails;
- if the external limit is determined by a vertical anthropic structure (like a wall or an elevated road) the water depth (WD) in that point will be different from 0, therefore also the second hypothesis can fail in urbanised area.

To minimise the errors produced due to the limitation of the method, improvements were proposed. The first one consisted in using, with the points above the flooded perimeter, additional points located along some cross-sections generated by the user. The water profile on the cross-sections was simulated with an interpolation procedure, based on the inverse distance weighted (IDW) interpolation method, that needs only the elevation of the two extreme points of the cross-section to draw the water profile. This additional set of points forced the interpolation procedure of the GIS-method producing a more realistic behaviour of the water.

The second one regarded the points that were against the two hypotheses. A polygon mask, created by the user depending on the area under analysis, deleted the points that were near the anthropic structures. The lowest error (section case) had: average = 12 cm, absolute average = 29 cm and standard deviation = 36 cm. The maximum precision that can be reached with this method was finally estimated, its errors were: average = 1 cm and standard deviation = 12.5 cm. After the validation of the new method, an application was performed using the *fascia P.A.I.* T=200 years. Then, a comparison with the R2D model was performed, but it produced higher errors.

The explanation can be attributed to the difference in the discharge used to compute the *fascia P.A.I.*, that is around 300 m^3/s lower than the one used in the R2D model.

From the results observed, it was resulted that the implemented method was not able, at the moment, to fully substitute the traditional hydraulic modelling. However, being aware of its limitations and its degree of accuracy, it can be considered a useful tool for the first estimation of flood damages.

Considering all the results obtained, the future developments of this study can be:

- The use of a faster software that can remove a degree of uncertainty accumulated during the various steps. In fact, a great computational effort required for the unsteady modelling made the sensitivity analysis and the calibration impossible to be performed directly on the same model. The use of these new software can lead to obtain more reliable results in less time.
- The use of a DTM with higher resolution (for example 1x1 meter) which can lead to obtain higher accuracy both in traditional hydraulic modelling and in the GIS-method. Furthermore, it should be considered that extreme resolution of data and models may create false confidence in the precision of the model (Dottori et al., 2013).
- Collecting and sharing the measured or computed data. This practice should be encouraged in this field since due to the lack of robust observed data, calibration of the model and validation of results are not always possible.

BIBLIOGRAPHY

Alcrudo, F. (2004). Mathematical modeling techniques for flood propagation in urban areas. *Buscar*, 1–34.

Alfieri, L., Cohen, S., Galantowicz, J., Schumann, G. J.-P., Trigg, M. A., Zsoter, E., … Salamon, P. (2018). A global network for operational flood risk reduction. *Environmental Science & Policy*, *84*(March), 149–158. https://doi.org/10.1016/j.envsci.2018.03.014

Autorità di bacino del fiume Po. (2003). Studio di fattibilità della sistemazione idraulica.

Bazin, P. H., Mignot, E., & Paquier, A. (2017). Computing flooding of crossroads with obstacles using a 2D numerical model. *Journal of Hydraulic Research*, *55*(1), 72–84. https://doi.org/10.1080/00221686.2016.1217947

Beretta, R., Ravazzani, G., Maiorano, C., & Mancini, M. (2018). Simulating the Influence of Buildings on Flood Inundation in Urban Areas. *Geosciences*, *8*(3), 77. https://doi.org/10.3390/geosciences8020077

Bettiga, A. (2016). Scenario di rischio alluvionale per la città di Sondrio.

Brunner, G. (2010). HEC-RAS river analysis system, Hydraulic reference manual, Version 4.1. *US Army Corps of Engineers Hydrologic Engineering Center, Davis CA*, (January), 1–790. https://doi.org/CPD-68

Chow, V. Te. (1959). Open Channel Hydraulics. *Open Channel Hydraulics*. https://doi.org/10.1016/B978-0-7506-6857-6.X5000-0

Cohen, S., Brakenridge, G. R., Kettner, A., Bates, B., Nelson, J., Mcdonald, R., … Zhang, J. (2017). Estimating Floodwater Depths from Flood Inundation Maps and Topography. *Journal of the American Water Resources Association*, *76019*, 1–12. https://doi.org/10.1111/1752-1688.12609

Cunge, J. a. (2003). Of data and models. *Journal of Hydroinformatics*, *5*(2), 75–98.

Dottori, F., Di Baldassarre, G., & Todini, E. (2013). Detailed data is welcome, but with a pinch of salt: Accuracy, precision, and uncertainty in flood inundation modeling. *Water Resources Research*, *49*(9), 6079–6085. https://doi.org/10.1002/wrcr.20406

Dottori, F., Figueiredo, R., Martina, M. L. V., Molinari, D., & Scorzini, A. R. (2016). INSYDE: A synthetic, probabilistic flood damage model based on explicit cost analysis. *Natural Hazards and Earth System Sciences*, *16*(12), 2577–2591. https://doi.org/10.5194/nhess-16-2577-2016

Dung, N. V., Merz, B., Bárdossy, A., Thang, T. D., & Apel, H. (2011). Multi-objective automatic calibration of hydrodynamic models utilizing inundation maps and gauge data. *Hydrology and Earth System Sciences*, *15*(4), 1339–1354. https://doi.org/10.5194/hess-15-1339-2011

Gatti, F., & Sterlacchini, S. (2016). STIMA DEL RISCHIO ALLUVIONALE PER LE ATTIVITA ' ECONOMICHE : IL CASO DI STUDIO DI OLBIA (OT).

Heideman, H. K. (2014a). LIDAR base specification (ver. 1.2). *U.S. Geological Survey Techniques and Methods 11-B4*, (October), 41. https://doi.org/10.3133/tm11B4

Heideman, H. K. (2014b). LIDAR base specification (ver. 1.2). *U.S. Geological Survey Techniques and Methods 11-B4*, (October), 41. https://doi.org/10.3133/tm11B4

Jaroslav Mysiak, & Martina Gambaro. (2011). Scheda Tecnica: Il bacino del fiume Adda.

Krause, P., Boyle, D. P., & Bäse, F. (2005). Comparison of different efficiency criteria for hydrological model assessment. *Advances in Geosciences*, *5*, 89–97. https://doi.org/10.5194/adgeo-5-89-2005

Legates, D. R., & McCabe Jr., G. J. (2005). Evaluating the Use of "Goodness of Fit" Measures in Hydrologic and Hydroclimatic Model Validation. *Water Resources Research*, *35*(1), 233–241. https://doi.org/10.1029/1998WR900018

Lilburne, L., & Tarantola, S. (2009). Sensitivity analysis of spatial models. *International Journal of Geographical Information Science*, *23*(2), 151–168. https://doi.org/10.1080/13658810802094995

Menoni, S., & Margottini, C. (2011). *Inside Risk: A Strategy for Sustainable Risk Mitigation*.

Natale, L. (2003). Delimitazione delle aree inondabili ad assegnati tempi di ritorno - Fiume Adda.

Ozdemir, H., Sampson, C. C., de Almeida, G. A. M., & Bates, P. D. (2013). Evaluating scale and roughness effects in urban flood modelling using terrestrial LIDAR data. *Hydrology and Earth System Sciences*, *17*(10), 4015–4030. https://doi.org/10.5194/hess-17-4015-2013

Paoletti, A., Bianchi, A., & Becciu, G. (1999). *Disponibilità ed ottimizzazione nell'uso della risorsa idrica*. *Quaderni Regionali di Ricerca n. 33*.

Pastormerlo, M., & Zazzeri, M. (2016). SWAM (SURFACE WATER ANALYSIS METHOD): UN METODO SPEDITIVO PER LA MODELLAZIONE DI UN EVENTO ALLUVIONALE, 1–112.

Poljanšek K., De Groeve T., Marín Ferrer M., C. I. (2017). *Science for disaster risk management 2017*. https://doi.org/10.2788/688605

Radice, A., & Crotti, G. (2016a). River2D quick guide.

Radice, A., & Crotti, G. (2016b). *Two-dimensional river modelling*.

Rossetti, S., & Cella, O. W. (2010a). *Relazione Idrologico-Idraulica*.

Rossetti, S., & Cella, O. W. (2010b). *Relazione Tecnica Generale*.

Saltelli, A. (2002). Sensitivity analysis for importance assesment.

Steffler, P., & Blackburn, J. (2002). River2D Two-Dimensional Depth Averaged Model of River Hydrodynamics and Fish Habitat Introduction to Depth Averaged Modeling and User â€™ s Manual by. *Software Manual*, 1-.

LIST OF ABBREVIATIONS

AdbPo: *Autorità di Bacino del fiume Po* / District basin authority of the river Po;

BC: Boundary Condition;

cms: cubic metre per second;

DEM: Digital Elevation Model;

DSM: Digital Surface Model;

DTM: Digital Terrain Model;

FwDET: Floodwater Depth Estimation Tool;

GIS: Geographic Information System;

h: hours;

HEC-RAS: Hydrologic Engineering Center's River Analysis System (name of the software);

HP: hypothesis;

m a.s.l.: metre above sea level;

OB: OverBank

Q: Discharge;

R2D: River 2D (name of the software);

SA: Sensitivity Analysis;

sec or [s]: seconds;

SW: Software;

SWAM: Surface Water Analysis Method;

SWE: Shallow Water Equations;

T: Return period;

V=velocity;

VER.: Version;

WD: Water Depth;

WSE: water surface elevation;

APPENDIX

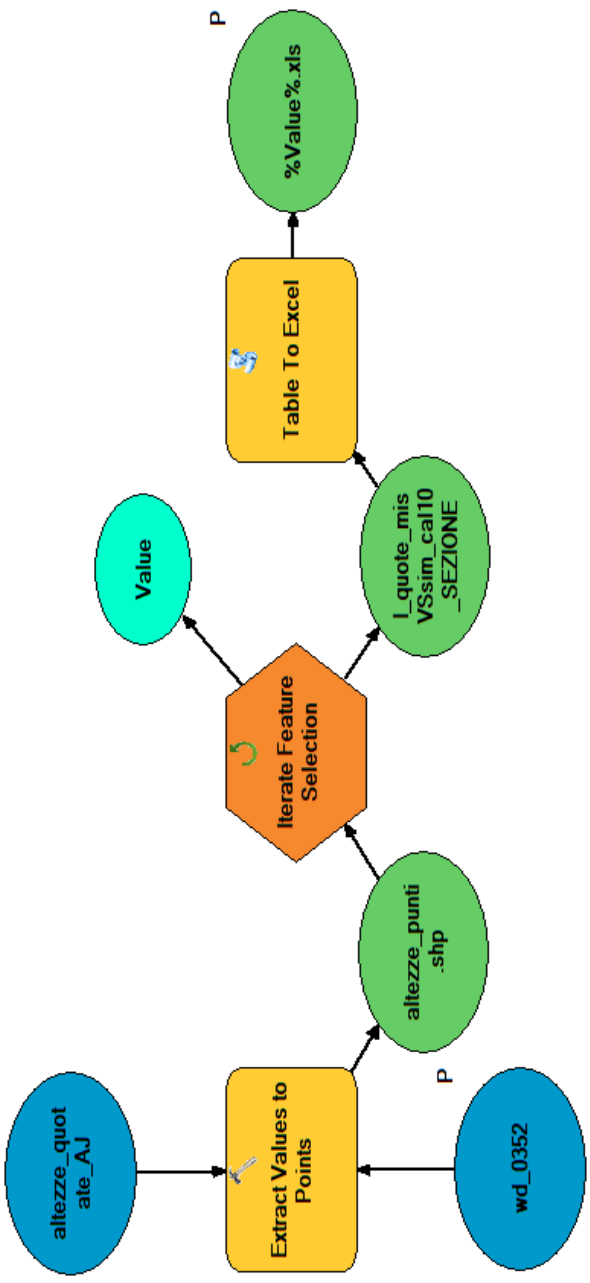

Appendix A Model used to evaluate the depth parameter in the sensitivity analysis

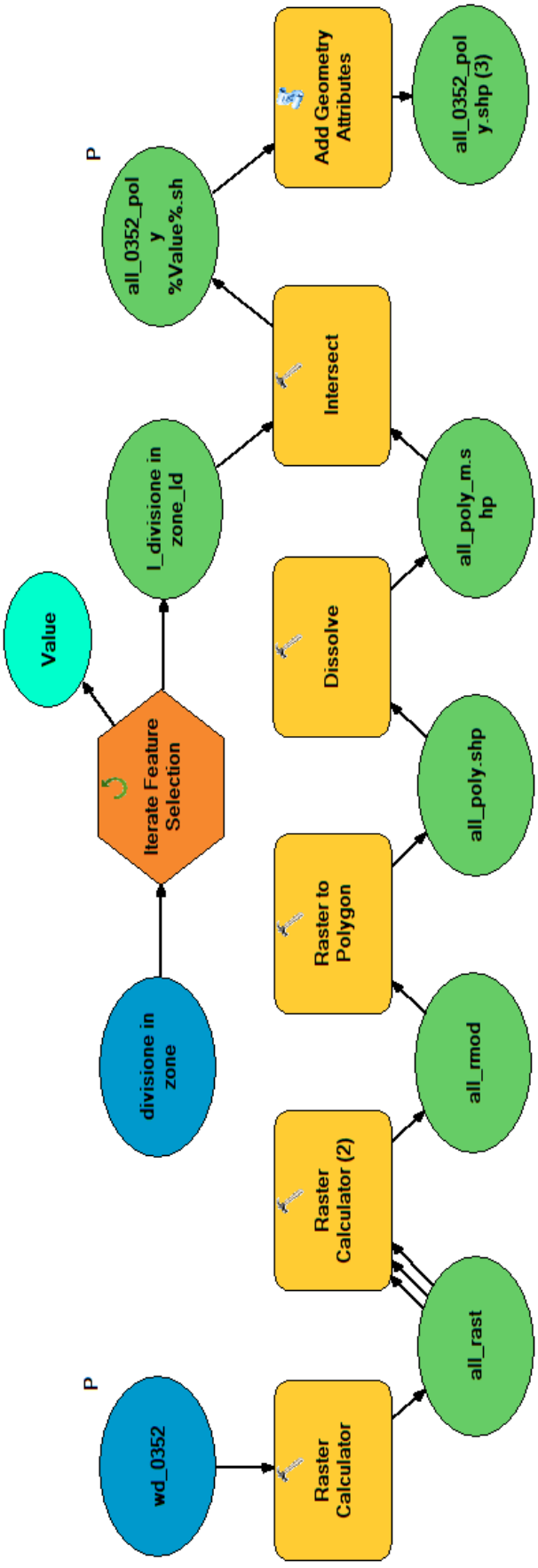

Appendix B Model used to evaluate the areal parameter in the sensitivity analysis

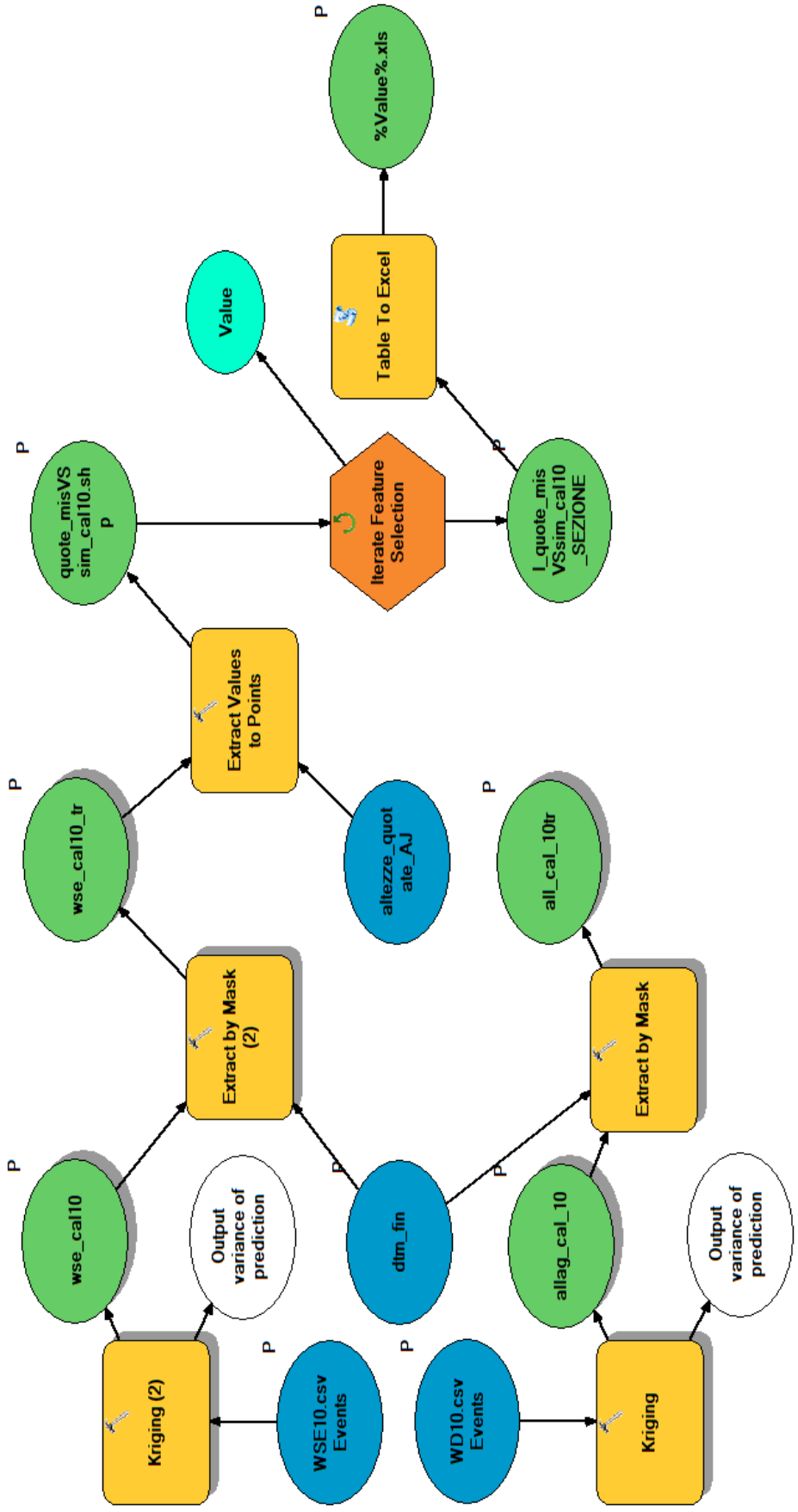

Appendix C Model used to evaluate the F_1 in the calibration phase

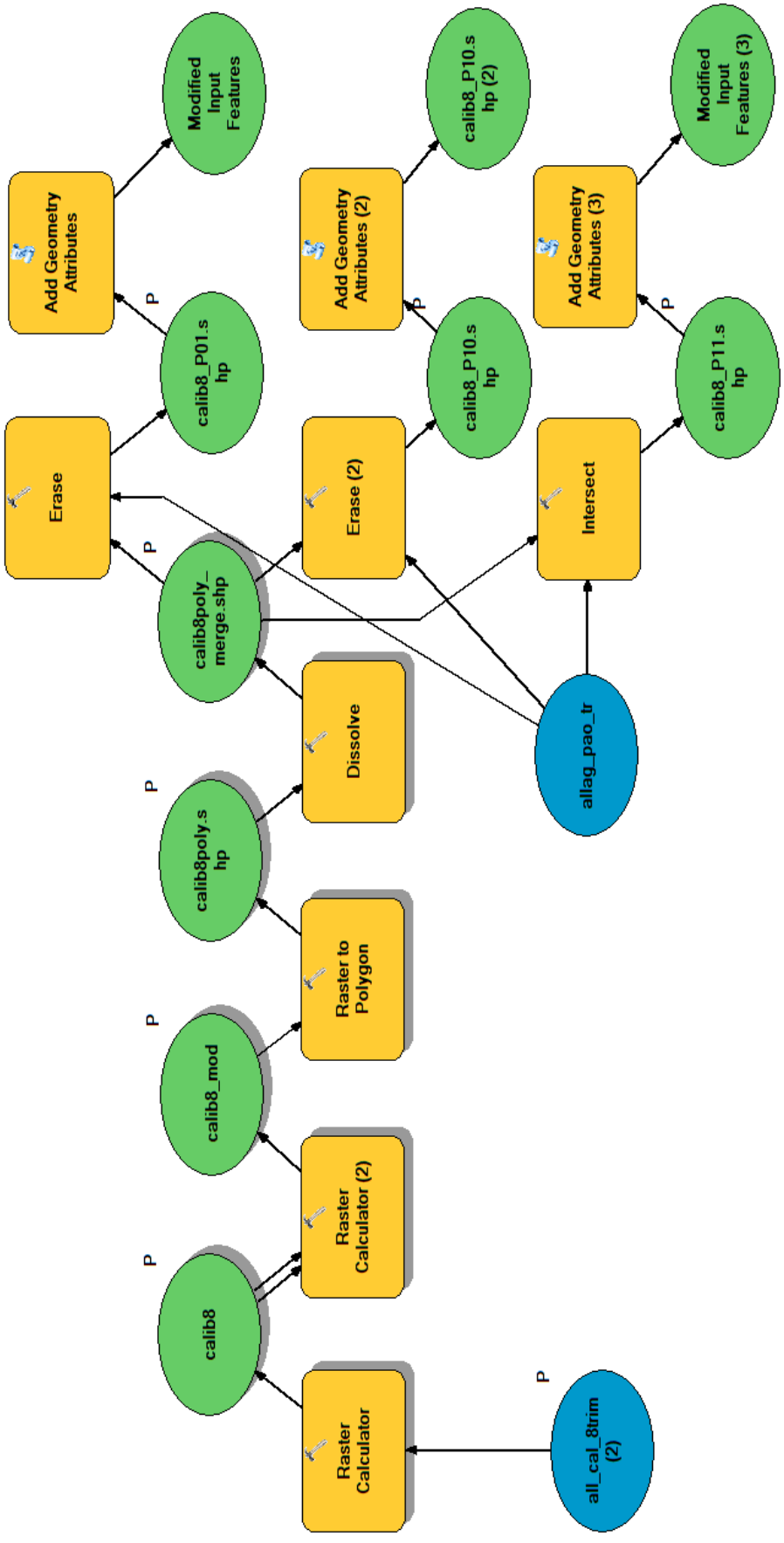

Appendix D Model used to evaluate the F_2^M in the calibration phase

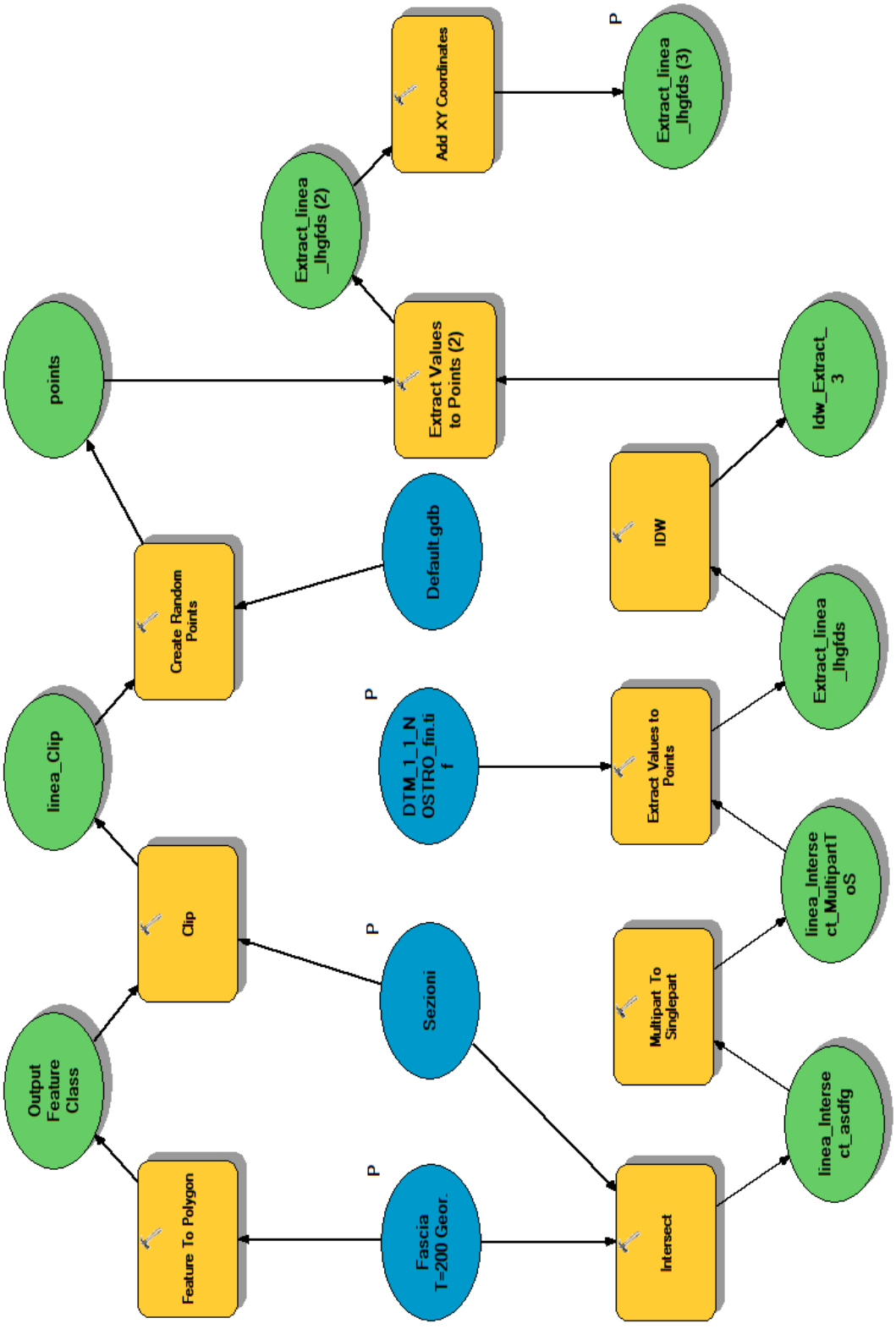

Appendix E Model used to interpolate the WSE within the defined section

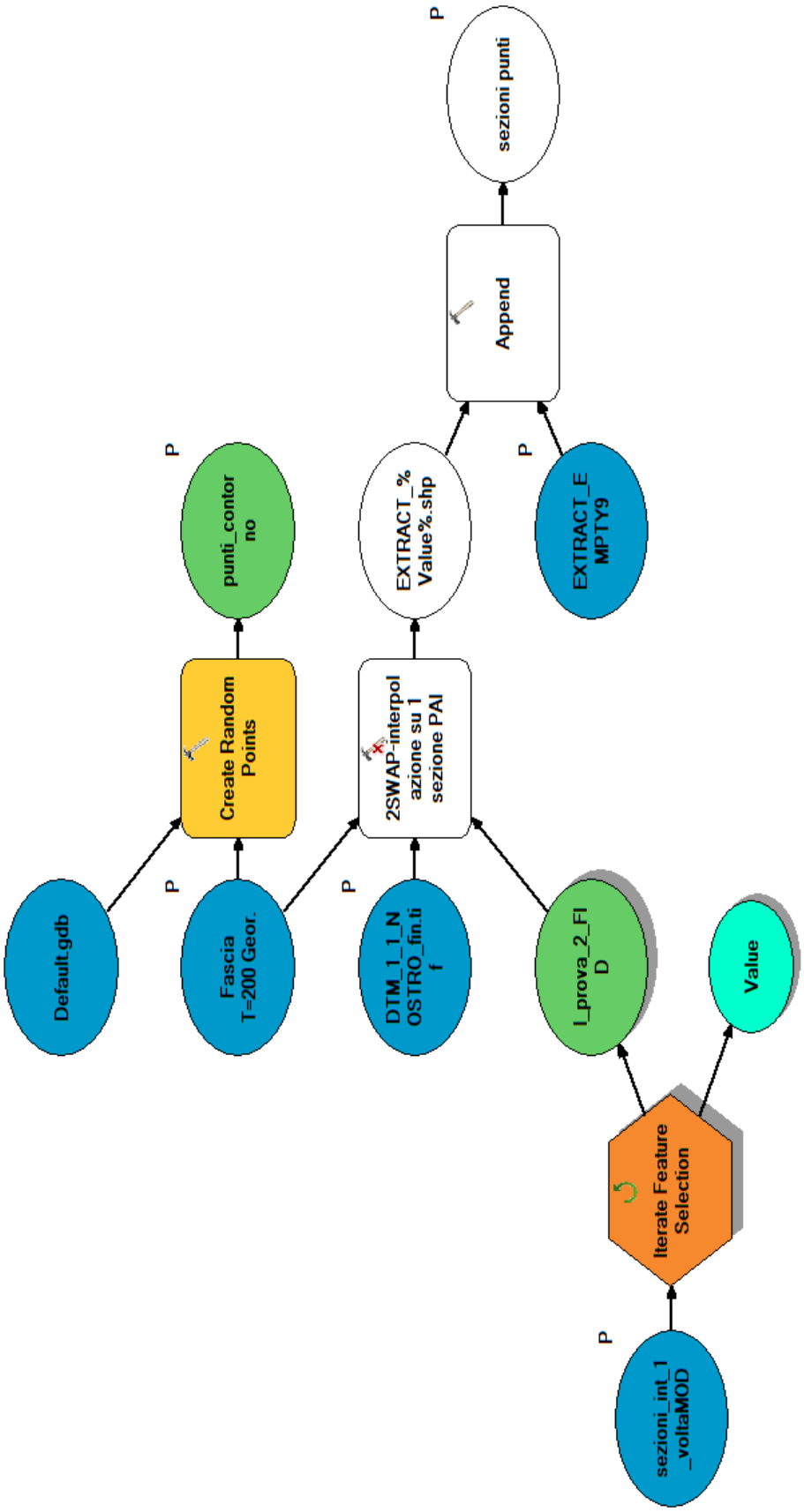

Appendix F Model used to produce the boundary points and iterate the model in Appendix E through all the sections

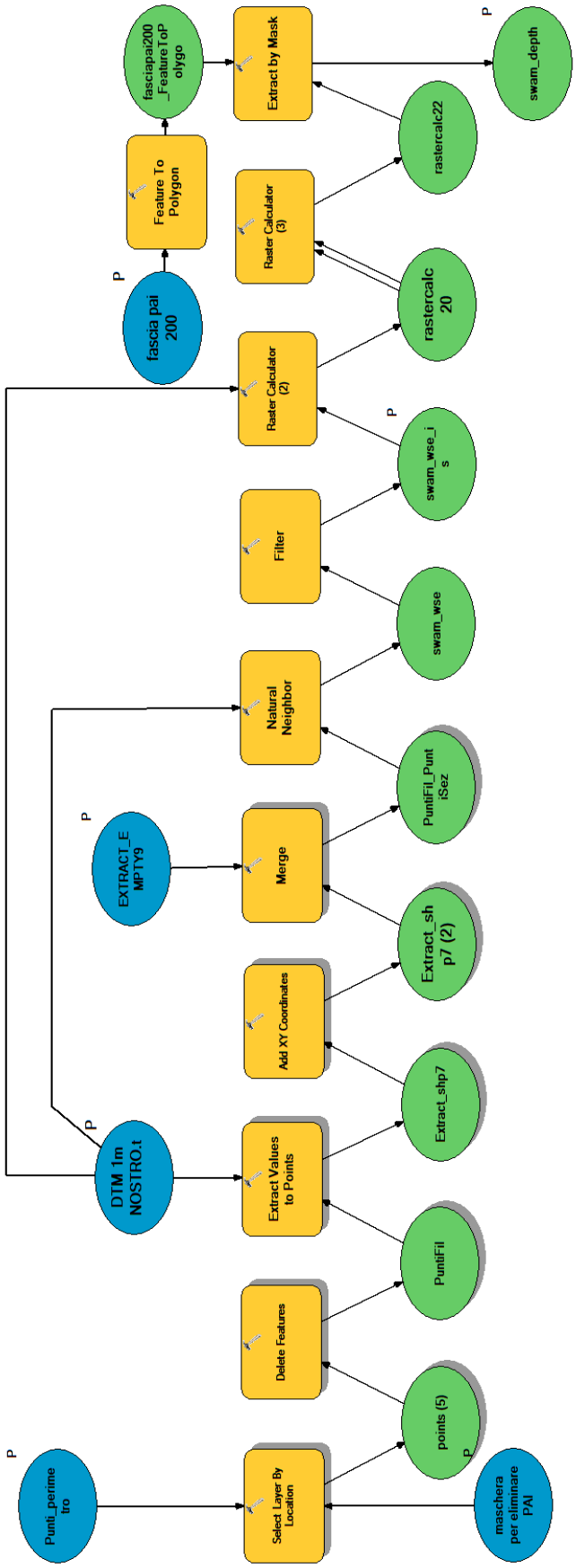

Appendix G Model 4 Model used to calculate the WSE and the WD starting from the perimeter points and the sections points

Raster calculator:

Builds and executes a single Map Algebra expression using Python syntax in a calculator-like interface.

http://desktop.arcgis.com/en/arcmap/10.3/tools/conversion-toolbox/raster-to-polygon.htm

Raster To Polygon:

Converts a raster dataset to polygon features.

http://desktop.arcgis.com/en/arcmap/10.3/tools/spatial-analyst-toolbox/raster-calculator.htm

Dissolve:

Aggregates features based on specified attributes.

http://desktop.arcgis.com/en/arcmap/10.3/tools/data-management-toolbox/dissolve.htm

Iterate Feature Selection:

Iterates over features in a feature class.

http://desktop.arcgis.com/en/arcmap/10.3/tools/modelbuilder-toolbox/iterate-feature-selection.htm

Intersect:

Computes a geometric intersection of the input features. Features or portions of features which overlap in all layers and/or feature classes will be written to the output feature class.

http://desktop.arcgis.com/en/arcmap/10.3/tools/analysis-toolbox/intersect.htm

Add geometry Attributes:

Adds new attribute fields to the input features representing the spatial or geometric characteristics and location of each feature, such as length or area and x-, y-, z-, and m-coordinates.

http://desktop.arcgis.com/en/arcmap/10.3/tools/data-management-toolbox/add-geometry-attributes.htm

Create Random Points:

Creates a specified number of random point features. Random points can be generated in an extent window, inside polygon features, on point features, or along line features.

http://desktop.arcgis.com/en/arcmap/10.3/tools/data-management-toolbox/create-random-points.htm

Extract values to points:

Extracts the cell values of a raster based on a set of point features and records the values in the attribute table of an output feature class.

http://desktop.arcgis.com/en/arcmap/10.3/tools/spatial-analyst-toolbox/extract-values-to-points.htm

Add XY Coordinates:

Adds the fields **POINT_X** and **POINT_Y** to the point input features and calculates their values. It also appends the **POINT_Z** and **POINT_M** fields if the input features are Z- and M-enabled.

http://desktop.arcgis.com/en/arcmap/10.3/tools/data-management-toolbox/add-xy-coordinates.htm

Table To Excel:

Converts a table to a Microsoft Excel file.

http://desktop.arcgis.com/en/arcmap/10.3/tools/conversion-toolbox/table-to-excel.htm

Kriging:

Interpolates a raster surface from points using kriging.

http://desktop.arcgis.com/en/arcmap/10.3/tools/3d-analyst-toolbox/kriging.htm

IDW:

Interpolates a raster surface from points using an inverse distance weighted (IDW) technique.

http://desktop.arcgis.com/en/arcmap/10.3/tools/3d-analyst-toolbox/idw.htm

Extract by Mask:

Extracts the cells of a raster that correspond to the areas defined by a mask.

http://desktop.arcgis.com/en/arcmap/10.3/tools/spatial-analyst-toolbox/extract-by-mask.htm

Erase:

Creates a feature class by overlaying the **Input Features** with the polygons of the **Erase Features**. Only those portions of the input features falling outside the erase features outside boundaries are copied to the output feature class.

http://desktop.arcgis.com/en/arcmap/10.3/tools/analysis-toolbox/erase.htm

Append tool:

Appends multiple input datasets into an existing target dataset. Input datasets can be point, line, or polygon feature classes, tables, rasters, raster catalogs, annotation feature classes, or dimensions feature classes.

To combine input datasets into a new output dataset, use the Merge tool.

http://desktop.arcgis.com/en/arcmap/10.3/tools/data-management-toolbox/append.htm

Select layer by location:

Selects features in a layer based on a spatial relationship to features in another layer.

Each feature in the **Input Feature Layer** is evaluated against the features in the **Selecting Features** layer or feature class; if the specified **Relationship** is met, the input feature is selected.

http://desktop.arcgis.com/en/arcmap/10.3/tools/data-management-toolbox/select-layer-by-location.htm

Feature To Polygon:

Creates a feature class containing polygons generated from areas enclosed by input line or polygon features.

http://desktop.arcgis.com/en/arcmap/10.3/tools/data-management-toolbox/feature-to-polygon.htm

Clip:

Extracts input features that overlay the clip features.

Use this tool to cut out a piece of one feature class using one or more of the features in another feature class as a cookie cutter. This is particularly useful for creating a new feature class—also referred to as study area or area of interest (AOI)—that contains a geographic subset of the features in another, larger feature class.

http://desktop.arcgis.com/en/arcmap/10.3/tools/analysis-toolbox/clip.htm

Multipart To Singlepart:

Creates a feature class containing singlepart features generated by separating multipart input features.

http://desktop.arcgis.com/en/arcmap/10.3/tools/data-management-toolbox/multipart-to-singlepart.htm